UCRL-16535

University of California

Ernest O. Lawrence Radiation Laboratory

CONVECTIVE TRANSFER PROCESSES IN LAMINAR GAS-LIQUID CHANNEL FLOW

TWO-WEEK LOAN COPY

This is a Library Circulating Copy which may be borrowed for two weeks. For a personal retention copy, call Tech. Info. Division, Ext. 5545

Berkeley, California

DISCLAIMER

This document was prepared as an account of work sponsored by the United States Government. While this document is believed to contain correct information, neither the United States Government nor any agency thereof, nor the Regents of the University of California, nor any of their employees, makes any warranty, express or implied, or assumes any legal responsibility for the accuracy, completeness, or usefulness of any information, apparatus, product, or process disclosed, or represents that its use would not infringe privately owned rights. Reference herein to any specific commercial product, process, or service by its trade name, trademark, manufacturer, or otherwise, does not necessarily constitute or imply its endorsement, recommendation, or favoring by the United States Government or any agency thereof, or the Regents of the University of California. The views and opinions of authors expressed herein do not necessarily state or reflect those of the United States Government or any agency thereof or the Regents of the University of California.

Special thesis (Byers)

UCRL-16535

UNIVERSITY OF CALIFORNIA

Lawrence Radiation Laboratory
Berkeley, California

AEC Contract No. W-7405-eng-48

CONVECTIVE TRANSFER PROCESSES IN LAMINAR GAS-LIQUID CHANNEL FLOW

Charles Harry Byers and C. Judson King

May 20, 1966

CONVECTIVE TRANSFER PROCESSES IN LAMINAR GAS-LIQUID CHANNEL FLOW

Contents

List of Illustrations

List of Tables

Abstract

I. General Introduction 1

A. Historical Background. 2

B. Objectives of the Study. 4

II. Equipment Design 5

A. Design Criteria. 5

1. Hydrodynamics. 5

2. Heat Transfer Criteria 6

3. Test Section Criteria. 7

B. Choice of Equipment. 8

C. Final Design 12

1. The Channel. 12

2. The Gas System 16

3. The Liquid System. 18

4. Sampling and Control 18

5. A typical Run. 19

III. Effect of Interfacial Motion upon Gas Phase Controlled Mass Transfer 21

A. Simple Models for Mass Transfer to Laminar Streams 21

1. The Graetz Solution. 22

2. The Leveque Model. 25

3. The Penetration Model. 27

B. Mass Trasnfer with Tangential Interfacial Motion 28

1. The Solution of the Modified Graetz Problem. 29

2. Gas-Phase Mass Transfer Near a Moving Interface. 33

3. Mass Transfer to Countercurrent Flow 42

C. Experimental Results 45

1. The Liquid Phase 45

2. The Graetz Runs 46

3. Cocurrent Mass Transfer with Resistance in a Single Phase 48

4. Countercurrent Data 55

D. Experimental Errors 62

E. Conclusions 65

IV. Interphase Mass Transfer 67

A. Introduction 67

B. An Analytic Solution to the Equations for Interphase Mass Transfer 71

C. Computer Colutions to Interphase-Mass-Transfer Problems . . . 80

1. Method of Solution 80

2. Results of the Computer Solution 83

D. Countercurrent Interphase Mass Transfer 90

E. Experimental Investigations of Interphase Mass Transfer . . . 91

1. Cocurrent Experiments 91

2. Countercurrent Interphase Experimental Data 94

F. Conclusions . . . . . .

V. Effect of a Surfactant Film upon Interphase Mass Transfer 99

A. Previous Investigations 99

1. Vertical Surfaces 99

2. Spherical Geometry 100

3. Horizontal Surfaces 102

B. The Present Study 104

1. Experimental Data 104

2. Theory of the Growth of Surfactant Films 109

3. Mass-Transfer Models 116

C. Conclusions 122

D. Recommendations for Further Study 122

Acknowledgments 126

Appendices

A. The Hydrodynamics of Laminar Two-Phase Flow 127

B. Design Details 140
C. Experimental Data. 148
D. Collection of Programs for Solving the Convective Transport Equation 176
E. Physical Properties. 243
F. Nomenclature 248
References 252

List of Illustrations

Figure number	Title	Page
1.	Cross sectional view of the laminar interphase mass transfer channel showing a typical velocity profile	10
2.	Schematic diagram of the experimental apparatus	13
3.	Overall view of the rectangular channel apparatus	14
4.	The rectangular channel with supporting table	15
5.	Close-up view of the test section	17
6.	Mass transfer to laminar flow between two flat plates	23
7.	Simple mass transfer models	26
8.	Mass transfer to a fluid in laminar flow between two parallel walls, one of which is in cocurrent motion	30
9.	Mean fraction saturation as a function of the Graetz number	34
10.	A logarithmic representation of the local Nusselt number as a function of the Graetz number	35
11.	A comparison of concentration profiles for different Graetz numbers in a falling film	36
12.	A comparison of solutions for cup-mixing concentration in a falling film as a function of Graetz number	37
13.	The Beek and Bakker model for mass transfer to an infinite medium with an interfacial velocity	38
14.	The solution of the Beek and Bakker problem	41
15.	Concentration profiles for the Beek and Bakker problem	43
16.	The countercurrent flow of a gas and a liquid showing a typical velocity profile	44
17.	A comparison of runs with zero interfacial velocity with the solution of Butler and Plewes	47
18.	Concentration profile for run 9	49
19.	Concentration profile for run 10	50
20.	Mean fraction saturation as a function of Graetz number for cocurrent motion of CO_2 and ethanol (18.0 cc/sec)	51

Figure number	Title	Page
21.	Mean fraction saturation as a function of Graetz number for cocurrent motion of CO_2 and ethanol(30.0 cc/sec)	52
22.	Mean fraction saturation as a function of Graetz number for cocurrent motion of CO_2 and ethanol(51.0 cc/sec)	53
23.	Concentration profiles for cocurrent flow of CO_2 and ethanol	56
24.	A comparison of average mass transfer coefficients based upon the solution of Beek and Bakker with experimental data	57
25.	Countercurrent mass transfer of ethanol into CO_2 with ethanol flow rate = 17.65 cc/sec	58
26.	Countercurrent mass transfer of ethanol into CO_2 with ethanol flow rate = 35.20 cc/sec	59
27.	Countercurrent mass transfer of ethanol into CO_2 with ethanol flow rate = 53.70 cc/sec	60
28.	A comparison of laminar single phase controlled cocurrent and countercurrent data	61
29.	Concentration profile for mass transfer in countercurrent flow	63
30.	A simplified model for gas liquid mass transfer	72
31.	Interphase mass transfer solution for two unbounded media	79
32.	Interphase mass transfer between two flat plates	81
33.	Theoretical concentration profiles for various values for Graetz number for two streams flowing at the same velocity, with 3/4 of the mass transfer resistance in the upper stream	84
34.	Theoretical concentration profiles for various values of the Graetz number for two streams with the same properties flowing at the same velocity. The resistance to mass transfer is 3/4 in the lower phase	85
35.	Overall Nusselt number as a function of Graetz number with various degrees of control in the upper phase as the parameter	86

Figure number	Title	Page
36.	Local Nusselt number curves as a function of Graetz number for different values of the parameter, U_m/U_o	88
37.	The ratio of the Nusselt given by the exact solution to that given by the addition of resistances as a function of Graetz number	89
38.	Cocurrent gas phase controlled and interphase mass transfer data	93
39.	Interphase mass transfer and a comparison with an exact computer solution	95
40.	Interphase countercurrent mass transfer data and theory	96
41.	End effect in rotating-Drum apparatus after Kennedy	101
42.	(a) Channel used by Merson and Quinn for observation of film growth (b) Surface flow pattern observed by Merson and Quinn	103
43.	Data for the evaporation of ether into oxygen from dilute aqueous solutions	105
44.	Data for the evaporation of ether into CO_2 from dilute aqueous solutions	106
45.	Data for the evaporation of ether into helium from dilute aqueous solutions	107
46.	Surface concentration diagram at a given time, also showing the corresponding channel position with velocity profiles	111
47.	Hydrodynamic models for adsorption and desorption from a horizontal surface	112
48.	(a) Mass transfer model with a stagnant interface (b) Model with a slowly moving interface	117
49.	Average mass transfer coefficient as a function of oxygen flow rate for $Q_1 = 15.43$ cc/sec	119
50.	Average mass transfer coefficient as a function of Oxygen flow rate for $Q_1 = 30.86$ cc/sec	120

Figure number	Title	Page
51.	Average mass transfer coefficient as a function of oxygen flow rate for Q_1 = 51.46 cc/sec	121
52.	Calculated interfacial velocity as a function of oxygen flow rate for three liquid flow rates	123
53.	Average mass transfer coefficients as a function of gas rate	124
54.	Single phase and two phase laminar velocity profiles between two flat plates	128
55.	Geometry of single phase and two phase rectangular channels	132
56.	Interfacial velocity profiles in two phase flow as a function of aspect phase aspect ratio	141
57.	Flow diagram for two phase pipe flow after Hoogendoorn	144
58.	Detailed drawing of the micrometer probe	147
59.	Concentration profiles for single phase controlled mass transfer showing profiles for various values of the Graetz number. The velocity ratio, U_m/U_o = 10.0	185
60.	Concentration profiles for single phase controlled mass transfer showing profiles for various values of the Graetz number. The velocity ratio, U_m/U_o = 4.0	186
61.	Concentration profiles for single phase controlled mass transfer showing profiles for various values of the Graetz number. The velocity ratio, U_m/U_o = 2.0	187
62.	Concentration profiles for single phase controlled mass transfer showing profiles for various values of the Graetz number. The velocity ratio, U_m/U_o = 1.0	188
63.	Concentration profiles for single phase controlled mass transfer showing profiles for various values of the Graetz number. The velocity ratio, U_m/U_o = 0.667	189
64.	Concentration profiles for single phase controlled mass transfer showing profiles for various values of the Graetz number. The velocity ratio, U_m/U_o = 0.5	190

Figure number	Title	Page
65.	Concentration profiles for single phase controlled mass transfer showing profiles for various values of the Graetz number. The velocity ratio, U_m/U_o = 100.0 (may be assumed to be the Graetz solution)	191
66.	Cup mixing concentration as a function of Graetz number (theoretical) for evaporation of ether from ethanol into helium flowing at different values of the parameter U_m/U_o	206
67.	Cup mixing concentration as a function of Graetz number (theoretical) for evaporation of ether from ethanol into CO_2 flowing at different values of the parameter U_m/U_o	207
68.	Interphase concentration profiles for the evaporation of ether from ethanol solution into helium for different values of the Graetz number. U_m/U_o = 10.0	208
69.	Interphase concentration profiles for the evaporation of ether from ethanol solution into helium for different values of the Graetz number. U_m/U_o = 4.0	209
70.	Interphase concentration profiles for the evaporation of ether from ethanol solution into helium for different values of the Graetz number. U_m/U_o = 2.0	210
71.	Interphase concentration profiles for the evaporation of ether from ethanol solution into helium for different values of the Graetz number. U_m/U_o = 1.0	211
72.	Interphase concentration profiles for the evaporation of ether from ethanol solution into helium for different values of the Graetz number. U_m/U_o = 0.667	212
73.	Interphase concentration profiles for the evaporation of ether from ethanol solution into helium for different values of the Graetz number. U_m/U_o = 0.5	213
74.	Interphase concentration profiles for the evaporation of ether from ethanol solution into CO_2 for different values of the Graetz number. U_m/U_o = 10.0	214
75.	Interphase concentration profiles for the evaporation of ether from ethanol solution into CO_2 for different values of the Graetz number. U_m/U_o = 4.0	215
76.	Interphase concentration profiles for the evaporation of ether from ethanol solution into CO_2 for different values of the Graetz number. U_m/U_o = 2.0	216

Figure number	Title	Page
77.	Interphase concentration profiles for the evaporation of ether from ethanol solution into CO_2 for different values of the Graetz number. $U_m/U_o = 1.0$	217
78.	Interphase concentration profiles for the evaporation of ether from ethanol solution into CO_2 for different values of the Graetz number. $U_m/U_o = 0.667$	218
79.	Interphase concentration profiles for the evaporation of ether from ethanol solution into CO_2 for different values of the Graetz number. $U_m/U_o = 0.50$	219
80.	Local Nusselt number as a function of the Graetz number for interphase mass transfer with the liquid phase velocity constant. The parameter is U_m/U_o and $\sigma\mathcal{H} = 2.00$	228
81.	Local Nusselt number as a function of the Graetz number for interphase mass transfer with the liquid phase velocity constant. The parameter is U_m/U_o and $\sigma\mathcal{H} = 5.00$	229
82.	Local Nusselt number as a function of the Graetz number for interphase mass transfer with the liquid phase velocity constant. The parameter is U_m/U_o and $\sigma\mathcal{H} = 0.50$	230
83.	Local Nusselt number as a function of the Graetz number for interphase mass transfer with the liquid phase velocity constant. The parameter is U_m/U_o and $\sigma\mathcal{H} = 0.25$	231
84.	Cup mixing concentration as a function of Graetz number for interphase mass transfer with the liquid phase velocity constant. The parameter is U_m/U_o and $\sigma\mathcal{H} = 1.00$	232
85.	Cup mixing concentration as a function of Graetz number for interphase mass transfer with the liquid phase velocity constant. The parameter is U_m/U_o and $\sigma\mathcal{H} = 2.00$	233
86.	Cup mixing concentration as a function of Graetz number for interphase mass transfer with the liquid phase velocity constant. The parameter is U_m/U_o and $\sigma\mathcal{H} = 5.00$	234
87.	Cup mixing concentration as a function of Graetz number for interphase mass transfer with the liquid phase velocity constant. The parameter is U_m/U_o and $\sigma\mathcal{H} = 0.50$	235
88.	Cup mixing concentration as a function of Graetz number for interphase mass transfer with the liquid phase velocity constant. The parameter is U_m/U_o and $\sigma\mathcal{H} = 0.25$	236

List of Tables

Table number	Title	Page
C-1	Data for the evaporation of pure ethanol into flowing nitrogen	149
C-2	(a) Concentration profiles for Graetz run number 9, (b) Concentration profiles for Graetz run number 10	151
C-3	Data and calculations for cocurrent single phase runs	152
C-4	Concentration profiles for cocurrent runs with control in a single phase	156
C-5	Single phase countercurrent data	157
C-6	Concentration profiles for countercurrent runs with control in a single phase	160
C-7	Interphase cocurrent experimental data	161
C-8	Countercurrent interphase experimental data	162
D-1	Graetz numbers for which profiles are plotted in Figures 59 to 65	184
D-2	Concentration profile plots	205
D-3	Graetz Numbers of profiles in Figures 68 to 79	220
D-4	A listing of the plots for different values of $\sigma\lambda$	227
E-1	Gas diffusivities at 25°C	243
E-2	Experimental diffusion coefficients in $cm^2/sec \times 10^5$	245
E-3	Viscosities	246
E-4	Important vapor pressures	247

CONVECTIVE TRANSFER PROCESSES IN LAMINAR GAS-LIQUID CHANNEL FLOW

Charles Harry Byers and C. Judson King

Lawrence Radiation Laboratory
University of California
Berkeley, California

May 20, 1966

ABSTRACT

Interphase mass transfer has been studied experimentally and theoretically for cases where resistance to mass transfer is confined to the gas phase and where control is distributed between phases. A horizontal, rectangular channel of high aspect ratio has been built. The gas and liquid phases, which move in stratified laminar flow, are contacted in an 18-in-long test section. The exit streams are analyzed in a gas-liquid chromatograph.

A numerical solution was performed of the laminar transport equation for a parabolic velocity profile with a cocurrently moving boundary. Experiments in which pure ethanol was evaporated into two gases, CO_2 and oxygen, showed agreement with this theory within the estimated experimental error of 10%. An earlier solution of a simplified theory for mass transfer to an infinite medium with an interfacial velocity and a linear slope in velocity has been modified. The appropriate experimental results agree with this theory to better than 10%. It may be concluded from this study that cocurrent motion of the interface increases mass transfer. Experiments were carried out with the same fluids in countercurrent flow. Mass transfer is hindered by a flow reversal in the gas phase. A phenomenological model developed for this case, involving the addition of a stagnant film resistance to the resistance to mass transfer of a parabolic velocity profile, correlated the data to within the experimental error of the method.

Numerical solutions were performed of two cases of interphase mass transfer. The first is for parabolic velocity profiles in both phases, and the second assumes a parabolic profile in the gas and a constant velocity in the liquid. Experiments were carried out in which ether was evaporated from

dilute ethanol solutions into two gases, CO_2 and helium, in cocurrent flow. The experimental results agreed with the first interphase mass transfer solution to within 15% in all cases. Equations for a more simplified model in which the liquid has a constant velocity and the gas velocity varies linearly with distance from the interface have been solved analytically. Results of the appropriate interphase experiments agree with this theory. Interphase countercurrent experimental results agree substantially with a model that postulates penetration for the liquid phase and with the aforementioned countercurrent model for the gas phase.

A series of cocurrent interphase experiments was made, using water as the solvent. Experimental results were lower than the predicted values by at least a factor of two. The apparent cause of the difficulty was accumulation of surfactants at the interface. Experimental mass-transfer coefficients indicate that the interfacial velocity was about 10 to 20% of the predicted velocity. This was confirmed by visual observation.

I. GENERAL INTRODUCTION

If gradients in concentration exist within a single-phase physical system at a given time, there will be a movement of molecules within the system which in time will bring about complete chemical homogeneity. In multiphase systems an equilibrium will be established. The estimation of the rate at which such processes occur is the province of the field of study known as mass transfer. In an isothermal system mass transfer may occur in two ways. First the gradient in concentration provides a driving force for the movement of individual molecules. Secondly, bulk movement of a portion of the fluid from an area of one concentration to another with a different concentration causes a net movement of the individual chemical species. Normally, the problems in which we are interested involve a coupling of the two processes.

Of particular interest in the present study is interphase transfer of material. To be more specific, the case of mass transfer across a gas-liquid interface is investigated because devices in which gas-liquid contacting is important are so numerous in the chemical industry. These include absorption towers, distillation columns, and cooling towers. While the complexity of these operations forces us to adopt a somewhat empirical approach to the design of industrial units, an understanding of the basic processes involved in gas-liquid contacting is of considerable importance in meeting new problems.

One major division must still be made before the specific area of this study is defined. The equations describing mass transfer in laminar flow are substantially different from those for turbulent flow because of the unsteady components added by the turbulent flow. This study considers only cases involving laminar fluid mechanics.

A. Historical Background

Before 1800 very little of a quantitative nature was known about evaporation. Dalton in his classic paper on evaporation in 1801 summarizes what was known about the field prior to his paper[14]:

"1. Some fluids evaporate much more quickly than others.

2. The quantity evaporated is in direct proportion to the surface exposed, all other circumstances alike.

3. An increase of temperature in the liquid is attended with an increase of evaporation, not directly proportionable.

4. Evaporation is greater where there is a stream of air than where the air is stagnant.

5. Evaporation from water is greater the less the humidity previously existing in the atmosphere, all other circumstances the same."

With this as his basis, and with a series of evaporation experiments at different temperatures he determined that the driving force for evaporation is the difference between the equilibrium vapor pressure of the liquid and the partial pressure of the transferring substance in the medium to which it is exposed. Later workers have shown that when the liquid is a mixture, with only one transferring component, the driving force is the partial pressure of that component.

Adolf Fick,[19] in 1855, attempted to analyze his data for the diffusion of salt through water, following a mathematical approach originally proposed by Fourier for conductive heat transfer.[20] His result for unsteady-state mass transfer where convection can be neglected is

$$\frac{\partial c_A}{\partial t} = \frac{k\,\partial^2 c_A}{\partial y^2} \quad . \qquad (1\text{-}1)$$

The constant, k, has become known as the diffusion coefficient and is given the special symbol, D. Since that time it has been found that the diffusion coefficient is not generally a constant but is a function of concentration. A modern treatment of the estimation of gas-phase diffusivities, based upon

statistical mechanics, is presented in the monographs by Chapman and Cowling[9] and Hirschfelder, et al.[33] The various theories that have been developed in the liquid-phase case are found in the review of the subject by Johnson and Babb.[37]

Most early engineering studies of mass transfer involved turbulent flow. One result of particular importance to the present study was a postulate by Nernst that in turbulent flow the entire concentration gradient is across a "stagnant film" at the interface.[50] Within the film all transfer of material occurs by molecular processes. Before 1922 fluid-fluid contacting operations in which there was mass transfer were a source of some confusion. Applying the Nernst stagnant film approach to both sides of the interface, Lewis[46] and Whitman[76] were able to correlate such data. Their famous "two-film" theory for interphase mass transfer predicted that the individually measured resistances to mass transfer could be added when one desired to ascertain the overall resistance to mass transfer. It has since been found that this approach need not be confined to films but can describe many laminar situations with considerable accuracy.

The more basic approach, using the partial-differential equations of convective transport as a starting point, was developed by the German engineers Thoma,[69] Schmidt,[60] and Nusselt[51] in the 1920's. Higbie in developing his "penetration" model for liquid-phase mass transfer[18] and Drew in his theoretical approach[58] introduced this method to chemical engineering. Gilliland and Sherwood[21] used the wetted-wall column to obtain a better understanding of the underlying processes of interphase mass transfer. This use of a simple flow geometry to study mass transfer has been an important step towards a fundamental approach to mass transfer. Recent developments in the field of laminar convective mass transfer have centered on the more fundamental approach to the problem, with simple experimental devices.

There have been no interphase mass-transfer experiments in which there has been significant resistance to mass transfer in both phases and in which the flow geometry of both phases is sufficiently simple to allow solution of the convective transport equations. The behavior of the interface under mass-transfer conditions has been a subject of interest to chemical engineers for a number of years. First it was found that equilibrium is established in a

shorter time than can be measured.[62] The accumulation of trace contaminants on the interface as a surfactant film has been investigated. Finally phenomena associated with high mass flux are presently under study. These include surface flow patterns which tend to be turbulent in nature. They are caused by gradients in surface tension. Another such phenomenon was discovered in 1901 by Bénard.[3] Cellular patterns are exhibited by thin layers of fluid across which there is a gradient in density. While the phenomenon observed by Bénard was caused by gradients in temperature, "Bénard cells" might also be caused by gradients in concentration, which arise in rapid interphase mass transfer.

B. Objectives of the Study

The objectives of this study fall logically into two categories, the overall goals of the major program being undertaken in this field and the immediate goals of this part of the program. We first discuss the long-range plans of the entire project. The area of simultaneous heat and mass transfer is one which has received little attention from the research point of view. Of particular interest is the intimate interrelation between the two processes when one is discussing problems of high mass flux rates and high concentration levels. Hence the ultimate goal of this study is to gain a better understanding of the processes involved in high flux, interphase, simultaneous heat and mass transfer. Before this study can be undertaken the areas of pure mass transfer, pure heat transfer, and simultaneous heat and mass transfer with the simplification of low mass flux rates must be investigated. Only the pure mass transfer aspects of the problem are considered in the present work.

The specific objectives of the present study are:

1. Construction of a piece of experimental apparatus in which a gas and a liquid could be contacted under conditions where the hydrodynamics of both phases are well-known. The equipment must be planned in such a way that it will serve the future studies as well as the present mass-transfer objectives.

2. Study of mass transfer with control resident in the gas phase, in the hydrodynamic situation where the gas-liquid interface is in motion.

3. Investigation of interphase gas-liquid mass transfer with control divided between the two phases.

4. Examination of the mass-transfer behavior of an interface which is covered by natural surfactants.

II. EQUIPMENT DESIGN

In any major study of an experimental nature, much effort must be expended in design and construction of the apparatus. It was pointed out in Chapter I that the present work is only the first of a sequence of studies. From the standpoint of productivity as well as economy, it was desirable to construct an apparatus which in its basic concept would serve the purpose of the entire program. Hence with the overall goals of the program in mind, a series of criteria were established to serve as a guide in the choice of an appropriate design for the apparatus. Based upon these criteria, the possible designs were compared. The design best suited to the established criteria was built. This chapter is an account of these three fundamental steps.

A. Design Criteria

In an effort to design a piece of equipment which minimizes the inherent difficulties involved in studying simultaneous heat and mass transfer, the following criteria were established upon which a logical decision could be made concerning choice of equipment.

1. Hydrodynamics

The solution of any convective mass- or heat-transfer problem must necessarily be based upon a knowledge of the hydrodynamics of the particular flow geometry. In a basic transfer study it is of interest to study situations where the hydrodynamics are simple so that the underlying transfer processes may be thoroughly investigated. As a result it would be desirable for the hydrodynamics of the proposed system to be laminar in both phases. Further it would be quite important for the velocity of both phases to be expressible in simple algebraic terms.

Many previous studies have been hampered because there were hydrodynamic disturbances of the normal laminar flow pattern. Some of the more important undesirable effects are:

a. Ripples. The natural occurence of ripples on the surface of the liquid in many of the classical mass-transfer experiments has made it difficult to gain a true picture of the mass-transfer process underlying the experiment.

An apparatus where the growth of ripples is not a fundamental problem was necessary for the present experiment.

b. Surfactants. While a portion of the present study is concerned with mass transfer where there is a surfactant on the gas-liquid interface, for the remainder of the experiments it was desirable to have a system which is completely free from the accumulation of surfactants at the interface.

c. End effects. Hydrodynamic end effects are always present in fixed-exposure convective-transfer experiments. Hence the effectiveness with which one minimizes their importance relative to the overall exposure determines the validity of the normal assumption that the fluid mechanics are fully developed. The entrance-end effect is caused by the fact that a developing velocity profile must be dealt with in the region of the greatest mass-transfer coefficient. It is generally very much simpler to deal with the convective-transfer equations when the velocity is fully developed, and therefore this condition is almost always assumed. At the downstream end of the exposure it is normal to find a small capillary wave very close to the exit divider plate. This ripple which is caused by the subsequent stagnation of the interface is discussed by Lamb.[42] Very little can be done about this effect.

2. Heat-Transfer Criteria

While it is sufficient to separate two streams by a solid boundary to prevent mass transfer from occuring prematurely, the same cannot be said concerning heat. Hence the adopted apparatus must be designed so that this heat leak does not occur in the entry region. It must also be possible to insulate the entire apparatus from the surrounding atmosphere, so that a proper heat transfer study may be carried out.

3. Test Section Criteria

Since different lengths of exposure may be needed for various experiments, the length of the test section must be variable. It would be desirable to have available a wide variety of gas and liquid flow rates, so that the best experiments could be carried out in both heat and mass transfer. The possibility of operating both cocurrent and countercurrent experiments would be an interesting adjunct to the experiment. It would be important that the countercurrent experiments be the exact reverse of the cocurrent ones so that a comparison could be made. It must be possible to observe the transfer area clearly, and it would be of some advantage to be able to photograph the interface. It is quite evident that all these requirements could not be filled by any single piece of equipment. Hence some compromise was the only intelligent choice.

B. Choice of Equipment

Most devices are designed with particular attention to the hydrodynamics of one phase. The hydrodynamics of the other phase involved in the interphase mass are usually quite complex and as a result a solution of the convective transport equations for only one phase is possible. Therefore experiments are usually performed with the mass-transfer control totally within the phase with simple flow characteristics, the other phase being a medium saturated with the fluid of the first phase. When an experiment is attempted in which the control is distributed, empirical methods must be used to correlate the results. A good example of this is the laminar jet. Scriven and Pigford used a jet to study mass transfer to a liquid, where carbon dioxide was absorbed into the moving jet.[61,62] Their data are successfully correlated by use of a modified penetration theory. Several years later Hatch and Pigford altered the system to allow flow of the gas continuously through the vessel which surrounded the jet.[29] The fluid mechanics in the gas phase were found to be quite complex and dimensional analysis was used to correlate the data. The wetted sphere used by Cullen and Davidson,[13] the rotating drum of Dankwerts and Kennedy,[15] and the moving-band experiment of Govindan and Quinn[27] all suffer from the same difficulty as the laminar jet.

The wetted-wall column offered a possible solution to the problems posed by the previously mentioned devices. Here a gas and a liquid may be contacted in a controlled fashion. The long wetted-wall column, which was introduced by Gilliland and Sherwood,[21] suffers because, at liquid film Reynolds numbers above 4, visible ripples appear on the liquid interface. These disturbances greatly increase the mass-transfer coefficient. The short wetted-wall column, which may have lengths varying from 1/2 to 6 in., was first built by Vivian and Peaceman.[22] The short exposure makes the end effects a quite important portion of the overall length. In addition, the short wetted-wall column does not lend itself to widely varying conditions.

The device found to suit most closely the criteria for this program is a horizontal, rectangular channel of sufficiently high aspect ratio that the side walls do not affect the velocity profile in the central portion of the channel width. For sufficiently low flow rates in both phases, laminar stratified hydrodynamic conditions may be expected, with the velocity profile in the central section of the channel width approaching that of fluid flow between two flat plates. By segregating the effluent fluids from the center portion of the channel, one can study a mass-transfer situation that is essentially two-dimensional. Historically rectangular channels have often been used by hydraulics engineers in their experimental studies.

The first reference to a channel in chemical-engineering mass-transfer research concerns a device built by Van Krevelan and Hoftijzer in 1949.[70] The apparatus consisted of a shallow pan in which the liquid flowed. The pan was placed inside a slightly inclined circular pipe, which contained the gas phase. In 1957 Westkaemper and White reported an experiment in a horizontal rectangular channel in which they studied the evaporation of a moving stream of carbon tetrachloride into a turbulent air stream.[75] An empirical correlation was found for the mass-transfer coefficient. Since then this rectangular geometry has been used in several investigations. These include studies by Jamond, who worked with an inclined channel and carried out a liquid-phase controlled absorption with chemical reaction,[35] and by Gartside and Goodridge, who measured velocity profiles in a slightly inclined channel.[23,24] They also performed an absorption of carbon dioxide into water. The hydrodynamic studies showed basic agreement with the equations for the flow of a fluid down

an inclined plane at angles as low as 20 min to the horizontal. Their mass-transfer studies were in basic agreement with the penetration model.

Probably the most influential work as far as the present project is concerned is the study of Tang and Himmelblau.[67] Their channel was a two-phase flow channel in which the liquid was water and the gas was carbon dioxide. They observed the rate of absorption of carbon dioxide into water. They proposed three theories to explain their data--the penetration model, a solution of the mass transfer to the parabolic profile, and a boundary-layer-type model. All three models fit the data very well. It is interesting to note that there was really no reason to believe that the parabolic profile would give any better agreement than the penetration model since, at most the difference between the two models is perhaps 10% and the data are not any better than that figure. An important fact about all of these studies is that no invalidating facts concerning operation of the channels are presented in any of the publications.

The hydrodynamic simplicity of the channel device is probably the outstanding point in its favor. The hydrodynamics of flow in a two-phase channel are discussed in detail in Appendix A. The velocity profile is parabolic in both phases. No ripples are induced on the liquid interface by the flowing gas, if the gas is in laminar flow. Cohen and Hanratty have shown that a turbulent gas stream is necessary to induce ripples to appear upon a horizontal liquid surface.[10]

The fundamental experimental device is shown in crossection in Fig. 1, along with a schematic of the basic flow geometry. There was some question of the degree of development of the velocity profiles of the two streams at the downstream end of the entry section. Schlichting has shown that the parabolic velocity profile is fully developed in flow between two flat plates after an entry length, ℓ_e, given by the following expression:

$$\ell_e = 0.04\ b^2 U_m/\nu \quad . \tag{2-1}$$

The longest entry length would exist in the gas phase, where the entering velocity, U_m, is about 80 cm/sec. The entry length corresponding to this velocity is about 28 cm. Since the calming section is 76 cm long, we can

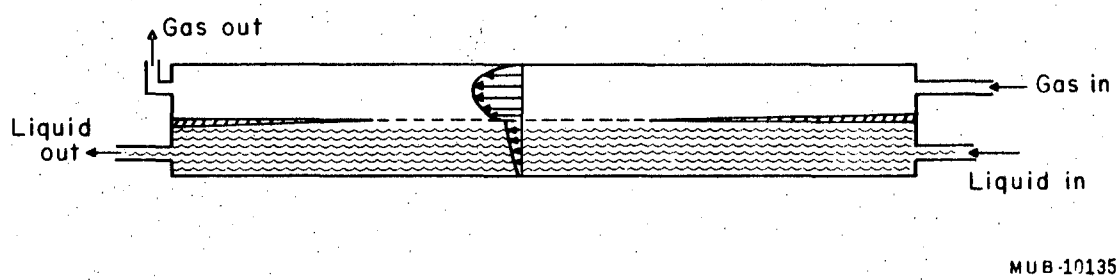

Fig. 1. Cross sectional view of the laminar interphase mass transfer channel showing a typical velocity profile.

assume that, at the point where the two phases are in contact, fully developed parabolic velocity profiles exist in both phases.

This fact gives rise to another hydrodynamic entry region. The development of the interfacial velocity of a liquid with a suddenly-freed interface has been studied by Goren.[26] Generally speaking, the development of the interfacial velocity should be essentially complete within the first few channel widths downstream from the liquid inlet. Hence if the channel is made sufficiently long, no measurable effect of the entry region should be manifest.

The horizontal geometry makes it possible to operate under a wide variety of hydrodynamic conditions. Countercurrent flow is quite simple to arrange. Finally the flat walls make it quite simple to view the interface as well as to photograph the interface if that ever became necessary.

There are some disadvantages to the use of such a device. Perhaps the most important is the fact that surfactant films tend to grow to great lengths on a horizontal surface. The magnitude of such a problem was not realized at the time of the design of the equipment, basically because none of the previous workers had reported any surfactant film in their studies. It was realized that this was a real problem at a much later date when a film arose to alter results significantly (see Chapter V). The second disadvantage is the possibility of creating surface instabilities at higher flux rates. While these phenomena are of interest in themselves, they might not be desirable when one is attempting to study high flux rates in a relative simple manner. The two problems can be overcome to a considerable extent, if not completely eliminated, by the proper choice of gas and liquid phases in which to carry out experiments.

A third potential problem with the operation of the device was realized during its operation. Since the liquid is more viscous than the gas phase, it appears to the gas as almost a solid wall. At the start of the exposure the liquid interface accelerates and the gas near the interface follows it. This causes a minimum to occur within the gas-phase velocity profile. This may lead to a violent rearrangement in the gas phase, because of the existence of a point of inflection in the velocity profile, which could explain any observation of unduly high mass-transfer coefficients.

C. Final Design

This section describes the device built to carry out the proposed series of experiments. It is not the object of this part of the report to give a detailed account of the design procedure, but rather to give a broad view of the final design. Details of design important to this study are included in Appendix B. Appendix A deals with the fluid mechanics of flow in a rectangular channel. A typical run is described at the end of this section.

Figure 2 is a schematic drawing of the overall system. The main piece of equipment is the channel in which the liquid and the gas are contacted. Two independent systems operate within the apparatus--the gas system and the liquid system. Figure 3 is a photograph of the entire system.

1. The Channel

The central portion of the equipment is a rectangular channel whose interior cross-sectional dimensions are 1 in. deep by 3 in. wide. An analysis of the hydrodynamics of two-phase flow in a rectangular channel (Appendix B) shows that this aspect ratio is sufficiently high that the central inch of the channel width has the hydrodynamics of flow between two flat plates. The overall length of the apparatus is 6.5 ft, consisting of two calming sections, each 2.5 ft in length, and an 18-in. test section designed to fit between the two calming sections. Several materials of construction were considered, with the final choice being "Lexan" polycarbonate. Use of this material made possible operation at temperatures up to 100°C, while maintaining the feature of visibility of flow within the channel. The entire channel is mounted on a 1/2-in. thick steel plate, which in turn is attached to a table. At the downstream end a sturdy hinge attaches the plate to the table; the other end merely lies upon the table. A rack and pinion gear apparatus may be used to raise and lower the upstream end of the channel when it is desirable to carry out experiments with an inclined channel. A photograph of this part of the overall equipment is the subject of Fig. 4.

The two calming sections are divided into an upper and a lower half by a horizontal divider plate. The plate consists of three sheets of 25-gauge stainless steel put together such that they form a sandwich with the center piece being only a border strip on three sides. The fourth side of the border

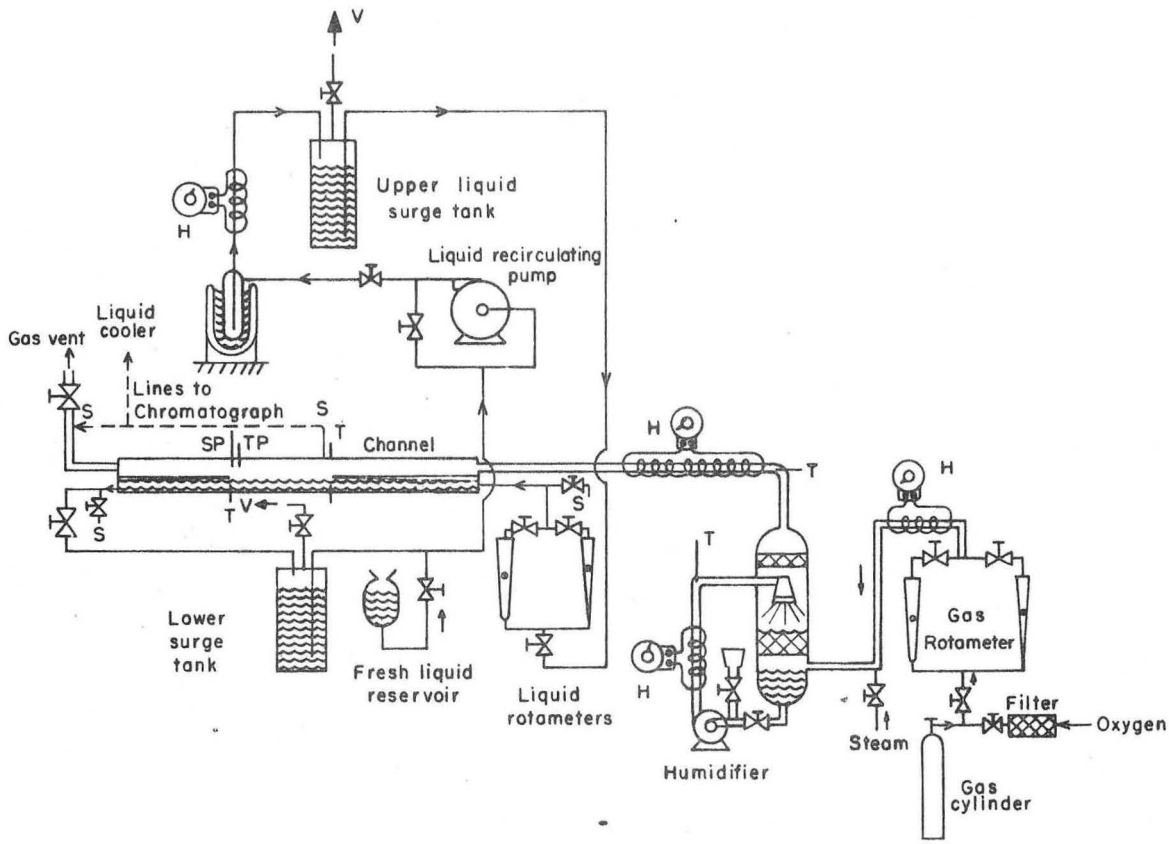

Fig. 2. Schematic diagram of the experimental apparatus.

MUB-10906

H - Heater using heating tape and controlled by a "Variac"
S - Sample point. SP. Sample probe used in taking profiles
T - Temperature measurement point
TP - Temperature probe designed for taking profiles
V - Vent on surge tanks.

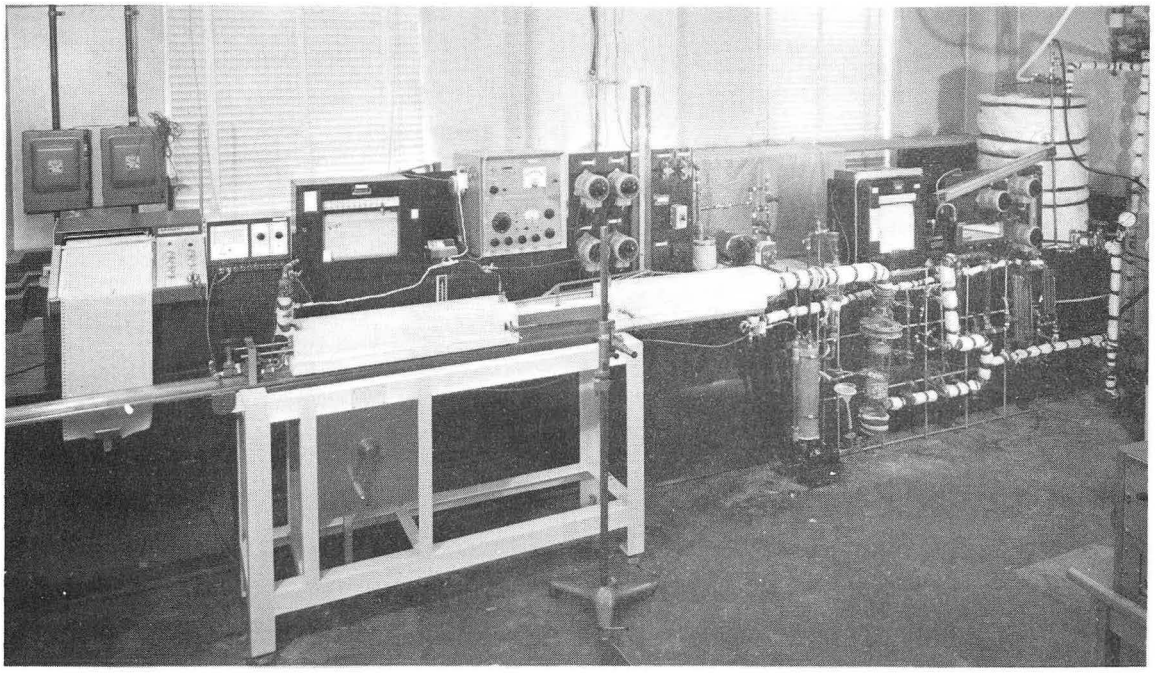

ZN-5608

Fig. 3. Overall view of the rectangular channel apparatus.

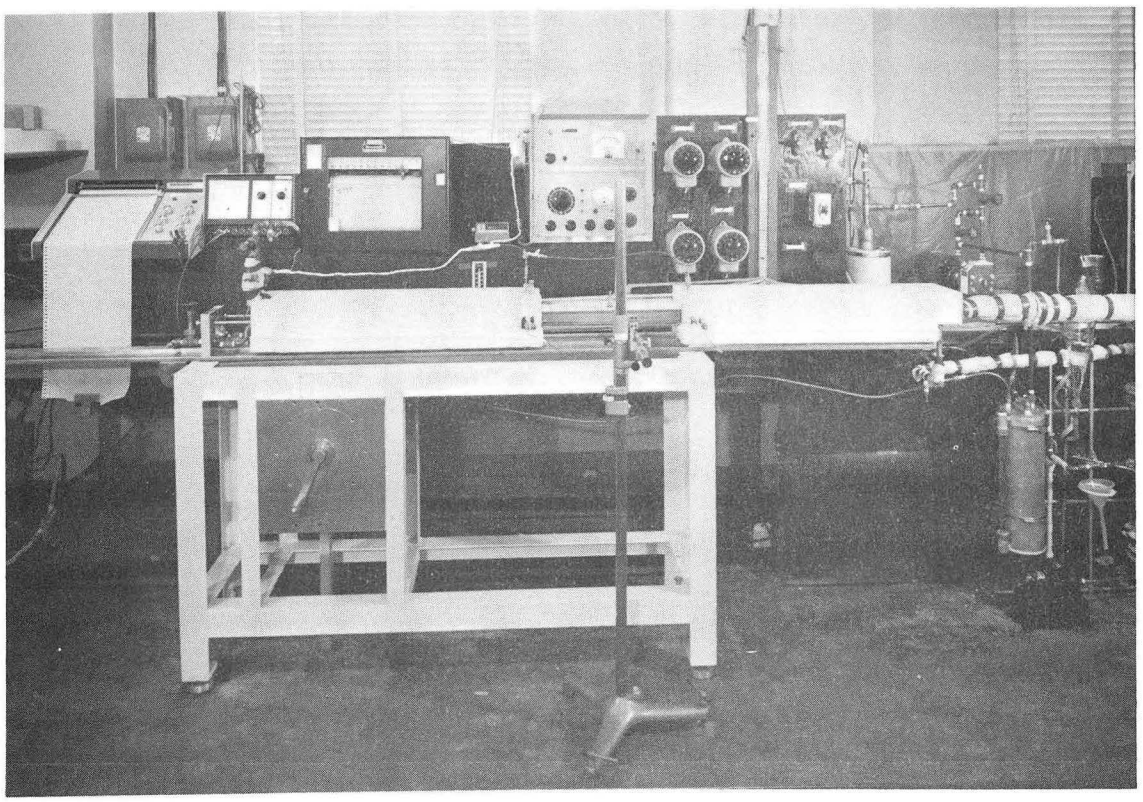

ZN-5609

Fig. 4. The rectangular channel with supporting table.

is fitted with a nose plate which is a metal wedge with an angle of 7 deg. This apparatus is welded together with the space between the two plates left void except for a thin strip of cork which is used to keep the plates from collapsing. A vacuum can be pulled on this apparatus which should discourage heat transfer between fluids. The long calming sections are considered necessary to prevent any turbulence from disturbing the flow pattern in the channel.

The test section is shown in the photograph in Fig. 5. The size of the apparatus is discussed in Appendix B. This section has a plain rectangular cross section so that the fluids are exposed to one another only within this 18-in. length. While the calming sections are covered on all sides with Styrofoam thermal insulation, the test section is designed so that a vacuum may be drawn on the plastic jacket surrounding it. This feature allows for insulation of the test section while maintaining the visibility of the fluids within the channel.

The three sections of the channel are interlocking, and a seal is maintained by O-rings. The downstream calming section is on a sliding track, so that the test section may be replaced with another of different length if desirable.

2. The Gas System

The gas was drawn from two sources; oxygen was taken from the building supply, filtered, dried and used directly, while the other gases came from cylinders. Oil-pumped-grade gas was used in the latter cases.

The gas flow rate was monitored with rotameters appropriate to the flow rate; in all, four rotameters were used to cover the range of flows from 50,000 cc/min (3/8-in. stainless steel ball) to 100 cc/min (3/16-in. stainless steel ball). From the rotameters the gas flows to a small glass humidifier, 4 in. in diameter and 2 ft high, where it passes up through a 6-in.-deep bed of 1/2-in. Raschig rings. The humidifying liquid in the bottom of the column is recirculated by a pump through a sparger and over the bed of Raschig rings. A bed of small beads is above the first bed to prevent entrainment. The gas is thermally regulated by the liquid in the humidifier. Any necessary small adjustment in temperature is made by heating tape at the exit of the humidifier.

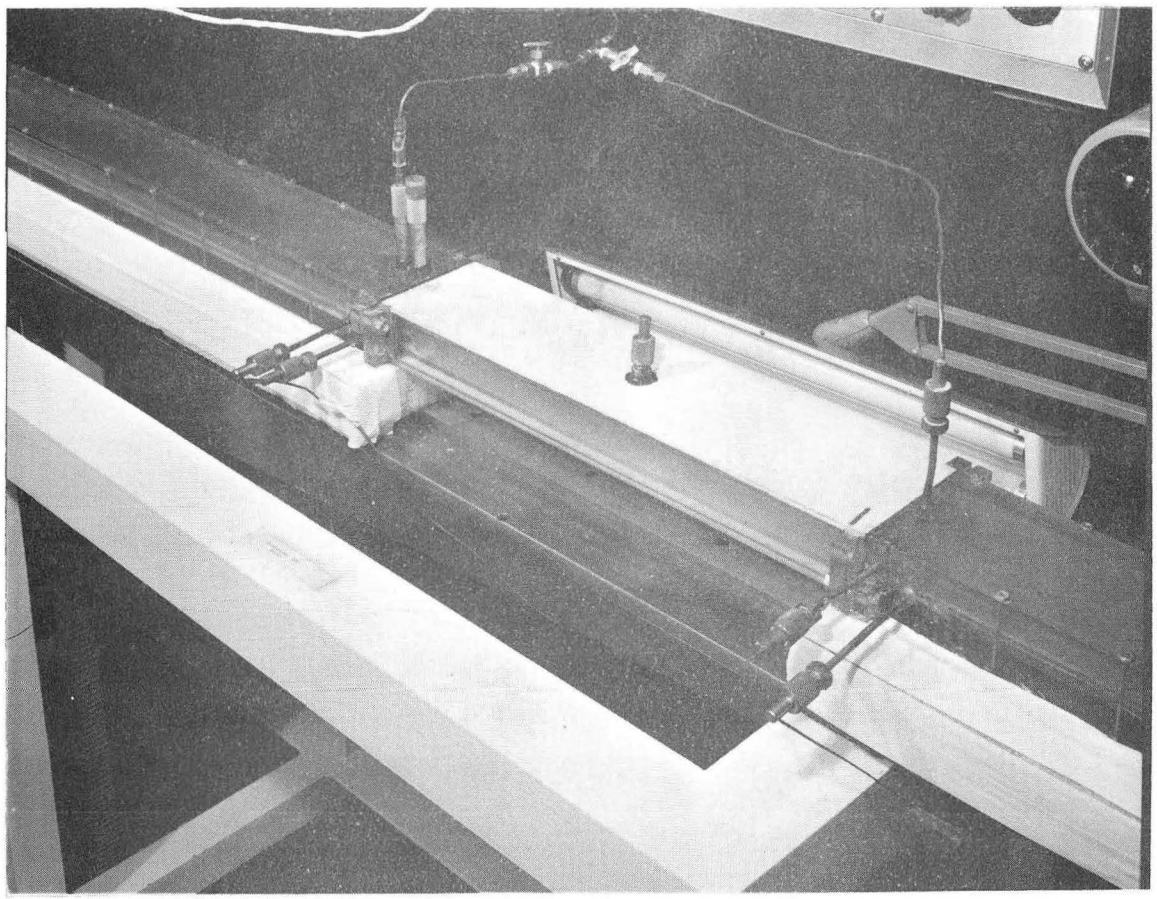

ZN-5610

Fig. 5. Close-up view of the test section showing micrometer probes on the left.

The gas then flows through the top half of the inlet calming section, where it contacts the liquid, and then the phases are divided once more at the downstream calming section. The last 2 in. of the length of this calming section is divided into three 1-in.-wide sections, by means of two thin metal plates placed vertically in the channel. Only the center section is of interest from a sampling viewpoint. Gas in this section leaves the channel through a 1/4 in. pipe. Before it is sampled, the gas must pass through a piping system which has two 90-deg elbows. The two sharp changes in flow direction and the initial drastic reduction in area provided sufficient mixing to assure that the sample taken subsequent to these disruptions is a representative cup-mixing concentration. After sampling, all the gas is vented to the atmosphere.

3. The Liquid System

Early problems with liquid-level control in the channel made conversion from a once-through-type system to a recirculating system desirable. A "Vanton" pump is used to recirculate the liquid. Because of the tendency of the pump to surge slightly, surge tanks were placed before and after the pump. These are small brass tanks with a capacity of two gallons each. One is situated near the ceiling and the other near the floor. When it is necessary to add liquid to the system, this operation is carried out by means of a reservior which feeds into the system just before the pump. A bypass on the pump is used to regulate the head created by the pump. Liquid leaving the pump passes through a cooling unit, which is necessary to counteract the high temperatures near the ceiling. It then flows to the ceiling surge tank, from whence it moves down to the rotameters where it is metered and fed into the lower half of the channel. After contacting the gas, liquid is drawn from the channel and flows to the lower surge tank. From there is is recycled.

4. Sampling and Control

All sampling of the gas phase was carried out with an Aerograph A-90-P2 Chromatograph. After some testing it was found that a dual column consisting of 10 ft. of Halomid M-18 and 10 ft. of Ethofat best suited the analyses that were necessary in the entire study. The chromatograph was fitted with a capillary flowmeter in order to observe closely the carrier-gas flow rate.

Helium was used as the carrier gas for all the runs. Sampling was carried out in a 5-cc sample valve which is an integral part of the instrument. The results were recorded on a Honeywell recorder equipped with a Disc integrator.

Sampling in the gas side of the channel may be done in three places--just before the start of the test section, in the central portion of the exit, or at the end of the test section. The last sample port is a micrometer type sampler used to obtain concentration profiles. This apparatus is described in Appendix B. All sample ports are directly connected to the sample valve. The flow rate to these ports is regulated by the pressure in the channel and by needle valves on the sample lines. Flow through the sample valve is metered by a rotameter. To avoid condensation within the sample lines, they are heated by means of nichrome wires.

Where necessary, sampling in the liquid phase is carried out at the inlet and exit of the channel. If the two components of the mixture in question have a sufficient different in refractive index, a Zeiss differential interferometer can be used to analyse the mixture. In the other cases, the liquid sampling facilities of the chromatograph were used.

Temperatures were measured with copper-constantan thermocouples at some points and by thermistors at others. All places at which measurements were made are indicated by a "T" in Fig. 2. A thermal probe, almost identical in design to the micrometer probe used for concentration profiles, is mounted on the test-section exit. Temperature profiles could be measured with this probe, whose sensing element is a thermistor.

Control of the liquid level was a problem throughout the experiment. The desired level was found on a cathetometer which was placed in front of the channel. If the level was too low, some liquid was added by means of the reservior, while if the liquid level was too high, a vacuum was drawn on the air pocket in the lower surge tank. This controlled liquid level adequately, but tired the experimenter quickly. It is suggested that some automatic control device be used in future experiments.

5. A Typical Run

The procedure described in this section is for the most complex series of runs, where control is divided between the phases. Other, simpler operations are carried out in the same way except that the unnecessary steps are omitted.

(a). The liquid rate is set and allowed to settle. Because pressures within the surge tanks must have time to come to steady state, this settling operation normally requires at least on-half hour. Once the level in the channel has settled, it remains fairly stable.

(b). At the beginning of a set of runs it is necessary to ascertain the chromatograph reading which corresponds to a gas-phase mixture that has been equilibrated with the liquid phase. This value is found in the channel by operating the liquid phase at normal flow rates while the gas phase flows at extremely low rates (50 to 100 cc/min). Several values of the chromatograph reading for saturation are taken, and their average is used as the saturation reading. The concentration of the liquid phase is also measured.

(c). The gas rate is set, and the system is allowed to come to steady state. Several samples are made of the cup-mixing exit concentration in the center section of the gas phase. Slow sampling is necessary to prevent any sudden momentary changes from affecting the results. At the same time, liquid samples are taken; these are analysed after the series of runs.

(d). In the runs where concentration profiles are taken, flow through the sampler is closely regulated so that only the impinging gas is taken as a sample. Hence one of these runs often takes several hours to complete.

(e). During all of the runs the liquid temperature was kept as close as possible to the gas temperature of 25±3°C. Because of the time consumed in taking a concentration profile it is necessary to sample the liquid phase several times during one of these runs.

(f). When the liquid flow rate is changed, reestablishment of a steady interface requires some time. As a result, all the runs at one liquid flow are carried out before the liquid flow rate is changed.

III. EFFECT OF INTERFACIAL MOTION UPON GAS-PHASE-CONTROLLED MASS TRANSFER

Before one can undertake a meaningful study of mass transfer with a distribution of the resistance between the phases, the individual mass-transfer behavior of both phases must be known. In laminar channel flow the mass-transfer process is quite well understood in the liquid phase. There is still an area of doubt in the case of the gas phase, concerning the effect of interfacial motion upon the mass-transfer coefficient. This chapter is devoted to the investigation of that effect.

A. Simple Models for Mass Transfer to Laminar Streams

The starting point of any theoretical study of mass transfer must be the convective-transport equation. A derivation of this basic equation is discussed by Bird et al.[4d] In vector notation the equation for a binary system may be written as

$$\frac{\partial C_A}{\partial t} + \mathcal{V} \cdot \nabla C_A = D_{AB} \nabla^2 C_A \quad . \tag{3-1}$$

This simplified equation contains the following assumptions:

(a). The diffusion coefficient, D_{AB}, is a constant. Since the diffusivity is a function of concentration, we are limited to small changes in concentration; since it is also a function of temperature, isothermal systems are assumed.

(b). The molar density is a constant. This implies the same restrictions as were imposed by a constant diffusivity.

(c). There is no chemical reaction which either produces or removes any of either component.

(d). The narrow range of concentration dictated by assumptions (a) any (b) allows the simplification that the velocity vector, $\mathcal{V}$, may be either the molar-average or the mass-average velocity.

Even with these restrictions Eq. (3-1) is more general than the form which is used throughout the present study. The added restrictions for this study are:

(e). Only the form of the equation in Cartesian coordinates is used, and further only cases where one of the three coordinate directions does not enter are considered. This implies that the z direction is infinite in extent and that concentration is not a function of z.

(f). Only cases where there are laminar, fully developed fluid mechanics are considered.

(g). Steady-state situations are the only ones considered.

(h). If the main fluid flow by forced convection occurs in the x direction, then the diffusive term of the equation in this direction is assumed to be negligibly small compared to the other terms in the equation.

(i). Restriction "a" confines us to a narrow concentration range. This range is now defined as the region where the concentration of component A is low and where one can assume that the diffusion of the component in question does not affect the hydrodynamics of the system. This may be called the assumption of low mass-transfer fluxes. Solutions with higher flux rates are considerably more complex. A good discussion of this area is contained in Bird, Stewart, and Lightfoot.[4b]

(j). All cases discussed in the present study are simplified by the fact that there is no y component of velocity. As a result it is dropped from the equation for the remainder of this report. Therefore Eq. (3-1) reduces to

$$U(x)\frac{\partial c_A}{\partial x} = D_{AB}\frac{\partial^2 c_A}{\partial y^2} \quad . \qquad (3\text{-}2)$$

The solution of this equation for the various important situations occupies a considerable portion of the remainder of this chapter.

1. <u>The Graetz Solution</u>

The earliest important solution to Eq. (3-2) was carried out by Graetz.[28] His solution involved heat transfer from a circular tube at a constant temperture to a fluid flowing in the tube. The corresponding solution in a Cartesian system involves flow between two flat plates of infinite width. The velocity profile in this case is parabolic, and therefore the same type of solution is possible. The particular solution of interest in this study is that carried out by Butler and Plewes.[6] The physical situation is illustrated in Fig. 6.

A fluid flowing in fully developed flow between two flat plates has the following velocity profile:

$$U_{(x)} = 6\, U_m\, [y/b - (y/b)^2] \quad . \qquad (3\text{-}3)$$

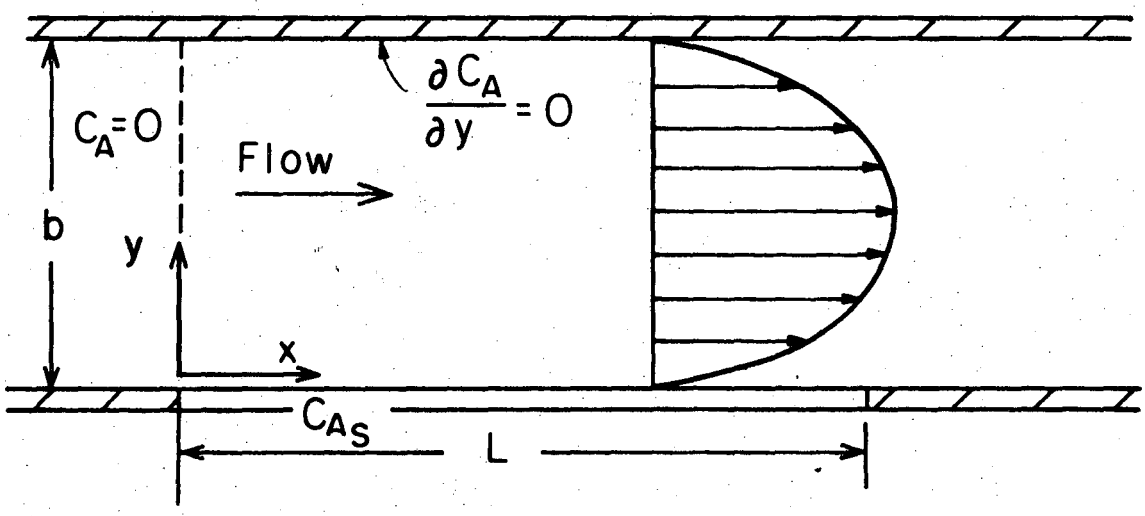

MUB-10904

Fig. 6. Mass transfer to laminar flow between two flat plates.

If one introduces the nondimensionalizing parameters

$$C = C_A/C_{As} - 1, \quad Y = y/b, \quad \text{and} \quad X = D_{AB}x/6\, U_m b^2, \tag{3-4}$$

the convective-transport equation becomes

$$(Y-Y^2)\ \frac{\partial C}{\partial X} = \frac{\partial^2 C}{\partial Y^2} \quad , \tag{3-5}$$

with the boundary conditions

$$C = 0 \quad \text{at } Y = 0 \tag{3-6a}$$

and

$$\partial C/\partial Y = 0 \quad \text{at } Y = 1. \tag{3-6b}$$

This problem is solved by a separation of variables. It is assumed that

$$C = X(X) \cdot \Omega(Y) \quad . \tag{3-7}$$

The equation becomes

$$\frac{X'}{X} = \frac{\Omega''}{(Y-Y^2)\Omega} = \beta^2. \tag{3-8}$$

The two solutions are

$$X = Ae^{-(\beta^2 X)} \tag{3-9}$$

and

$$\Omega = k_0 + k_1\ Y + k_2\ Y^2 + --- + k_n\ Y^n \quad . \tag{3-10}$$

The constants are evaluated in Ref. 6. The concentration at any point is given by

$$C = -2.1766\ e^{-(14.582\ X)}.\ \mathfrak{f}_1\ (Y) - 1.431\ e^{-(141\ X)}.\ \mathfrak{f}_2(Y) - \cdots\ , \tag{3-11}$$

where the numerical values for the series $\mathfrak{f}_1(Y)$ and $\mathfrak{f}_2(Y)$ are tabulated by Butler and Plewes. Overall results are expressed in terms of mean fractional saturation at exit. For flow between two flat plates the Graetz number becomes

$$\psi = D_{AB}\, L/U_m\, b^2 \tag{3-12}$$

and the mean fraction saturation is

$$\phi = 1 - 0.8956\, e^{-(2.4303\psi)} - 0.1044\, e^{-(23.5\psi)} - \cdots \quad . \tag{3-13}$$

2. <u>The Leveque Solution</u>

At low Graetz numbers the solution of the Graetz problem requires a great number of terms in the series. At low values of $D_{AB}\, L/U_m\, b^2$ only the velocity profile near the wall has an effect upon the mass transfer. Leveque[44] approximated the velocity profile in this region by the linear form

$$u = ay \quad . \tag{3-14}$$

The physical situation is illustrated in Fig. 7a. If one carries out the transformations

$$C = \frac{C_A - C_{AO}}{C_{As} - C_{AO}} \qquad \eta = y/L \qquad \text{and} \qquad \lambda = D_{AB}x/a\, L^3 \;, \tag{3-15}$$

the convective transport equation reduces to,

$$\eta \frac{\partial C}{\partial \lambda} = \frac{\partial^2 C}{\partial \eta^2} \quad . \tag{3-16}$$

Equation (3-16) may converted to an ordinary differential equation by the following transformation

$$X = \eta/(9\lambda)^{1/3} \quad . \tag{3-17}$$

In these new coordinates the boundary conditions are

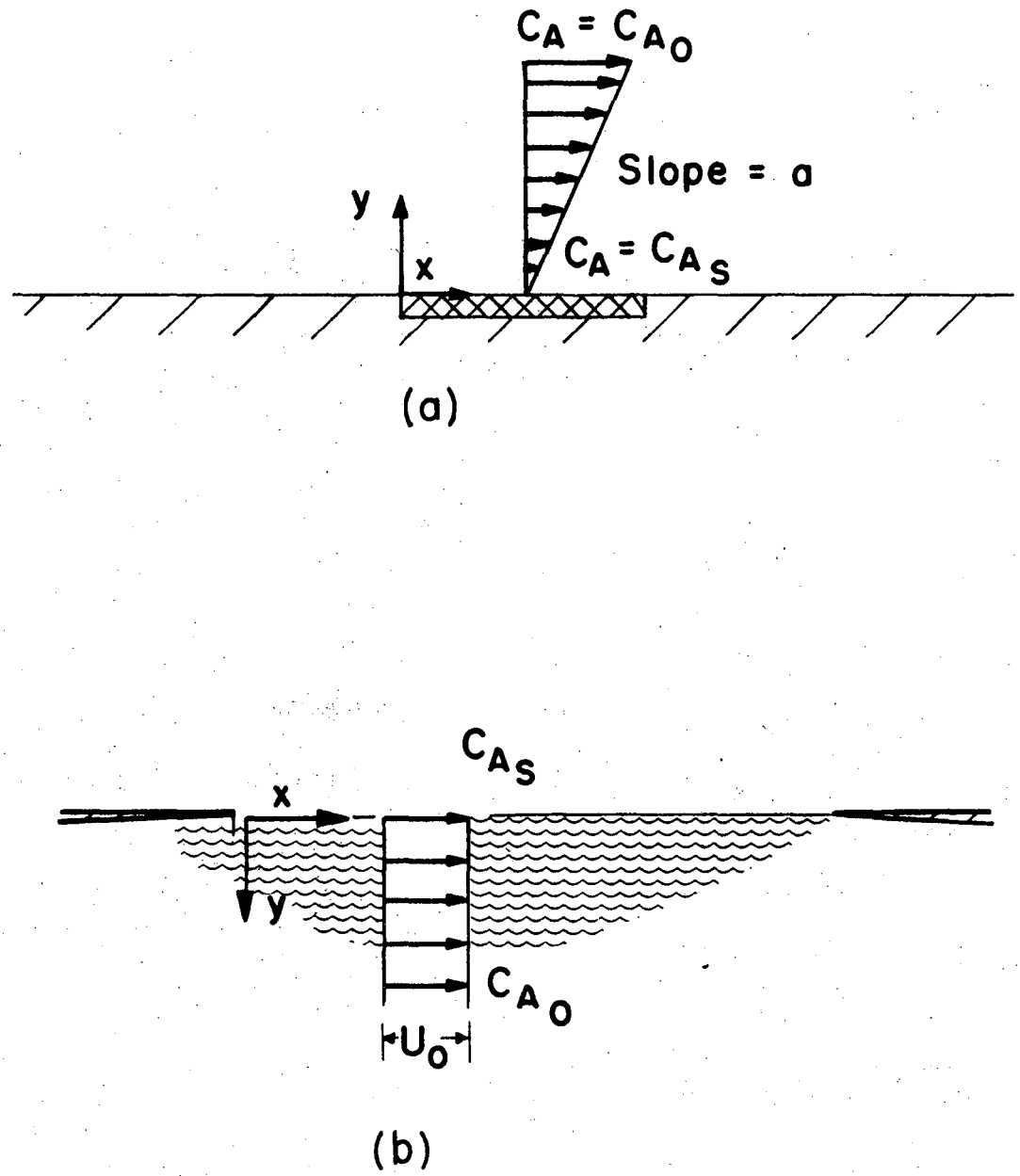

MUB-11334

Fig. 7. Simple mass transfer models; (a) the Leveque model, (b) the penetration model.

$$C = 1 \quad \text{at } x = 0$$
$$C = 0 \quad \text{at } x = \infty \tag{3-18}$$

The solution is

$$C = \frac{3}{\Gamma(1/3)} \int_x^\infty x e^{-x^3} dx \quad . \tag{3-19}$$

The mass-transfer coefficient is given as

$$k_C = \frac{D \partial C}{\partial y} = 0.538 \ (D^2 a/x)^{1/3} \quad . \tag{3-20}$$

In Eq. (3-20) the concentration, C, is the dimensionless quantity given in Eq. (3-15) which defines the driving force for mass transfer as the initial difference in concentration, $C_{As} - C_{AO}$. In order to maintain a uniformity of approach, all the cases considered in this study are based upon the assumption of an initial concentration difference as the driving force. This solution is almost always applicable in the case of mass transfer to liquids with extremely low diffusion coefficients. In the present study the solution is applicable when a gas is flowing in the channel at a high velocity.

3. <u>The Penetration Model</u>

If, instead of considering mass transfer to a fixed wall, we turn our attention to the case of a free interface, the situation shown in Fig. 7b is applicable. This case is the familiar Higbie penetration model.[30] The convective-transport equation for this model is

$$U_0 \frac{\partial C_A}{\partial x} = D_{AB} \frac{\partial^2 C_A}{\partial y^2} \quad . \tag{3-21}$$

Now if we again let $C = \dfrac{C_A - C_{A_0}}{C_{As} - C_{AO}}$ and $Y = y \ U_0/(4D_{AB}x)^{1/2}$

then Eq. (3-21) becomes an ordinary differential equation:

$$\frac{d^2C}{dy^2} + 2y\,\frac{dC}{dy} = 0. \tag{3-22}$$

Transforming the boundary conditions we get

$$C = 1 \quad \text{at} \quad y = 0$$
$$C = 0 \quad \text{at} \quad y = \infty \quad .$$

The solution to this equation is

$$C = 1 - \mathrm{erf}\left[y\,\frac{U_0}{4D_{AB}x}\right]^{1/2} \tag{3-23}$$

and

$$k_1 = \left[\frac{D_{AB}U_0}{\pi x}\right]^{1/2} \quad . \tag{3-24}$$

The penetration model has proved to be quite accurate for a free laminar liquid interface. Its prediction of a one-half-power dependence on diffusivity can be extended to many important industrial situations. For example, Vivian and King have shown that it is apparently applicable to the very complex flow of the liquid phase of a packed column.[71]

Several simple models have been omitted from this section, not because they are not important but merely because they do not bear directly upon our problem. Such models as the film and the boundary-layer flow models as well as those for common turbulent flow are discussed in standard texts in the field.[4,65]

B. Mass-Transfer Models with Tangential Interfacial Motion

When a flowing gas is exposed to a liquid that is concurrent with it the mere fact that the interface is in motion enhances mass transfer between phases. In the past many studies have been carried out with wetted-wall columns in which the mass transfer was controlled by the gas phase. In laminar flow it has commonly been assumed that the Graetz solution, or in the case of short columns the Leveque solution, describes the situation. That the interface is in motion is entirely neglected. Another approach is to subtract the interfacial velocity from the velocity of the gas flow. The remaining

velocity is solved for in the usual manner. The degree to which each of these methods is in error is of considerable interest.

A gas-liquid mass-transfer model, in which there is an interfacial velocity due to the motion of the liquid, may be built upon the addition-of-resistances principle if good models are known for both phases. The penetration model has been shown to be a good model for a liquid phase; however, for the gas phase an appropriate model for a parabolic profile with interfacial motion has not been proposed. The model corresponding to the Leveque solution with an interfacial velocity has been solved by Beek and Bakker.[2] This solution is investigated and modified in the present study. Concentration profiles are also calculated for this model.

1. <u>The Solution of the Modified Graetz Problem</u>

The modification in the velocity profile. Fig. 8 shows the problem that is the subject of discussion for the remainder of this section. There is one moving wall which has a velocity U_0 and a concentration C_{a_s}. The other wall is stationary and has zero flux. If the average incoming gas velocity is U_m, then the velocity profile may be expressed as

$$U = U_0 + (6U_m - 4U_0)\, y/b + (3U_0 - 6U_m)(y/b)^2 \quad . \tag{3-25}$$

The equation of convective transport is

$$U \frac{\partial C_A}{\partial x} = D_{AB} \frac{\partial^2 C_A}{\partial y^2} \quad . \tag{3-26}$$

If we let:

$$C = \frac{C_A - C_{A_0}}{C_{A_s} - C_{A_0}} \qquad \psi = \frac{D_{AB} L}{U_0 b^2} \qquad Y = y/b$$
$$X = x/L \qquad U = U_m/U_0 \quad , \tag{3-27}$$

then we have

$$1 + (6U-4)Y + (3-6U)Y^2 \; \frac{\partial C}{\partial X} = \psi \frac{\partial^2 C}{\partial Y^2} \; , \tag{3-28}$$

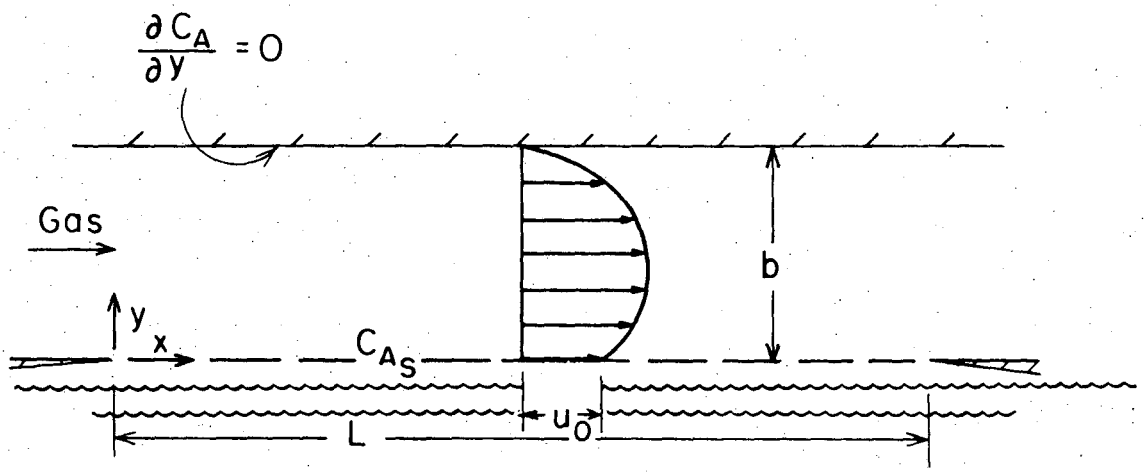

MUB-10903

Fig. 8. Mass transfer to a fluid in laminar flow between two parallel walls, one of which is in cocurrent motion.

with the boundary conditions

$$C = 0 \quad \text{at} \quad X = 0$$

$$C = 1 \quad \text{at} \quad Y = 0$$

and

$$\frac{\partial C}{\partial y} = 0 \quad \text{at} \quad Y = 1 \quad . \tag{3-29}$$

This problem may be solved directly in the same way the Graetz problem was handled. Unfortunately there is the added parameter, U, in this equation with which we must deal. It would be necessary to generate constants for each different case of U, the ratio of the average velocity to the interfacial velocity which was encountered. With the computer this is not a particularly difficult task. The real problem is in tabulating all of the constants and later in putting them to use. Many terms would have to be generated if the solution were to be valid near the entry region. On the other hand we may choose to solve the equation numerically as it stands and thus generate the concentration profiles and Nusselt numbers in a graphical manner. It is this latter course which was chosen to carry out the solutions.

Since Eq. (3-28) is a parabolic partial differential equation, a marching solution may be used. One solves one entire row of concentrations in the direction perpendicular to the motion before moving on to the next step in the direction of fluid motion. As a result the x-direction calculation may be carried out for as many steps as one desires. The Crank-Nicholson six-point implicit formula was used in the solution of the partical differential equation.[43a] The boundary condition at the initial line, x = 0. allows us to start the marching solution. The first problem encountered was with the interface condition at the point of first exposure. The infinite gradient at that point tends to make the solution unstable at the start. This instability tends to persist for several lines downstream. If, on the other hand, we used the Laasonen four-point formula to solve for this area of the problem, the point would be ignored. It was found that this approach was effective in removing the instability.

Another problem that arises in solving these equations is a result of the zero-flux condition at the wall where there is also a zero-velocity condition. When this condition is put into finite-difference form, the final line is no longer diagonally dominant (that is, the sum of the off-diagonal terms is equal to or greater than minus the diagonal term). The solutions for the matrix are not stable unless diagonal dominance is satisfied. A new approach was tried, which involved making a material balance upon the half element nearest the wall. This new approach gives a diagonal dominance to the entire matrix and proved to give satisfactory results.

The tridiagonal matrix that resulted from this analysis was solved directly by the Thomas method.[43b] However, because of truncation and round-off error it was necessary to seek more accuracy. Hence a Gauss-Seidell iterative analysis[43c] with an overrelaxation factor of 1.25 was used to cut down the error. No more than two iterations per row were needed to give four-decimal reproducibility of all points on a concentration profile.

Once the concentration profile was available, the fluxes could be calculated. A five-point formula was used in calculating the interfacial mass-transfer fluxes. The method used to nondimensionalize the solution leads to a direct calculation of the local Nusselt number based upon the initial difference in concentration. The five-point formula is

$$Nu_x = k_c b/D = (19\ C_1 - 30\ C_2 + 18\ C_3 - 10\ C_4 + 3\ C_5)/(12H)\ . \quad (3\text{-}30)$$

The interfacial concentration is C_1; the remaining concentrations have interesting subscripts with increasing distance from the interface. The dimensionless increment is denoted by H. The cup-mixing concentration was also calculated. Here the concentration profile was integrated by means of Simpson's rule. These two calculations are quite accurate at points away from the beginning of the exposure. Near the beginning of the exposure, local Nusselt numbers tend to be slightly inaccurate because of the steep gradients. This inaccuracy almost completely disappears after the first few steps downstream.

The Fortran source program for this solution is included in Appendix D, along with an explanation of how to use it. Even though all the output was printed, it was decided that the "Calcomp" plotter would be used as the means of presentation of the data. Concentration profiles, the cup-mixing concentration as a function of the modified Graetz number ($DL/U_m b^2$), and a log-log representation of the Nusselt number as a function of the Graetz number were plotted for the velocity ratio (U_m/U_0) equal to 10, 4, 2, 1, 2/3, and 1/2. The concentration profiles are included with the program in Appendix D. Figures 9 and 10 are the cup-mixing-concentration and the Nusselt number graphs. Figure 9 shows the overall effect of increasing interfacial velocity. The amount of mass transfer increases considerably with increasing motion of the interface in the direction of the fluid motion.

Of particular interest is the case where the average velocity is two-thirds of the interfacial velocity. This is the case of mass transfer to the free surface of a fluid which is flowing down a plane, with zero shear stress upon the interface. The most practical example of this is the wetted-wall column. It is common to use the penetration model to predict the mass-transfer coefficient and the concentration profile. Figure 11 shows a comparison of concentration profiles predicted by the penetration model (the dotted line) and the present solution (the solid line). It is evident that above a Graetz number of 0.04 (cup-mixing concentration of 40% of saturation) the penetration model is no longer valid. Pigford carried out an eigenvalue solution of this problem.[54] It is compared with the present solution on a log-log plot of cup-mixing concentration against the reciprocal of Graetz number in Fig. 12. The Pigford solution (dotted line) is only valid down to concentrations of about 15% of saturation.

2. Gas-Phase Mass Transfer Near a Moving Interface

The problem of mass transfer near a moving interface may be simplified in the same way Leveque was able to approximate the Graetz solution. In the case shown in Fig. 13, a medium of infinte extent with a linear slope in velocity, a, is exposed to a fluid of different constant concentration, C_{a_s}, which is moving with an interfacial velocity, Uo. The initial concentration of the upper phase is C_{a_o}. Beek and Bakker[2] have solved the equations in the following way:

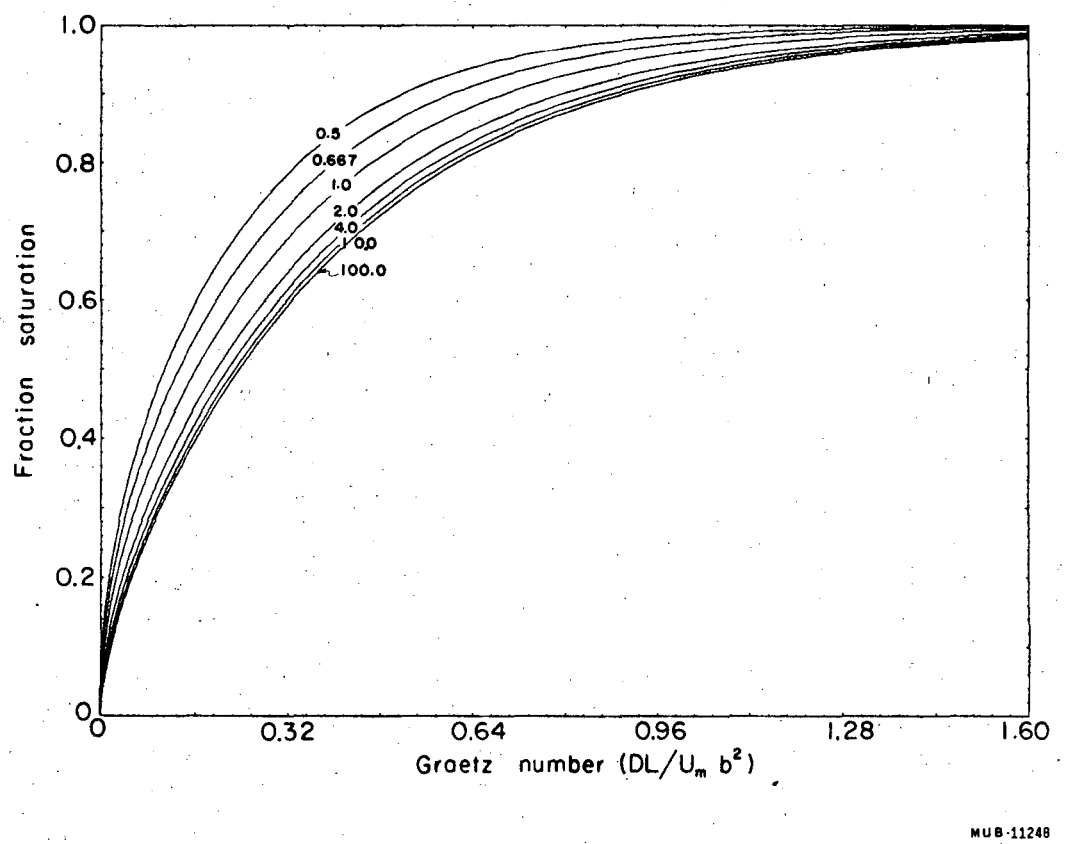

Fig. 9. Mean Fraction Saturation as a Function of the Graetz Number.

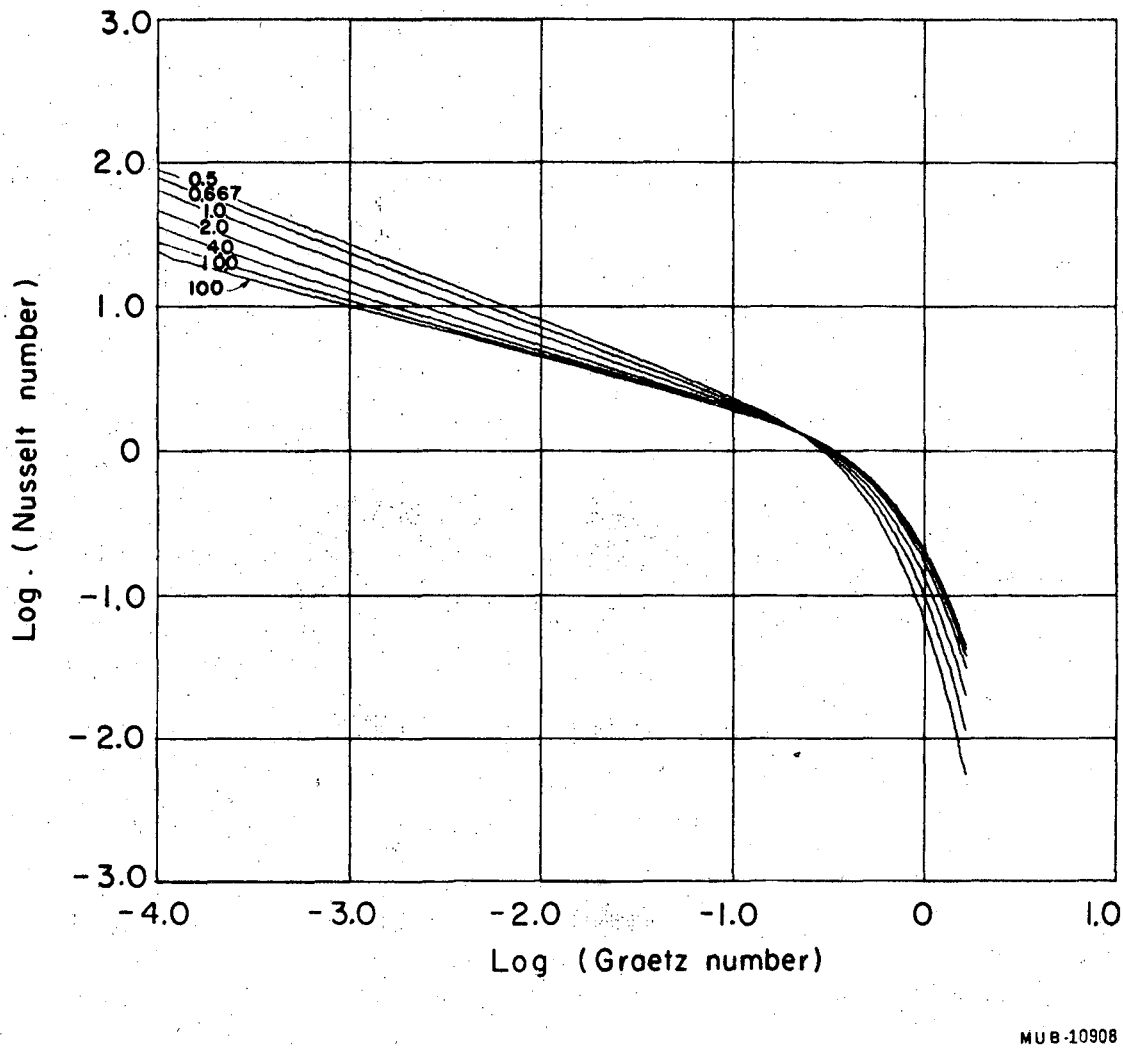

Fig. 10. A logarithmic representation of the local Nusselt number as a function of the Graetz number for different values of the parameter U_m/U_o.

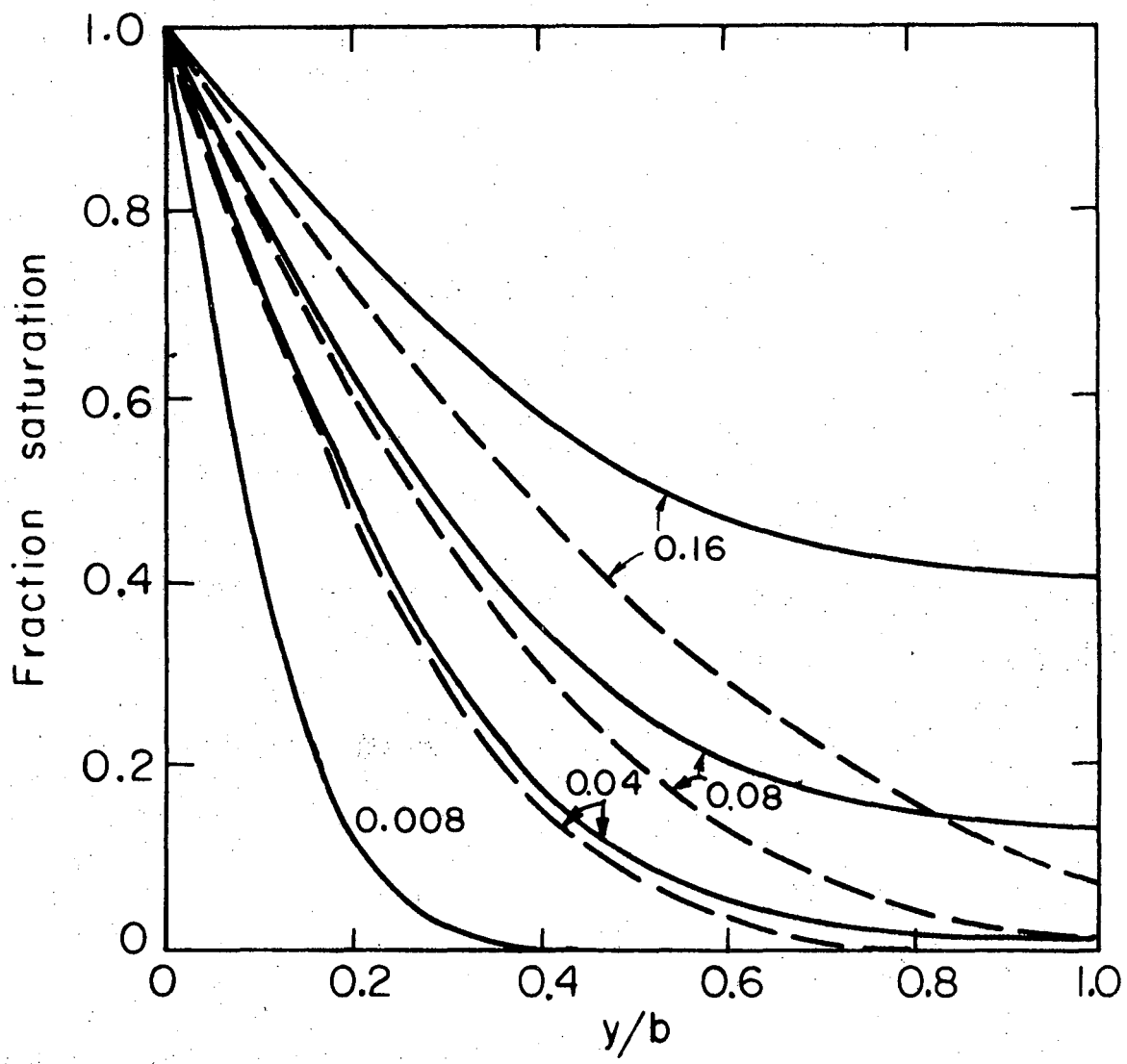

MUB-10909

Fig. 11. A comparison of concentration profiles for different Graetz numbers in a falling film. —— The exact solution. --- The penetration model.

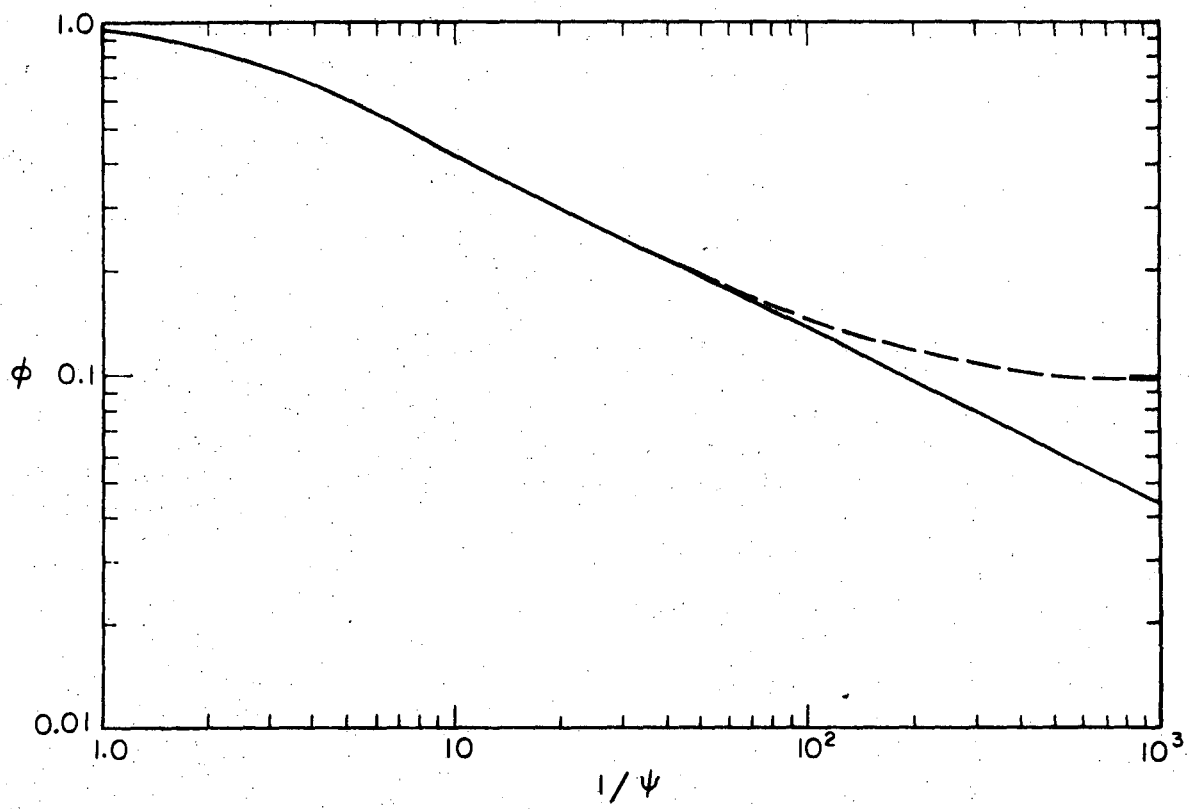

MUB-10905

Fig. 12. A comparison of solutions for cup-mixing concentration in a falling film as a function of Graetz number. —— The present solution. --- Pigford's solution (Ref. 54).

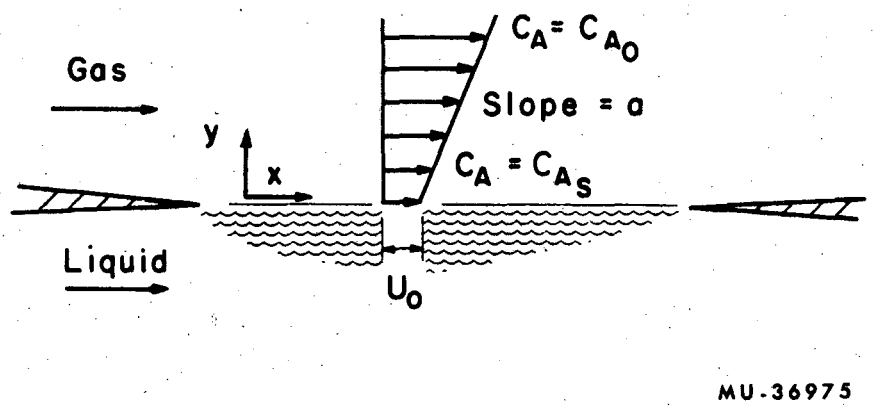

Fig. 13. The Beek and Bakker Model for Mass Transfer to an Infinite Medium with an Interfacial Velocity.

The convective mass transfer equation for this case is

$$(U_0 + ay)\frac{\partial C_a}{\partial x} = D_{AB}\frac{\partial^2 C_a}{\partial y^2} \tag{3-31}$$

with the boundary conditions

$$C_A = C_{A_0} \quad \text{at} \quad x = 0$$

$$C_A = C_{A_S} \quad \text{at} \quad y = 0 \tag{3-31a}$$

and

$$C_A = C_{A_0} \quad \text{at} \quad y = \infty \quad .$$

For $\eta = ay/U_0$ and $\xi = a^2Dx/U_0^3$

we have $$(1-\eta)\frac{\partial C_A}{\partial \xi} = \frac{\partial^2 C_A}{\partial \eta^2} \quad . \tag{3-32}$$

The problem is solved by means of the Laplace transformation (ξ is transformed to p). After all the boundary conditions are satisfied, the solution in the Laplace domain for concentration is

$$\bar{C} = \frac{(1+\eta)^{1/2}}{p}\,\frac{K_{1/3}\left[2/3\ p^{1/2}(1+\eta)^{3/2}\right]}{K_{1/3}\left[2/3\ p^{1/2}\right]} \tag{3-33}$$

No general solution for the concentration profile was presented because of the complexity of the equation. However, it is possible to solve for the mass-transfer coefficient:

$$-\frac{d\bar{c}}{d\eta}\Big|_0 = \frac{K_{2/3}(2/3\ p^{1/2})}{p^{1/2}\ K_{1/3}(2/3\ p^{1/2})} \quad . \tag{3-34}$$

This equation may then be inverted to obtain the asymptotes for both long and short exposures. The solution for short exposures ($a^2Dx/U_0^3 \ll 1$) is

$$k\left(\frac{x}{U_0 D}\right)^{1/2} = \frac{1}{\sqrt{\pi}} + \frac{1}{4}\left(\frac{a^2Dx}{U_0^3}\right)^{1/2} \quad , \tag{3-35}$$

while for long exposures ($a^2Dx/U_0^3 \gg 1$) the solution is

$$k\left(\frac{x}{U_0D}\right)^{1/2} = 0.538\left(\frac{a^2Dx}{U_0^3}\right)^{1/2}\left[1+0.375\left(\frac{U_0^3}{a^2Dx}\right)^{1/3}\right] . \qquad (3\text{-}36)$$

This solution is shown in graphical form in Fig. 14. The limits of the model are of some interest. As the group a^2Dx/U_0^3 approaches zero we would expect the solution to approach the penetration model. Since for the penetration model $k(x/U_0D)^{1/2}$ is a constant equal to $(\pi)^{-1/2}$, it is represented in Fig. 14 as a horizontal straight line. On the other hand for high values of a^2Dx/U_0^3 the Leveque model becomes more accurate. If we multiply both sides of the Leveque solution (Eq.(3-20)) by $(x/U_0D)^{1/2}$, the result becomes

$$k\left(\frac{x}{U_0D}\right)^{1/2} = 0.538\left(\frac{a^2Dx}{U_0^3}\right)^{1/6} . \qquad (3\text{-}37)$$

The Leveque solution is also shown as a dotted line. It approaches the solution for a moving interface when a^2Dx/U_0^3 exceeds 100.

Since the above solutions are not valid in the region of a^2Dx/U_0^3 near unity, Beek and Bakker extended both asymptotes to an abscissa of one, and the solution was assumed to be an interpolation between them. In justifying this they say "We made some calculations to find the right interpolation between the two given relationships in the neighborhood of $\xi = 1.0$". They conclude that their interpolation is valid to within 10%. Since this section of the curve is where the greatest difference from the limiting models occurs, some further investigation of the interpolation seems in order.

If the asymptotic solution for high values of ξ is calculated for values of ξ below unity, it reaches a minimum. It crosses the low values of ξ at about 0.2. It must be understood that the asymptote for high ξ values is not valid in the region in question, but the fact that the two solutions cross leaves grave doubts about the validity of an interpolation between them in this region. This question led to a search for a true solution in this region.

Since the computer program for a parabolic profile was available, it was modified for use with an infinite medium. The velocity profile was modified to make it linear. This program appears in Appendix D under the title "Bakker".

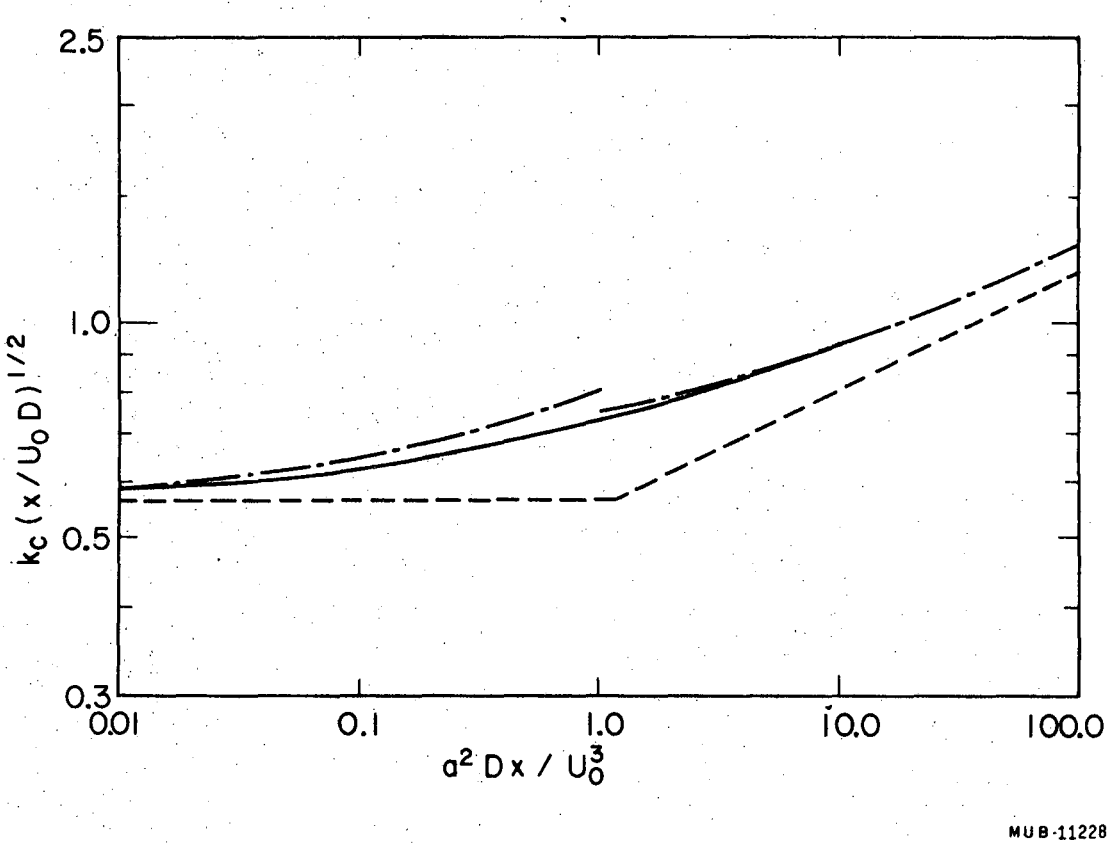

Fig. 14. The Solution of The Beek and Bakker Problem.
Legend: ——— Exact solution to the problem including computer solution. ---- limiting models - —— - asymptotic solutions.

Figure 15 is a plot of concentration profiles for this solution. Where there appears to be penetration to the wall, the profiles are not valid. The solid line in the region of Fig. 14 is the computer solution to this problem. Note that it meshes with the two asymptotic solutions. It does, however, fall below the two lines in the central region, proving that interpolation is not a proper procedure in this case. With a correct solution in the region of interest, it is possible to find overall mass-transfer coefficients.

3. Mass Transfer to Countercurrent Flow

In all previous cases, cocurrent flow was assumed. However countercurrent flow is of much more importance industrially. It is normal practice to assume that the mass-transfer coefficient for countercurrent operation is the same as that for cocurrent flow, and that there is an increased driving force. The question of the effect of interfacial velocity upon mass-transfer coefficients again casts some doubt upon this procedure.

A typical velocity profile for counterflow confined by two walls is shown in Fig. 16. The interfacial velocity, which is opposed to the main flow, causes a flow reversal in the less viscous upper medium. Since only molecular diffusion may take place at that point, it would be expected that the mass-transfer coefficient would be substantially less that would be predicted by the corresponding cocurrent theory.

The fact that there is a flow reversal makes an exact solution to this problem much more difficult. The problem lies in the fact that the part of the gas which flows in the same direction as the liquid enters the test section at the downstream end of the exposure with a definite but unknown concentration. Any numerical solution of this problem would necessarily be iterative. Since this involves major changes in the existing solutions, the idea of carrying out such a solution was abandoned.

A simpler approximation can be made in this case. Since the backflow enters at a concentration close to equilibration, it is assumed that, as a limiting case, the area between the interface and the flow reversal is a stagnant film. The Graetz model is assumed to hold in the remainder of the channel. If it is assumed that the resistances to mass transfer may be added, the result is

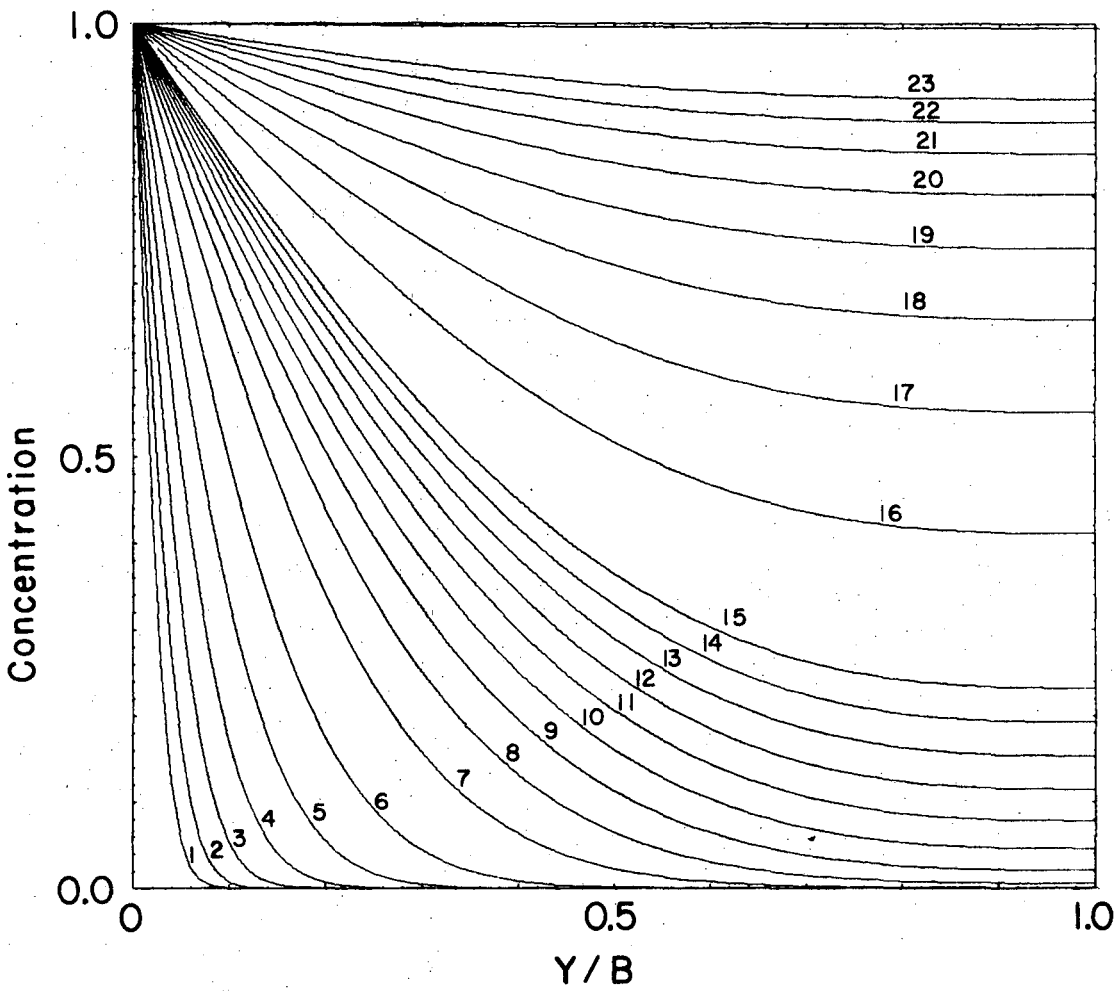

MUB-11250

Fig. 15. Concentration Profiles for the Beek and Bakker Problem. Profiles given for different values of the Parameter, $a^2 D\, x/U_0^{\,2}$.

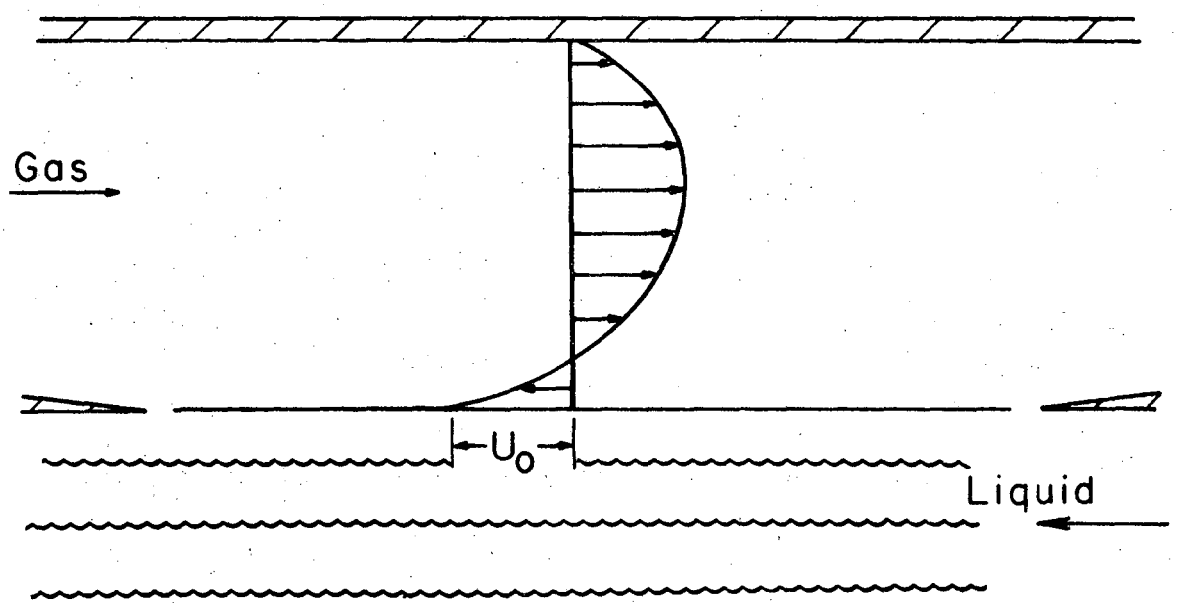

MUB-10907

Fig. 16. The countercurrent flow of a gas and a liquid showing a typical velocity profile.

$$\frac{1}{K_{c_{avg}}} = \frac{1}{k_{Gz_{avg}}} + \frac{1}{k_{F_{avg}}} \tag{3-38}$$

where

$$k_{F_{avg}} = D_{AB}/\Delta \tag{3-39}$$

and

$$k_{gz_{avg}} = f\left(\frac{DL}{U_m(b-\Delta)^2}\right) \tag{3-40}$$

The variable, Δ, is the distance between the interface and the flow reversal. The point of flow reversal may easily be found from Eq.(A-14). The velocity used in the Graetz portion of the solution is the average velocity of the inlet gas plus the average velocity of the backflow. The driving force is based upon the inlet concentration difference. The proposed film model will give a conservative estimate of the amount of mass transfer which we may expect. It is, however, fairly safe to predict that the mass-transfer coefficient will decrease rather than increase with increasing interfacial velocity.

C. Experimental Results

1. The Liquid Phase

The hydrodynamics of the liquid phase of the channel used in this study are similar in many respects to those of the channel used by Tang and Himmelblau.[67] In their study they found that the rate of absorption of carbon dioxide into water in two-phase flow in a 1- by 6-in. channel obeys the penetration theory to better than 7%. The diffusivity used for their analysis was approximately 5% lower than the value found by most other workers (1.85×10^{-5} cm^2/sec vs 1.95×10^{-5} cm^2/sec). For complete liquid-phase control of the mass transfer, one would expect, on the basis of all the available experiments, that the penetration model would be applicable. In order to ascertain the effect of the parabolic velocity profile upon mass transfer in the liquid phase, Tang solved the appropriate transport equation by a separation-of-variables method. The small depth of penetration of the mass transfer precluded any visible change in the solution from the penetration solution. This is especially true when one considers that the experimental error in the study was appreciable and that

one must attain a concentration of 40% saturation before there is a substantial difference between the two solutions.

There has been no previous experimental study of gas-phase-controlled mass transfer in the presence of a moving interface in a channel. Therefore, before interphase studies were undertaken, an experimental program was performed which filled this gap.

2. The Graetz Runs

The first series of runs was used as a check on the hydrodynamics of the gas phase. The channel was filled with pure liquid (industrial grade, 100% ethanol) and this stagnant phase was exposed to a series of flow rates of pure nitrogen. The liquid level was maintained by adding liquid between runs. A series of nine runs was performed in this fashion. In this series as in all the succeeding series, the velocities were calculated from the measured flow rate by means of the hydrodynamic equations developed in Appendix A. Butler and Plewes have solved for this situation.[6]

The temperature of the interface was a cause for some concern, since evaporation from the interface tends to have a cooling effect. Temperature profiles were taken at the channel exit, and the temperature at the interface was deduced from this profile by extrapolation. Since this temperature was always within 3°C of the temperature of the bulk gas, the interface temperature could be used as the temperature of the system without making a significant error in gas-phase properties. The interfacial velocity caused by drag on the liquid by the gas may be shown to be small and is neglected in this study.

The mean fraction saturation of the effluent gas stream was measured, and the data were reduced to 25°C using the properties tabulated in Appendix E. These data are listed in Table C-1 in Appendix C and are accompanied by a set of sample calculations. Theory and experiment are compared in Fig. 17. In this plot of mean fractional saturation (ϕ) as a function of Graetz number ($DL/U_m b^2$), the solution of Butler and Plewes is represented by a solid line, while the experimental data are shown as circular points. The agreement with theory was better than 5%, which is well within the limits of the estimated experimental error. Concentration profiles were taken for Runs 9 and 10. The experimental results are tabulated in Table C-2. The actual profiles and the

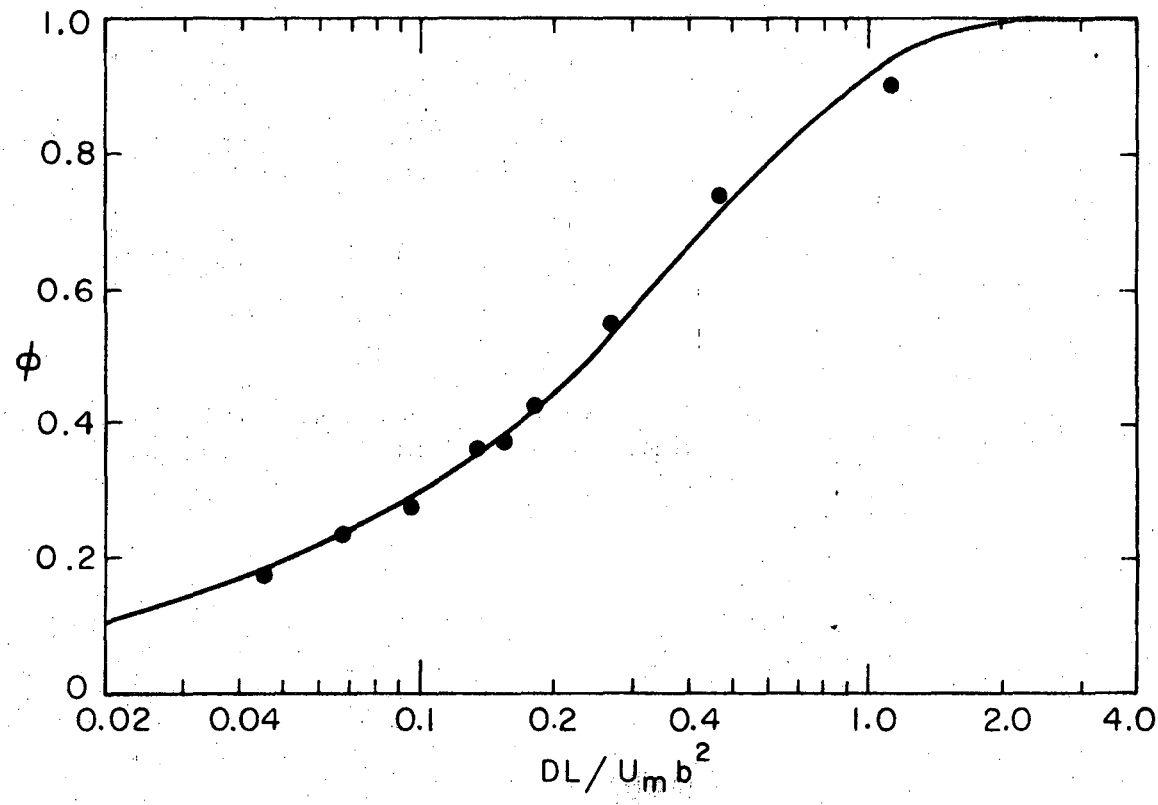

MUB-10915

Fig. 17. A comparison of runs with zero interfacial velocity with the solution of Butler and Plewes (Ref. 6). ●●● Data. —— Theory.

theoretically calculated values are compared in Figs. 18 and 19. Here the agreement is better than 7 mole percent, with no readily discernible trend in this error.

3. Cocurrent Mass Transfer with Resistance in a Single Phase

The next step was to put the liquid phase in motion. Again ethanol was used as the pure liquid while two gases, oxygen and carbon dioxide, were used as the other phase. The experiments were performed at 25°C ± 3°C, and therefore most properties were estimated at 25°C. The one exception is the vapor pressure of the ethanol, which was estimated at the interfacial temperature. Because of the rather low vapor pressure of ethanol (57 mm Hg at 25°C) and the substantial flow rates of the liquid, the possibility of an important secondary flow of a cellular nature is very remote. Under the most extreme conditions (the highest gas flow rate and the lowest liquid flow rate), the maximum possible temperature drop at the interface is 1.85°C. Only a few runs were made under these conditions. The majority of the runs were performed under conditions where temperatures at the interface differed from the bulk-phase temperatures by less than 1°C. The former case corresponds to an increase in density at the interface of roughly 0.004 gm/cc. Since the interface was cooled and the evaporating vapors were denser than the gas phase, there was no possibility of natural convection in the gas phase.

Since it was quite difficult to vary the liquid rate and maintain a constant level in the channel, the liquid rate was set, and then a series of runs was carried out with different gas rates. For each gas, three different liquid rates were used. The range of U_m/U_0 covered was from 0.5 to 12.0. Interfacial velocities were calculated from the liquid and gas flow rates by means of the hydrodynamic equations discussed in Appendix A. These ranged from 2.5 to 10.0 cm/sec. Concentration profiles were carried out on one run at each liquid rate. In all, 70 runs were carried out, three of them with concentration profiles. Since the accuracy of the runs with both gases is about equivalent, it was decided to present only the carbon dioxide data. All the data for both gases are presented in Appendix C.

The overall-mass-transfer data for carbon dioxide are shown in Figs. 20, 21, and 22. The mean fraction saturation is shown as a function of Graetz

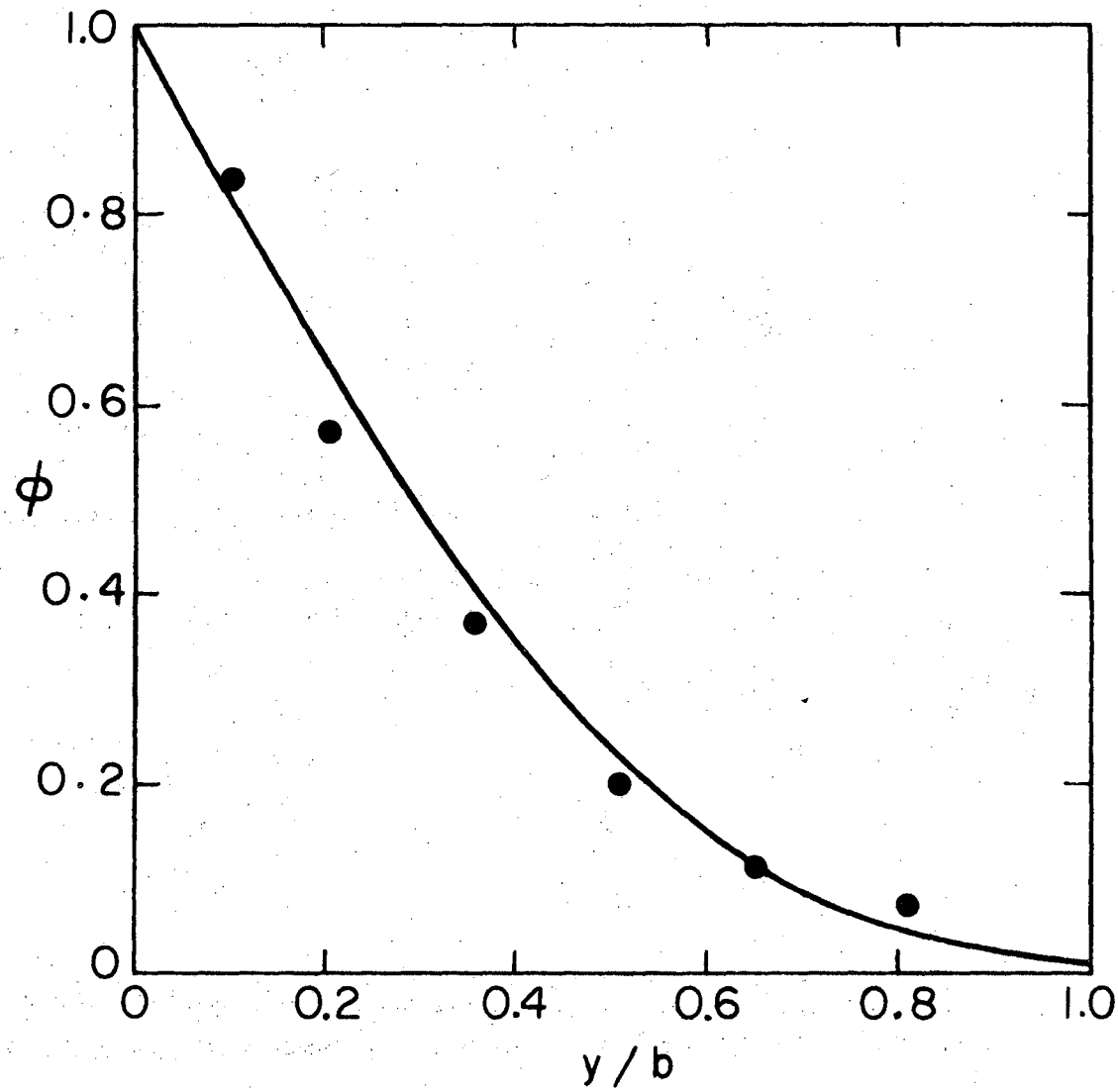

Fig. 18. Concentration profile for run 9. ●●● Data. —— Theory.

MUB-10918

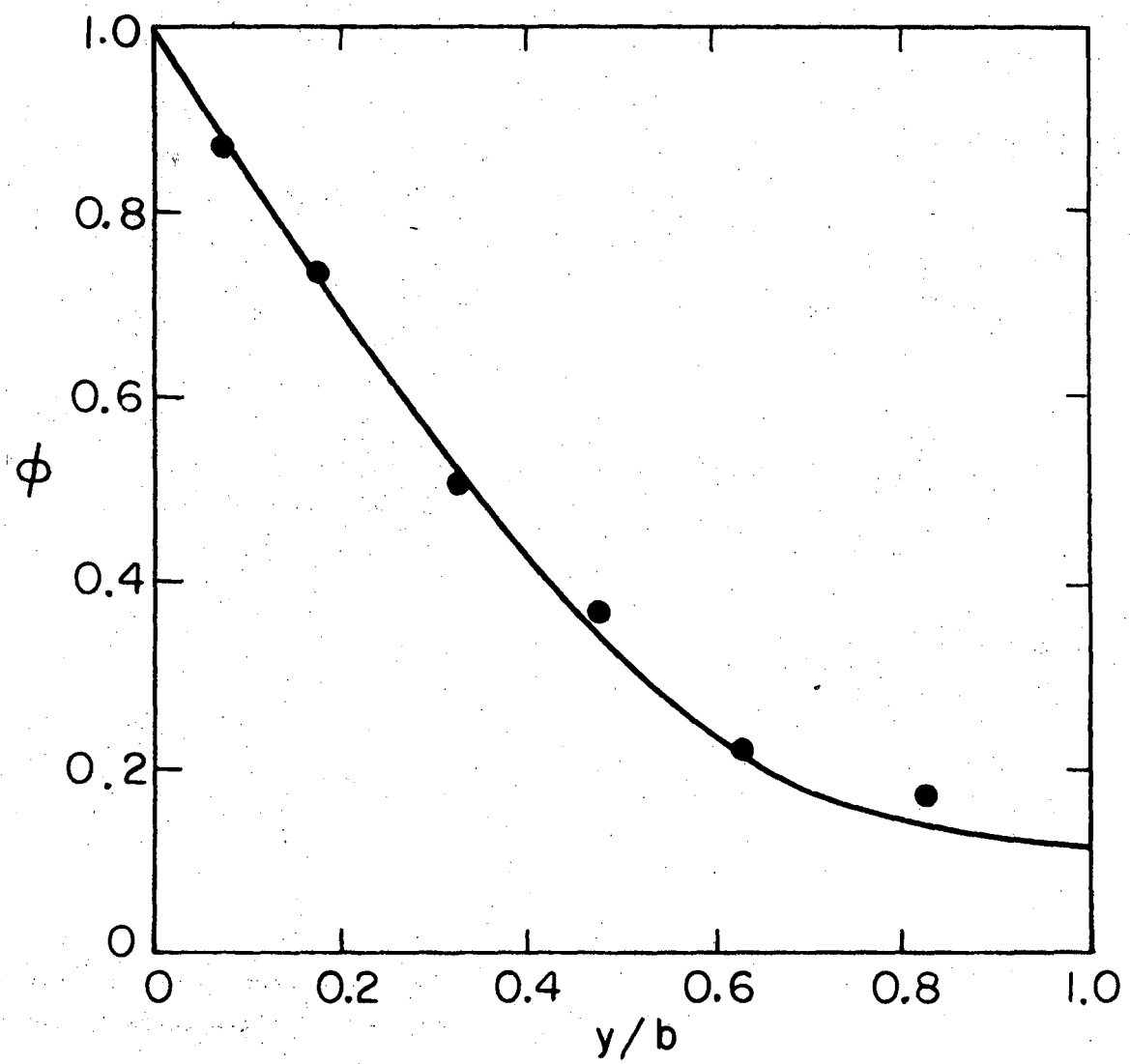

Fig. 19. Concentration profile for run 10. ●●● Data. —— Theory.

MUB-10919

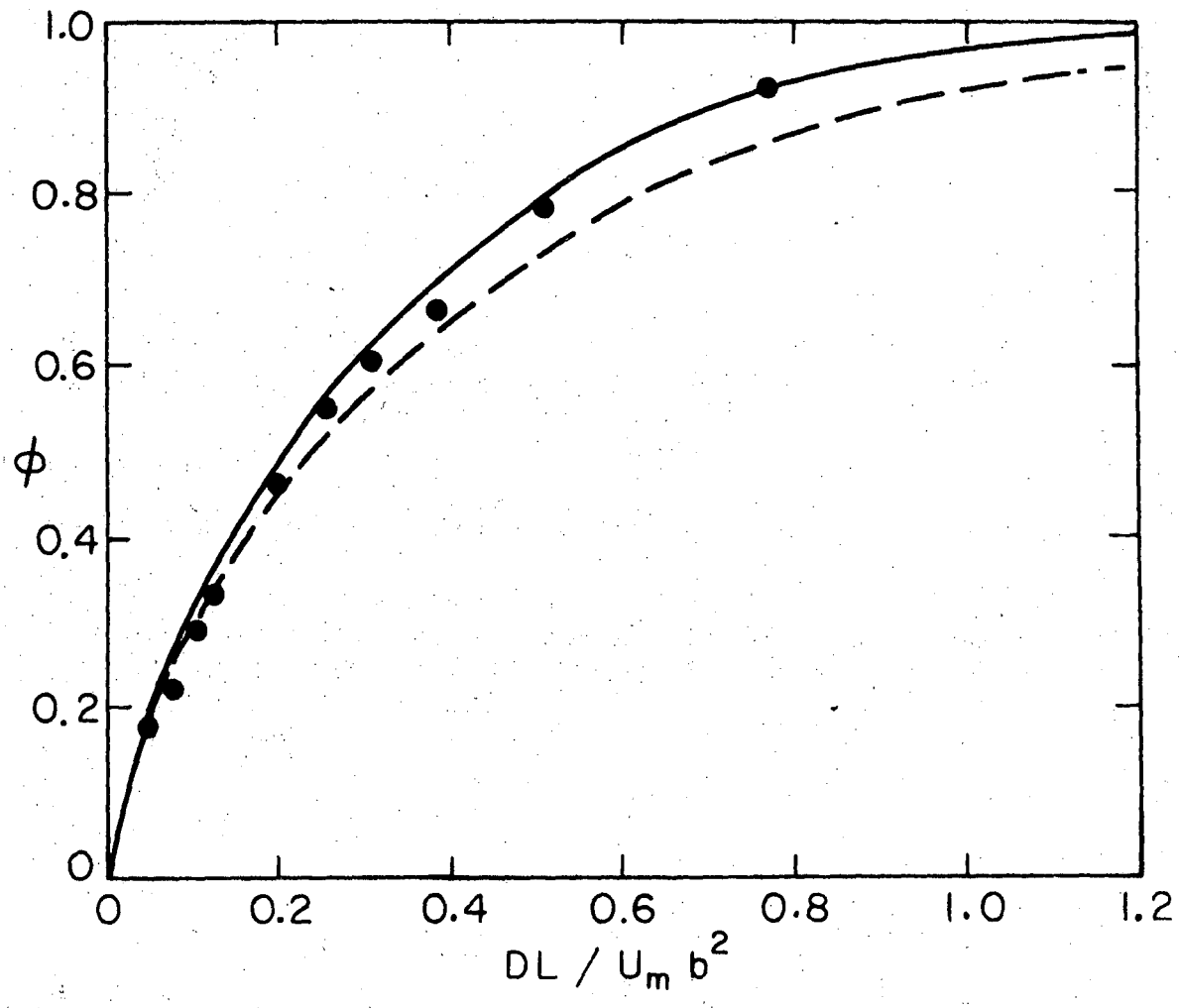

MUB-10914

Fig. 20. Mean fraction saturation as a function of Graetz number for cocurrent motion of CO_2 and ethanol (18.0 cc/sec); ●●● Data. --- Theory for zero interfacial velocity. —— Computer solution for experimental conditions.

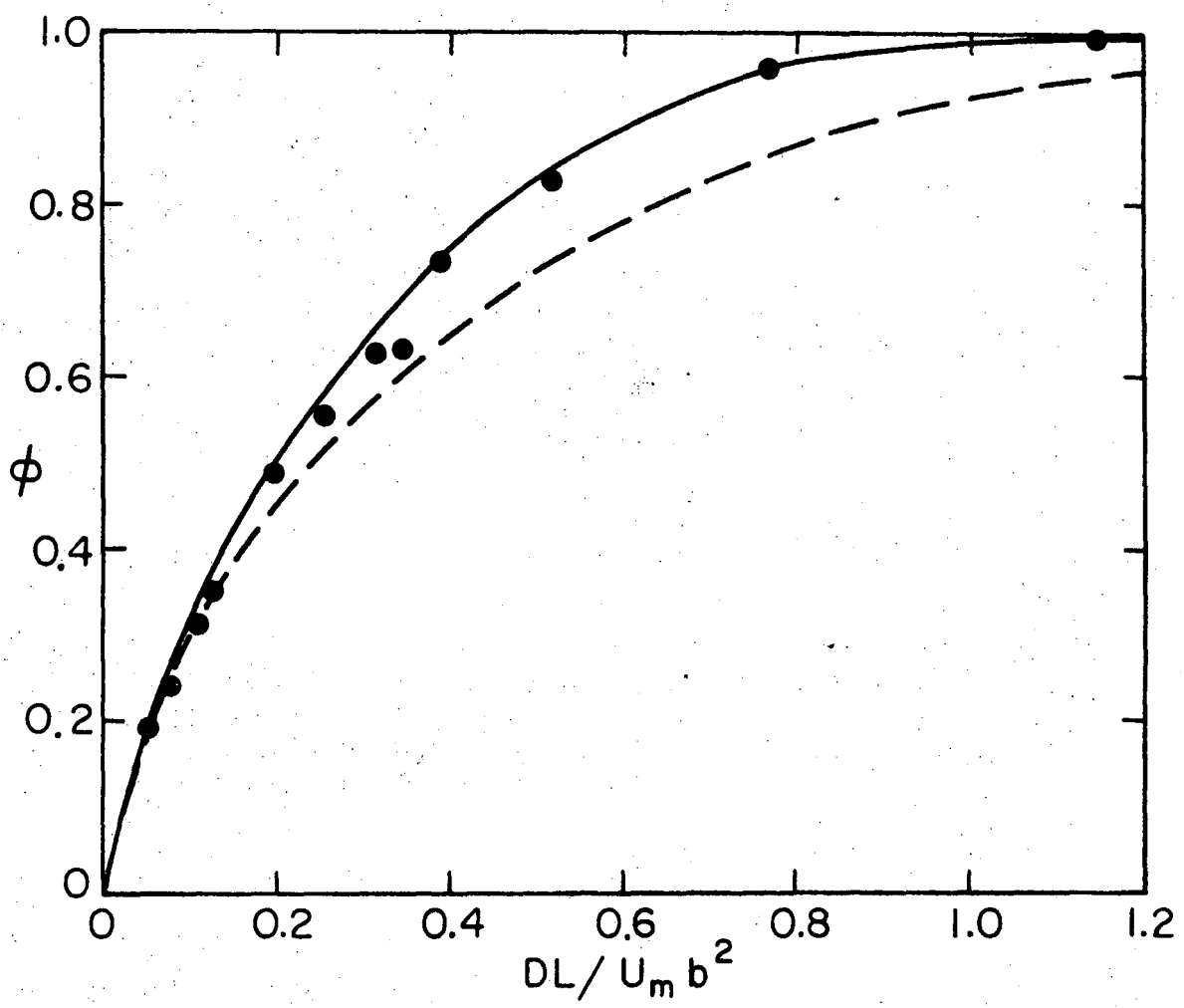

MUB-10913

Fig. 21. Mean fraction saturation as a function of Graetz number for cocurrent motion of CO_2 and ethanol (30.0 cc/sec); ●●● Data. --- Theory for zero interfacial velocity. —— Computer solution for experimental conditions.

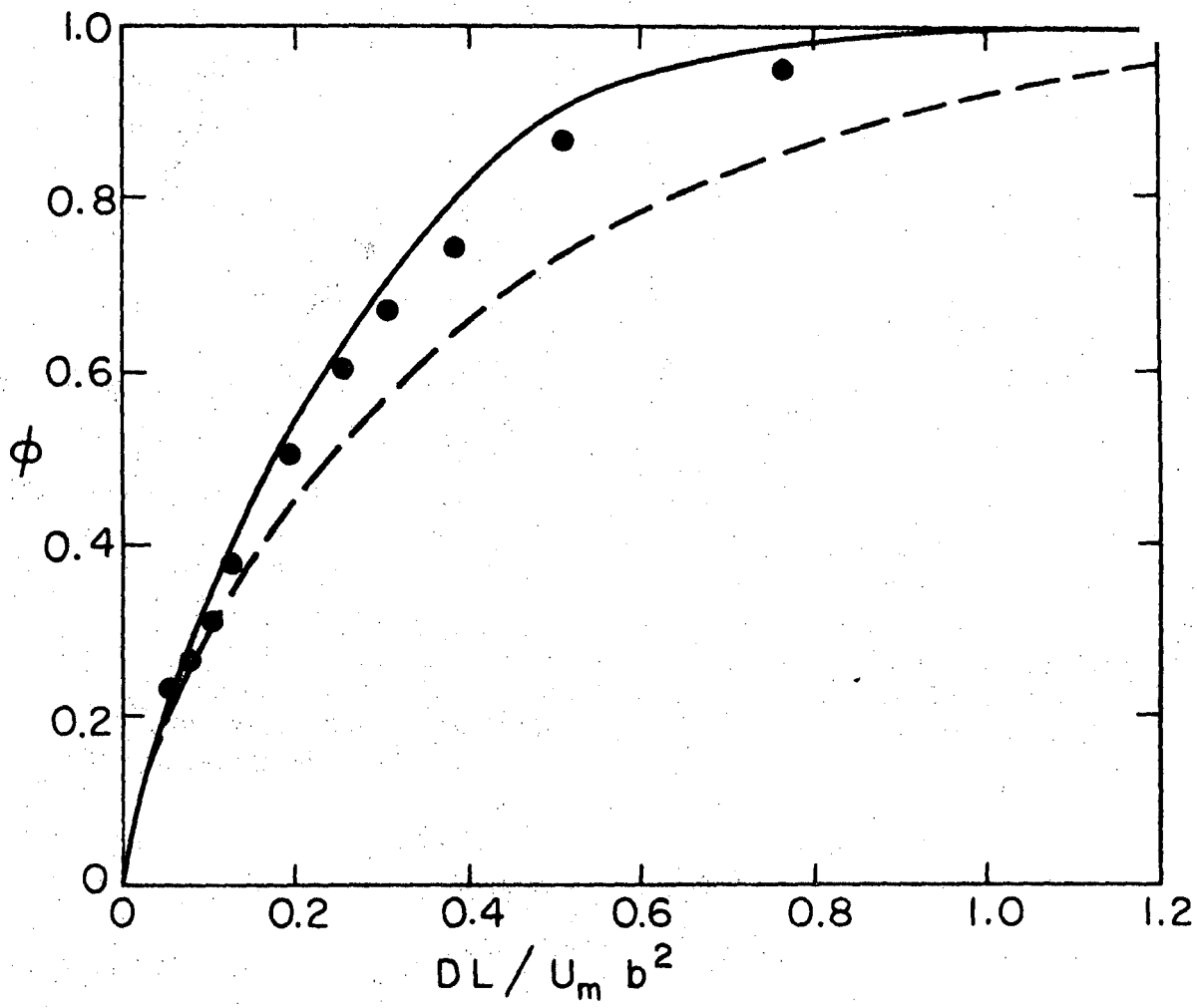

MUB-10912

Fig. 22. Mean fraction saturation as a function of Graetz number for cocurrent motion of CO_2 and ethanol (51.0 cc/sec); ●●● Data. --- Theory for zero interfacial velocity. —— Computer solution for experimental conditions.

number for liquid flow rates of 18.0, 30.0, and 51.0 cc/sec, respectively. The solid line represents the theory for a moving interface, and the dotted line is that presented by Butler and Plewes for zero interfacial motion. At the highest gas flow rates, low Graetz numbers, there is some error in the data, especially for the lowest liquid flow rate (Fig. 20). However with an increase in the liquid flow rate, where there is greater difference in fraction saturation between the two solutions, the effect of the interfacial motion becomes more evident. The fact that the data are generally lower than theory might be explained by two effects. Although we checked for any slowing of the interface by the action of surfactants in later runs and found no effect, there is a possibility that they might have been a factor in the earlier runs. The saturation value might have been a little high causing all the runs to appear a little low.

The experimental results given in Figs. 17, 20, 21, and 22 for the mass transfer are in terms of the mean fraction saturation. A conversion to average mass-transfer coefficient based upon the initial driving force may be performed using the following relationship:

$$k_{c_{av}} = \phi \, Q_g / 0.915 \, W \, L \quad . \tag{3-40}$$

Here W and L are, respectively the width and length of the mass-transfer area, while 0.915 is the corner correction. A discussion of this correction is contained in Appendix B. From this point it is a simple matter to compute the Stanton number:

$$St \equiv k_{c_{av}} / U_m = \phi b / L \tag{3-41}$$

Finally we may define the mass-transfer Nusselt number (the Sherwood number) based upon the overall length as

$$Nu = k_{c_{av}} L / D = \phi Q_g / 0.915 \, D \, W \quad . \tag{3-42}$$

Since the mass-transfer coefficient is defined on the basis of the initial difference in concentrations, the two dimensionless groups are also defined on this basis.

The three concentration profiles are shown in Fig. 23. The theoretical profiles corresponding to the three runs are also included. The data follow theory quite well except for one point in Run 63, which is probably erroneous. All the carbon dioxide data were generally within the estimated experimental error limit of 10%. While the points tended to be systematically low, they are sufficiently accurate to show the effect of interfacial velocity.

All the data for which the Beek and Bakker solution should be applicable--i.e., experiments where the mean exit concentration was less 50% of saturation--are shown in Fig. 24. The solid line indicates the theory. Within the estimated experimental error, the data agree with theory. The data using oxygen as the gas phase are included in this graph.

4. Countercurrent Data

The carbon dioxide runs discussed in the previous section were repeated, but this time the two fluids flowed in opposite directions. It was anticipated that there might be some trouble with ripples and level control with this mode of operation. However, no particular problem was encountered in operating countercurrently. A series of 33 runs was carried out at three different liquid rates. The results are reported in Figs. 25, 26, and 27. The results are compared with the Graetz model (the dotted line) and with the proposed theory of adding a stagnant zone between the surface and the point of flow reversal. The stagnation zone varied in thickness from 0.009 to 0.29 cm. The data agree almost quantitatively with the proposed theory and certainly within the error of the experimental method. For the highest liquid flow rate the cocurrent data are compared with the countercurrent data in Fig. 28. The solution for zero surface motion is included for comparison. The ordinate may be converted from mean fraction saturation to Stanton number by multiplying by the factor b/L. It is quite evident that the direction of motion of the interface is very important and that one must exercise great care in applying cocurrent data to countercurrent design.

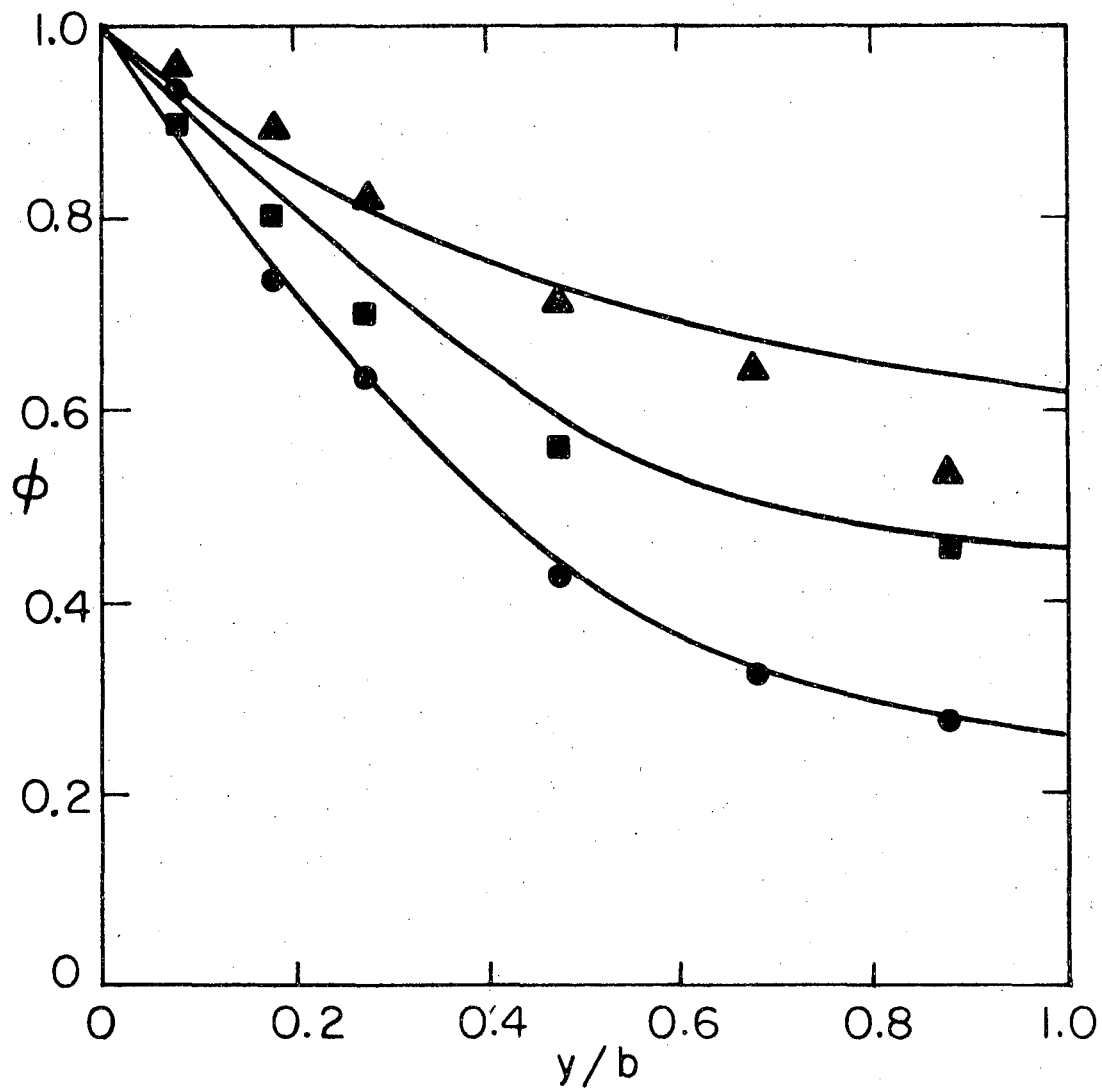

MUB-10917

Fig. 23. Concentration profiles for cocurrent flow of CO_2 and ethanol; ▲ Data for run 63. ■ Data for run 58. ● Data for run 46. —— Theory for all runs.

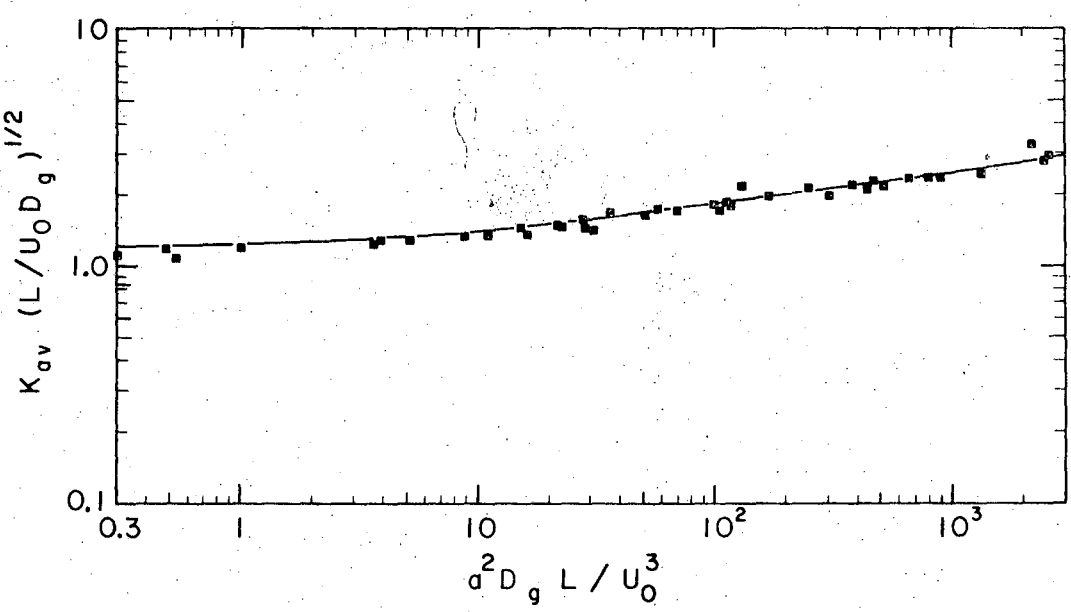

MUB-10136

Fig. 24. A comparison of average mass transfer coefficients based upon the solution of Beek and Bakker with experimental data.

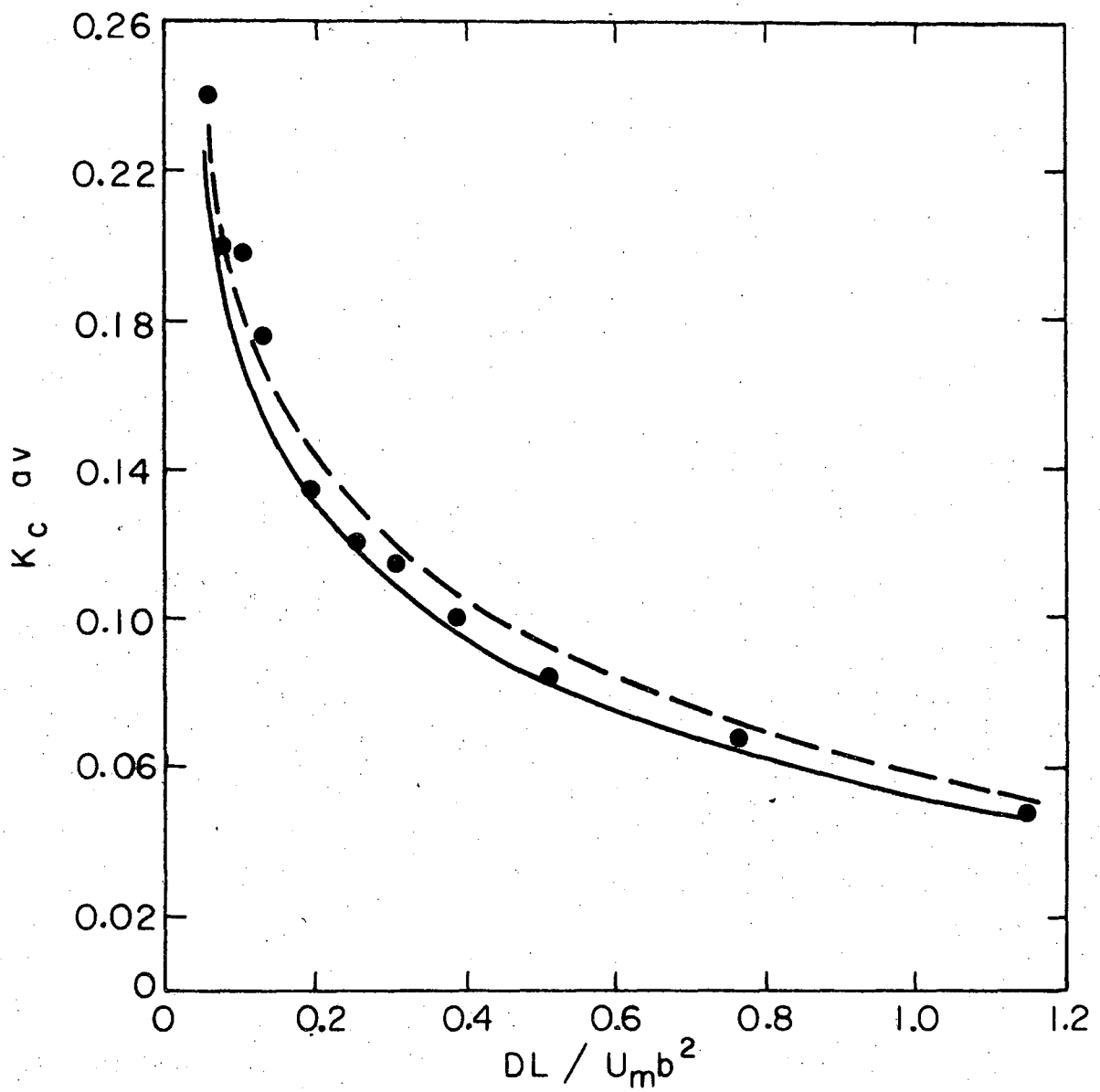

MUB-10910

Fig. 25. Countercurrent mass transfer of ethanol into CO_2 with ethanol flow rate = 17.65 cc/sec. ● Data. —— Countercurrent theory. --- Graetz solution (zero interfacial velocity).

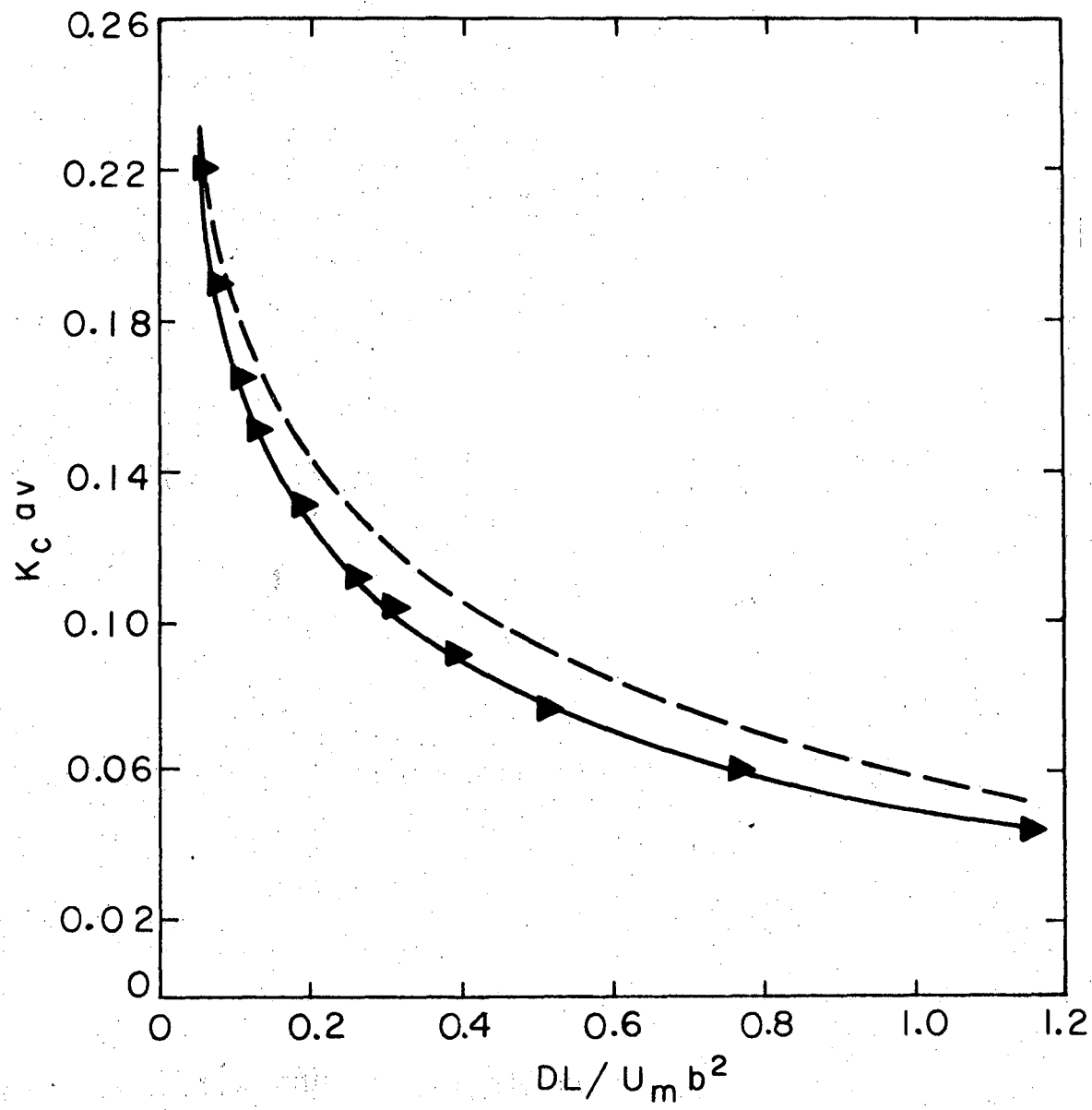

MUB-10920

Fig. 26. Countercurrent mass transfer of ethanol into CO_2 with ethanol flow rate = 35.20 cc/sec. ▲ Data. —— Countercurrent theory. --- Graetz solution (zero interfacial velocity).

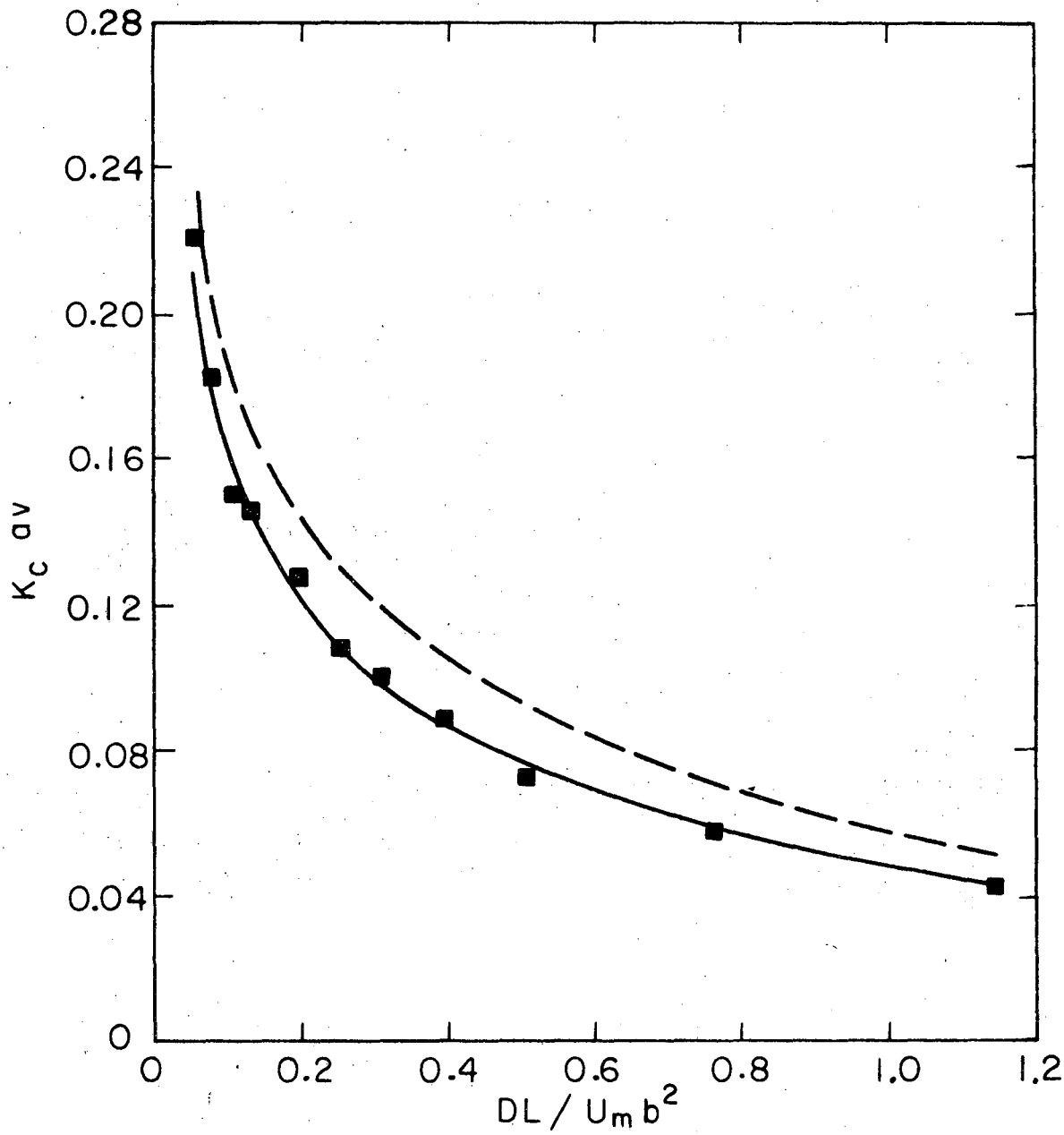

MUB-10911

Fig. 27. Countercurrent mass transfer of ethanol into CO_2 with ethanol flow rate = 53.70 cc/sec. ■ Data. —— Countercurrent theory. --- Graetz solution (zero interfacial velocity).

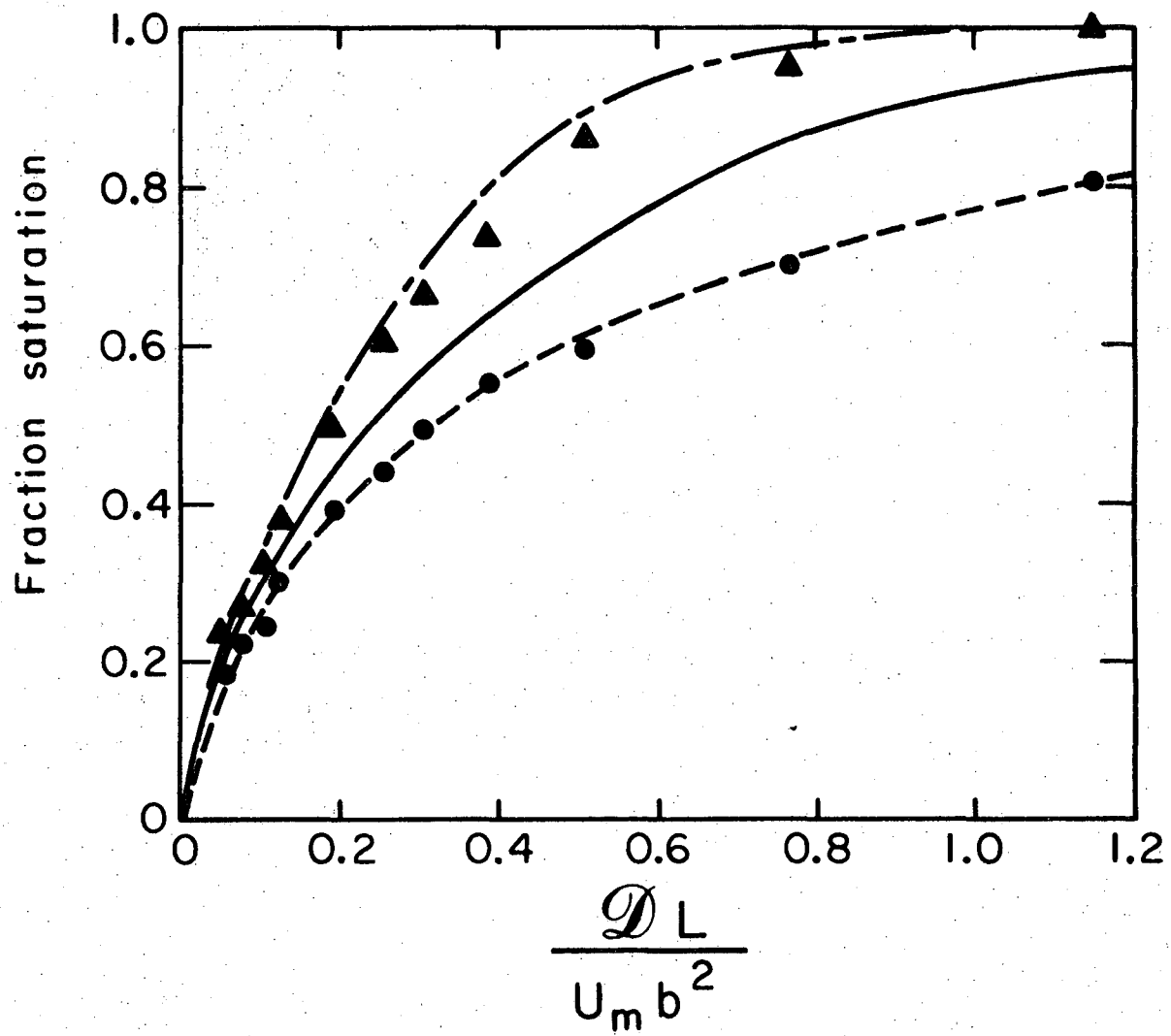

MUB-10137

Fig. 28. A comparison of laminar single phase controlled cocurrent and countercurrent data; ▲ cocurrent data, — — — cocurrent theory, —— the Graetz solution, ● countercurrent data, – – – countercurrent theory.

Three concentration profiles were carried out with countercurrent operation. One of these (Run 100) is presented in Fig. 29. The best line is drawn through the data, and the profile is compared with that expected for the corresponding cocurrent case. The difference is quite sizeable.

D. Experimental Errors

Several sources of error apply to all experiments discussed in this chapter and in the following two chapters. Some of the more important of them are discussed in the following section.

(a). The reference value for the gas analysis, using the gas-liquid chromatograph, is dependent upon the attainment of a saturation value for the component that is being transferred. In this work this was accomplished by flowing the liquid phase at the normal rate and flowing the gas at extremely low rates. The gas flow was held at about 50 to 75 cc/min, and a saturation composition was measured. Then the flow rate was doubled. There was no change in the amount of component in the sample. It was then concluded that this was the saturation value.

The number of units that the integrator on the recorder indicates is directly proportional to the carrier-gas flow rate. As a result the flow rate of the helium carrier gas must be maintained at a constant value, once a saturation value has been established. The carrier gas flow was monitored by means of a capillary flow meter. It was observed that the flow rate tended to drift to some extent, and a correction was necessary in the flow rate. Control of the carrier flow rate was better than 2%. Other errors of a lesser magnitude are involved in the control of temperatures within the detector of the unit, small variations in filament current, and in transmission and recording of the signal.

Implicit in the method of analysis is the assumption that the peak area recorded for each sample is a linear function of concentration. Since very low concentrations were measured in all cases (less than 8 mole%), this assumption is probably the source of very little error.

A rotameter on the sample line from the apparatus to the sample valve on the chromatograph was used to insure that sufficient gas had flowed from the apparatus to the sampler to purge it completely before the sample was

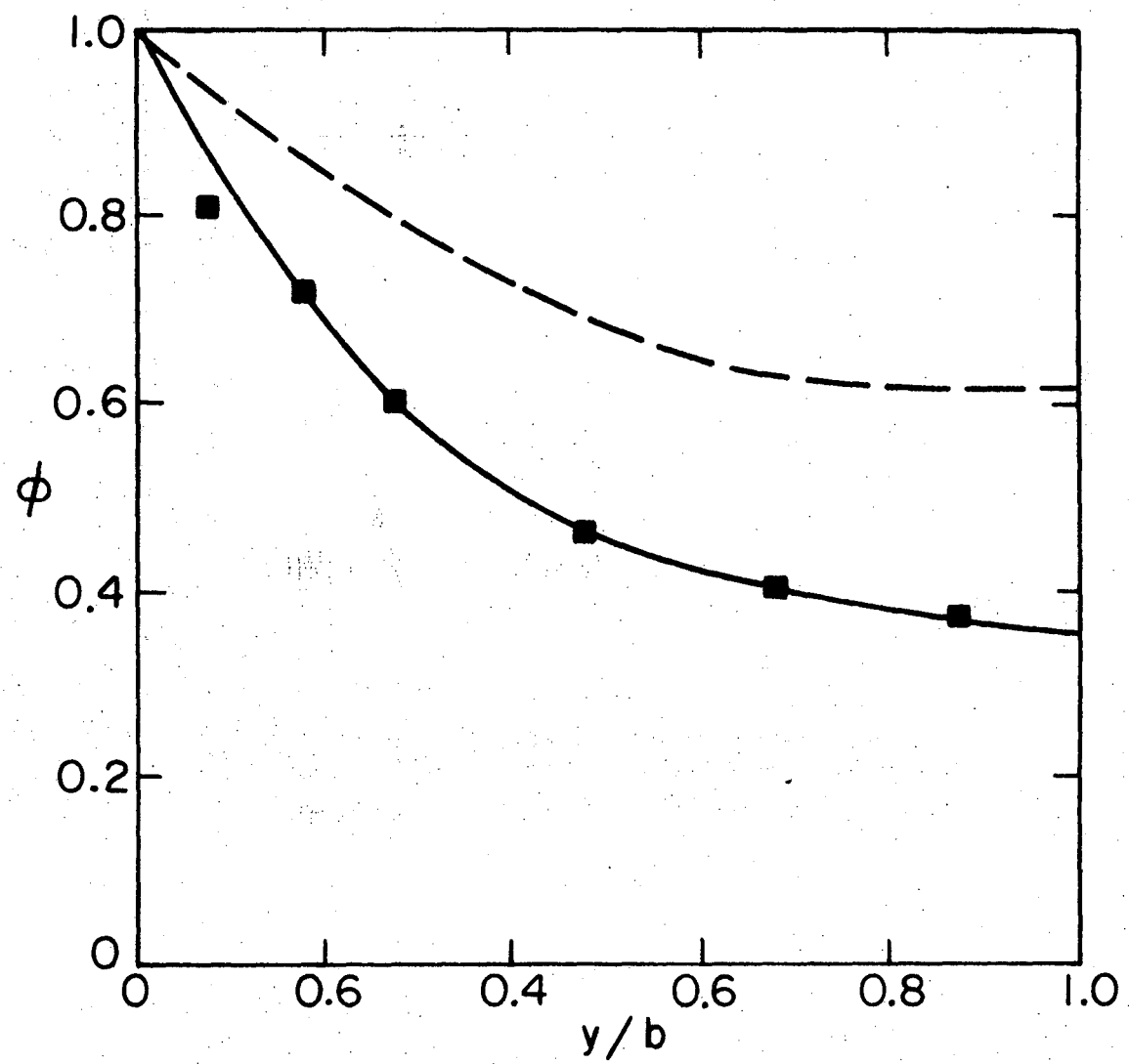

MUB-10916

Fig. 29. Concentration profile for mass transfer in countercurrent flow. ■ Data, —— Best fit of data, --- Theoretical concentration profile for the corresponding cocurrent conditions.

analysed in the chromatograph. A set time was used in flushing the sample valve, so that desorption from the sampler wall would be uniform. There were small human errors in timing of the length of purging. All of these small errors were probably not responsible for more than a total of 1% error. Successive samples of the same concentration tended to confirm this estimate of the combined minor errors.

(b). The channel itself contained within its construction several sources of error. First the control of the height of the gas-liquid interface was one of the main sources of difficulty in operating the apparatus. Although it was closely controlled, it could vary to some extent. That extent could become disastrous if a close watch was not kept upon operations. The fact that the liquid was in a relative thick layer was helpful in that minor variations in liquid level tended to change the hydrodynamics of the liquid in only a minor way. However a slightly too high liquid level for instance, would increase gas velocity and thus increase the mass transfer coefficient. It is estimated that this effect could not amount to more than 2% error in any one run, because of the close observation which was made of the level.

The hydrodynamics of the entry region tend to introduce a systematic effect into the data. The result should be mass-transfer results lower than predicted by the fully developed flow models used. It is difficult to estimate whether this effect was important, since the entry region was probably quite short compared to the overall length of the exposure. The cocurrent data were between 0 and 8% below the theoretically predicted value for fully developed hydrodynamics. While the entry region might have been a partial cause, it cannot account for all of the error.

Although tests showed that there was no visible slowing of the interface due to the presence of surfactants if ethanol was used as the solvent, it is entirely possible that some small effect might have passed unnoticed. Certainly the possibility should not be overlooked. The problem of the existence of a surfactant on the surface is discussed in detail in Chapter V.

Minor disturbances were noted at the interface, especially when the flow rates were high. These were probably due to the vibrations of the pump. However the wave length of these ripples was sufficiently long that their effect upon the mass-transfer coefficient should be negligible.

(c). Rotameters were used to measure the gas and liquid flow rates. They can be relied upon, in their central range of operation, to have an accuracy of about 5% in metering flow. The meters used in this study were found to follow the calibration curves provided by the manufacturer to better than 2%. However, since the flow rates are almost impossible to keep exactly where one would like them, small inaccuracies in flow rate must be accepted. With the ball-type rotameter used to meter the gas flow, it is often difficult to decide the exact positon of the center of the ball. Thus the proposed figure of 5% would seem to be a valid one.

(d). Temperatures within the system could be controlled to the closest degree Celsius. Thus at any one time the bulk gas and bulk liquid might have a temperature difference of about 1°C. Furthermore, temperatures read by means of thermistors and thermocouples were accurate to only about 0.2°C. This introduced an error of about 1% in the estimation of the vapor pressure and hence an error of 1% in the data.

(e). In all the runs an extrapolation had to be used to estimate the surface temperature. The vapor pressure was estimated on this basis. Since vapor pressure is a sensitive function of temperature, any error in the extrapolation has a direct effect upon the accuracy of the data. The temperatures were measured at the end of the exposure where the temperature would be highest. Due to the sharp curvature of the temperature profile in the gas phase near the interface and the difficulty in accurately measuring temperature in the region of the interface with the available probe, an error in the estimate of the vapor pressure of about 2% was possible. The error was probably responsible to some degree for the low values obtained in the cocurrent mass-transfer runs.

As a result of this analysis it is evident that an estimated error of about 10% would not be unexpected for this experiment.

E. Conclusions

The following may be concluded from the results discussed in this chapter.

(a). The channel gas phase effectively follows the Graetz solution both in its overall mass transfer and in point concentrations.

(b). A computer solution to the problem of mass transfer from a moving interface to a parabolic velocity profile proved quite effective in describing many different situations. This procedure is as effective as the generation of eigenvalues and eigenfunctions and is much less difficult. The use of the "Calcomp" plotter makes the method even more effective. When the present solution was compared with penetration theory for the case of the wetted-wall column, the penetration theory proved substantially in error at cup-mixing concentrations above 40% of saturation.

(c). Experiments generally confirmed the theoretical solution. The effect of an interfacial velocity is to enhance the mass-transfer coefficient in cocurrent flow. Concentration profiles also agree with theory within the experimental error of the method.

(d). If the effect of the interfacial velocity on gas-phase mass transfer is ignored in wetted-wall column studies, a substantial error may occur. If one attempts to correct for this effect by subtracting the velocity of the liquid interface from the gas-phase velocity and using a Graetz model, the resulting correction will be in the wrong direction.

(e). A computer solution has shown that the solution of Beek and Bakker must be modified to be made correct. Concentration profiles were developed for this case. Generally, experimental data confirmed the validity of the theory with the suggested modifications.

(f). Counterflow experiments indicated a substantially lower mass transfer coefficient than would be expected if there were no motion at the interface. This fact may be attributed to the flow reversal in the gas phase, which tends to create a stagnant area near the interface, thereby adding to the mass-transfer resistance. Adding a film resistance for the area between the flow reversal and the interface to the resistance of the Graetz model for the remainder of the channel width provided quantitative agreement with the data. It must be concluded that in packed-tower design, cocurrent data cannot be used to estimate countercurrent coefficients for the gas phase.

(g). The estimated experimental error is about 10%. The major sources of error are the measurement of flow, the estimation of concentration, and the uncertainty of the hydrodynamics of the channel.

IV. INTERPHASE MASS TRANSFER

While mass transfer controlled by the resistance of a single phase finds some application in industrial practice, a large majority of design problems involve estimation of mass-transfer coefficients where there is resistance to mass transfer in both of the contacting phases. This problem is the subject of this chapter.

A. Introduction

The question of designing contacting devices in which there is resistance to mass transfer in both phases stood in a state of confusion until Lewis[46] and Whitman[76] proposed their two-film theory for resistance to mass transfer. Since then the theory has been interpreted more generally as applying to whatever models are employed for the two phases under consideration. In this latter way the theory is applied in the remainder of this study. The mass transfer coefficients (k_c and K_l) are defined as

$$k_c = \frac{N_A}{C_g - C_g^{\,i}} \quad \text{and} \quad k_l = \frac{N_A}{C_l^{\,i} - C_l} \tag{4-1}$$

It is inconvenient to have an equation that included the interfacial concentrations, $C_g^{\,i}$ and $C_l^{\,i}$, since it is not possible to measure these quantities. As a result, one defines an overall mass-transfer coefficient based upon the overall difference in concentration between the bulk phases. This coefficient is defined as

$$k_c = \frac{N_A}{C_g - C_g^{\,*}} \tag{4-2}$$

where $C_g^{\,*} = \mathcal{H}\, C_l$.

The second part of Eq. (4-2) is the assumption that Henry's law is a valid equilibrium relationship between the two phases. A simple algebraic manipulation of these equations produced the final expression for the two film theory:

$$\frac{1}{K_C} = \frac{1}{k_C} + \frac{\mathcal{H}}{k_l} \quad . \tag{4-3}$$

This relationship is necessarily valid at any given point at the interface, as long as k_c and k_l are indeed the prevailing individual phase coefficients at that point.

On the other hand, experimentally measured mass-transfer coefficients must be values which are estimated over a finite region. Usually k_c and k_l will vary from position within the region. In such cases the fact that Eq. (4.3) holds for each point of interface within the region does not imply that a similar relationship will hold true for the average coefficients measured for the entire region.

In addition, most common usages of the two-resistance theory imply that independently measured resistances to mass transfer may be added by Eq. (4-3) to obtain an overall mass-transfer coefficient at any point or for a region of interface. This is the addition-of-resistances principle. If this practice were universally applicable to all models there would be no need for interphase mass-transfer studies. Recently, however, the universal validity of such an assumption has been questioned.

King has discussed the validity of adding individually measured resistances to ascertain the overall mass-transfer coefficient in physically important cases.[39-41]

King points out the following five criteria that must be satisfied in order for the additivity of resistances to be valid.[40]

(1). The Henry's law coefficient, $\mathcal{H}$, must be a constant throughout the region of the exposure. The equilibrium relationship at the interface may take on the form

$$C_g = \mathcal{H}C_l + b' \quad , \qquad (4\text{-}4)$$

provided $\mathcal{H}$ and b' are both constants for the exposure in question.

(2). The resistances added must be the only ones present. Equilibrium must be achieved at all points along the interface instantaneously upon the exposure of the two phases.

(3). The hydrodynamic conditions used in formulating the two-single-phase models must be the same as those that actually exist in the interphase mass-transfer case.

(4). The existence of either resistance to mass transfer must not materially affect the value of the other.

(5). The ratio, $H\ k_g'/k_l'$, must be a constant at all points on the interface. The reason for the necessity for this condition is thoroughly discussed by King.[40]

The other, and more fundamental way in which the problem may be approached is to solve the partial differential equations for the two-phase problem, with the proper coupling interfacial conditions. However, very few situations are sufficiently simple to allow a comparison between the theory of addition of independently measured resistances and a solution to the overall mass-transfer problem by using the basic transport equation. Additivity can be compared with several models where solutions exist. For instance King has solved for the case where penetration theory applies in the liquid phase and the film model is assumed in the gas phase.[40] A comparison of the analytic solution for the average overall mass-transfer coefficient with the one found by adding average individual resistances shows that the deviation is at most 5%. However, since the addition of resistances gives the lower values, it is conservative. On the other hand the true local overall coefficient at any point is considerably less than that derived by the additivity principle from the local coefficients exhibited by either phase in the absence of resistance in the other phase.

In general for single exposures of gases and liquids, no deviation from additivity is observed if the chosen models predict the same dependence of the mass transfer coefficient upon distance from the start of the exposure. An example of this type of solution is given by Potter.[55] Mass transfer between two streams whose initial velocities are different but constant is considered. Upon contact the interface achieves a velocity between the two bulk velocities. The development of the velocity profiles in both phases may be described by means of a boundary-layer approach. This produces a solution to the convective-transport equations for each phase. The two independent resistances to mass transfer may be added because both have the same dependence upon the length of exposure, and therefore the interfacial concentration is constant. The special case of equal entering velocities may be treated by the penetration model in both phases. Here again the addition of the two resistances yields exact agreement with the analytical solution.

When counterflow is involved, even the simplest situations must be solved on the computer. Even then some unrealistic models must be chosen in order to maintain some simplicity. Two models for countercurrent flow are examined by King.[41] Model 1 assumes slip at the interface with counter-flow of two phases with constant velocities, while Model 2 assumes the same model in the liquid while flow in the gas phase is assumed to follow a simplified boundary-layer model (the first term of the Pohlhausen polynomial approximation). The maximum deviation of the true overall average coefficients from those predicted by the additivity of resistances was found to be 20% for Model 1, while Model 2 gave maximum deviations of approximately 14%. These two models are approximate, but they show the trend to be expected in the counterflow cases.

There are two primary reasons for the scarcity of interphase mass-transfer studies. Until recently, no critical analysis had been made of the assumptions underlying the principle of addition of independently measured resistances. As a result, the assumption has always been made that the principle was valid and therefore most studies only considered cases where the resistance to mass transfer was entirely resident in one phase. The second reason is that no device had been developed in which the principle could be tested under controlled conditions in both phases. The few plate and packed- and plate- column studies which have dealt with interphase mass transfer have shown that the addition of independently measured resistances predicts mass transfer coefficients which are in error by as much as a factor of two. These studies may not be considered as being completely valid,[80,66] since no experiments were made with complet liquid-phase control. On the other hand, the stirred-flask study carried out by Goodgame and Sherwood indicated that addition of the resistances was valid at least to the accuracy of the method.[22] The validity of the principle has not been tested experimentally in laminar flow.

The geometry of the device developed for this study is particularly well adapted to a thorough study of interphase mass transfer. The simple hydrodynamics of both phases allow for the development of exact models for single-phase controlled mass transfer. It is possible to solve the transport equation for interphase mass transfer to the same degree of precision. A comparison may then be made on the addition of the individual resistances with the exact interphase model. Finally all the models may be checked experimentally.

B. Analytical Solution to the Equations for Interphase Mass Transfer

It would be of some interest to develop a general model for interphase gas-liquid mass transfer for cocurrent laminar flow, which would also be applicable to the case of flow between two flat plates. With the fact in mind that mass transfer is most dependent upon the velocity profile very near the interface, the model shown in Fig. 30 is proposed as an interphase transfer model. A liquid with interfacial velocity U_0 and a gas with slope a in the velocity profile are contacted. Initially the gas has a concentration C_{g_0}, and the liquid has a concentration C_{l_0}. Near any gas-liquid interface this approximation will be valid. Only where a long exposure is encountered will the fact that the velocity profile is oversimplified have any effect. A solution to the equations of change for this interphase case is now considered.

In the liquid phase, since the velocity is a constant, the equation reduces to

$$U_0 \frac{\partial C_l}{\partial x} = D_l \frac{\partial^2 C_l}{\partial y^2} \tag{4-5}$$

with the following boundary conditions

$$\begin{aligned} C_l &= C_{l_0} \quad \text{at} \quad x = 0 \\ C_l &= C_{l_0} \quad \text{at} \quad y = -\infty \quad . \end{aligned} \tag{4-6}$$

This equation may be solved by means of the Laplace transformation. If $\bar{C}_l$ is defined as

$$\bar{C}_l = \int_0^\infty C_l \, e^{-sx} dx \quad , \tag{4-7}$$

then Eq. (4-5) transforms to

$$U_0 s \, \bar{C}_l - U_0 C_{l_0} = D_l \frac{d^2 C_l}{dy^2} \quad . \tag{4-8}$$

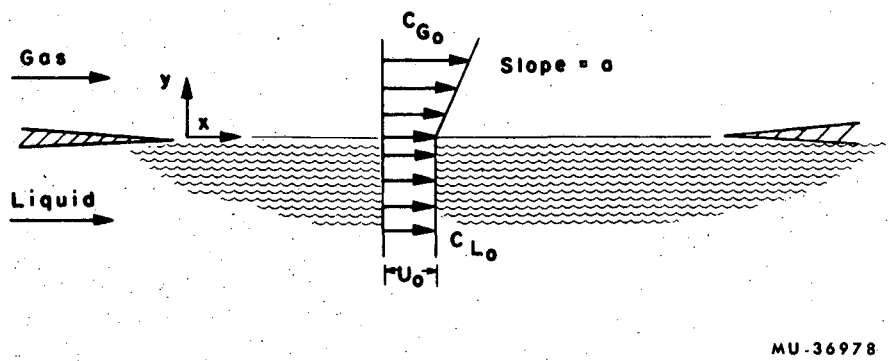

Fig. 30. A Simplified Model for Gas Liquid Mass Transfer.

The boundary conditions are used to eliminate an integration constant, and the solution of this differential equation in the Laplace domain is

$$\bar{C}_1 = \frac{C_{1_0}}{S} + \Lambda \exp\left[\left(\frac{U_0 s}{D_1}\right)^{1/2} y\right] \tag{4-9}$$

$$\frac{d\bar{C}_1}{dy} = \Lambda \left(\frac{U_0 s}{D_1}\right)^{1/2} \exp\left[\left(\frac{U_0 s}{D_1}\right)^{1/2} y\right] \tag{4-10}$$

The interface has two conditions that relate the two phases.

(1). Equilibrium is assumed to exist between the two phases at the interface. If we assume that this system obeys Henry's Law, then we have

$$C_g = \frac{H}{RT} C_1 \quad . \tag{4-11}$$

(2). There must be equality of fluxes across the interface

$$D_g \frac{\partial C_g}{\partial y}\Big|_{o^+} = D_1 \frac{\partial C_1}{\partial y}\Big|_{o^-} \tag{4-12}$$

As is shown in Fig. 30, the velocity in the gas phase is

$$U = U_0 + ay \tag{4-13}$$

Therefore the transport equation for the gas phase is

$$(U_0 + ay) \frac{\partial C_g}{\partial x} = D_g \frac{\partial^2 C_g}{\partial y^2} , \tag{4-14}$$

with the boundary conditions:

$$\begin{aligned} C_g &= C_{g_0} \quad \text{at} \quad x = 0 \\ C_g &= C_{g_0} \quad \text{at} \quad y = \infty \quad . \end{aligned} \tag{4-15}$$

The transformed equation in the Laplace domain is

$$\left(\frac{a^2 D_g}{U_0^3}\right) \frac{d^2\bar{C}_g}{d\left(1+\frac{a}{U_0}y\right)^2} - \left(1+\frac{a}{U_0}y\right) s\bar{C}_g + \left(1+\frac{a}{U_0}y\right) C_{g_0} = 0 \tag{4-16}$$

This is a form of the Bessel equation. Hildebrand[31] gives its solution as

$$\bar{C}_g = \frac{C_{g_0}}{s} + \theta_1\left(1+\frac{a}{U_0}y\right)^{1/2} I_{\frac{1}{3}}\left[\frac{2}{3}\left(\frac{U_0^3}{a^2 D_g}\right)^{1/2} s^{1/2}\left(1+\frac{a}{U_0}y\right)^{3/2}\right]$$
$$+ \theta_2\left(1+\frac{a}{U_0}y\right)^{1/2} K_{\frac{1}{3}}\left[\frac{2}{3}\left(\frac{U_0^3}{a^2 D_g}\right)^{1/2} s^{1/2}\left(1+\frac{a}{U_0}y\right)^{3/2}\right]. \tag{4-17}$$

When the boundary conditions are taken into account, the result in the Laplace domain is

$$\bar{C}_g = \frac{C_{g_0}}{s} + \theta\left(1+\frac{a}{U_0}y\right)^{1/2} K_{\frac{1}{3}}\left[\frac{3}{3}\left(\frac{U_0^3}{a^2 D_g}\right)^{1/2} s^{1/2}\left(1+\frac{a}{U_0}y\right)^{3/2}\right] \tag{4-18}$$

and

$$\frac{d\bar{C}_g}{dy} = -\theta\frac{a}{U_0}\left(1+\frac{a}{U_0}y\right)\left(\frac{U_0^3}{a^2 D_g}\right)^{1/2} s^{1/2} K_{-\frac{2}{3}}\left[\frac{2}{3}\left(\frac{U_0^3}{a^2 D_g}\right)^{1/2} s^{1/2}\left(1+\frac{a}{U_0}y\right)^{3/2}\right]. \tag{4-19}$$

The two constants, Λ and θ, are obtained by simultaneous application of the two interfacial conditions to the solutions in the Laplace domain.

$$\Lambda = \frac{\Delta C}{s}\left[\frac{\mathcal{H}\sigma K_{-2/3}\left[2/3\ Rs^{1/2}\right]}{\mathcal{H}\sigma K_{-2/3}\left[2/3\ Rs^{1/2}\right] + K_{1/3}\left[2/3\ Rs^{1/2}\right]}\right] \tag{4-20}$$

$$\theta = -\frac{\Delta C}{s}\ \frac{\mathcal{H}}{\mathcal{H}\sigma K_{-2/3}\left[2/3\ Rs^{1/2}\right] + K_{1/3}\left[2/3\ Rs^{1/2}\right]} \tag{4-21}$$

where

$$\sigma = \left(D_g/D_1\right)^{1/2}$$
$$R = \left[\frac{U_0^3}{a^2 D_g}\right]^{1/2} \tag{4-22}$$
$$\Delta C = \frac{C_{g_0}}{\mathcal{H}} - C_{1_0}\ .$$

and

$$z = \frac{2}{3} Rs^{1/2} \quad . \tag{4-23}$$

It is quite obvious that concentration profiles would be very difficult to generate. As a result only a solution for the mass transfer coefficient is sought. The local overall mass-transfer coefficient is defined as

$$\bar{k} = -\frac{D_g}{\Delta C} \frac{d\bar{C}_g}{dy}\bigg|_{y=0} \quad . \tag{4-24}$$

In the Laplace domain this is found to be

$$\bar{k} = \frac{2\mathcal{N}U_0^2}{3za} \cdot \left[\frac{K_{-2/3}(z)}{\alpha\mathcal{N}\left[K_{-2/3}(z)\right] + K_{1/3}(z)}\right] \quad . \tag{4-25}$$

No simple general solution is available for this problem. However it is possible to find asymptotic solutions for short and long exposures. For large values of the function z the following simple functionality may be given to the Bessel function of the second kind.

$$K_n(z) = \left[\frac{\pi}{2z}\right]^{1/2} e^{-z}\left[R_n + S_n\right] \quad , \tag{4-26}$$

where R_n and S_n are series in n and z given by Carslaw and Jaeger.[8] If this approximation is included in the solution, the result is

$$\bar{k} = G\left[\frac{1 + \frac{7}{72}\xi + \frac{455}{10365}\xi^2}{\alpha - \beta\xi}\right] \quad , \tag{4-27}$$

where

$$\begin{aligned} \xi &= 1/z \quad , \\ G &= 2\mathcal{N}U_0^2/3a \quad , \\ \alpha &= \alpha\mathcal{N} + 1 \quad , \\ \beta &= \frac{5 - 7(\alpha\mathcal{N}+1)}{72} \quad , \end{aligned} \tag{4-28}$$

The binomial in the denominator is made into a series, and this is multiplied by the existing terms in the numerator. The result is

$$\bar{k} = \frac{G}{\alpha}\left[\xi + \left(\frac{\beta}{\alpha} + \frac{7}{72}\right)\xi^2 + \left(\frac{\beta^2}{\alpha^2} + \frac{455}{10,368} + \frac{7}{72}\frac{\beta}{\alpha}\right)\xi^3 + \ldots\right] \qquad (4\text{-}29)$$

This series may be inverted term by term. The overall mass-transfer coefficient based upon the gas phase is

$$K_C = \frac{G}{\alpha}\left[\frac{3}{2(R)\ (\pi x)^{1/2}} + \frac{9}{4R^2}\left(\frac{\beta}{\alpha} + \frac{7}{72}\right) + \ldots\right] \quad . \qquad (4\text{-}30)$$

Rearrangement gives

$$K_C\left(\frac{x}{U_O D_g}\right)^{1/2} = \frac{\mathcal{H}R}{\sigma\mathcal{H}+1}\left[\frac{1}{R\sqrt{\pi}} + \frac{6x^{1/2}}{4R^2}\left(\frac{5-7\sigma\mathcal{H}}{72(\sigma\mathcal{H}+1)} + \frac{7}{72}\right) + \ldots\right] \quad . \qquad (4\text{-}31)$$

The grouping, $\sigma\mathcal{H}$, is of interest since it denotes the degree of control that is resident in a single phase. If its value is much greater than 5, the second term on the right side of Eq. (4-31) drops out, and the equation becomes

$$K_c\left(\frac{x}{U_O D_g}\right)^{1/2} = \frac{1}{\sigma\sqrt{\pi}} \quad . \qquad (4\text{-}32)$$

Now if we rearrange and find the overall mass-transfer coefficient based upon the liquid phase, then

$$K_l = \frac{D_L U_O}{\pi x} \qquad (4\text{-}33)$$

Thus in the limit the model becomes the penetration model. This is the anticipated result. On the other hand if the grouping, $\sigma\mathcal{H}$, is very small the equation becomes

$$K_C\left(\frac{x}{U_O D_a}\right)^{1/2} = \frac{1}{\sqrt{\pi}} + \frac{\sqrt{x}}{4R} \quad . \qquad (4\text{-}34)$$

This is merely the Beek and Bakker short-exposure solution. Hence the variation of $\alpha\mathcal{H}$ serves to change the degree of control between the phases.

The solution for low values of Z is a good deal more difficult, and the solution in this case is not quite as satisfactory. For small values of Z we have

$$K_p(x) = 2^{p-1}(p-1)!x^{-p} \quad . \tag{4-35}$$

For this case Eq. (4-25) becomes

$$\bar{k} \simeq \frac{G}{z}\left(\frac{1}{\alpha\mathcal{H}+Dz^{1/3}}\right) \quad . \tag{4-36}$$

A solution is very difficult in this case and we therefore seek a solution only for the situation where

$$\alpha\mathcal{H} \rangle Dz^{1/3} \quad , \tag{4-37}$$

with

$$D = \frac{2^{-1/3}(-2/3)!}{(-1/3)!} \quad .$$

Let $\tau = \alpha\mathcal{H}/D$. Then for $z^{1/3}/\tau$ much greater than one we have

$$\bar{k} = \left(1-z^{1/3}/\tau + z^{2/3}/\tau - \cdots\right) \quad . \tag{4-38}$$

The solution is inverted and rearranged. Finally the coefficients are evaluated. The result is

$$K_c \frac{x}{D_g U_0}^{1/2} = \frac{1}{\alpha\mathcal{H}}\left[\frac{1}{\sqrt{\pi}} \frac{-0.515}{\alpha\mathcal{H}} \left(\frac{a^2 D_g x}{U_0^3}\right)^{1/6} + \frac{0.343}{(\alpha\mathcal{H})^2} + \left(\frac{a^2 D_g x}{U_0^3}\right)^{1/3} + \cdots\right] \tag{4-39}$$

Note that for high values of $\alpha\mathcal{H}$ the solution becomes the penetration model. For low values of the control function, the solution does not become the

limiting gas-phase-controlled model. This is not unexpected since Eq. (4-37) has already precluded the agreement between the models in the limit.

The results of this solution are shown graphically in Fig. 31. A log-log presentation of $K_g(x/U_0D_g)^{1/2}$ as a function of a^2D_gx/U_0^3 is made for different values of the parameter $\alpha\mathcal{H}$. The solid line represents the analytic solution, while the dotted line shows the results of a computer solution of the same problem in the regions where the analytic solution is not valid (see Section C).

The additivity of resistances should be quite a good theory for the prediction of this result, since both phases obey penetration at very short times, and the deviation thereafter is from a minus one-half power dependence on the length of exposure to a minus one-third power dependence at very long exposures. The additivity principle is used for prediction of K_c from the local coefficients exhibited by either phase in the absence of resistance in the other phase. It is assumed that the penetration model holds in the liquid phase.

$$\frac{1}{K_c\left(\frac{x}{D_gU_0}\right)^{1/2}} = \frac{1}{k_g\left(\frac{x}{D_gU_0}\right)^{1/2}} + \frac{\mathcal{H}}{k_l\left(\frac{x}{D_lU_0}\right)^{1/2}}\left(\frac{D_l}{D_g}\right)^{1/2} \quad . \qquad (4\text{-}41)$$

If this equation is rearranged and put in the nomenclature of the previous derivation, we have

$$K_c\left(\frac{x}{D_gU_0}\right)^{1/2} = \frac{k_c\left(\frac{x}{D_gU_0}\right)^{1/2}}{1+\sqrt{\pi\alpha\mathcal{H}}\,k_c\left(\frac{x}{D_gU_0}\right)^{1/2}} \qquad (4\text{-}42)$$

The value of $k_c(x/DU_0)^{1/2}$ is taken from Fig. 14, which is a composite of Eqs. (3-35) and (3-36) and a computer solution. The solution using the additivity of resistances was compared with the analytical solution where it is applicable and the computer solution in the remainder of the region. It was found that the deviations of the additivity solution were greatest in the region where $\alpha\mathcal{H}$ is unity, that is where control is evenly divided between phases. Also the deviation tends to increase as a^2D_gx/U_0^3 increases. The maximum deviation is less than 2% for any reasonable value of the length group (100,000). Since it has already been shown that the estimated experimental error for this method is 10%, no effect of the nonadditivity of local resistances can be expected in the experimental data.

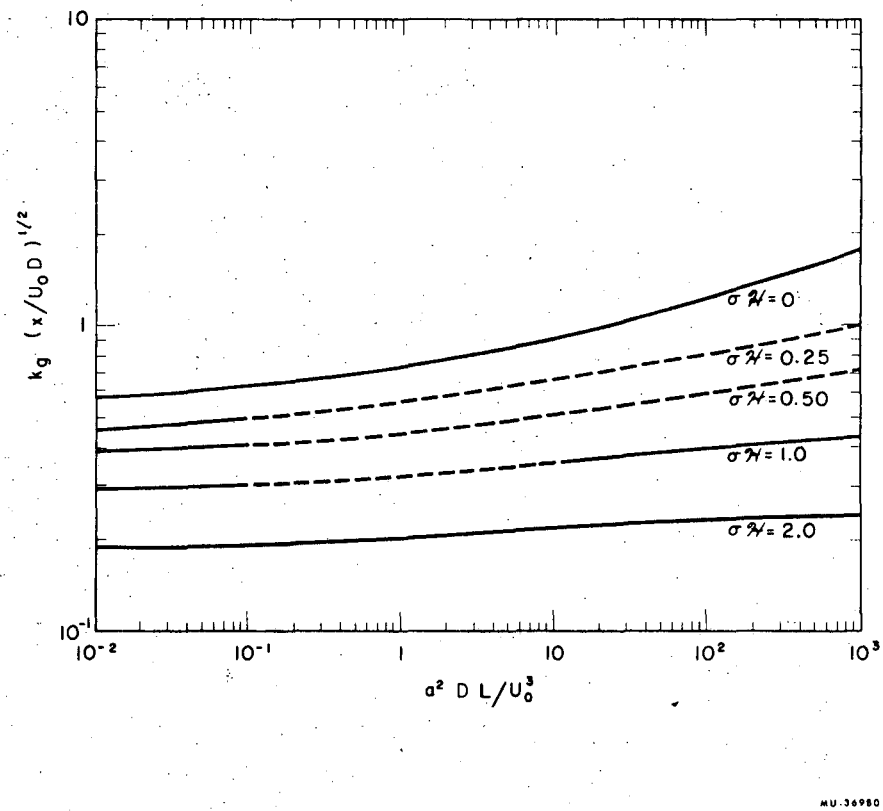

Fig. 31. Interphase Mass Transfer Solution for Two Unbounded Media. ——Analytic solution ---- Computer solution.

The local mass-transfer coefficients cannot be estimated experimentally, and as a result the average mass-transfer coefficients must be computed from the theory for the local coefficients. The local coefficient is integrated over the entire exposure and divided by the length of the exposure. Since the solution for the central region of the exposure is a computer solution, the integration had to be carried out in sections with the central portion integrated by first fitting the computer solution to a fourth-order polynomial and then integrating the polynomial. The final equation is given as part of the "SURFER" program in Appendix C.

C. Computer Solutions to Interphase Mass-Transfer Problems

While the solution discussed in the previous section is adequate for most mass-transfer studies where low percent saturation is achieved, the full parabolic profile must be taken into account when higher concentrations are considered. It is also anticipated that the corresponding heat-transfer problem will require a solution of this kind in order to describe the behavior of the channel. With these objectives in mind it was decided to write three different programs to solve for cases with different degrees of approach to the actual situation in the channel. These solutions examine the problems with parabolic profiles in velocity in both phases, with a parabolic profile in the gas and a linear profile in the liquid, and with a linear slope in profile in the gas and a constant velocity in the liquid.

1. Method of Solution

All three programs used the same numerical approach. In this section the most complex program (with two parabolic profiles) is discussed. Figure 32 is a drawing of the physical situation for which a solution is sought. The partial differential equation to be solved in this case for the gas phase is

$$\left[1 + (6U_m/U_0 - 4)y + \left(3-6\ U_m/U_0\right)y^2\right]\frac{\partial C_g}{\partial x} = \frac{D_L}{U_0}\frac{\partial^2 C_g}{\partial y^2} \quad , \qquad (4\text{-}43)$$

with the boundary conditions

$$\begin{aligned} x &= 0 \qquad C_g = C_{g_0} \\ y &= a \qquad \partial C_g/\partial y = 0 \end{aligned} \qquad (4\text{-}44)$$

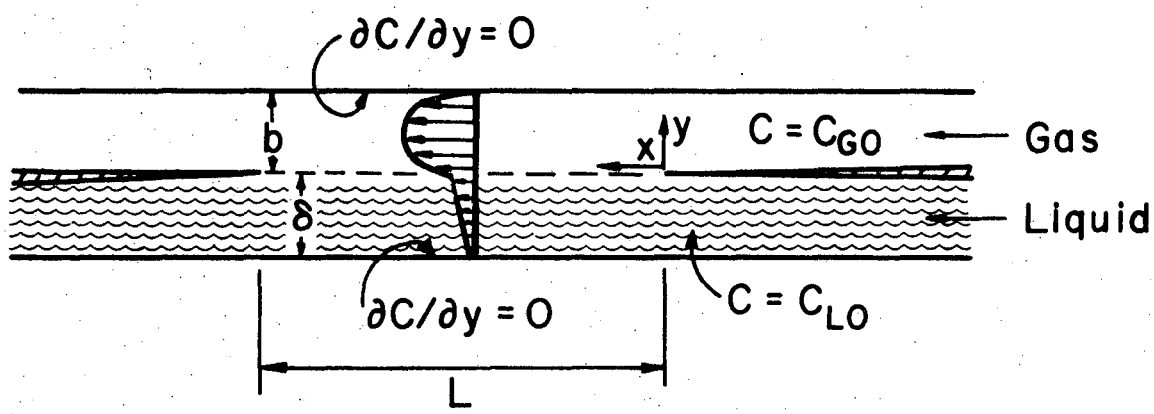

MUB-11249

Fig. 32. Interphase Mass Transfer between Two Flat Plates.

In the liquid phase we have

$$(1-y^2)\frac{\partial C_1}{\partial x} = \frac{D_L}{U_0}\frac{\partial^2 C_1}{\partial y^2} \tag{4-45}$$

with the boundary condition

$$\begin{aligned} x &= 0 \qquad C_1 = C_{1_0} \\ y &= -b \quad \partial C/\partial y = 0 \end{aligned} \tag{4-46}$$

At the interface the equilibrium condition assumed is Henry's law:

$$C_g = \mathcal{H} C_1 \tag{4-47}$$

at $y = 0$, while the other condition is the continuity of the flux.

$$D_g \left.\frac{\partial C_g}{\partial y}\right|_{0^+} = D_1 \left.\frac{\partial C_1}{\partial y}\right|_{0^-} \tag{4-48}$$

If the velocity profiles are compared with those for the general case of confined flow, it will be found that the profiles used in this solution are not exact. The error is the assumption that there is no drag of the gas upon the liquid. Thus the liquid profile in velocity is slightly different from the actual solution. If the exact profile is specified, much of the generality of the solution is removed because the viscosities of both phases must be known as well as the physical dimensions of the channel and the flow rates. By allowing the small error in the velocity of the liquid, the number of variables necessary to define the hydrodynamics of the system may be reduced to one, the ratio of the average gas velocity to the interfacial velocity.

The mass-transfer variables are the gas diffusivity group ($D_g L/U_0 a^2$), the liquid diffusivity group ($D_1 L/U_0 b^2$), and the interfacial group ($D_g b\mathcal{H}/D_1 a$). Of these four variables, only three are independent. A Crank Nickolson six-point iterative technique was used to solve the coupled equations.[43a] The solution was carried out in exactly the same way as the solution for the single phase case. That solution is discussed in Chapter III. At the interface it is

necessary to use the interfacial boundary condition in order to eliminate the definition of concentrations in the gas phase in terms of the liquid phase and vice versa. The source program is reproduced in Appendix D along with an explanation of mechanics of using the program.

The three independent parameters that must be established for each case of flow between two flat plates make a general solution of this case on the computer very time-consuming. For mass transfer in the liquid phase, the curvature of the velocity profile is not very important, because of the small penetration depth during mass transfer. Therefore a second interphase mass-transfer program was written in which the liquid phase has a constant velocity. This reduces the number of independent parameters by one.

2. Results of the Computer Studies

A computer solution for the first case, where there are two parabolic velocity profiles, was carried out for the two experimental systems. The concentration profiles and Nusselt-number curves for these cases are included in Appendix D with the remainder of the information pertaining to the "GRAGRA" program. A few other cases of interest were also solved.

Figure 33 is an example of the concentration profiles which may be expected for the exposure of two phases where the average velocity of the gas phase is twice that of the liquid interface and the mass-transfer control is three-quarters in the liquid phase. The gas and liquid have equal diffusivity groups. Figure 34 shows the results for the same situation with the mass-transfer control three-quarters in the liquid. Figure 35 is a comparison of the average Nusselt number, defined as $K_c(av)L/D_g$, as a function of the gas-phase Graetz number, $D_g L/U_m b^2$. As the Graetz number approaches zero, the average mass-transfer coefficient approaches infinity with a half-power dependence upon the length of exposure, L. Therefore, Nusselt approach infinity with decreasing L with a half-power dependence upon distance. The middle curve indicates the case where control is equally divided between the two phases, while the other two cases are those considered in Figs. 33 and 34.

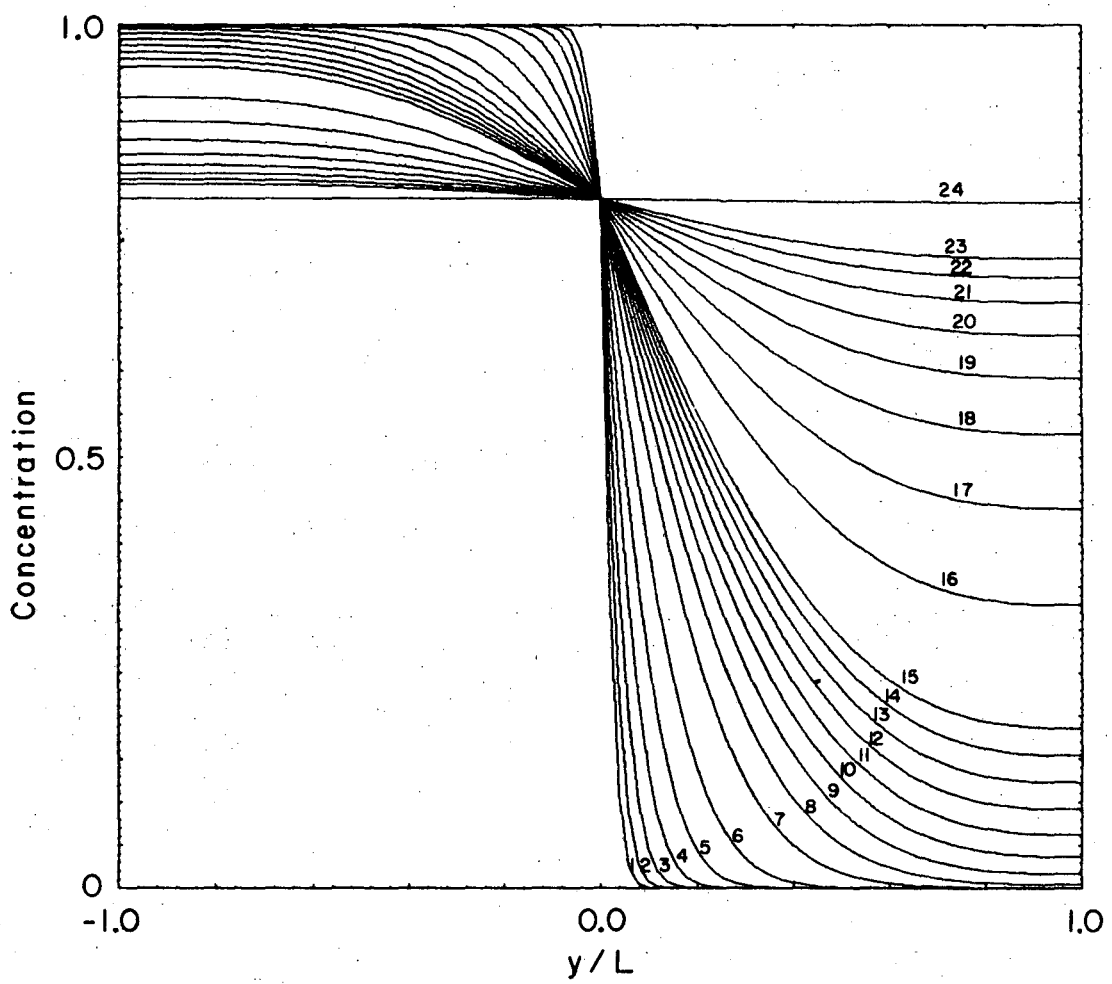

Fig. 33. Theoretical concentration profules for various values of Graetz number for two streams flowing at the same velocity, with 3/4 of the mass transfer resistance in the upper stream.

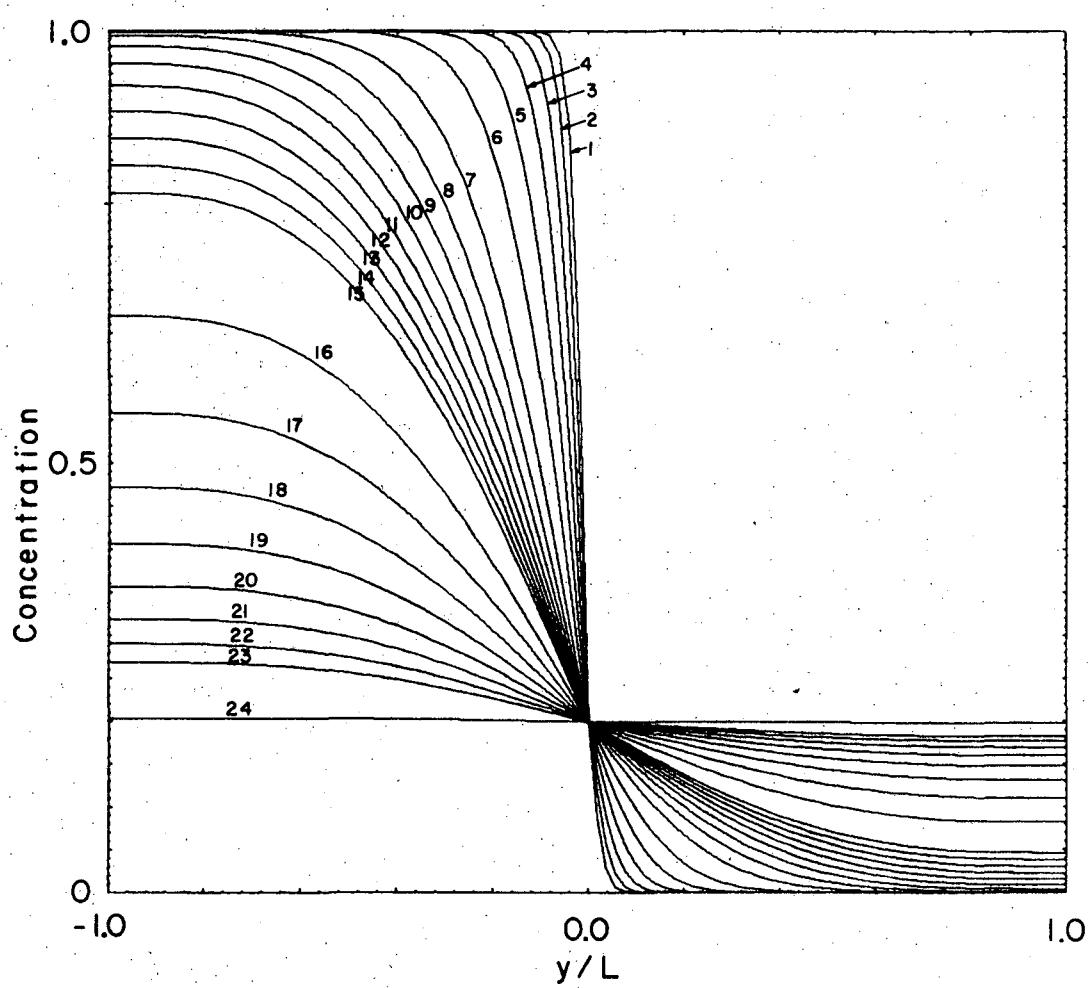

MUB-11316

Fig. 34. Theoretical concentration profiles for various values of the Graetz number for two streams with the same properties flowing at the same velocity. The resistance to mass transfer is 3/4 in the lower phase.

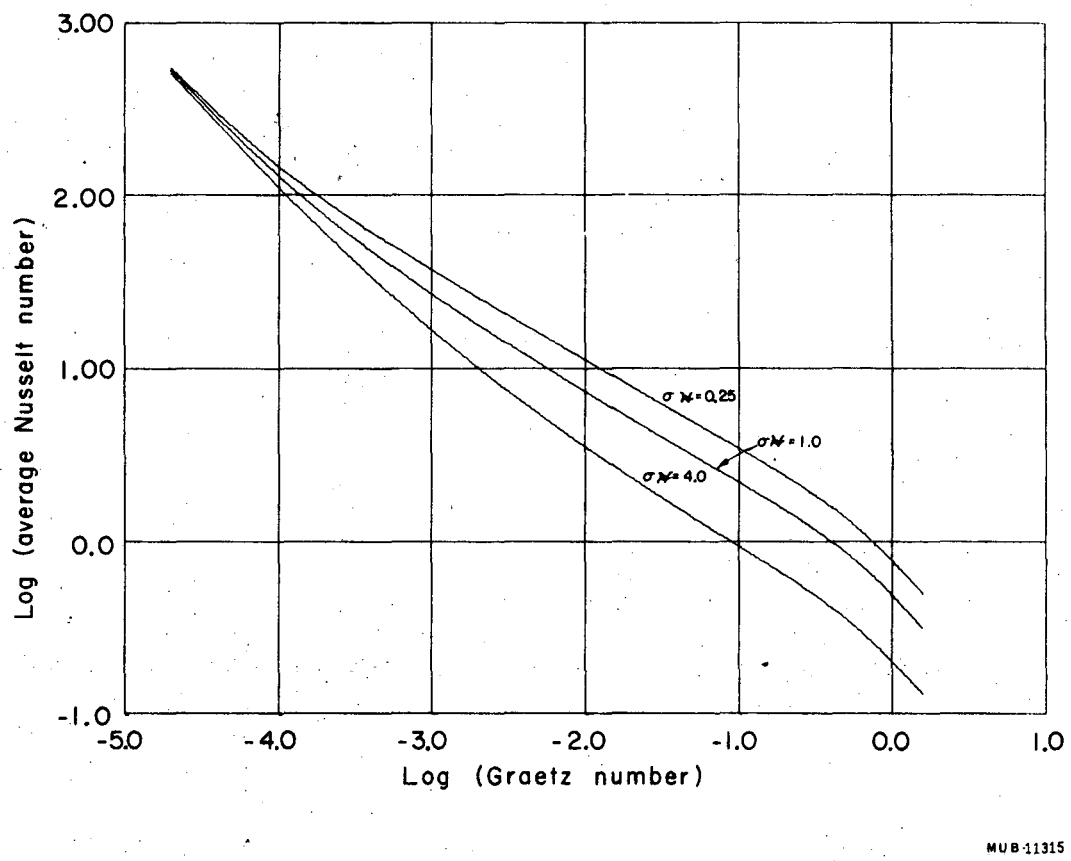

Fig. 35. Overall Nusselt number as a function of Graetz number with various degrees of control in the upper phase as the parameter for interphase mass transfer between phases with equal velocities.

The second program, with the velocity of the liquid phase a constant, could be used to find a general solution to the mass-transfer problem. Five different values of the control parameter, varying from 80% to 20% gas-phase-controlled were chosen, and for each, the velocity parameter U_m/U_0 was varied from 0.5 to infinity in seven steps. The results for the local Nusselt number based upon the initial concentration difference and for the cup-mixing concentration are given as a series of ten graphs in Appendix D, as a part of the information included with the "GRAPEN" program. Figure 36 is representative of the local Nusselt-number curves. It shows equal distribution of resistances between phases. For low values of the Graetz number the numerically computed derivative at the interface is quite inaccurate. The Nusselt numbers for Graetz numbers less than 0.001 are not shown because of this inaccuracy.

This program was used to compare interphase mass-transfer coefficients with those predicted by the addition of the two individual resistances to mass transfer. It has been found that when the resistance to mass transfer is evenly divided between the two phases the greatest deviations from additivity occur. The case of 50% gas-phase control was used as the test case. The penetration model was used in the liquid phase and the computer-solved case of mass transfer to a confined phase with an interfacial velocity was used as the gas-phase model. The ratio of the actual local mass-transfer coefficient to that predicted by addition of the two resistances is plotted as a function of Graetz number $(D_g x/U_m b^2)$ for a value of the velocity parameter, U_m/U_0, equal to 4 in Fig. 37 as a solid line. The addition of resistances is very much in error at high Graetz numbers (by as much as a factor of 4) because of the changing nature of the gas-phase resistance as saturation is approached by this phase while the liquid-phase resistance does not change. Thus we are in error because one of the conditions for the addition of resistances has been violated. If the same comparison is made using the local driving force in the calculation of Nusselt numbers, the dashed curve in Fig. 37 is the result. It is evident that the use of the cup-mixing concentration in the gas phase as the local driving force overcorrects in the area of very high concentration. The other two curves on the figure are comparisons of average Nusselt numbers. The upper curve is based on the local driving force, while

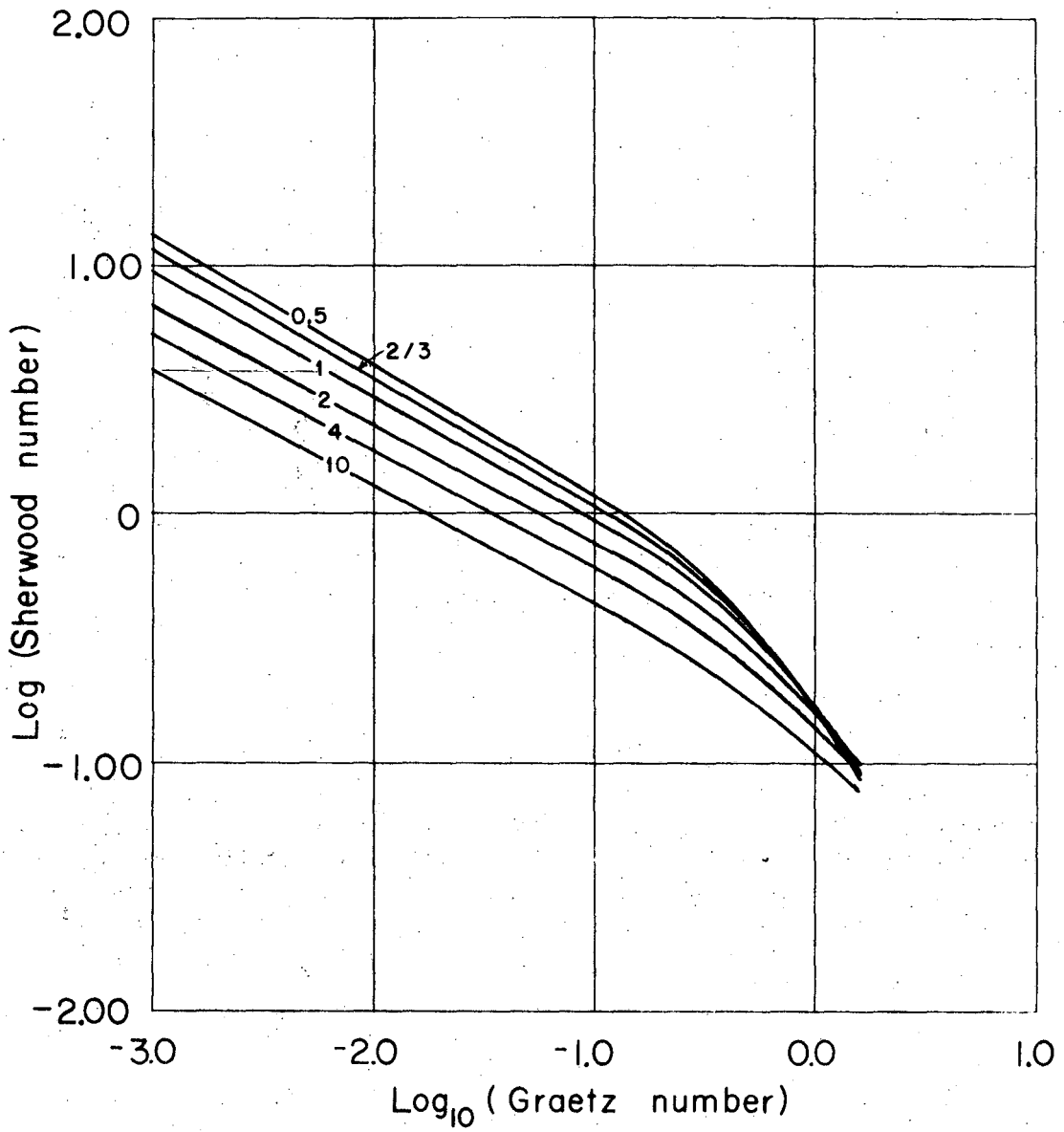

MUB-11252

Fig. 36. Local Nusselt number curves as a function of Graetz number for different values of the parameter, U_m/U_o. A constant velocity is assumed in the liquid with mass transfer control equally divided between phases.

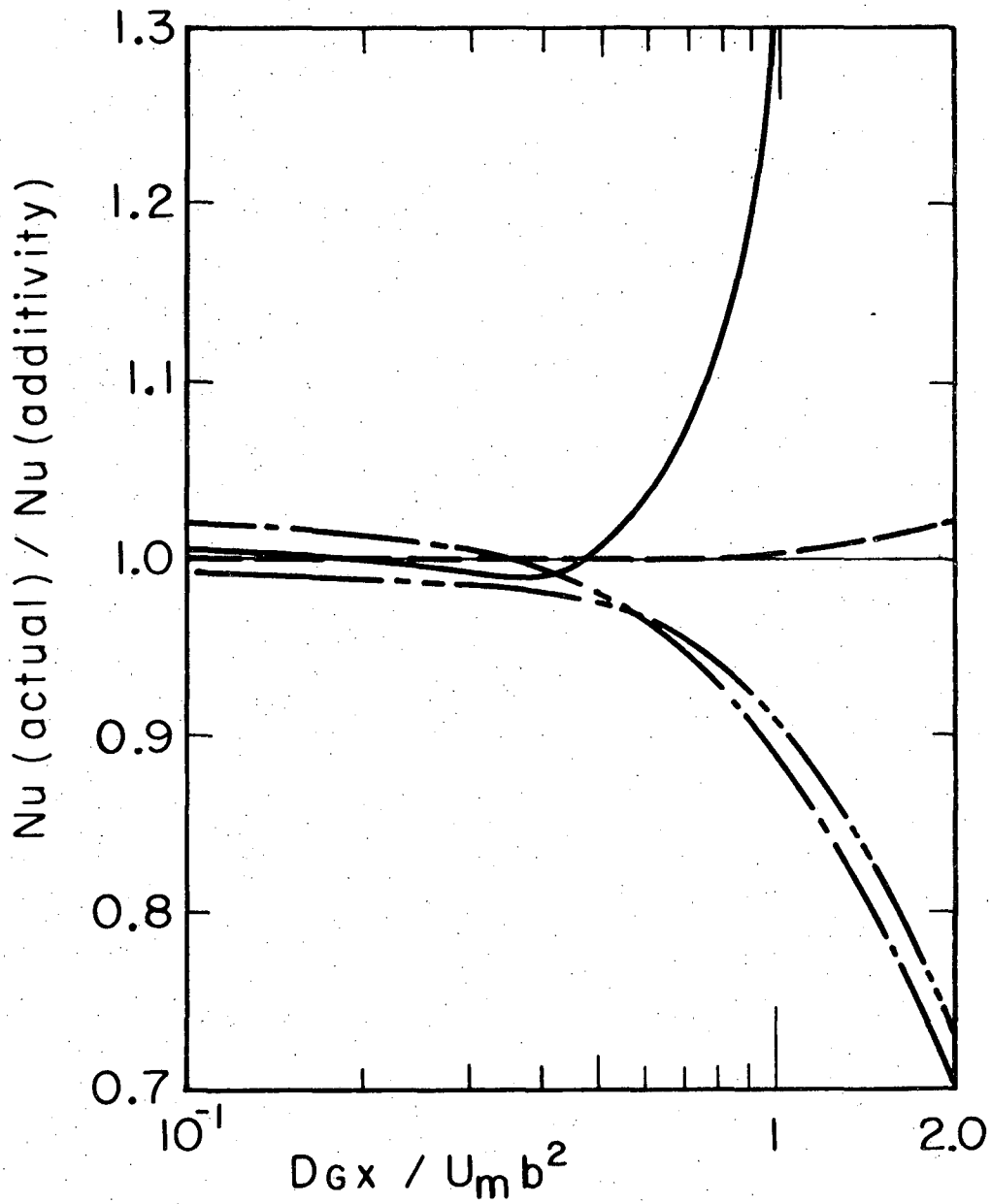

MUB-11194

Fig. 37. The ratio of the Nusselt given by the exact solution to that given by the addition of resistances as a function of Graetz Number.

the lower one is based on a logarithmic-mean driving force. In the area of experimental interest, between a Graetz number of 0.1 and 1.5, the average Nusselt number based on the initial driving force may be predicted to within 2% by the addition of the two independent resistances to mass transfer. The average Nusselt number based on the logarithmic-mean driving force yields a prediction that is much less accurate. Therefore the former is preferred because it is more simply calculated and more accurate.

The results of the third program have already been discussed in Section A of this chapter. It postulates two phases of infinite extent with a constant velocity in the liquid and a linear velocity profile in the gas. Care must be taken to insure that there is no significant penetration of either phase. Hence the solutions were limited in length of exposure due to the limitations of the storage space in the computer. The addition of resistances gave excellent agreement with theory, so that this program is not really necessary except for estimating the extent to which this type of solution is valid and to check the addition equation.

D. Countercurrent Interphase Mass Transfer

Interphase mass transfer is normally carried out in countercurrent flow in industrial practice. The fundamental difference between cocurrent and countercurrent flow is that in the countercurrent case a flow reversal occurs in one of the phases. Only molecular diffusion may occur across this plane. If the gas-phase velocity is rapid compared to that of the liquid phase, only a small difference in mass-transfer coefficient is observed between the two types of flow. However, if the flows rates are comparable about 50 cc/sec in both phases) a 20 to 30% difference may be observed between the two. In single-phase mass transfer (Chapter III, Section B-3) it is found that the resistance of the area between the interface and the flow reversal is that of an essentially stagnant layer. If we are considering interphase mass transfer in the flow between two flat plates, the resistance of the liquid phase must be added to the two assumed for the gas phase alone in Eq. (3-38). The resulting equation is

$$\frac{1}{K_{C_{avg.}}} = \frac{1}{k_{GZ_{avg.}}} + \frac{1}{k_{F_{avg.}}} + \frac{H}{k_{L_{avg.}}} , \qquad (4\text{-}38)$$

where the individual gas-phase resistances are defined in Eq. (3-39) and the liquid-phase mass-transfer coefficient is defined as

$$K_{L_{avg}} = 2\left(\frac{DU_0}{\pi L}\right)^{1/2} \quad . \tag{4-39}$$

The fact that the counterflow models chosen by King[41] showed an appreciable deviation from additivity suggests that this model might predict mass-transfer coefficients slightly higher than one would actually measure.

E. Experimental Investigation of Interphase Mass Transfer

No good experimental studies of interphase mass transfer have been carried out under conditions where the situation could be analysed using the convective equations of change. The series of experiments discussed in this section are the interphase extension of the ones discussed in the experimental sections of Chapter III. It was desirable to choose a system of gases and liquid which had roughly the viscosity of water, was nontoxic, and most important, divided control of the mass transfer between the two phases. Initial calculations showed that the ether-water system would be a desirable mixture, since water is available in such large quantities. Experiments with such a system proved to be unsatisfactory, because the liquid interface became covered with surfactants, which drastically altered the results. These experiments are discussed in Chapter V. After this system proved to be unsatisfactory, we decided to shift to dilute solutions of ether in ethanol. These experiments proved more satisfactory.

1. Cocurrent Experiments

Two series of experiments were carried out in cocurrent flow. In the first, carbon dioxide was the gas phase, while in the second, the gas was helium. In both cases solutions of reagent grade ether (about 0.5 mole percent) in 100% ethanol were used as the liquid. Both gases were saturated with ethanol in the humidifier, so that only ether would be transferred. The constant, $(D_g/D_l)^{1/2}\mathcal{H}$, is equal to 0.427 in the first series while in the second series it is 0.948. Thus the control lay about 80% in gas phase in the first series, and 50% in the gas in the second series. Because of the low concentration of ether, the maximum drop in the interfacial temperature was less than 0.1°C. Hence this factor was not a problem in these runs.

The results of this study are tabulated at Table C-7 in Appendix C. Generally speaking, the interphase studies were much more difficult to control, because the liquid-phase hydrodynamics played a much more important role in the mass transfer. No variations of liquid level could be tolerated. The fact that the liquid concentration was always decreasing made it necessary to remove samples from the system and readjust the liquid level frequently. Because concentration profiles require the maintenance of control over the apparatus for several hours, none were attempted in the interphase studies.

Each series of runs was carried out using four different liquid flows and several different gas flow rates. Forty four runs were made in all. It was found that if the gas rate was greater than about 200 cc/sec, somewhat greater mass-transfer coefficients were observed than could be explained by laminar theory. Since this was not observed in the analysis of the single-phase case, it must be concluded that some rippling of the liquid interface was being induced. Towards the end of the runs some difficulty was experienced with the carrier-gas flow to the chromatograph. As a result there is some uncertainty concerning some runs in the helium series.

The simplified model could be applied to all runs in which a sufficiently low fraction saturation was obtained to make the assumption of an infinite gas phase applicable. In Fig. 38, all gas-phase flow rates above 60 cc/sec satisfy this condition. The results are given as a plot of $k_c(av)(L/U_0D)^{1/2}$ as a function of the group a^2D_gL/U_0^3 for different values of the parameter $(D_g/D_l)^{1/2}\mathcal{H}$. The line that shows complete control of the gas phase is given for comparison. The triangles give values for carbon dioxide, while the circles are the points for helium. The theoretical lines are shown to agree with the theory within the limits of the accuracy of this series of experiments. With the added difficulties, it is estimated that the experimental error is about 15 to 20%. A few points were deleted because the data were of a dubious nature, due to changes in the flow of the Carrier in the chromatograph. The tendency for the values at high values of the abscissa to be high is possibly due to rippling of the liquid interface at relatively high gas flows, while the tendency to be low at low values is attibutable to the curvature of the velocity profile in the gas phase and the presence of the wall. Except for a few runs which were discarded, the error is less than 15%.

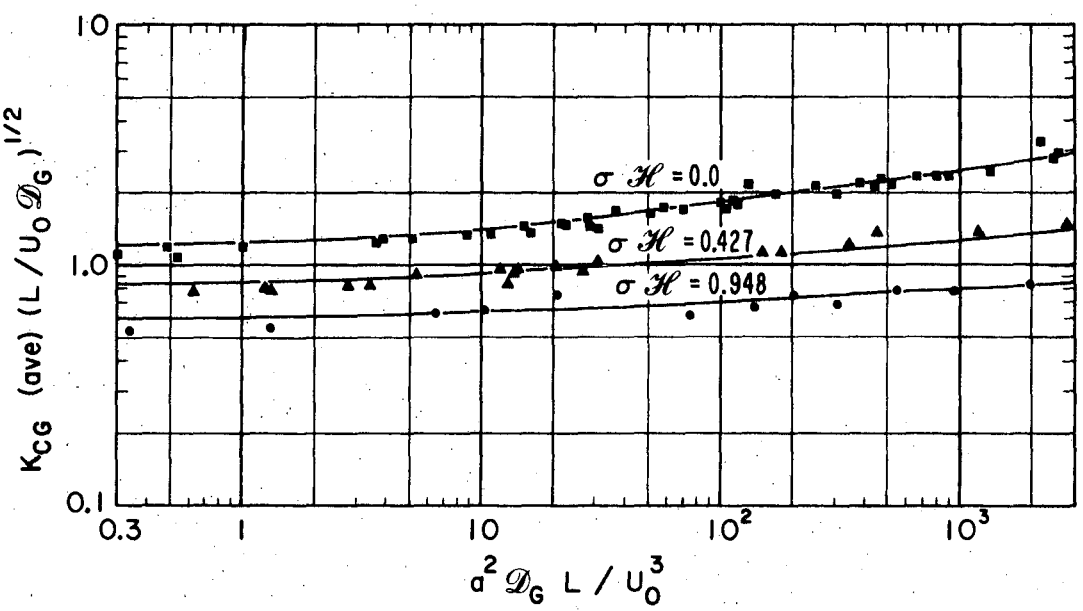

Fig. 38. Cocurrent gas phase controlled and interphase mass transfer data ▮ gas phase controlled data, ▲ data for the evaporation of ether into carbon dioxide, ● data for the evaporation of ether into helium, —— theory for the corresponding data.

Since it is not possible to present the comparison of all data with the exact computer solution, some typical data were selected. In the carbon dioxide series, Runs 222 to 228 were used. In this case the liquid rate was 30.86 cc/sec. Note that in Fig. 39 the experimental points indicated by the squares are in substantial agreement with the theory, which is shown as a solid line. As has been mentioned previously the points at high flow rates (low Graetz number) show a slight positive deviation from theory. The other point in disagreement with theory is probably a piece of spurious data. The helium runs for the same liquid rate (Runs 243-247) are shown as circular points. The theoretical prediction for these data is shown as a dashed line. The high-flow-rate run is considerably spurious. The remainder of the data are compared in tabular form as a part of Table C-7. Generally the agreement with the theoretical line is of the same order as has been illustrated in Fig. 39.

Within the experimental error of the method, data followed theory in all but a few cases. We may conclude therefore that a valid model has been developed to predict interphase mass-transfer coefficients in laminar cocurrent flow.

2. Countercurrent Interphase Experimental Data

The final runs in this study involved mass transfer in countercurrent flow with the control of the mass transfer distributed between the two phases. Generally speaking these runs were a repetition of the previous series with the liquid phase flowing in the opposite direction. The emphasis was laid on helium data because the control was more evenly divided between the phases in this case. The results of these experiments are tabulated in Table C-8 in Appendix C. In runs 258 to 283 the carrier gas in the channel was helium, while carbon dioxide was used in runs 284 to 288.

In Fig. 40 the data are compared with the theory developed in section C of this chapter. Runs 258 to 262 were chosen as representative of the helium data, while the carbon dioxide data for runs 284 to 288 are also shown. The liquid flow rates in these series of runs were 61.82 cc/sec and 39.86 cc/sec, respectively. The solid line in each case represents Eq. (4-38), which postulates a stagnant region between the flow reversal and the interface,

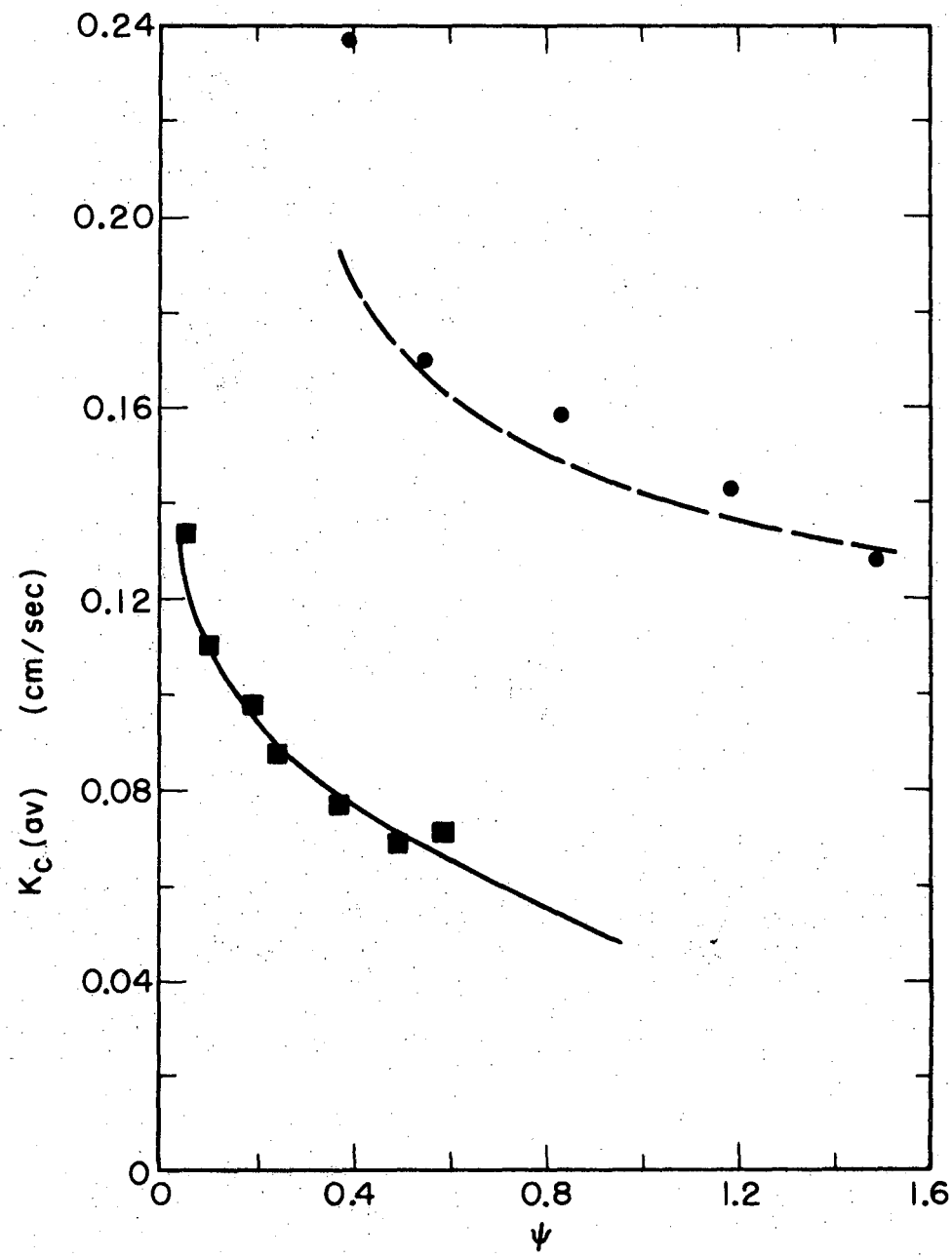

MUB-11196

Fig. 39. Interphase mass transfer and a comparison with an exact computer solution: ▮ Carbon dioxide data, —— carbon dioxide theory ● helium data, --- helium theory.

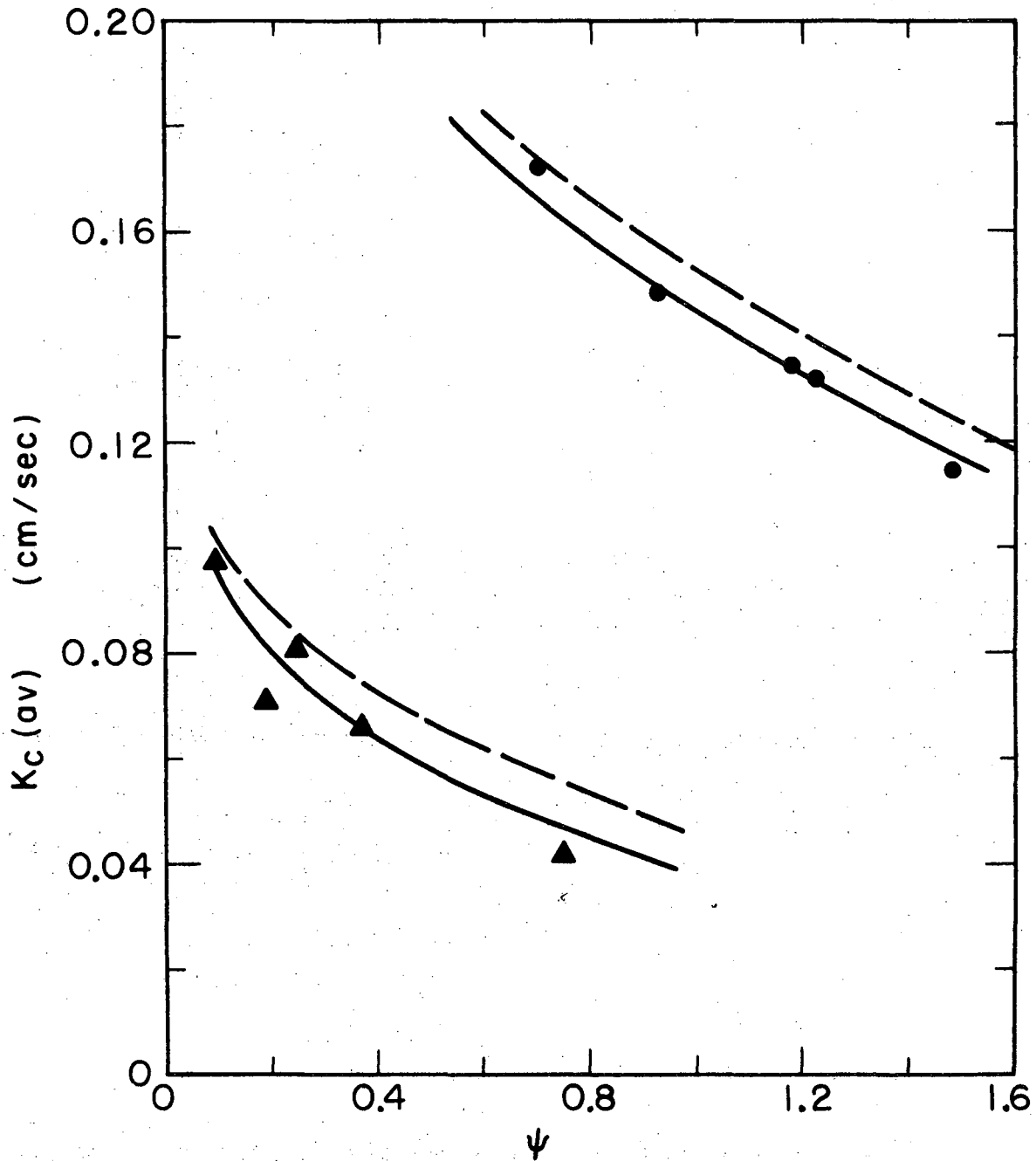

MUB-11195

Fig. 40. Interphase countercurrent mass transfer data and theory. A CO_2 data, o helium data, —— countercurrent theory ---- Theory with no flow reversal.

while the dotted line represents the addition of the Graetz solution and a penetration model with no regard for flow reversal. The theoretical curves for the experimental conditions are calculated by means of a simple computer program and are listed as a part of Table C-8. It is evident that the helium data, shown by circles, follow the predictions of the simple model for interphase mass transfer proposed in Section C of this chapter. The carbon dioxide data are more scattered, and agreement with theory is not as good as in the helium runs.

The trouble in carrier-gas control experienced in the previous series of runs became more acute in the present series. There seems little doubt that this trouble led to a good deal more inaccuracy in the carbon dioxide data than in the previous runs.

F. Conclusions

The following may be concluded from the studies in interphase mass transfer:

(a) A model has been developed for laminar cocurrent interphase mass transfer. For normal lengths of exposure, this model agrees to within 2% with the prediction derived from the addition of the resistances of the two phases, provided the correct model is used in both phases.

(b) A computer solution has been made of the problem of interphase mass transfer between two streams in cocurrent laminar flow between two flat plates. This solution is of particular use to the present study in that it provides the theory necessary when saturation is approached in the gas phase.

(c) The cocurrent experimental data, which are probably only valid to about 15% agree with the model developed for this study. That the data are high at high values of the parameter $a^2 D_g L/U_0^3$ may attributable to the induction of ripples by the high gas flow rate. However there was no visible change in the condition of the interface. At the other end of the scale, low values are attributable to penetration of the gas phase.

(d) Countercurrent data generally agreed with the model postulated for the laminar countercurrent flow of two streams. This postulates that the liquid phase obeys penetration theory, the area between the interface and the

flow reversal is stagnant, and the area between the flow reversal and the wall obeys the Graetz solution. The three models are reciprocally added, and the overall mass-transfer coefficient is calculated. The error in these data is slightly higher than in the previous runs because some difficulty was encountered in the control of the carrier gas flow to the chromatograph.

V. EFFECT OF A SURFACTANT FILM UPON INTERPHASE MASS TRANSFER

Contamination of interfaces by surfactant films has been a subject of continuing interest to engineers in the field of mass transfer for the past 15 years. In our case the topic arose when a series of mass transfer data points for the evaporation of ether from water into various gases gave results that did not follow theory. After the equipment was checked for possible operational difficulties, it was decided to check the interfacial velocity, which was found to be about 15% of the expected velocity. Upon examination of two papers by Merson and Quinn,[40,49] in which the contamination of horizontal surfaces is discussed, it was decided that contaminants in the water caused a surface film to form. The resulting surface stagnation caused a change to occur in the velocity profiles near the interface and in this way drastically altered the mass-transfer coefficients. This chapter is devoted to a study of these data and the behavior of surface films.

A. Previous Investigations

Recent publications in the field of mass transfer contain many references to the occurrence of surface films upon virtually every kind of gas-liquid mass-transfer device used. A review of the observations of others is desirable for comparison. The experiments have been classified according to the vertical orientation to the liquid interface.

1. Vertical Surfaces

This class of devices includes laminar jets and different types of wetted-wall columns. Where surface active molecules are present, a stagnant film about 2 cm or less in length is observed at the downstream takeoff point. Several examples have been reported. Matsuyama in his laminar-jet study absorbed carbon dioxide into aqueous barium hydroxide solutions.[47] He found that the precipitated barium carbonate tended to collect in a stagnant film at the receiver. Cullen and Davidson in 1957 found that the addition of a surfactant (Teepol) to a jet of water caused a stagnant film to appear at the

liquid collector.[12] Stagnant films of about the same length as those observed in laminar jets have been found by Wendel[74] and Lynn, Straatemeier, and Kramers[16] in their studies of mass transfer in short wetted-wall columns. Motion within the films has been described as a "pinwheel" type circulation. Danckwerts and Kennedy found that their rotating-drum apparatus manifested the same type of behavior.[15] A photograph of the interface of the apparatus[38] is shown in Fig. 41. Water enters at the 12 o'clock position, is contacted with a gas, and is removed at the 3 o'clock position. The white band at the bottom of the exposure is powder, that has collected within the stagnant film. Since the length of the exposure is about 6 cm, the length of the film appears to be about 1 cm. They too found lazy irregular motion within their film.

2. Spherical Geometry

Whether one is considering flow over a solid sphere or the movement of bubbles and drops through a medium, one finds that if a surfactant is present, a film or cap accumulates on the downstream side of the sphere. In an experiment with flow of a liquid in a laminar regime over a string of spheres, Davidson, et al. found that the presence of a surfactant prevented mixing of the fluid between spheres.[16] More recently Ratcliffe and Reid have found that the same sort of phenomenon occurs with a liquid-liquid system.[56,57] They found that the cap on the downstream side of the solid sphere attained an equilibrium length.

A vast amount of literature exists concerning the motion of bubbles and drops. Generally speaking, the rate of fall is retarded by the existence of a cap of surfactant on the downstream side of the bubble or drop. Levich[45] and Davies and Rideal[17] go into considerably more detail on the subject.

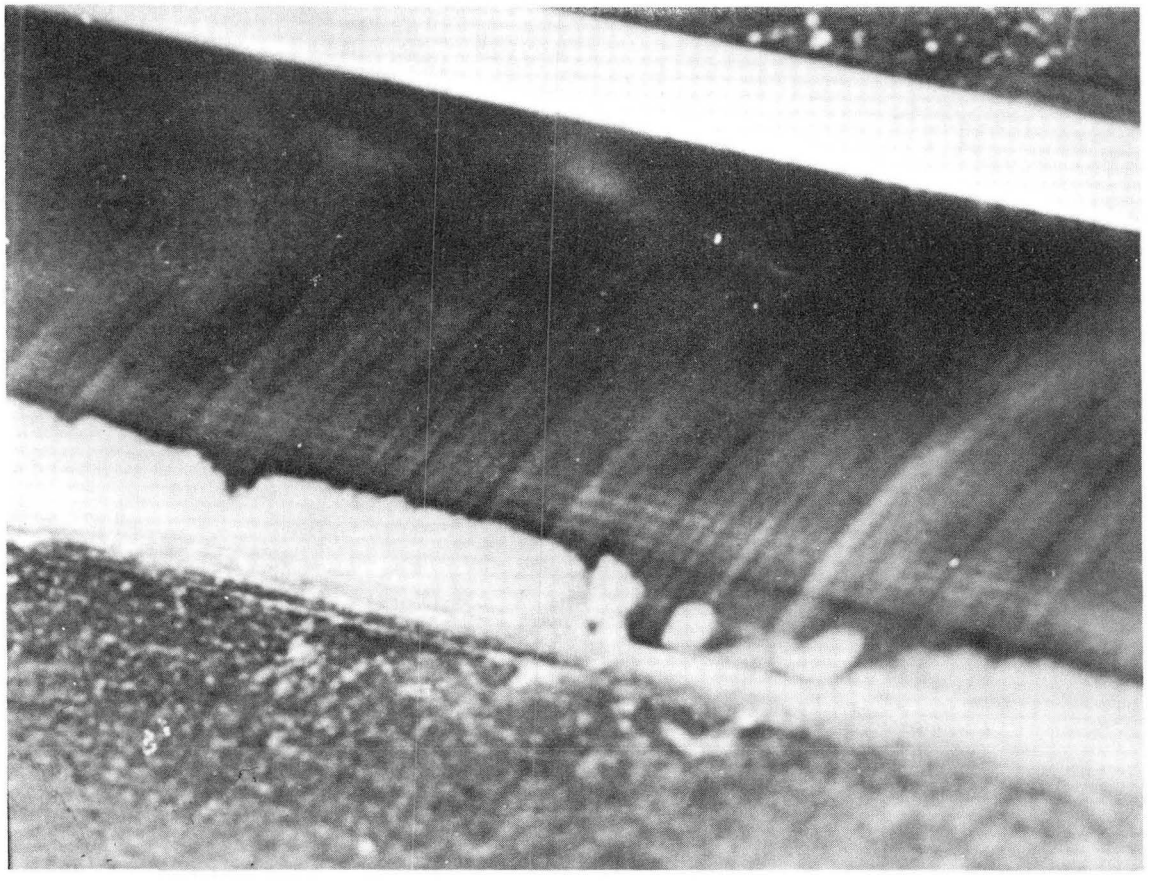

ZN-5611

Fig. 41. End effect in rotating-drum apparatus after Kennedy.

3. Horizontal Surfaces

Merson and Quinn in carrying out absorption with a radially moving horizontal interface encountered stagnation when the interfacial tension exceeded 10 dynes/cm.[48] In their experiment, liquid issued radially onto a horizontal surface and was removed at the wall of the cylindrical containing vessel. The exposure to the other medium occurred during the radial motion. It was found that when water was used as the radially flowing fluid and such substances as benzene, carbon dioxide and air were used as the other medium, the surface became stagnant with the film of surfactant building up from the wall towards the center of the apparatus. The entire interface was quickly stagnated. The data for the transfer of carbon dioxide into water and benzene into water when the surface was stagnated indicated that the mass-transfer coefficients fell between a theory for the case where there was motion of the interface uninhibited by surface-active agents and one for the case where the surface was entirely stagnant. This indicated motion might be attributable to circulation patterns within the film on the interface.

Subsequent to this study, Merson and Quinn studied the growth of films on a horizontal surface using a rectangular channel (Fig. 42).[49] Their main conclusions concerning naturally-occurring contaminants in distilled water are as follows:

(a) The surfactants contained in their water tended to form films that were in an expanded state. Adsorption into a moving interface was quite rapid and was definitely the rate-determining step in the growth of films.

(b) The greatest pains must be taken to exclude any other surfactants from an experimental device.

(c) Once formed the film is very difficult to disrupt and tends to reform quickly after being disturbed.

(d) Circulation patterns such as the one shown in Fig. 42 were observed within the film.

(e) The concentration based upon controlled runs carried out with dodecyltrimethyl ammonium chloride was estimated to be 0.2 to 0.4 weight parts per million. It was thought likely that the surfactant was ionic in nature.

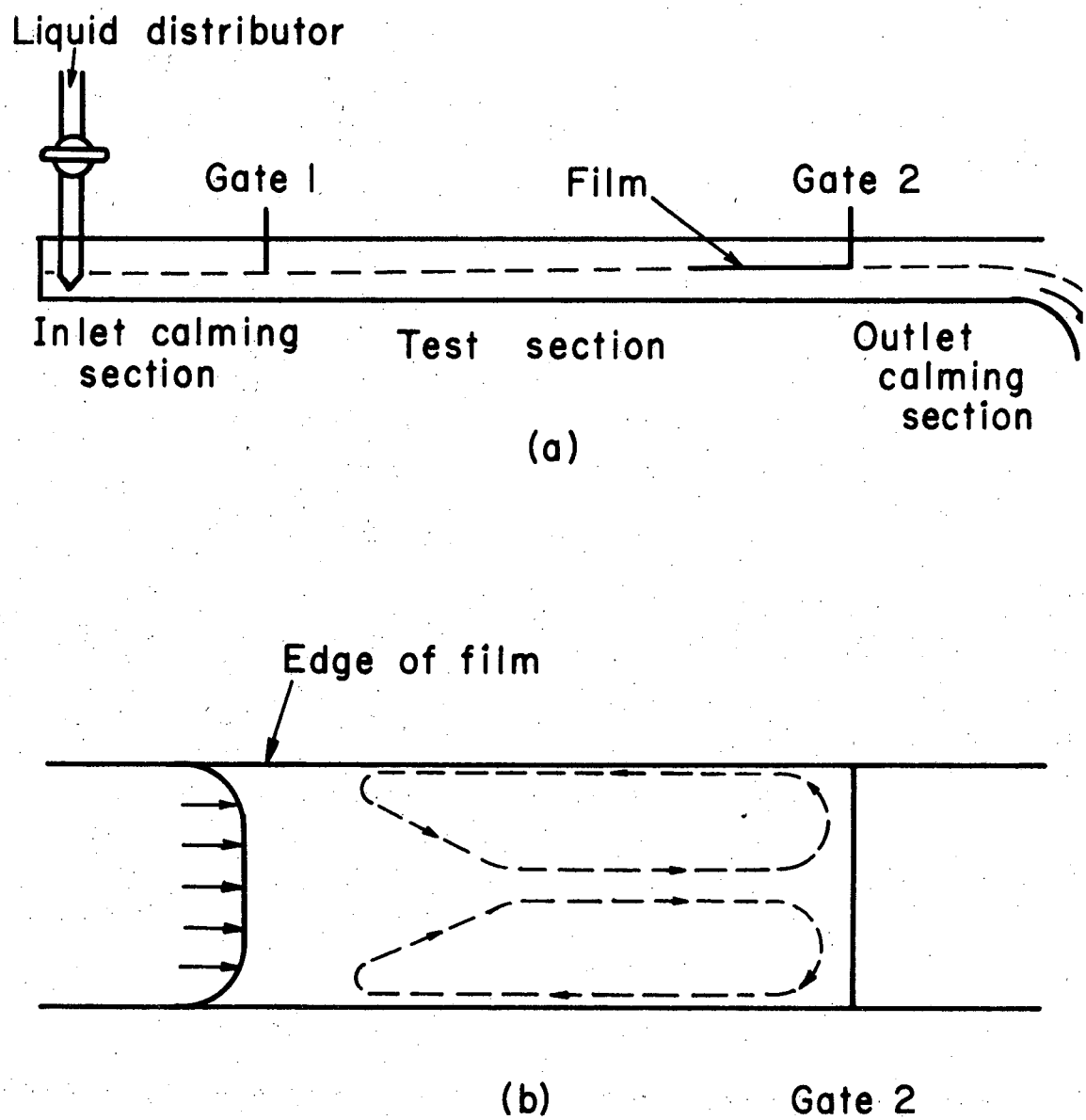

MUB-11289

Fig. 42. (a) Channel used by Merson and Quinn for observation of film growth; (b) surface flow pattern observed by Merson and Quinn.

During the writing of this report, a paper has appeared by Acrivos and Kashiwagi,[1] which deals with the flow of different fluids issuing from a nozzle and moving down a plane that is slightly inclined to the horizontal. At the downstream end of the plane there is a stagnant pool of the liquid. They found that materials with high surface tension—such as water, glycerin, and formaldehyde—tend to exhibit a backflow near the edges of film, while materials with low surface tensions—such as methanol, 1-octanol, and benzene—show no backflow tendency. They found that the addition of a surfactant to 1-octanol creates a backflow. This confirms the work of Merson and Quinn who also reported a backflow near the wall. According to this report one would expect that water would be affected by surfactants, while ethanol would be relative free from such disturbances.

These last two studies on essentially horizontal surfaces are applicable in a direct way.

B. The Present Study

1. Experimental Data

The ether-water system was chosen for the study of distributed mass-transfer control because the physical size of the original apparatus precluded consideration of most other solvents. Ether was evaporated from approximately 0.5 mole percent solutions in water into three gases—carbon dioxide, oxygen, and helium—in the channel. For each gas a series of runs was carried out at different gas flows for each of three liquid rates (15.43, 30.86, and 51.64 cc-sec). Since it was assumed that the experiments would agree with the theory for interphase mass transfer which was presented in Chapter IV, the data (see Appendix C) for the different gases were plotted on graphs of the type suggested by the theory. Figures 43, 44, and 45, in which $K_{avg}(L/U_0D_g)^{1/2}$ is given as a function of a^2D_gL/U_0^3, show the data for the three different gases as well as the theoretical line for each gas. The physical properties of the system are discussed in Appendix E. It was observed that the experimental mass-transfer coefficients were lower than the theoretical values by at least a factor of two. This fact along with the visual observation that the interface was moving much more slowly than one would expect for the given hydrodynamic conditions led to the conclusion that the conditions at the interface were being affected by accumulation of surfactants.

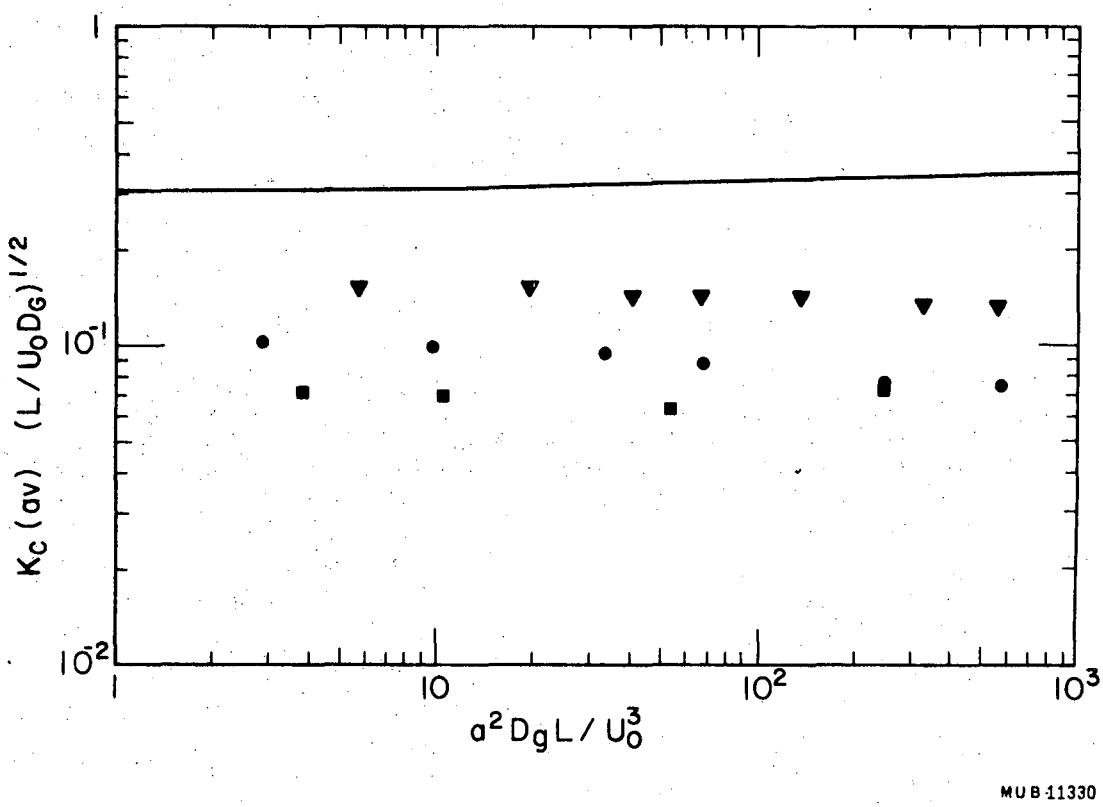

Fig. 43. Data for the evaporation of ether into oxygen from dilute aqueous solutions. —— Theory, ▼ Q_l = 15.43 cc/sec, ● Q_l = 30.86 cc/sec, ■ Q_l = 51.46 cc/sec.

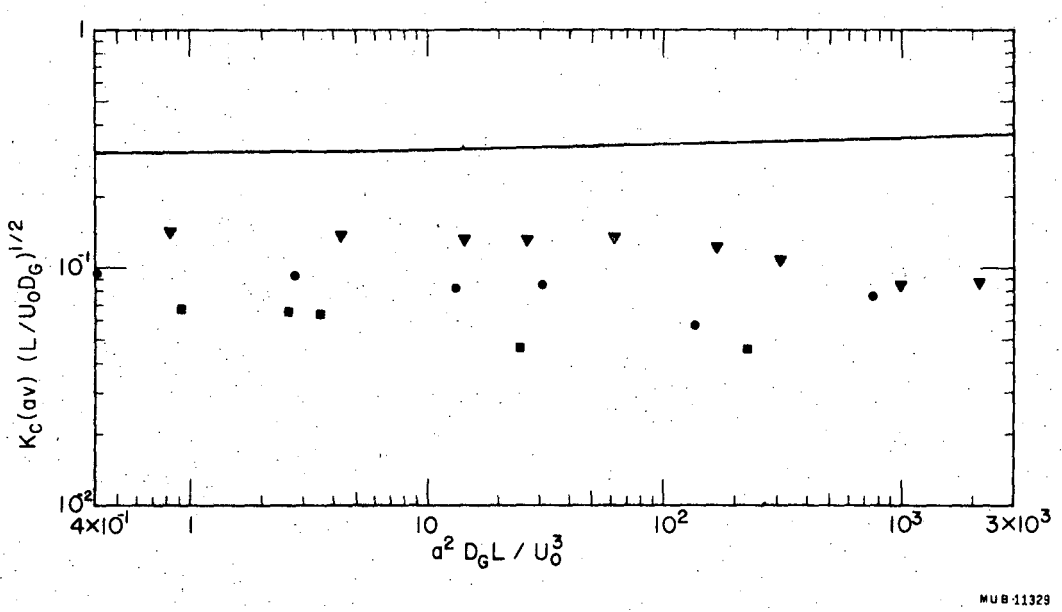

Fig. 44. Data for the evaporation of ether into CO_2 from dilute aqueous solutions. —— Theory, ▼ Q_l = 15.43 cc/sec, ● Q_l = 30.86 cc/sec, ■ Q_l = 51.46 cc/sec.

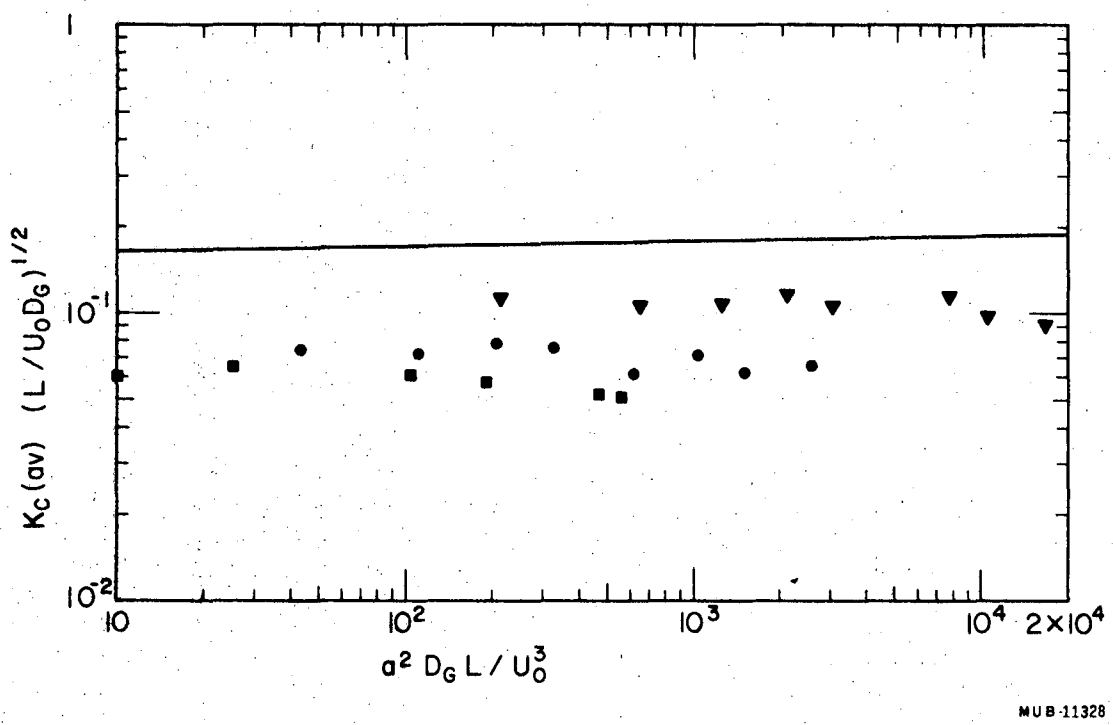

Fig. 45. Data for the evaporation of ether into helium from dilute aqueous solutions. —— Theory, ▼ Q_l = 15.43 cc/sec, ● Q_l = 30.86 cc/sec, ■ Q_l = 51.46 cc/sec.

The water used in the study was ordinary building distilled water, which had not been treated by an ion-exchange column. Furthermore, it was exposed to a large system which could have contained many sources of surfactant molecules (for example, pumps and valves). Finally a recirculatory flow system was used for the liquid phase; this would tend to hold captive any dissolved surfactants.

Small bubbles were introduced into the liquid side of the channel to facilitate observation of the interfacial motion. Free motion of the interface could not be detected at any point in the channel. Since observation was quite difficult near the inlet of the liquid it is possible that some motion occurred in this region. Within the film, a circulation pattern similar to that found by Merson and Quinn and reproduced in Fig. 42 was observed.[49] An interfacial velocity of about 10 to 20 percent of the calculated free velocity was observed in the center of the channel. The observation was made at a liquid rate of 15.43 cc/sec. The fact that the channel was not especially designed for the injection of material onto the interface made such observations relatively difficult.

It was felt that if the surface could be temporarily released from the confining influence of the downstream divider plate, data might be taken before the surface became stagnant. To this end, the downstream portion of the outlet calming section was raised so that liquid would not touch the downstream divider plate and hence the liquid at the interface would be removed. The surfaces of the channel outlet and the divider plate were made nonwetting by coating them with paraffin. Runs that reproduced flow conditions of previous runs were made with the liquid not touching the divider plate. Data taken as little as a minute after the channel was filled reproduced the previous runs to within the accuracy of the method, even when the entire system had been thoroughly cleaned with hot chromic acid and then with acetone, before putting in a new solution. It must be concluded that the water available to this study must have contained a great deal of surfactant, or that the small amount of surfactant present had a great effect.

This preliminary analysis of the experimental observations indicates that the development of some theory would be helpful in the interpretation of data taken in this portion of the study. In particular the growth of films as well as motion within circulating films is considered important.

2. Theory of Growth of Surfactant Films

Since the exact nature of the surfactant present in this study is unknown, any theoretical development must be based upon some assumption concerning the physical state of the film. Merson and Quinn found that their contaminant was compressible in nature.[49] It is probably fair to assume that the same is true in the case of our study.

If a gas and a liquid are flowing cocurrently between two flat plates, and we assume that the liquid contains a concentration, Co, of surfactant contaminant, we would like to be able to assess the rate of film growth and the final equilibrium length of the film. A zero time is chosen at which the entire surface is moving and the film at the downstream divider has just begun to form. If we assume that the stagnant film obeys the ideal two-dimensional gas law, then Γ_s, the concentration in the stagnant portion of the interface, may be expressed as

$$\pi/\Gamma_s = kT \tag{5-1}$$

The surface pressure, π, in the stagnant portion of the interface is composed of two contributions. The moving part of the interface is assumed to be subject to no shear stress; however, the accumulation of a concentration on the surface causes a surface pressure which acts on the leading edge of the stagnant region. Its magnitude may be estimated by means of the two-dimensional ideal gas law,

$$\pi_m = \Gamma_m kT \quad . \tag{5-2}$$

The other contribution is the constant shear on the interface, caused by the two moving fluids close to the interface. Therefore we have

$$\Gamma_s(1) = \pi_\tau(1)/kT + \Gamma_m \quad . \tag{5-3}$$

If we assume that the velocity profile at the point of stagnation develops instantly, then the shear stress is a constant for any given set of flow rates.

Therefore it follow that

$$\pi_\tau = F_\tau/W = \tau_s A/W = \tau_s l \qquad (5\text{-}4)$$

and

$$\Gamma_s = \Gamma_m + \tau_s l/kT \quad . \qquad (5\text{-}5)$$

As a result of this argument one would expect the concentration profile at the interface at any arbitrary time after time zero to be as shown in Fig. 46. The interface between A and B is moving, while it is stagnant between B and C. A picture of the effect upon velocity profiles within the channel is included below the surface-concentration profiles.

When the molecules strike the stagnant film they are compressed by the shear stress to which they are submitted. As a result they may desorb back into the bulk. When the new liquid surface is exposed we would expect adsorption to take place. A material balance upon these two processes gives a value for the net rate of accumulation of contaminants at the interface:

$$\left\{\begin{array}{c}\text{Rate of increase}\\ \text{of material at}\\ \text{the interface}\end{array}\right\} = \left\{\begin{array}{c}\text{Rate of adsorption}\\ \text{on the moving}\\ \text{surface}\end{array}\right\} - \left\{\begin{array}{c}\text{Rate of desorption}\\ \text{from the Stagnant}\\ \text{film}\end{array}\right\} \qquad (5\text{-}6)$$

This precludes desorption in the moving surface and adsorption in the stagnant film. In the light of the physical situation, these assumptions seem quite reasonable.

The model for adsorption onto the moving interface is now considered. If we assume that there are no molecules on the interface at the instant of exposure and that molecules in the molecular layers directly below the surface are completely depleted by the subsequent adsorption at the interface, then it can be assumed that the driving force for adsorption is merely Co, the bulk concentration of surfactant. A penetration model like that shown in the moving of Fig. 47 is invoked here, and the result is

$$\Gamma m = 2Co\ N \sqrt{DX/\pi u_i} \qquad (5\text{-}7)$$

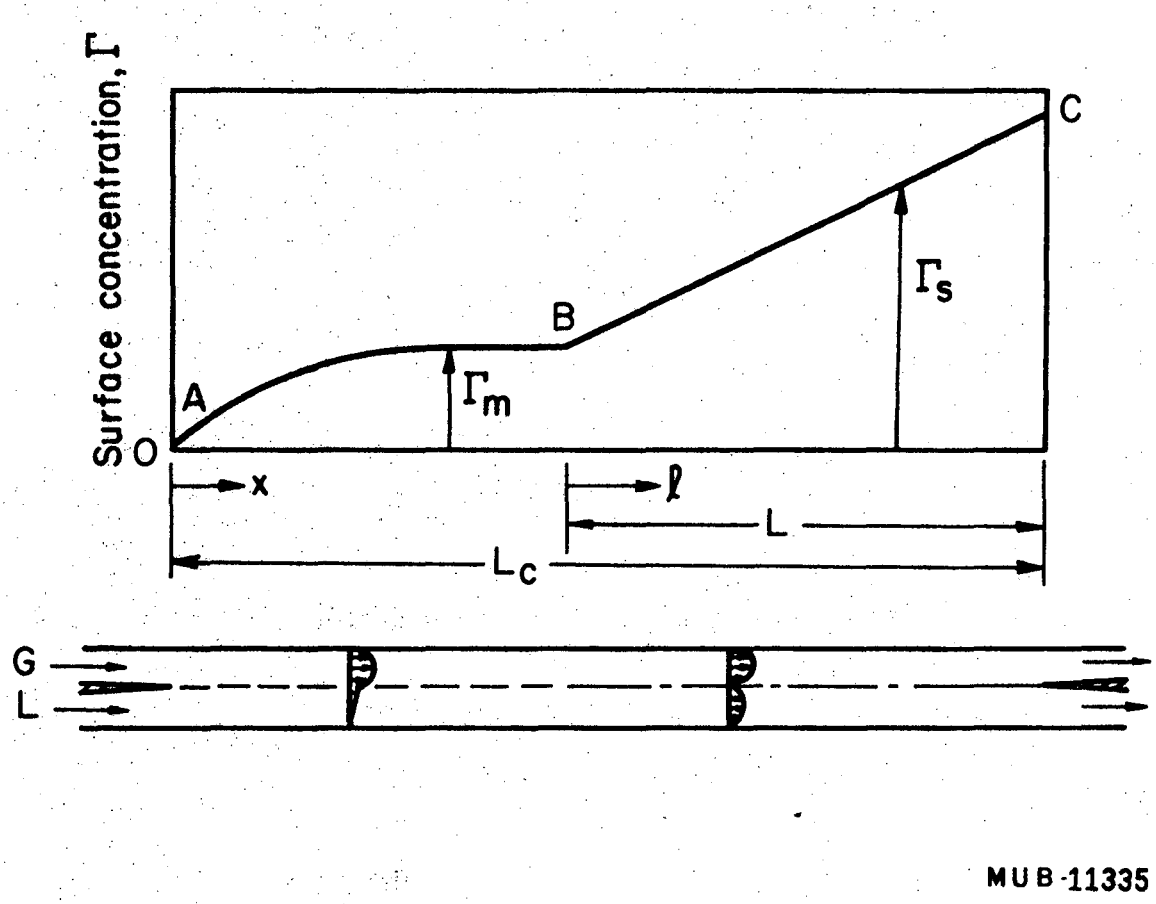

Fig. 46. Surface concentration diagram at a given time, also showing the corresponding channel position with velocity profiles.

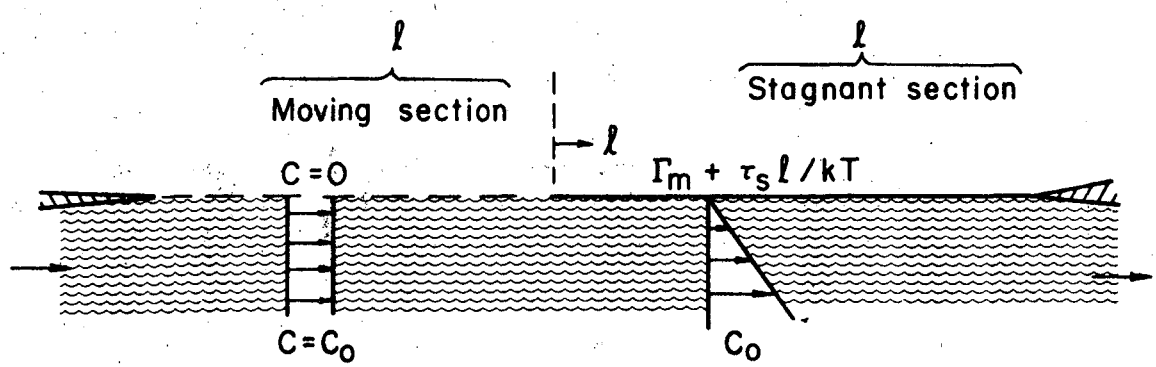

MUB-11288

Fig. 47. Hydrodynamic models for adsorption and desorption from a horizontal surface.

where N is Avogadro's number, D is the diffusivity of the impurity in the liquid, x is the distance downstream from the entry and u_i is the interfacial velocity. The total rate of adsorption is given given by the following relationship,

$$\phi = u_i \Gamma m \quad . \tag{5-8}$$

Actually this equation is only valid for very short exposures, since the subsurface will eventually have an appreciable concentration. A method of handling the back diffusion term is discussed by Ward and Tordai.[73] It is neglected here because of the short exposure times.

In the stagnant portion of the surface, the model shown in Fig. 47 for the stagnant part is used. Fluid with a concentration in equilibrium with Γm flows past a solid wall with a concentration profile $\Gamma m + \tau sl/kT$. Close to the wall the classical Leveque model for mass transfer applies. However, the wall boundary condition differs from the orginal solution. The driving force is assumed to be $(\Gamma s - \Gamma m)$ since in the area near the start there is equilibration with Γm. No simple solution was found for the problem with this boundary condition; however, Tribus et al.[63] have solved the Graetz problem for this condition and for a constant wall temperature (the condition solved for in the Leveque solution) for the case of heat transfer near the wall of a cylindrical tube. For constant wall temperature

$$NU_{cwt} = 1.3565\ (x^+)^{-1/3} \tag{5-9}$$

while for linearly varying wall temperature

$$NU_{lwt} = 2.0348\ (x^+)^{-1/3} \tag{5-10}$$

Therefore the solution is

$$k_l = (NU_{lwt}/NU_{cwt}) x 0.538 (D^2 a/l)^{1/3} \tag{5-11}$$

Therefore the rate of desorption from the film is

$$\phi = \int_0^L 0.807(D^2a/l)^{1/3}(\Gamma s(l) - \Gamma m)dl \qquad (5\text{-}12)$$

Integrating

$$\phi = 0.484\ (D^2a)^{1/3}\ \tau_s\ l^{5/3}/kT \qquad (5\text{-}13)$$

The total rate of adsorption is equal to the rate of growth of the film. Since at the arbitrary zero time Γm is fully developed, the excess amount at the interface at any given time is equal to

$$W\int_0^{Lc}(\Gamma-\Gamma m)dx = W\int_{Lc-l}^{Lc}(\Gamma s-\Gamma m)dx = W\int_0^L \tau_s l/kTdl = \tau_s L^2W/2kT \qquad (5\text{-}14)$$

The rate of accumulation of surfactant on the interface per unit width of the channel is

$$\frac{d(\tau_s L^2/2kt)}{dt}$$

As a result of the material balance (Eq. (5-6)) the following relationship may be written:

$$\frac{d(\tau_s L^2/2kT)}{dt} = (\tau_s L/kT)\frac{dL}{dt} = 2CO\ N\ \ Du_i/\pi(Lc-L)^{1/2} - 0.484(D^2a)^{1/3}\tau_s L^{5/3}/kt \qquad (5\text{-}15)$$

While an analytic solution for L as a function of time is highly improbable, the equilibrium length of the film may be found quite easily

$$\frac{X^{5/3}}{(1-X)^{1/2}} = 2.33\ \frac{CoN\ D^{1/6}kT}{Lc^{7/6}}\ \frac{u_i^{1/2}}{a^{1/3}\tau_s} \qquad (5\text{-}16)$$

Where $X = L/Lc$

A simple calculation of the film length for the conditions which existed in the channel show that a concentration of 10^{-6} molar would be sufficient to cover 90 percent of the interface. Hence the visual observation that a moving region, if it existed, was quite short, appears to be quite reasonable.

If it is assumed that the surface is completely covered, what interfacial velocity could be produced by desorption alone? We assume that there is infinitely fast adsorption, so that the interfacial concentration profile consists of only the stagnant part of the profile shown in Fig. 47. The velocity at any point is equal to the desorption rate from that point to the end of the exposure divided by the concentration at the point in question.

$$U(l) = \frac{1/(Lc-L)\int^{Lc} l\,\phi dl}{\tau_s\ l/kT + \Gamma m} = \frac{0.485(D^2a/(Lc-L))^{1/3}\ \tau_s(Lc-L)/kT}{\tau_s\ l/kT + \Gamma m} \tag{5-17}$$

The average velocity is

$$Uavg = K\int_0^1 \frac{(1-x)}{X + B}^{2/3} dX \tag{5-18}$$

where $X = l/Lc$, $K = .485(D^2a/Lc)^{1/3}$, and $B = \Gamma mkT/\tau sLc$

The maximum velocity occurs at the beginning of the exposure where

$$u(0) = 0.485(D^2a/Lc)^{1/3}\ \tau_s Lc/kT\Gamma m \tag{5-19}$$

For a typical run (Run 110 for example) if we assume a diffusivity of 10^{-5} and an initial area per molecule is about 10 $A^{\circ 2}$ the maximum velocity would be of the order of 10^{-2} cm/sec. It must therefore be concluded that this cannot be an important effect.

Another possible cause of motion within the stagnant film stems from the fact that the side walls on the channel are not infinitely far away. Since the shear stress upon the film at the wall is zero, one would expect the concentration of contaminant at that point to be Γm. Thus there is a gradient in pressure between the center of the channel and the wall at all at all points along the length of the channel. This difference increases

linearly with distance downstream from the inlet. A backflow along the walls is probably the result of this gradient in surface pressure. Any attempt to solve for the backflow is hindered by the fact that we do not know the surface viscosity, which might even be non-Newtonian, and by the complexity of the flow pattern which develops. Since in the case of simple two-phase flow, it is shown in Appendix A that the interfacial velocity attains its center velocity quite a short distance from the wall and since the viscosity if the many films is comparable to that of butter,[17a] one might expect the forward flow in the center to be rather a small fraction of the flow which would occur where there no film on the interface.

The backflow at the wall was quite rapid compared to the forward flow of the interface in the central portion of the channel width. Since concentration samples were taken only in the central inch of the channel width, the effect of the backflow upon the mass transfer would not be seen in the present study. It would be logical to expect that a model in which there is a small cocurrent motion of the interface would correlate the data. This topic is discussed in the next section.

3. Mass Transfer Models

Since it appears that a totally covered interface with surface circulation is a more accurate description of the physical situation than the partially stagnant and partially uninhibited interface, the former approach will be used in the development of a mass transfer model.

If the interface is completely stagnated, the velocity profiles of the two phases near the interface are approximated by linear slopes and a zero interfacial velocity, as indicated in Fig. 48a. The additivity of resistances is used to find the overall mass transfer coefficient.

$$1/K_g = 1/k_g + \alpha/k_i + H/k_l \qquad (5\text{-}20)$$

where H is the Henry's law constant which expresses the equilibrium relationship between the bulk gas and the main liquid, and α is defined as the Henry's law constant describing the interfacial relationship between the gas and the interfacial phase. The constant, α, is generally smaller than H because the

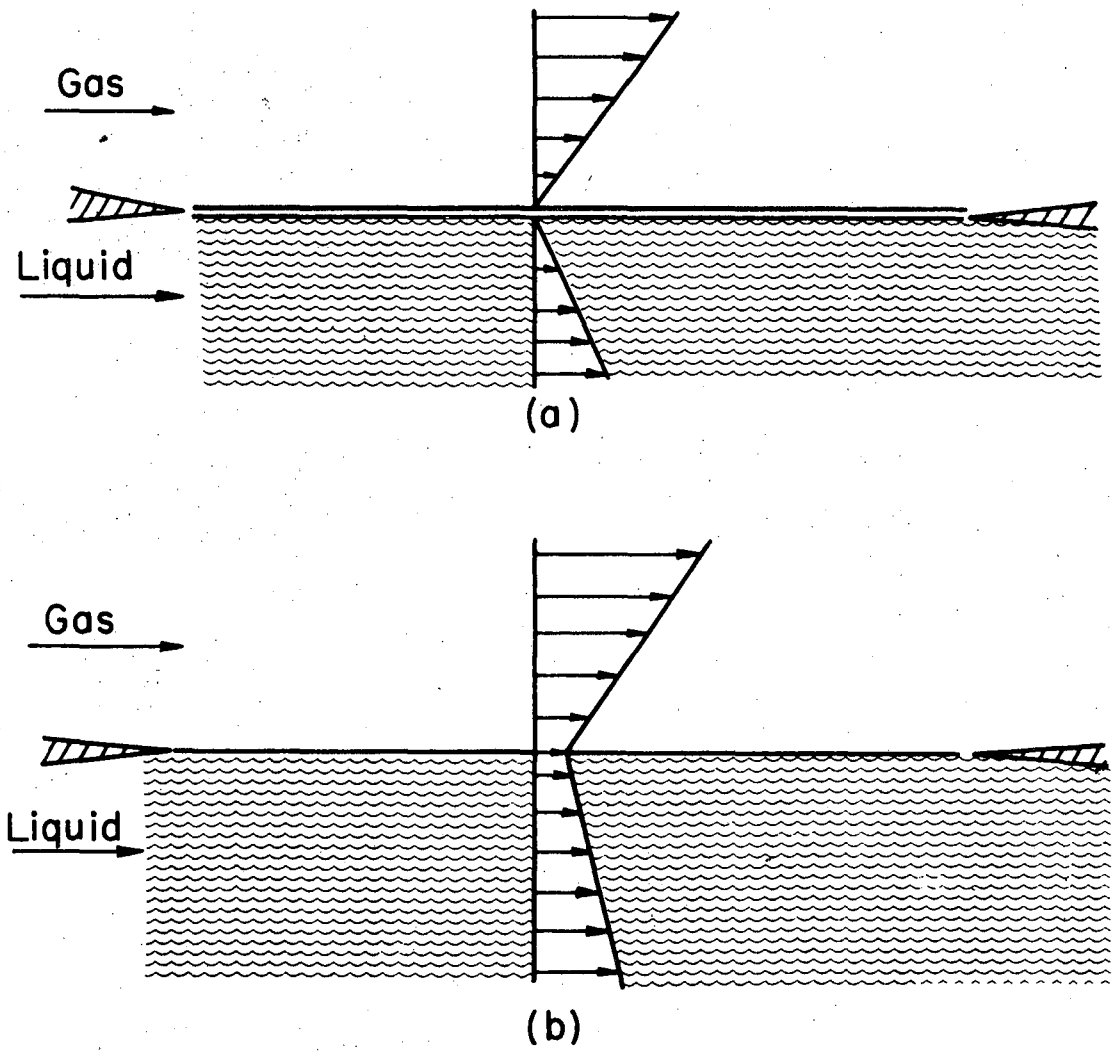

MUB-11291

Fig. 48. (a) Mass transfer model with a stagnant interface; (b) model with a slowly moving interface.

surfactant is always of higher molecular weight than the water. The Leveque model is applied to the liquid and gas phases,

$$k_l = 0.538\ (D_l^2\ a_l/x)^{1/3}$$
$$k_g = 0.538\ (D_g^2\ a_g/x)^{1/3} \qquad (5\text{-}21)$$

The film model is used for the interfacial resistance.

$$k_i = D_i/\Delta \qquad (5\text{-}22)$$

The film thickness is normally about 10^{-7} cm[17] and, therefore, if we assume this value for Δ and a value of about 10^{-9} cm^2/sec for the diffusivity[5] of the interfacial phase, the resistance to mass transfer of the film will never become greater than 1% of the total resistance. Interfacial resistance cannot therefore be of importance and is neglected in the remainder of the discussion. The overall average mass transfer coefficient is

$$K_g avg = 0.808(D_g^2\ a_g/L)^{1/3}/(1+(a_g D_g^2/a_l D_l^2)^{1/3} H) \qquad (5\text{-}23)$$

The other extreme is the case where there is no retardation of the interface. This model is fully discussed in Chapter IV. A comparison of the oxygen data with the two models is made in Figs. 49, 50, and 51. Generally these data indicate that there is some surface motion but that its importance tends to decrease with increasing flow rate. The data for helium and carbon dioxide indicate the same trend. At the highest flow rate carbon dioxide data fall below the theoretical line for no interfacial motion. If one postulates a model as is shown in Fig. 48b, where there is a small interfacial velocity (as might be the case where there is circulation within the film) the model one must use for mass transfer in both phases is the Beek and Bakker model which has been fully discussed in Chapter III. The resistances of both phases are added, and from a knowledge of the interfacial velocity and flow rates the mass transfer coefficient may be calculated. However, since we know the mass transfer coefficient and the flow rates and would like to calculate the interfacial

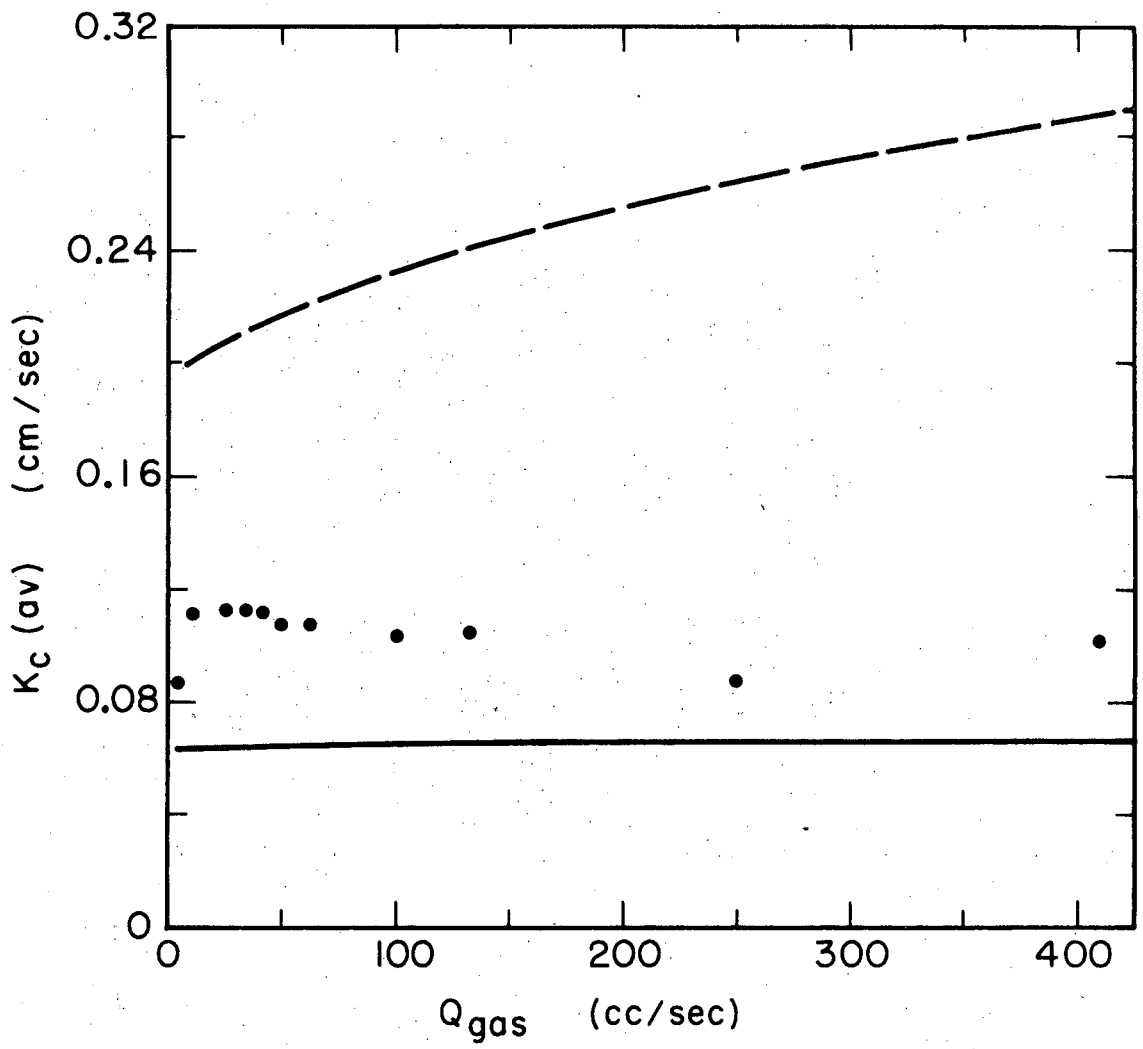

MUB-11295

Fig. 49. Average mass transfer coefficient as a function of oxygen flow rate for Q_l = 15.43 cc/sec. --- Model for free interface, —— model for stagnant interface, ● data.

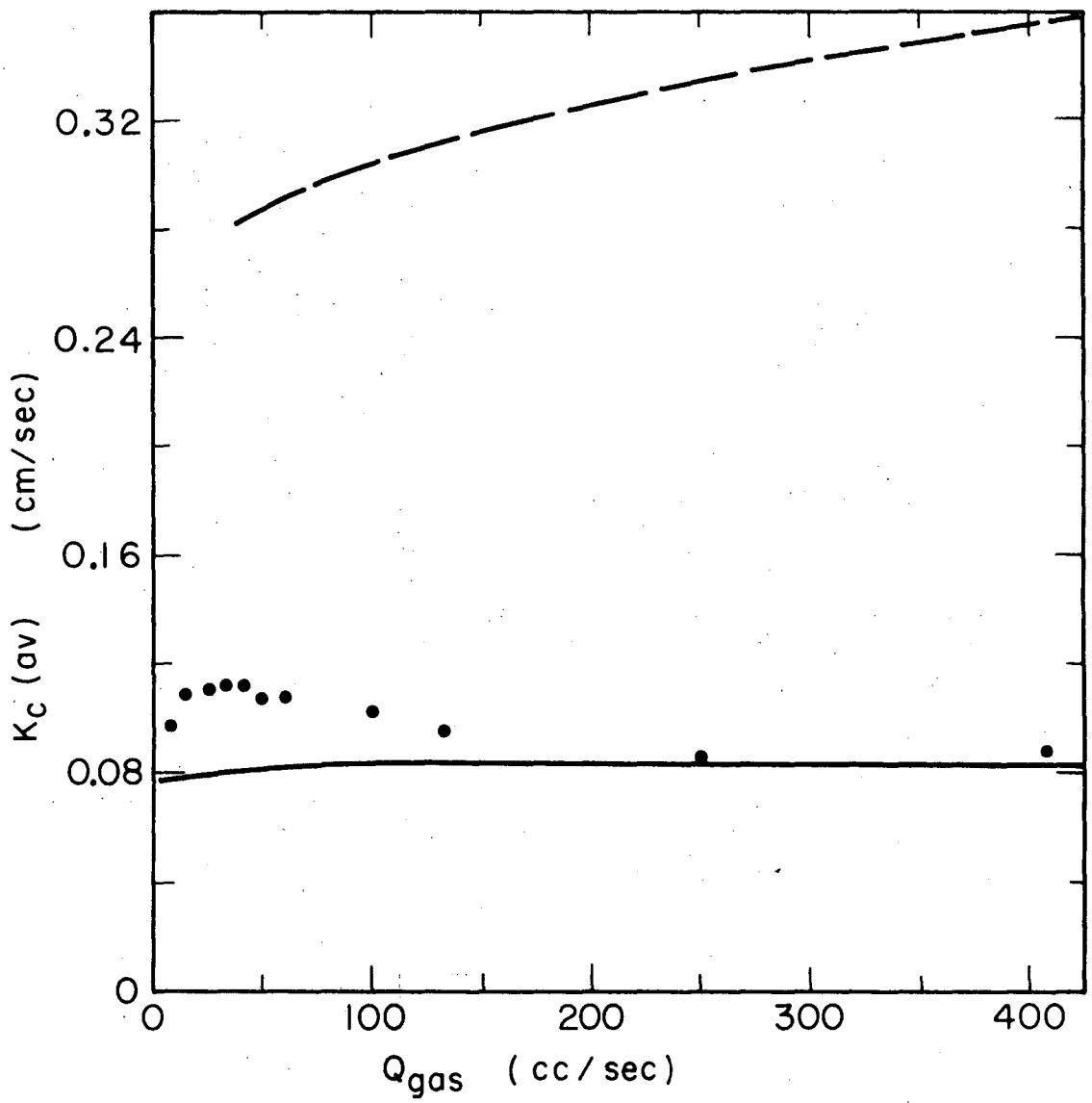

MUB-11296

Fig. 50. Average mass transfer coefficient as a function of oxygen flow rate for Q_l = 30.86 cc/sec. --- Model for free interface, —— model for stagnant interface, ● data.

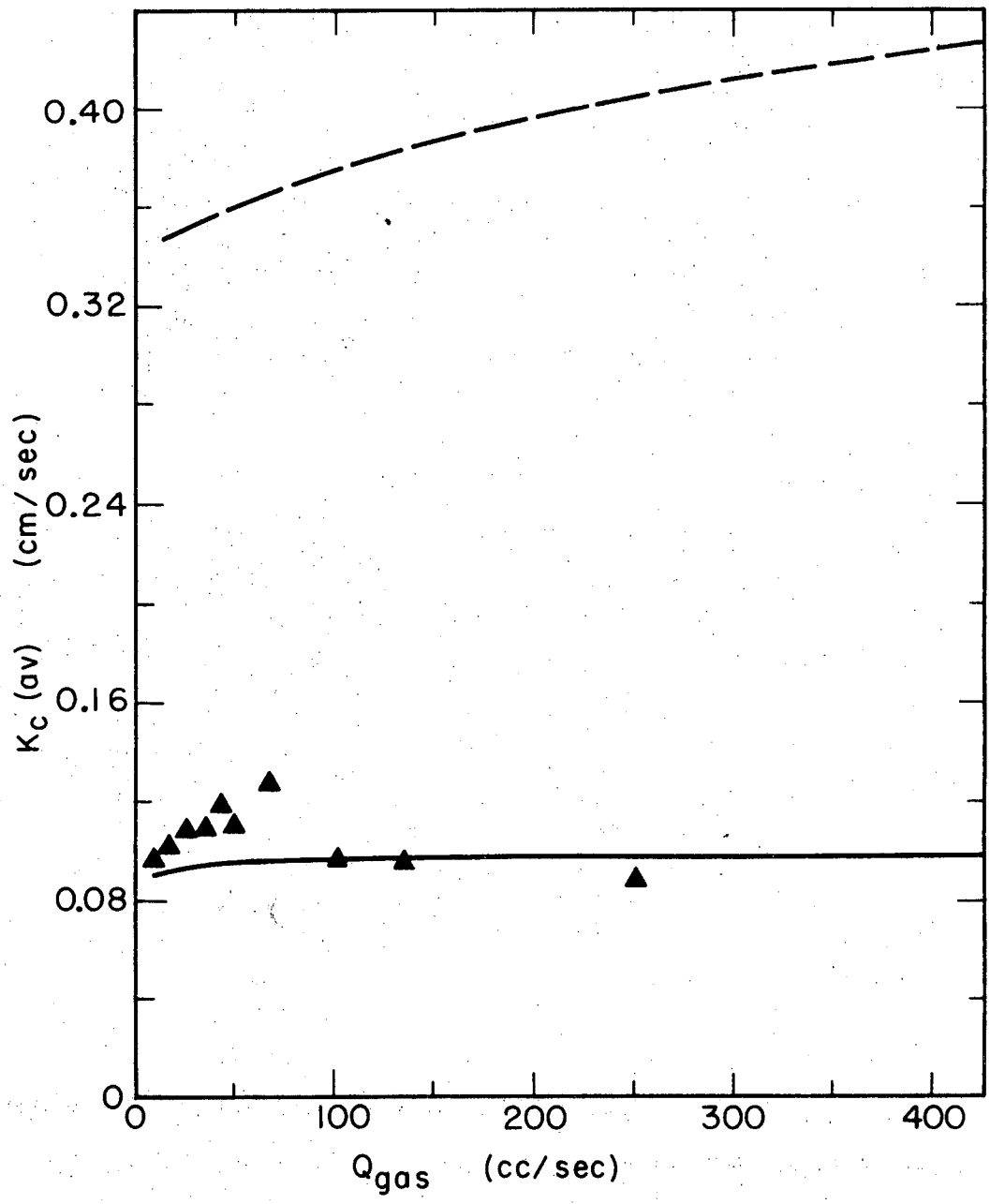

MUB-11287

Fig. 51. Average mass transfer coefficient as a function of oxygen flow rate for Q_1 = 51.46 cc/sec. --- Model for free interface, —— model for stagnant interface, ▲ data.

velocity, the calculation becomes a complex trial and error exercise. In order to save time, the procedure was programed for calculation on the computer. The program was also used to do the other mass transfer calculations considered in this chapter. It is fully described in Appendix C. Figure 52 shows interfacial velocity data for the oxygen experiments. The velocities calculated here for typical runs are of the same order of magnitude as observed on the actual interface. It is evident that increased shear tends to decrease the interfacial velocity. The experimental scatter present in all the data makes it difficult to come to definite conclusions. It does however seem justified to say that there is some interfacial motion especially at the lower flow rates.

It has already been shown that the gas flow rate has only a small effect upon the mass transfer coefficient. In Fig. 53 the average mass transfer coefficient is plotted as a function of gas rate for all the points observed. It is noted that the mass transfer coefficient does not seem to be a function of liquid rate, in spite of the fact that theory tells us that for surface stagnation the mass transfer should be liquid phase controlled.

C. Conclusions

(1) The results of the mass transfer calculations made in this section show the marked effect a surfactant can have upon the mass transfer through its effect upon the velocity profiles.

(2) The surfactant appeared to cover the entire interface. A circulatory pattern within the interfacial film is probably caused by surface pressure gradients.

(3) The forward motion of the central portion of the channel is confirmed by the fact that mass transfer data tend to be higher than is expected for zero motion at the interface.

D. Recommendations for Further Study

The present data tend to be unsatisfactory because 1. The data were taken under conditions where no surfactant was assumed to be present. As a result far too few observations were made of the condition of the interface. 2. The surfactant was unknown. 3. The channel was not designed to enable observation of surfactant films.

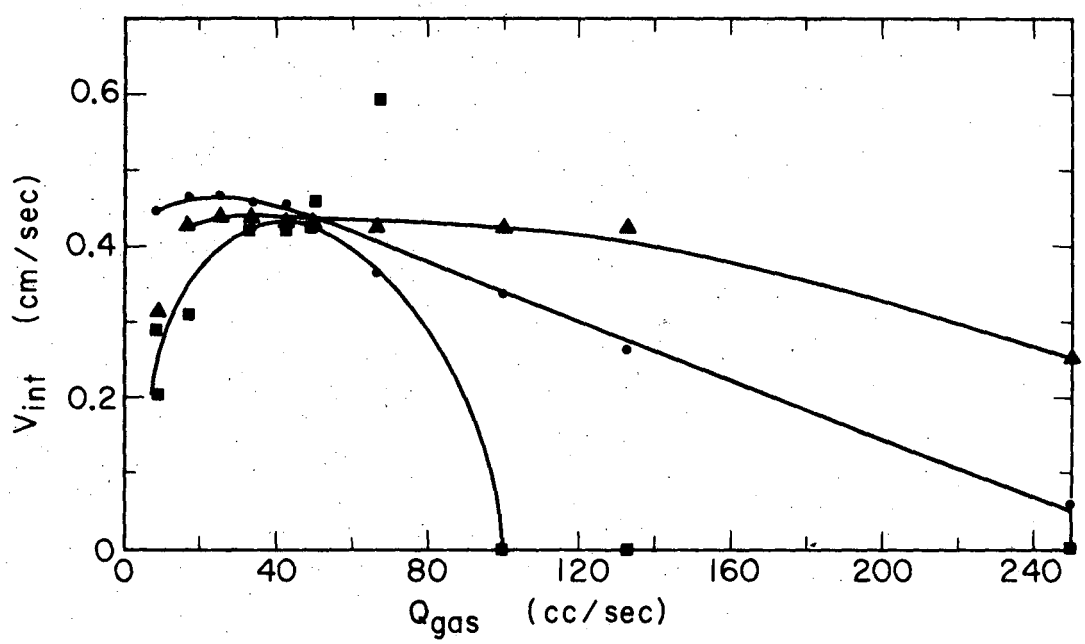

MUB-11294

Fig. 52. Calculated interfacial velocity as a function of oxygen flow rate for three liquid flow rates. —— Best curve through flow data for noted liquid rate. ▲ Data for Q_l = 15.43 cc/sec, ● Data for Q_l = 30.86 cc/sec, ■ Data for Q_l = 51.46 cc/sec.

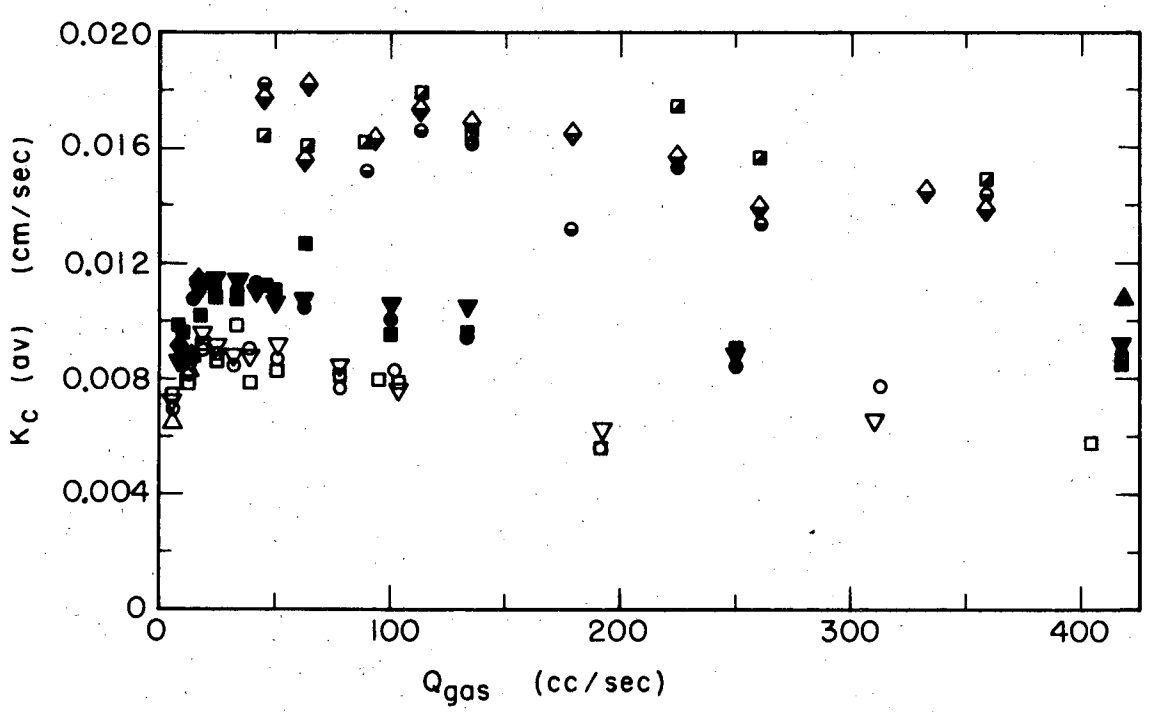

MUB-11293

Fig. 53. Average mass transfer coefficients as a function of gas rate. ▼●▲◆■ O_2 data, ▽△○□ CO_2 data, ◪◒◆ helium data.

It is recommended that:

(a) A new channel be built to serve more fully the needs of a surfactant study.

(b) Some of the data taken in this study be repeated in an attempt to test their validity. In this study more attention should be paid to the condition of the interface.

(c) The effect of different types of added impurities upon the mass transfer would also be of interest.

(d) The effect of inclination of the channel upon the equilibrium film length would be of interest.

ACKNOWLEDGEMENTS

The authors wish to express their appreciation to J. S. Newman and R. A. Seban for their helpful suggestions; to G. G. Young and J. Byce for their aid in the design and construction of the experimental equipment; and to Carl Quong for his help in computer programming.

APPENDIX A

THE HYDRODYNAMICS OF LAMINAR TWO-PHASE FLOW

A knowledge of the hydrodynamics of the experimental device is essential to any convective mass transfer study. The fluid mechanics of laminar two phase flow between two flat plates and in rectangular channels are discussed in this chapter. Other general information of a hydrodynamic nature is also included.

A. Flow Between Two Flat Plates

1. Flow of a Single Phase

The simplest situation for flow between two flat plates is steady state flow of a single phase. This is illustrated in Fig. 54a. The Navier-Stokes equations in this situation reduce to;

$$\frac{dP}{dx} = \mu \frac{d^2V}{dy^2} \qquad \text{(A-1)}$$

with the boundary conditions

$$V = 0 \quad \text{at} \quad y = \pm b/2$$

Since $\partial p/\partial y = 0$ then $\partial p/\partial x$ = a constant. Therefore the solution is

$$V = \frac{1}{2\mu}\frac{dP}{dx}\left(\frac{1}{2}\left(\frac{b}{2}\right)^2 - y^2\right) \qquad \text{(A-2)}$$

2. Stratified Flow of Two Immiscible Phases

The next case which is considered is illustrated in Fig. 54b. The equations of motion for this case reduce to the following:

$$\mu_g \frac{\partial^2 V_g}{\partial y^2} = \frac{dP}{dx} \quad \text{for } y > 0 \qquad \text{(A-3)}$$

$$\mu_l \frac{{}^2V_l}{y^2} = \frac{dP}{dx} \quad \text{for } y < 0 \qquad \text{(A-4)}$$

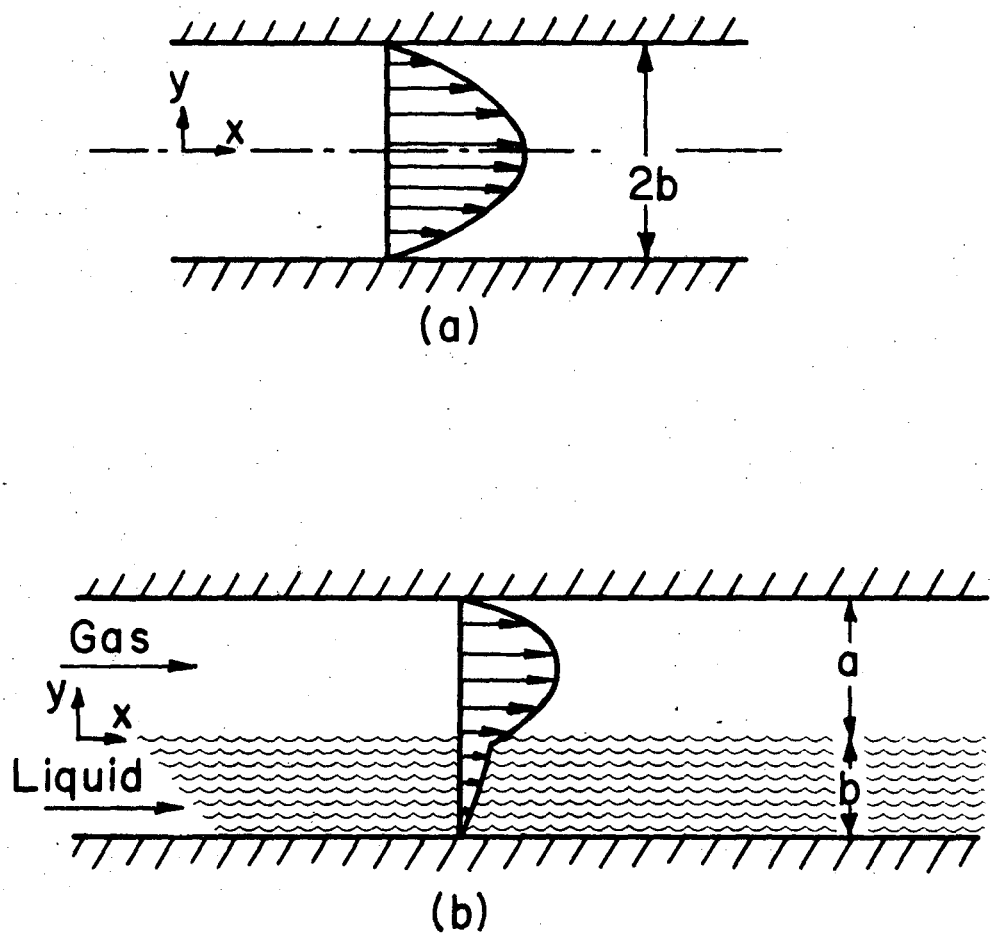

MUB-11290

Fig. 54. Single phase and two phase laminar velocity profiles between two flat plates. (a) Single phase, (b) two phase.

The above equations assume that dP/dx is the same constant in both phases. This means that the gas-liquid interface will be horizontal and is the defining condition for two-phase flow. The pressure gradient is a constant for the same reason as the single phase value is a constant. The four boundary conditions are:

$$\begin{aligned}
&\text{B.C.1} \quad \text{at} \quad y = 0 \qquad \mu_g \frac{\partial V_G}{\partial y} = U_1 \frac{\partial V_1}{\partial y} \\
&\text{B.C.2} \quad \text{at} \quad y = 0 \qquad V_g = V_1 \\
&\text{B.C.3} \quad \text{at} \quad y = a \qquad V_g = 0 \\
&\text{B.C.4} \quad \text{at} \quad y = -b \qquad V_1 = 0
\end{aligned} \tag{A-5}$$

If we solve the two equations applying B.C.1 so that the coefficients on the second term of each equation are equal, the solutions are:

$$\mu_g V_g = \frac{\Delta P}{2\Delta x} y^2 + k_1 y + k_2 \tag{A-6}$$

$$\mu_1 V_1 = \frac{\Delta P}{2\Delta x} y^2 + k_1 y + k_3 \tag{A-7}$$

If the other three boundary conditions are applied the three constants k_1, k_2, and k_3 are found to be

$$\begin{aligned}
k_1 &= \frac{-\Delta P}{2\Delta x} \frac{a^2\mu_1 - b^2\mu_g}{a\mu_1 + b\mu_g} \\
k_2 &= \frac{-\Delta P}{2\Delta x} \frac{\mu_g ab(a+b)}{a\mu_1 + b\mu_g} \\
k_3 &= \frac{-\Delta P}{2\Delta x} \frac{\mu_1 ab(a+b)}{a\mu_1 + b\mu_g}
\end{aligned} \tag{A-8}$$

When mass transfer models are considered, the interfacial velocity and the slope at the interface in the gas phase are the most important quantities. For this type of flow these variables are:

$$u_0 = \frac{\Delta P}{2\Delta x} \frac{ab(a+b)}{a\mu_l + b\mu_g} \tag{A-9}$$

$$a_g = \left.\frac{dV_g}{dy}\right|_0 = \frac{\Delta P}{2\mu_g \Delta x} \frac{a^2\mu_l + b^2\mu_g}{a\mu_l + b\mu_g} \tag{A-10}$$

The average velocities are of interest since they are related to the flow rate of fluid through the channel.

$$(u_g)m = \frac{1}{a}\int_0^a V_g \, dy$$

$$(u_g)m = \frac{\Delta P a^2}{6\Delta x \mu_g} + \frac{k_1 a}{2\mu_g} + \frac{k_2}{\mu_g} \tag{A-11}$$

Similarly

$$(u_l)m = \frac{\Delta P b^2}{6\Delta x \mu_l} - \frac{k_1 b}{2\mu_l} + \frac{k_3}{\mu_l} \tag{A-12}$$

The solution for the special case where a = b is given in Bird, Stewart and Lightfoot.[4a]

3. <u>Flow of Two Phases where the Lower Phase has a Hydraulic Gradient</u>

The flow rates of the two phases may be such that one phase is dragging the other. Unlike the case of two-phase flow, where both phases are horizontal, one of the phases (the liquid) will have a slight hydraulic gradient in this problem. It is shown in Appendix B that such a gradient is small when the viscosity is in the neighborhood of one centipoise. This solution is not restricted to cocurrent flow but will generate a solution for counterflow.

The solution of the equations of motion may be written in the general form as:

$$V_l = k_1 y^2 + k_2 y + k_3 \tag{A-13}$$

$$V_g = k_4 y^2 + k_5 y + k_6 \tag{A-14}$$

In the most convenient form for experimental analysis the boundary conditions are written as follows

$$\frac{Q_G}{W} = \int_0^b V_g dy \tag{A-15}$$

$$\frac{Q_L}{W} = \int_b^0 V_l dy \tag{A-16}$$

$$\text{at} \quad y = 0, \ \mu_g \frac{V_g}{y} = \mu_l \frac{V_l}{y} \tag{A-17}$$

$$\text{at} \quad y = 0, \ V_L = V_G \tag{A-18}$$

$$\text{at} \quad y = -b, \ V_l = 0 \quad \text{at} \quad y = b \quad V_G = 0 \tag{A-19}$$

for the special case where a is equal to b. As a result of Eqs. (A-17) and (A-18), k_5 may be replaced by $k_2(\mu_g/\mu_l)$ and k_6 by k3. The four independent constants are solved for simultaneously using the conditions in Equations (A-15), (A-16), and (A-19). These constants are:

$$\begin{aligned} k_3 &= \frac{1.5}{Wb} \quad \frac{Q_g+Q_l(\mu_l/\mu_g)}{1+(\mu_l/\mu_g)} \\ k_2 &= \frac{6}{Wb^2} \quad \frac{Q_g-Q_l}{1+(\mu_g/\mu_l)} \\ k_1 &= -(k_2 b+k_3)/b^2 \\ k_4 &= (k_2 b(\mu_g/\mu_l)-k_3)/b^2 \end{aligned} \tag{A-20}$$

For this situation k_3 is the interfacial velocity, and k_2 is the slope of the gas phase velocity at the interface.

B. Laminar Flow in Rectangular Channels

1. Flow of a Single Phase in a Rectangular Channel

Laminar flow in a rectangular duct was originally solved by Cornish.[11] A simpler solution, using Fourier transforms is presented here. The basic geometry of the channel is shown in Fig. 55a. For steady flow the general equations of motion reduce to

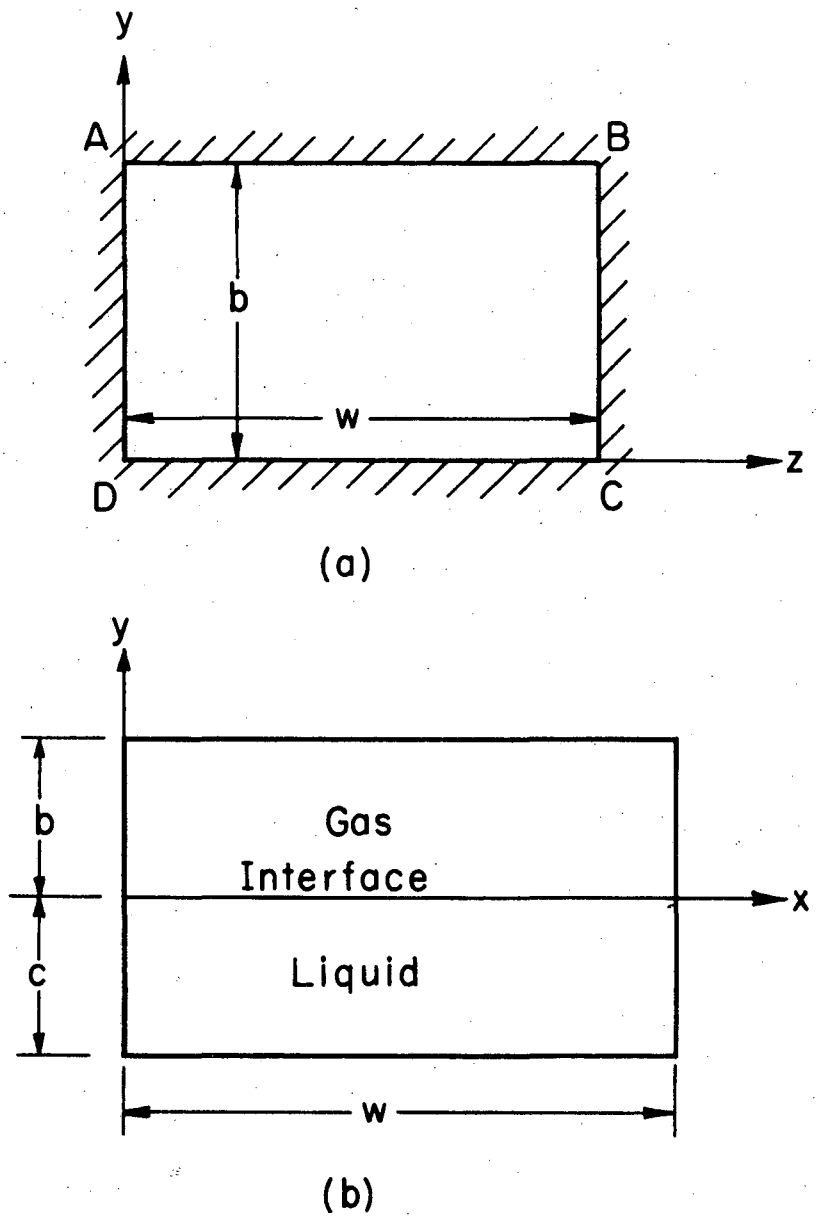

MUB 11333

Fig. 55. Geometry of single phase and two phase rectangular channels. (a) Single phase, (b) two phase.

$$\partial P/\partial z = \partial P/\partial y = 0 \tag{A-21}$$

$$\frac{\partial P}{\partial x} = \mu \frac{\partial^2 V}{\partial z^2} + \frac{\partial^2 V}{\partial y^2} \tag{A-22}$$

Let

$$K = \frac{1}{\mu}\frac{\partial P}{\partial x}$$

The boundary conditions the new coordinates are

$$V = 0 \quad \text{at} \quad z = 0 \quad \text{and} \quad z = w$$

$$\text{and } V = 0 \quad \text{at} \quad y = 0 \quad \text{and} \quad y = b \tag{A-24}$$

Transforming using Fourier sine transforms and bearing in mind the fact that an odd function is necessary here

$$\frac{d^2 U_s}{dy^2} - \left[\frac{(2n+1)\pi}{a}\right]^2 U_s = \frac{2wK}{(2n+1)\pi} \tag{A-25}$$

Where

$$U_s(n,z) = \int_0^w V \operatorname{Sin}\left(\frac{n\pi x}{a}\right) dx \tag{A-26}$$

The solution to this equation is:

$$U_s = A_n \operatorname{Sin} k \frac{(2n+1)\pi(b-y)}{w} + Bn \operatorname{Cosh} \frac{(2n+1)\pi y}{w} + \frac{2w^3 K}{(2n+1)^3\pi^3} \tag{A-27}$$

The boundary conditions are used to evaluate the constants. Upon retransformation the result becomes

$$V = \frac{4w^2 dP}{\pi\mu dx} \sum_{n=0}^{\infty} \frac{1}{(2n+1)^3} \operatorname{Sin}\left[\frac{(2n+1)\pi z}{w}\right] \cdot \left\{1 - \frac{\operatorname{Cosh}\frac{(2n+1)\pi y}{w}}{\operatorname{Cosh}\frac{(2n+1)\pi b}{w}} + \left(\frac{1-\operatorname{Cosh}\frac{(2n+1)\pi b}{w}}{\operatorname{Sinh}\frac{(2n+1)\pi b}{w}\ \operatorname{Cosh}\frac{(2n+1)\pi b}{w}}\right) \times \operatorname{Sinh}\frac{(2n+1)\pi(b-y)}{w}\right\} \tag{A-28}$$

The solution given by Cornish is stated in slightly different terms. This is due to the face that he chose the center of the channel as the origin. He also defined the dimensions of the channel differently. From Eq. (A-28) the volumetric flow rate may be determined.

$$Q = \int_0^w \int_0^b V dy dz \tag{A-29}$$

$$Q = \frac{4b^5}{w\mu} \frac{dP}{dx} \sum_{n=0}^{\infty} \frac{1}{\xi_n^5}\left(1-\mathrm{Cos}(\xi_n)\right) \cdot \left[\xi_n + 2\left(\mathrm{Csch}(\xi_n) - \mathrm{Coth}(\xi_n)\right)\right] \tag{A-30}$$

where $\xi_\eta = \frac{(2n+1)b}{w}$ (A-31)

For comparison the Cornish equation is

$$Q = \frac{4}{3} \frac{wb^3}{\mu} \left(\frac{dP}{dx}\right) \cdot \left[1 - \frac{192}{\pi^5} \frac{b}{w}\left(\tanh \frac{\pi w}{b} - \frac{1}{3^5} \tanh \frac{3\pi w}{b} + \ldots\right)\right] \tag{A-32}$$

2. <u>Two Phase Flow in a Rectangular Channel</u>

The equation for stratified two phase flow in a rectangular duct has been solved by Tang and Himmelblau.[47] The flow equations for each phase are the same as Eqs. (A-21) and (A-22). The zero velocity applies at three walls in each phase. Figure 55b shows the situation in this case. The interfacial conditions which couple the solutions of the two phases are:

$$V_G = V_L$$
$$\mu_g \frac{\partial V_g}{\partial y} = \mu_l \frac{\partial V_l}{\partial y} \tag{A-33}$$

The two equations are solved simultaneously using Fourier transforms. The results are.

$$V_g = \frac{4w^2}{\mu_g \pi^3} \frac{dP}{dx} \sum_{n=0}^{\infty} \frac{1}{(2n+1)^3} \mathrm{Sin}\left[\frac{(2n+1)\pi z}{w}\right] \cdot \left\{1 - \frac{\mathrm{Cosh}\left[(2n+1)\pi y/w\right]}{\mathrm{Cosh}\left[(2n+1)\pi b/w\right]} + \beta_n \mathrm{Cosh}\left[\frac{(2n+1)\pi c}{w}\right] \sinh\left[\frac{(2n+1)\pi(b-y)}{w}\right]\right\} \tag{A-34}$$

$$V_1 = \frac{4w^2}{\mu_1 \pi^3} \frac{dP}{dx} \sum_{n=0}^{\infty} \frac{1}{(2n+1)^3} \operatorname{Sin}\left[\frac{(2n+1)\pi z}{w}\right] \cdot$$

$$\cdot \left[1 - \frac{\operatorname{Cosh}[(2n+1)\pi y/w]}{\operatorname{Cosh}[(2n+1)\pi C/w]} - \beta_n \cosh\left[\frac{(2n+1)\pi C}{w}\right] \cdot \right. \qquad \text{(A-35)}$$

$$\left. \sinh\left[\frac{(2n+1)\pi(c+y)}{w}\right] \right]$$

where

$$\beta_n = \frac{\mu_g\left[1-\left[\operatorname{Cosh}(2n+1)\pi c/w\right]^{-1}\right] - \mu_1\left[1-\left[\operatorname{Cosh}(2n+1)\pi b/w\right]^{-1}\right]}{\mu_g \sinh(2n+1)\pi c/w \cosh(2n+1)\pi b/w - \mu_1 \operatorname{Sinh}(2n+1)\pi b/w \operatorname{Cosh}(2n+1)\pi c/w} \qquad \text{(A-36)}$$

It is evident that a solution of the velocity profile for any given aspect ratio would involve a great amount of tedious calculation. Added to this is the very great danger of making a computational error. As a result it was decided to write a program which would carry out the tedious calculations in Eqs. (A-34), (A-35), and (A-36). This program is included in the next three pages. Along with it is a description of how it is used. The primary use to which it was put in this study was in determining the aspect ratio which should be used in the construction of the channel.

```
C PROGRAM TO SOLVE EQUATIONS FOR LAMINAR VELOCITY PROFILES
C IN TWO PHASE FLOW IN A RECTANGULAR DUCT
      DIMENSION X(100),YB(100),YC(100),WB(100,100),WC(100,100),BETA(100)
     1  ,YG(100) ,YF(100)
  100 FORMAT (3F5.0 , 3I3 , 4F5.0 , 3F6.0,2I3)
  101 FORMAT (4H N= ,I3,10H      BETA=,E15.7)
  103 FORMAT(4H X= ,F10.5,10H      Y =  ,F10.5,10H      WB=  ,F10.5)
  104 FORMAT ( 4H X= ,F10.5,10H      Y =  ,F10.5,10H      WC=   ,F10.5)
  105 FORMAT (30H  VELOCITY PROFILES RUN NUMBER ,I3)
 1060FORMAT(24H CHANNEL DIMENSIONS, A= ,F5.2,  6H  B=  ,F6.4,6H  C=
     1,F6.4 )
 1070FORMAT(25H VISCOSITY OF AIR (CP) = ,F6.4,27H VISCOSITY OF WATER (C
     1P)= ,F5.2 )
 1080FORMAT(25H NUMBER OF X DIVISIONS =  ,I3,18H YB DIVISIONS =   ,I3,
     1 18H  YC DIVISIONS =  ,I4)
  109 FORMAT(22H DELTA P / DELTA L =  ,F6.2)
  110 FORMAT (35H CONVERGENCE NOT ACHIEVED AFTER N = ,I3)
  111 FORMAT(36H CONVERGENCE NOT ACHIEVED AFTER NO = ,I4 )
   25 READ (2,100) A,B,C,K,L,M,TOL,VISC1,VISC2,DELX,DELL,DELK,DELP,RUN
     1  ,KOUNT
      WRITE (3,105)  RUN
      WRITE (3,106)  A,B,C
      WRITE (3,107 )  VISC1,VISC2
      WRITE (3,108) M,L,K
      WRITE (3,109)    DELP
      F=C/A
      G=B/A
      DO 1 N= 1,KOUNT
      BETA(N)=(VISC1*(1.0-1.0/COSH(N,F))-VISC2*(1.0-1.0/COSH(N,G)))/
     1(VISC1*SINH(N,F)*COSH(N,G)+VISC2*SINH(N,G)*COSH(N,F))
    1 WRITE (3,101)  N,BETA(N)
      DO 6  I= 1,M
      X(I) = FLOAT(I)*DELX
      DO 3  JB =1,L
      YB(JB)=(FLOAT(JB)-1.0)*DELL
      YG(JB) =YB(JB)/A
      WB(JB,I)= 4.0*A*A*DELP*SIN(3.1416*X(I)/A)*(1.0-COSH(1,YG(JB))/
     1COSH(1,G)+BETA(1)*COSH(1,F)*SINH(1,(G-YG(JB))))/(VISC1*31.0065)
      DO 2 NI =2,KOUNT
      AN=FLOAT(NI)
      N=NI
      ADD=4.0*A*A*DELP*SIN((2.0*AN-1.0)*3.1416*X(I)/A)*(1.0-COSH(N,YG(JB
     1))/COSH(N,G)+BETA(N)*COSH(N,F)*SINH(N,(G-YG(JB))))/(VISC1*31.0065*
     2(2.0*AN-1.0)**3)
      WB(JB,I)=WB(JB,I)+ADD
      IF(ABS(ADD)-TOL)  11,11,10
   10 IF(N-KOUNT)  2,12,12
   12 WRITE(3,110) NI
      GO TO 18
    2 CONTINUE
   11 WRITE (3,103)  X(I),YB(JB), WB(JB,I)
    3 CONTINUE
      DO 4  JC  =1,K
      YC(JC)=-(FLOAT(JC)-1.0)*DELK
      YF(JC) =YC(JC)/A
      WC(JC,I)=4.0*A*A*DELP*SIN(3.1416*X(I)/A)*(1.0-COSH(1, - YF(JC)) /
     1COSH(1,F)-BETA(1)*COSH(1,G)*SINH(1,(F+YF(JC))))/(VISC2*31.0065)
      DO 7  NO=2,KOUNT
      AN=FLOAT(NO)
```

```
      N=NO
      ADC=4.0*A*A*DELP*SIN((2.0*AN-1.0)*3.1416*X(I)/A)*(1.0-COSH(N,-
     1YF(JC)) /COSH(N,F)-BETA(N)*COSH(N,G)*SINH(N,(F+YF(JC))))/(VISC2*
     231.0065*(2.0*AN-1.0)**3)
      WC(JC,I)=WC(JC,I) +ADC
      IF(ABS(ADC)-TOL) 16,16,15
   15 IF(NO-KOUNT)  7,17,17
   17 WRITE(3,111)  NO
      GO TO 18
    7 CONTINUE
   16  WRITE (3,104) X(I), YC(JC),WC(JC,I)
    4 CONTINUE
    6 CONTINUE
      GO TO 25
   18 STOP
      END
$IBFTC COSH1    LIST
      FUNCTION COSH(N,R)
      ARG = (2.0*FLOAT(N)-1.0)*3.1416*R
      COSH=1.0/SQRT(1.0-TANH(ARG)**2)
      RETURN
      END
$IBFTC SINH1    LIST
      FUNCTION SINH(N,R)
      ARG = (2.0*FLOAT(N)-1.0)*3.1416*R
      SINH= TANH(ARG)/SQRT(1.0-TANH(ARG)**2)
      RETURN
      END
```

Explanatory Notes

1. Required data must be in consistent units and are all read into the program in statement 25, according to Format 100. The data needed are A (the channel width), B (the height of the gas phase), C (the height of the liquid phase),K (the number of liquid phase divisions from the interface down), L (the number of gas phase divisions from the interface up), M (the number of divisions in a horizontal direction starting from the wall), TOL (the allowable error in the calculated velocity), VISC1 (viscosity of the gas), VISC2 (viscosity of the

liquid), DELX (size of divisions in the z direction), DELL (size of gas phase divisions), DELK (size of liquid phase divisions), DELP (dP/dx), RUN (run number), KOUNT (the maximum number of terms in the series).

2. The program calculates velocities at all points on the specified grid, using equations A-34 and A-35. The constant, Beta, is calculated for all possible terms in the series. The calculation proceeds from term to term in the series until the imposed comvergence criterion, TOL, is achieved or until the final term allowed by KOUNT is reached. In the latter case a print out informs one of the fact that convergence has not been achieved. (Setting KOUNT at 100 has been found to give convergence in all the cases which have been attempted.)
3. The program prints out all the physical data read into the program. The resulting velocity information appears as follows:

```
X=    0.45000     Y =    0.10000     WB=    0.12412
X=    0.45000     Y =   -0.          WC=    0.00855
```

X is the horizontal distance from the side wall, Y is the vertical distance from the interface, WB is the gas phase velocity , and WC is the liquid phase velocity.

C. Corner Corrections to be used in the Channel

The flow models used in solving the convective mass transfer equations are based upon flow between two flat plates. Actually the apparatus is a rectangular channel. We therefore must find a method of calculating the values of the interfacial velocity and the slope in the gas phase in the central region of the channel based upon the flow rates actually measured. This is accomplished by finding the ratio of the actual flow to the flow between two flat plates which would give the same interfacial velocity and interfacial slope in the gas phase as actually exists in the central region of the channel. If we consider both phases independently, we may compare the hydrodynamics between two flat plates and the Cornish solution which will give us the actual flow rate. It is found that the corner correction is an extremely weak function of the interfacial velocity, so that the correction for the single phase may be used for the case of two phase flow without making an error of more than 1%. The correction for the single phase case is given by the following ratio.

$$\frac{Q_{ACT}}{Q_{F.P.}} = 1 - \frac{192}{\pi^5}\frac{b}{w}\left(\tanh\frac{\pi w}{b} - \frac{1}{3^5}\tanh\frac{3\pi w}{b} + \ldots\right) \qquad \text{(A-37)}$$

APPENDIX B

DESIGN DETAILS

In every experimental thesis there are several details which are not sufficiently important to report in the main body of the work, but which deserve some explanation. Contained in this chapter are some of these considerations. They include the sizing of the channel, hydrodynamic details and a description of the micrometer sampling device.

A. Aspect Ratio

In sizing the channel it was felt that a good deal of importance should be laid upon keeping it as small as possible. A large piece of equipment would mean that it would not be economically feasible to use bottled gas as the upper phase. A fan would have to be used instead, while in the liquid phase large quantities of liquid would have to be pumped around. Both of these factors would cause undersirable vibrations in the channel. The smallest phase thickness which can be accurately probed with a common pitot type probe is about one half inch, which was the thickness chosen for the gas phase. The same thickness was chosen for the liquid phase since this thickness is necessary to keep errors in the hydrodynamics due to small changes in liquid level within reasonable bounds.

The width of the channel was then selected upon the criterion that in the central one third of the channel the velocity must be within five per cent of the centerline velocity. Again a minimum width of channel was necessary. For design purposes it was decided that the two-phase flow solution would provide an adequate representation of the true conditions. Using the equations of Tang and Himmelblau,[68] which are Eqs. (A-34) and (A-35), one can calculate for a given pair of fluids the complete velocity profiles. For design purposes the fluids chosen were water and air. From the profiles generated by the computer solution to this problem, it was surmised that the side walls have a fairly uniform effect upon the velocity profiles. As a result it was found that any single profile could be used as a representation of conditions throughout the channel. The interfacial velocity profile was calculated for a series of different flow geometries. Figure 56 shows these plotted for

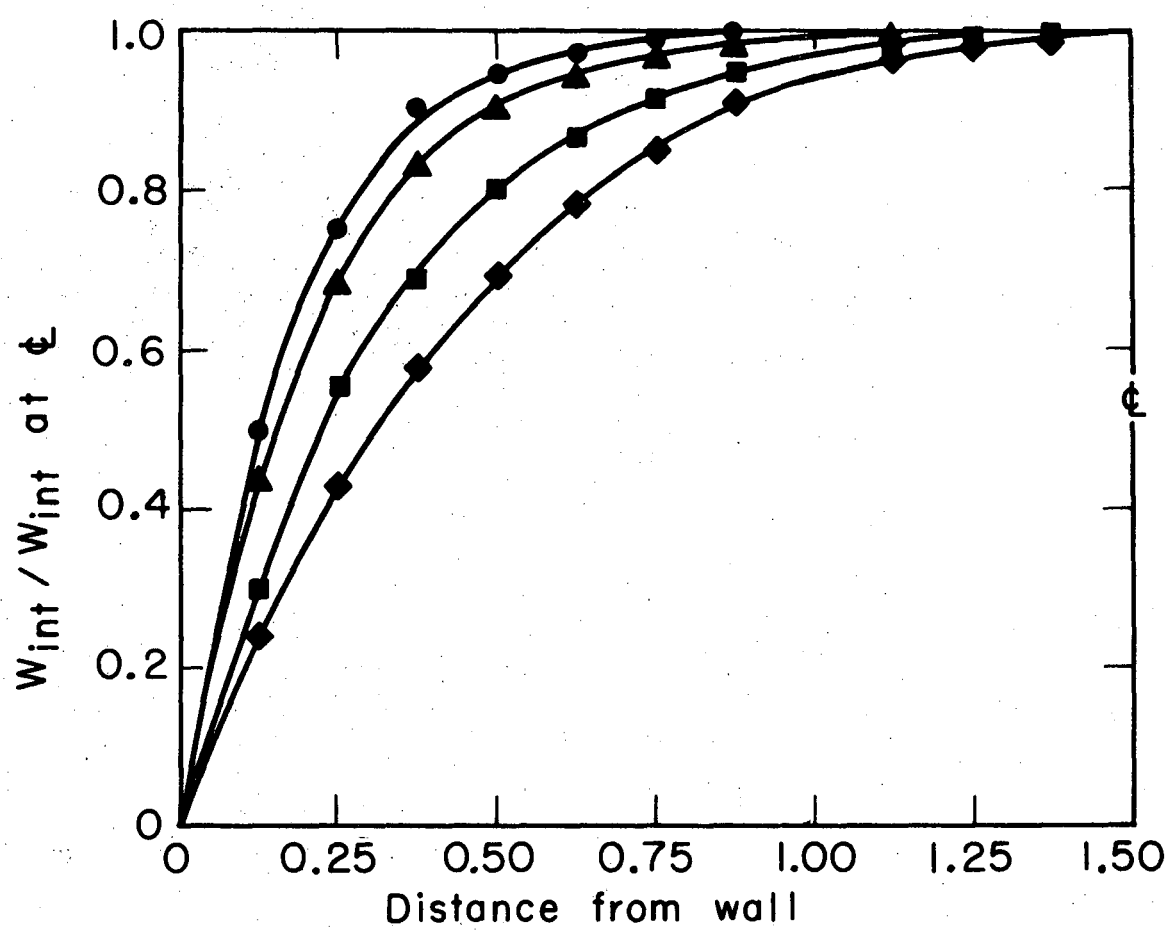

MUB 11332

Fig. 56. Interfacial velocity profiles in two phase flow as a function of aspect phase aspect ratio. ● Aspect ratio = 12:1, ▲ = 9:1, ■ = 6:1, ◆ = 4:1.

different aspect ratios (the ratio of the channel width to the depth of one phase). It will be noted that a channel width of three was chosen and that only half of each profile is shown. The abscissa is the ratio of the point velocity to the centerline velocity. The point 1.0 on the ordinate represents one-third of the channel width from the wall. A phase aspect ratio of four to one almost fits the criterion, but it was felt that an aspect ratio of six to one more safely suited the requirements of this study. Therefore each phase has the crossectional dimensions 1/2" by 3".

B. Maximum Flow Rates and Length of Channel

It was desirable to know the upper limits of flow rate. For this purpose it was decided to carry out some Reynolds number calculations using the ethanol-air system. Perry's handbook[52] gives the following equation for the Reynolds number in a noncircular duct

$$Re = 4Rh\mu m/\nu \qquad \text{(B-1)}$$

Where in the case of the gas phase

$$Rh = bW/2(b+W) \qquad \text{(B-2)}$$

and for the liquid

$$Rh = bW/(2b+W) \qquad \text{(B-3)}$$

If the maximum allowable gas phase Reynolds number if 1500, then the maximum gas flow rate is 900 cc/sec of air. Actually only about half that rate was ever used. In the liquid Jepson, Crosser and Perry[36] have shown that ripples become important at Reynolds numbers above 700, in a channel which was inclined at 9 degrees 44 minutes to the horizontal. Greater stability can be expected with the horizontal channel, since Yih[79] has shown that flow in a horizontal channel is neutrally stable to small disturbances while any inclination whatsoever creates an inherently unstable situation. We have assumed for the purposes of this study that a Reynolds number of 1000 is allowable. This

corresponds to a liquid flow rate of 55 cc/sec. Visual observation and mass transfer evidence later confirmed the validity of this assumption. It is interesting to locate the range of operation on the two phase flow diagram which has been presented by Hoogendoorn.[34] It must be noted that the chart applies strictly only to circular pipes. A portion of the original graph is reproduced in Fig. 57. The coordinates are defined as

$$V_m = (Q_g + Q_l)/(\frac{\pi}{4} D^2) \qquad \text{(B-4)}$$

$$C_g = Q_g/(Q_g + Q_l) \times 100\% \qquad \text{(B-5)}$$

For the case of a rectangular duct $D^2/4$ is replaced by 2bW. In our experiments V_m is a maximum of 0.275. C_g for that case corresponds to 94.3%. All other values are further away from the closest curve. The area in which the experiments fall is cross-hatched on the diagram. It will be noted that nowhere is the flow within a decade of the point where ripples should occur.

The length of the test section was the final consideration of the experimental design. Mechanical considerations governed the remainder of the design. It was desirable to use a test section which was long enough to minimize end effects. The length was limited by the fact that the gas phase would become saturated if very long exposures were permitted. Thus excessive length would seriously curb the flexibility of the apparatus. At the time this portion of the study was undertaken, experiments involving simultaneous heat and mass transfer of glycol from glycol-water mixtures to air were being contemplated. The object of the design was to find a length of channel which would give a complete range of control without allowing the number of transfer units to exceed two. A penetration model was used to characterize the liquid phase, while the resistance in the gas phase was calculated by means of the Leveque model. The resistances were added and the number of transfer units was calculated as well as the degree of control in either phase. The physical properties for the system, which are tabulated in Appendix E, predict gas phase control of the mass transfer at 25°C and liquid phase control at 100°C.

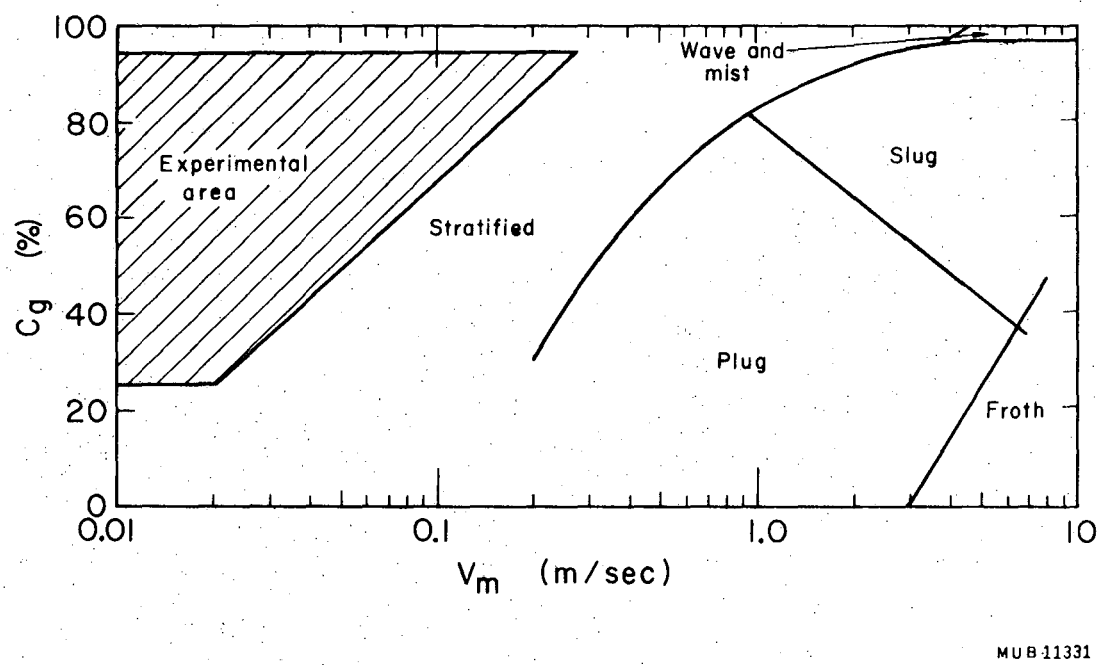

Fig. 57. Flow diagram for two phase pipe flow after Hoogendoorn. Greater turbulence to the right. Hatched area is experimental area.

It was found that the maximum permissible length was 1.5 ft. The physical system used in these calculations was not used in this series experiments, but the length of the channel proved quite satisfactory for the experiments which were actually carried out.

C. The Hydraulic Gradient of the Liquid Phase

When liquid is flowing over a horizontal surface, the film becomes thinner with distance downstream. It was necessary to estimate the size of this hydraulic gradient, in order to decide whether it would be necessary to incline the channel. The angle of the hydraulic gradient is approximately equal to the angle of inclination which will create a film of the same thickness as the film in question. The angle of the channel to the vertical is solved for by Bird, Stewart, and Lightfoot.[4c]

$$\beta = \mathrm{Cos}^{-1}\left\{3\mu U_m/\rho_g\delta^3\right\} \qquad \text{(B-6)}$$

For water flowing at an average velocity of 7.5 cm/sec and a film thickness, δ, of 1.27 cm, the angle of inclination is 0.0063 degrees to the horizontal. Since the channel is 18 inches long the change in film thickness over the length of the film is 0.002 inches. It would be reasonable to ignore this effect.

D. The Corner Correction

It has already been stated that all the complications brought into the calculations by the fact that we are dealing with the flow of two phases may be omitted, as far as the calculation of a corner correction is concerned, since this correction varies little with changes in the flow configuration. The correction is discussed in Appendix A, Sec. C and is given the following form:

$$Q_{act}/Q_{fp} = 1-192b/\pi^5 W\left\{\tanh(\pi W/b)-1/3^5 \times \tanh(3\pi W/b) + \ldots\right\} \qquad \text{(B-7)}$$

Since in our case W/b is 6.0, Qact/Qfp is equal to 0.915. This value was used throughout the experimental work.

E. The Design of the Sample Probe

The micrometer sample probe which was used to measure concentration profiles is slightly different from the normal, and because of its possible usefulness to others, a description is included here. The sampler design is shown schematically in Fig. 58, while the photograph of the test section (Fig. 5) shows it on the apparatus. The basic apparatus consists of a micrometer barrel whose center shaft (D) has been replaced by a brass shaft with a hole up through the middle. The sample probe (0.035"ID ss tube) which is shown as B in the diagram is soldered to the shaft, while a syringe adapter, C, is soldered to the top of the micrometer. The sample may be removed from the channel continuously of by means of a fixed-volume sample tube. By turning the head, E, the probe is moved up or down. Since the entire top assembly moves, samples may be taken only every 0.025 inches with the particular micrometer used. The position of the probe is directly read on the barrel, F. A thermal probe may be produced by mounting a sensing element at the tip and running the wires through the probe. Of course, the wires must be electrically insulated.

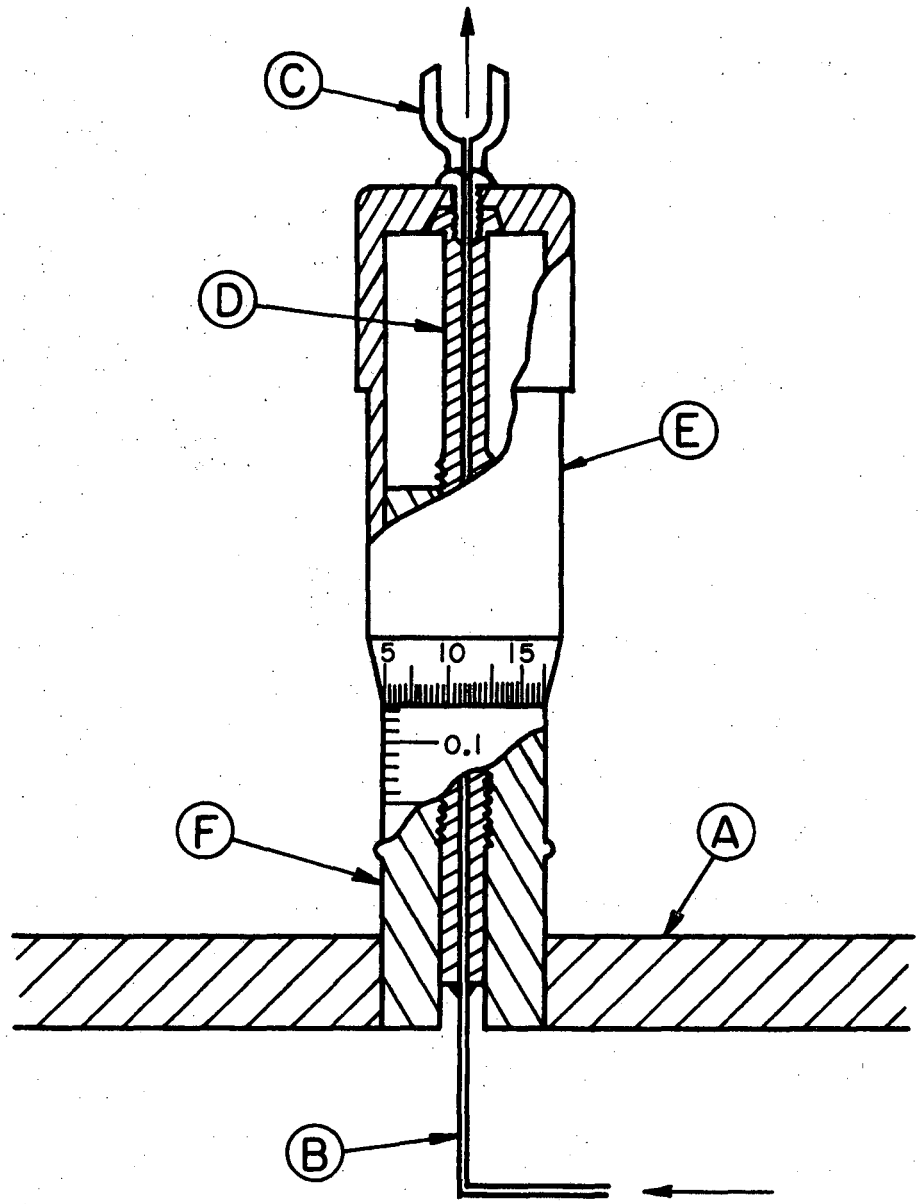

MUB-11292

Fig. 58. Detailed drawing of the micrometer probe. A, channel wall; B, sample probe; C, syringe adapter; D, central shaft; E, head; F, barrel.

APPENDIX C

EXPERIMENTAL DATA

This section of the report contains all the experimental data taken during this study. It takes on several forms; some data are simply tabulated while in other cases a brief computer program has been written to calculate the results where more complex equations were involved. In the latter cases the source programs are not included. The one exception is the care where a surfactant was found on the interface. The iteration method used is given in the computer program, and the source program is included.

At the end of each section of data, sample calculations are given.

Table C - 1

Data for the Evaporation of Pure Ethanol into Flowing Nitrogen

Run #	Gas Flow (cc./sec.)	Temperature (°C)	Graetz #	Kavg (cc/sec)	Per Cent Saturation Actual	Per Cent Saturation Calc.	% Error
1	117.4	22.1	0.2692	0.182	55.3	53.5	+3.3
2	235.5	22.3	0.1346	0.240	36.3	35.4	+2.6
3	483.0	21.3	0.0673	0.301	22.8	22.7	+0.4
4	709.	21.9	0.0449	0.347	17.5	17.6	-0.8
5	992.	----	-----	-----	----	----	----
6	68.2	20.0	0.466	0.143	74.2	71.0	+4.5
7	27.1	24.5	1.247	0.0686	90.0	94.0	+4.3
8	172.0	20.0	0.184	0.203	41.9	42.0	-0.2
9	334.0	21.2	0.0951	0.258	27.4	28.0	-2.1
10	203.0	22.5	0.1556	0.214	37.2	37.8	-1.7

Notes :

Run 5 is not reported since the result is in the turbulent region.

% Error = (% Satn. actual - % Satn Calc.)/ % Satn Calc. x 100

Sample Calculations: Runs 1 to 10

Run 1 $U_m = Q_g/0.915\ b\ W$ where 0.915 is the corner correction.

$Q_g = 117.$ cc/sec $b = 1.27$ cm $W = 7.62$ cm

Therefore $U_m = 14.5$ cm/sec.

$Gz = DL/U_m\ b^2$ where $D = 0.123\ cm^2/sec$ $L = 46.8$ cm

$Gz = 0.2692$

Saturation reading on the integrator at attenuation 32 and temperature 24.8°C is 35.8

$$\phi = \frac{\text{Chromatograph Reading x vap. press. ETOH at 25°C.}}{\text{Satn. Chromatograph Reading x V.P. EtOH at Run Temp.}}$$

$\phi = 17.8 \times 56.3/(35.8 \times 51.8) = 0.553$

$Kavg = \phi\ Q_g/LW \times 0.915 = 0.182$ cm/sec

According to the theory of Butler and Plewes

$\phi = 1-0.465\ -0.000 = 0.535$

% Error $= (0.553\ -0.535)/0.535 \times 100 = +\ 3.3\%$

Table C -2a
Concentration Profiles for Graetz Run # 9

Run #	y/B	Fraction Saturation Expt'l	Fraction Saturation Theoretical	% Error
9-1	0.104	0.842	0.81	3.8
9-2	0.204	0.571	0.64	11.0
9-3	0.354	0.375	0.42[illegible]	11.2
9-4	0.504	0.207	0.232	10.8
9-5	0.654	0.114	0.115	0.9
9-6	0.804	0.068	0.050	36.0

Table C - 2b
Concentration Profiles for Graetz Run # 10

Run #	y/B	Fraction Saturation Expt'l	Fraction Saturation Theoretical	% Error
10-1	0.075	0.876	0.885	2.4
10-2	0.175	0.734	0.735	0.1
10-3	0.325	0.507	0.524	3.2
10-4	0.475	0.363	0.350	3.7
10-5	0.625	0.220	0.222	1.0
10-6	0.825	0.167	0.140	19.2

Table C-3

Data and Calculations for Cocurrent Single Phase Runs

RUN	Q CC/SEC LIQUID	Q CC/SEC GAS	FR. SATURATION EXPTL	FR. SATURATION THEORY	GRAETZ NO	KAVG CC/SEC	GRP	KAVG(L/UOD)**.5 EXPTL	KAVG(L/UOD)**.5 THEORY	VEL. RATIO
39	51.00	387.00	.2310	0.210	0.0512	.2804	0.1414E 03	2.2150	1.9162	4.71
40	51.00	17.20	.9940	0.996	1.1514	.0537	0.1819E 01	0.4418	1.2918	0.23
41	51.00	25.80	.9510	0.975	0.7676	.0770	0.1005E 01	0.6321	1.2579	0.34
42	51.00	38.70	.9620	0.900	0.5117	.1046	0.2374E-00	0.8582	1.2178	0.51
43	51.00	51.50	.7370	0.790	0.3845	.1191	0.3889E-03	0.9751	1.1333	0.67
44	51.00	64.50	.6660	0.690	0.3070	.1348	0.2811E-00	1.1020	1.2203	0.84
45	51.00	77.40	.6010	0.625	0.2559	.1459	0.1066E 01	1.1916	1.2608	1.01
46	51.00	103.00	.4920	0.540	0.1923	.1590	0.4065E 01	1.2944	1.3488	1.33
47	51.00	154.30	.3790	0.395	0.1279	.1842	0.1568E 02	1.4911	1.4678	1.98
48	51.00	193.10	.3180	0.345	0.1026	.1926	0.2861E 02	1.5531	1.5661	2.45
49	51.00	258.00	.2690	0.280	0.0768	.2177	0.5822E 02	1.7432	1.7050	3.22
37	30.00	57.90	.6380	0.690	0.3426	.1157	0.5726E 01	1.2288	1.3677	1.27
50	30.00	17.20	.9950	0.995	1.1514	.0537	0.1271E 01	0.5747	1.2700	0.38
51	30.00	387.00	.1956	0.205	0.0512	.2375	0.6652E 03	2.3793	2.3988	7.57
52	30.00	258.00	.2370	0.265	0.0768	.1918	0.3097E 03	1.9649	2.1412	5.28
53	30.00	193.00	.3110	0.323	0.1026	.1883	0.1696E 03	1.9511	1.9651	4.04
54	30.00	154.90	.3510	0.385	0.1279	.1706	0.1038E 03	1.7795	1.8376	3.29
55	30.00	103.00	.4970	0.490	0.1923	.1606	0.3753E 02	1.6915	1.6162	2.23
56	30.00	77.40	.5300	0.595	0.2559	.1287	0.1628E 02	1.3619	1.4735	1.69
57	30.00	51.50	.7310	0.730	0.3845	.1181	0.3449E 01	1.2560	1.3376	1.14
58	30.00	64.50	.6220	0.650	0.3070	.1259	0.8752E 01	1.3352	1.3879	1.41
59	30.00	38.70	.8280	0.835	0.5117	.1005	0.5730E 00	1.0716	1.2364	0.86
38	30.00	25.80	.9540	0.960	0.7676	.0772	0.1355E-00	0.8251	1.2118	0.57
60	18.00	77.40	.5500	0.565	0.2559	.1335	0.1118E 03	1.8073	1.8560	2.76
61	18.00	258.00	.2270	0.265	0.0768	.1837	0.1333E 04	2.3596	2.6697	8.29
62	18.00	103.00	.4630	0.478	0.1923	.1496	0.2185E 03	2.0089	2.0364	3.62
63	18.00	51.50	.6050	0.705	0.3845	.0977	0.3730E 02	1.3333	1.6150	1.87
64	18.00	25.80	.9270	0.925	0.7676	.0750	0.2122E 01	1.0317	1.3024	0.95
65	18.00	17.20	.9540	0.985	1.1514	.0515	0.2269E-01	0.7098	1.1660	0.64
67	18.00	387.00	.1860	0.195	0.0512	.2258	0.2566E 04	2.8024	2.9598	11.62

Notes : KAVG(L/UOD)**.5 is $K_{c_{avg}}(L/U_oD)^{\frac{1}{2}}$ VEL.RATIO = U_m/U_o GRP = $a^2 D L/U_o^3$

Runs 11- 34 Oxygen is used as gas phase
Runs 35- 71 Carbon dioxide is used as gas phase.

Table C-3 Continued

RUN	Q CC/SEC LIQUID	Q CC/SEC GAS	FR. SATURATION EXPTL	FR. SATURATION THEORY	GRAETZ NO	KAVG CC/SEC	GRP	KAVG(L/DOD)**.5 EXPTL	KAVG(L/DOD)**.5 THEORY	VEL. RATIO
68	18.00	193.10	.3000	0.318	0.1026	.1817	0.7915E 03	2.3768	2.4631	6.44
69	18.00	154.90	.3300	0.370	0.1279	.1604	0.5169E 03	2.1205	2.3093	5.28
70	18.00	38.70	.7710	0.800	0.5117	.0936	0.1459E 02	1.2820	1.4572	1.41
71	18.00	64.50	.6040	0.620	0.3070	.1222	0.7016E 02	1.6605	1.7458	2.32
11	18.65	407.00	.2190	0.215	0.0604	.2796	0.2599E 04	2.9625	2.9658	11.06
12	18.65	207.00	.3170	0.340	0.1188	.2058	0.9079E 03	2.3296	2.5154	6.42
13	18.65	146.00	.4340	0.435	0.1685	.1988	0.4735E 03	2.2995	2.2793	4.73
14	18.65	73.50	.6310	0.650	0.3347	.1455	0.1036E 03	1.7299	1.8371	2.52
15	18.65	29.88	.9980	0.938	0.8517	.0904	0.4005E 01	1.0942	1.3478	1.02
24	18.65	35.30	.9420	0.895	0.6968	.1043	0.1045E 02	1.2591	1.4110	1.25
25	18.65	107.50	.5450	0.525	0.2288	.1838	0.2513E 03	2.1569	2.0774	3.58
26	18.65	47.00	.7980	0.800	0.5135	.1199	0.3128E 02	1.4401	1.5821	1.67
35	18.65	373.00	.2620	0.230	0.0659	.3066	0.2306E 04	3.2827	2.9099	10.35
16	37.30	407.00	.2100	0.235	0.0604	.2681	0.4405E 03	2.1482	2.2549	6.32
17	37.30	207.00	.3320	0.360	0.1188	.2156	0.1156E 03	1.7918	1.8645	3.46
18	37.30	146.00	.4190	0.405	0.1685	.1919	0.5090E 02	1.6137	1.6768	2.50
19	37.30	29.00	.9980	0.975	0.8785	.0877	0.4290E-00	0.7547	1.2286	0.50
20	37.30	73.50	.6610	0.695	0.3347	.1524	0.6151E 01	1.3001	1.3708	1.29
21	37.30	47.00	.8400	0.835	0.5135	.1262	0.5440E 00	1.0823	1.2348	0.85
22	37.30	107.50	.5190	0.550	0.2288	.1750	0.2221E 02	1.4829	1.5226	1.87
23	37.30	35.30	.9600	0.940	0.6968	.1063	0.1966E-01	0.9138	1.1634	0.63
36	37.30	373.00	.2620	0.255	0.0659	.3066	0.3766E 03	2.4711	2.2033	5.87
27	56.00	29.00	.9980	0.985	0.8785	.0877	0.1162E 01	0.6171	1.2651	0.34
28	56.00	47.00	.9070	0.907	0.5135	.1363	0.9570E-01	0.9568	1.2057	0.57
29	56.00	73.50	.7200	0.725	0.3347	.1660	0.4376E-00	1.1615	1.2291	0.87
30	56.00	107.50	.5250	0.585	0.2288	.1770	0.3687E 01	1.2330	1.3423	1.26
31	56.00	147.00	.4120	0.475	0.1673	.1900	0.1116E 02	1.3163	1.4197	1.71
32	56.00	207.00	.3210	0.375	0.1188	.2084	0.2930E 02	1.4328	1.5703	2.37
33	56.00	35.30	.9980	0.950	0.6958	.1105	0.6315E 00	0.7772	1.2395	0.42
34	56.00	407.00	.2210	0.235	0.0604	.2822	0.1360E 03	1.8910	1.9060	4.43

Sample Calculations: Runs 11 to 71

Run 49 Q_l = 51.00 cc/sec of Ethanol Q_g 258.0 cc/sec of CO_2

$D_g = 0.0789\ cm^2/sec$

The Graetz Number is $Gz = DL/U_m\ b^2$

$$U_m = Q_g/0.915\ bW$$

$$= 258.0/0.915 \times 1.27 \times 7.62$$

$$= 29.2\ cm/sec$$

and $Gz = 0.0768$

$$U_0 = \frac{1.5}{0.915Wb}\left[\frac{Q_G + Q_l(\mu_l/\mu_g)}{1+(\mu_l/\mu_g)}\right] \qquad \text{(A-20)}$$

Where $u_l = 1.15$ cp and $u_g = 0.0146$ cp

Therefore $U_0 = 9.07$ cm/sec

and $U_m/U_0 = 3.22$

It was found experimentally that the fraction saturation,

$$\phi_{exp.} = 0.269$$

From the computer solution the result for Gz = 0.768 and $U_m/U_0 = 3.22$ is

$$\phi_{th.} = 0.280$$

The average mass transfer coefficient is

$$Kavg = \phi Q_g/0.915\ LW = 0.2177\ cm/sec$$

The average Beek and Bakker distance group is

$$GRP = a^2DL/U_0^3$$

The value of a, the slope of the gas phase velocity profile at the interface, is

$$a = \frac{6}{Wb^2} \quad \frac{Q_g - Q_l}{1+(\mu_g/\mu_l)} \tag{A-20}$$

Therefore $a = 109.5 \text{ sec}^{-1}$

and $GRP = 109.5^2 \times 0.0789 \times 46.8/9.07^3 = 58.22$

According to the Beek and Bakker solution $Davg(L/U_0D)^{1/2} = 1.705$

The experimental value of $Kavg(L/U_0D)^{1/2} = 0.2177(46.8/9.07 \times 0.0789)^{1/2}$

$= 1.7432$

Cocurrent Interphase Mass Tranfer-Runs 213-257

These runs are calculated in almost exactly the same manner as the single phase controlled runs discussed above. The one difference is in the calculation of the theoretical values of the interphase mass transfer coefficient. Here the methods discussed in Chapter IV are used.

Table C-4

Concentration Profiles for Cocurrent Runs With Control in a Single Phase

Run 63
Graetz # = 0.385
Velocity Ratio = 1.87

y/b	Fraction Saturation Actual	Theoretical
0.075	0.957	0.940
0.175	0.890	0.875
0.275	0.816	0.810
0.475	0.712	0.725
0.675	0.645	0.670
0.875	0.533	0.640

Run 58
Graetz # = 0.3070
Velocity Ratio = 1.41

y/b	Fraction Saturation Actual	Theoretical
0.075	0.898	0.928
0.175	0.800	0.840
0.275	0.700	0.750
0.475	0.557	0.595
0.675	0.456	0.500
0.875	0.453	0.465

Run 46
Graetz # = 0.1923
Velocity Ratio = 1.33

y/b	Fraction Saturation Actual	Theoretical
0.075	0.932	0.895
0.175	0.737	0.760
0.275	0.634	0.647
0.475	0.424	0.443
0.675	0.294	0.326
0.875	0.251	0.279

Table C- 5
Single Phase Countercurrent Data

RUN	Q CC/SEC LIQUID	Q CC/SEC GAS	FR. SATN.	GRAETZ NO	MASS TRANSFER COEFFICIENT EXPTL	MASS TRANSFER COEFFICIENT GRAETZ	MASS TRANSFER COEFFICIENT MODEL
72	16.70	387.00	.1990	0.0512	.2416	.2317	.2263
73	17.65	258.00	.2480	0.0768	.2007	.1997	.1930
74	17.65	193.10	.3270	0.1026	.1981	.1796	.1724
75	17.65	154.90	.3630	0.1279	.1764	.1655	.1579
76	17.65	103.00	.4165	0.1923	.1346	.1415	.1337
77	17.65	77.40	.4990	0.2559	.1212	.1260	.1181
78	17.65	64.50	.5700	0.3070	.1153	.1164	.1086
79	17.65	51.50	.6230	0.3845	.1006	.1047	.0972
80	17.65	38.70	.7080	0.5117	.0860	.0901	.0831
81	17.65	25.80	.8250	0.7676	.0668	.0697	.0638
82	17.65	17.20	.8900	1.1514	.0480	.0510	.0465
83	35.30	387.00	.1850	0.0512	.2246	.2317	.2191
84	35.30	258.00	.2355	0.0768	.1906	.1997	.1861
85	35.30	193.10	.2844	0.1026	.1723	.1796	.1656
86	35.30	154.90	.3080	0.1279	.1497	.1655	.1513
87	35.30	103.00	.4030	0.1923	.1302	.1415	.1276
88	35.30	77.40	.4610	0.2559	.1119	.1260	.1126
89	35.30	64.50	.5145	0.3070	.1041	.1164	.1035
90	35.30	51.50	.5600	0.3845	.0905	.1047	.0926
91	35.30	38.70	.6280	0.5117	.0762	.0901	.0793
92	35.30	25.80	.7380	0.7676	.0597	.0697	.0612
93	35.30	17.20	.8420	1.1514	.0454	.0510	.0449
94	53.70	387.00	.1835	0.0512	.2228	.2317	.2128
95	53.70	258.00	.2230	0.0768	.1805	.1997	.1801
96	53.70	193.10	.2470	0.1026	.1496	.1796	.1598
97	53.70	154.90	.3010	0.1279	.1463	.1655	.1458
98	53.70	103.00	.3950	0.1923	.1276	.1415	.1228
99	53.70	77.40	.4410	0.2559	.1071	.1260	.1085
100	53.70	64.50	.4950	0.3070	.1002	.1164	.0998
101	53.70	51.50	.5520	0.3845	.0892	.1047	.0895
102	53.70	38.70	.5990	0.5117	.0727	.0901	.0768
103	53.70	25.80	.7040	0.7676	.0570	.0697	.0596
104	53.70	17.20	.8060	1.1514	.0435	.0510	.0440

Note; Graetz Number given in this table is equal to $D L / U_m b^2$ where b is the width of the gas phase

Sample Calculations: Runs 72 to 104

Run 95 Q_1 = 53.7 cc/sec of alcohol Q_g = 258.0 cc/sec of CO_2

This run is very similar to Run 49, which was used as the sample calculation for runs 11 to 71. Hence it is not necessary to go through all the preliminary calculations again. From the experimental readings it was found that:

$$Gz = 0.0768 \quad \phi = 0.223 \quad \text{and} \quad Kavg = 0.1805$$

This result is compared with the solution of Butler and Plewes

$$K_{avg} = Q_g(1-0.8956\ e^{-2.4304\ Gz}-0.006\ e^{-23.5\ Gz})/0.915\ WL$$
$$= 0.2053$$

Since Q_1 is a negative quantity in the constants in Eq. (A-20), there will be a point of zero velocity. This is found by setting the velocity at zero in Eq. (A-14). Therefore the distance from the interface to the flow reversal is

$$\Delta = (-k_2+(k_2^2-4 \times k_3k_4)^{1/2})/2\ k_4$$

$$k_2 = 6\left[(Q_g-Q_1)/(1+(\mu_g/\mu_1))\right]/W\ b^2 = 164.4\ sec^{-1}$$

$$k_3 = 1.5\left[(Q_g+Q_1(\mu_1/\mu_g))/(1+(\mu_1/\mu_g))\right]/W\ b^2 = 8.494\ cm/sec$$

$$k_4 = (k_2b(\mu_g/\mu_1)-k_3)/b^2 = 124.2\ cm/sec$$

From these quantities the point of flow reversal may easily be found. Δ = 0.05386 cm.

According to the film theory

$$K_{film} = D/\Delta$$
$$= 0.0789/0.0539$$
$$= 1.465\ cm/sec$$

In the remainder of the channel the Graetz number is

$$\psi = DL/U_m(B-\Delta)^2$$

$$= 0.0789 \times 46.8/29.14 \times (1.27 - 0.0539)^2$$

$$\psi = 0.0816$$

$$K_{Gz} = (1-0.8956\ e^{-(2.4302\psi)} - 0.0609\ e^{-(23.5\psi)})\ Q_g/WL \times 0.915$$

$$= (1-0.737 - 0.00926)258.0/0.915 \times 7.62 \times 46.8 = 0.202 \text{ cm/sec}$$

$$K_{th} = \frac{K_{film}\ K_{Gz}}{K_{film} + K_{Gz}} = 0.1801$$

<u>Countercurrent Interphase Mass Transfer Runs</u> Runs 258 to 288

Almost the same method of calculation was used in these runs as was used in Runs 72 to 104. The theoretical interphase mass transfer coefficient is predicted by the addition of the resistance of the gas phase predicted by the simplified countercurrent model and the resistance of the liquid phase predicted by the penetration model.

Table C-6

Concentration Profiles for Countercurent Runs
With Control in a Single Phase

Run 76
Graetz # =0.1923
Fr. Sat'n (avg) = 0.4165

y/b	Fraction Saturation
0.075	0.982
0.175	0.872
0.275	0.592
0.475	0.371
0.675	0.269
0.875	0.192

Run 90
Graetz # = 0.3845
Fr. Sat'n (avg) = 0.560

y/b	Fraction Saturation
0.075	0.783
0.175	0.709
0.275	0.643
0.475	0.571
0.675	0.479
0.875	0.439

Run 100
Graetz # = 0.307
Fr. Sat'n (avg) = 0.495

y/b	Fraction Saturation
0.075	0.810
0.175	0.710
0.275	0.604
0.475	0.460
0.675	0.407
0.875	0.377

Table C - 7

Interphase Cocurrent Experimental Data

RUN	Q CC/SEC LIQUID	Q CC/SEC GAS	FR. SATURATION EXPTL	FR. SATURATION THEORY	GRAETZ NO	KAVG CC/SEC	GRP	KAVG(L/UOD)**.5 EXPTL	KAVG(L/UOD)**.5 THEORY	VEL. RATIO
213	15.43	19.43	.6940	0.7360	0.9766	.0423	0.8558E 00	0.6425	0.8452	0.94
214	15.43	38.70	.5140	0.5260	0.4903	.0624	0.2784E 02	0.9416	0.9764	1.65
215	15.43	102.90	.2590	0.2580	0.1844	.0836	0.3460E 03	1.2350	1.1860	4.19
216	15.43	77.40	.3150	0.3260	0.2452	.0765	0.1826E 03	1.1393	1.1271	3.21
217	15.43	193.50	.1590	0.1600	0.0981	.0965	0.1208E 04	1.3854	1.3089	7.44
218	15.43	51.60	.3990	0.4340	0.3677	.0646	0.6552E 02	0.9704	1.0401	2.18
219	15.43	322.00	.1068	0.1080	0.0589	.1079	0.2849E 04	1.4907	1.3968	11.48
220	15.43	32.28	.4980	0.5810	0.5879	.0504	0.1479E 02	0.7626	0.9355	1.38
221	15.43	25.50	.5660	0.6630	0.7441	.0453	0.5356E 01	0.6863	0.8957	1.09
222	30.86	32.28	.7100	0.6710	0.5879	.0719	0.1357E-01	0.7731	0.8016	0.70
223	30.86	38.70	.5700	0.6060	0.4903	.0692	0.4110E-00	0.7433	0.8346	0.83
224	30.86	51.60	.4750	0.5130	0.3677	.0769	0.2838E 01	0.8240	0.8778	1.11
225	30.86	77.40	.3590	0.3790	0.2452	.0872	0.1392E 02	0.9301	0.9319	1.65
226	30.86	102.50	.3060	0.3070	0.1851	.0984	0.3215E 02	1.0454	0.9865	2.16
227	30.86	193.50	.1810	0.1840	0.0981	.1099	0.1514E 03	1.1499	1.1104	3.96
228	30.86	322.70	.1320	0.1280	0.0588	.1336	0.4305E 03	1.3699	1.2068	6.33
229	62.20	74.70	.4460	0.4750	0.2540	.1045	0.1278E-00	0.7910	0.8270	0.80
230	62.20	89.70	.3600	0.3990	0.2115	.1013	0.6139E 00	0.7657	0.8396	0.96
231	62.20	102.90	.3270	0.3690	0.1844	.1056	0.1336E 01	0.7969	0.8552	1.10
232	63.00	130.00	.2660	0.3140	0.1460	.1085	0.3439E 01	0.8120	0.8839	1.36
233	63.70	194.50	.2120	0.2210	0.0976	.1294	0.1229E 02	0.9579	0.9246	1.99
234	63.70	235.00	.1805	0.1950	0.0807	.1331	0.2066E 02	0.9822	0.9565	2.39
235	45.29	130.00	.2660	0.2820	0.1460	.1085	0.1442E 02	0.9537	0.9340	1.88
236	45.29	96.20	.3410	0.3470	0.1973	.1029	0.5333E 01	0.9082	0.8956	1.40
237	15.43	80.20	.4710	0.4190	1.1799	.1185	0.9292E 03	0.7826	0.7982	3.26
238	15.43	64.00	.5140	-----*	1.4786	.1032	0.5467E 03	0.6867	0.7776	2.64
239	15.43	37.45	.6150	-----*	2.5268	.0723	0.1212E 03	0.4869	0.7196	1.58
240	15.43	20.00	.6330	**---*	4.7314	.0397	0.5491E 01	0.2699	0.6294	0.86
241	15.43	114.89	.3510	0.3410	0.8236	.1265	0.1993E 04	0.8225	0.8276	4.52
242	15.43	240.00	.2880	0.1920	0.3943	.2168	0.7392E 04	1.3369	0.8760	8.50
243	30.86	80.20	.5680	0.5430	1.1799	.1429	0.7548E 02	0.6801	0.7022	1.69
244	30.86	114.89	.4400	0.4090	0.8236	.1586	0.2084E 03	0.7485	0.7402	2.38
245	30.86	240.41	.3150	0.2499	0.3936	.2376	0.1090E 04	1.0895	0.8044	4.71
246	30.86	172.50	.3140	0.3070	0.5486	.1699	0.5462E 03	0.7913	0.7775	3.48
247	30.86	63.75	.6400	0.6200	1.4844	.1280	0.3434E 02	0.6115	0.6748	1.36
248	46.29	240.41	.2370	0.2760	0.3936	.1787	0.3092E 03	0.6816	0.7554	3.26
249	46.29	172.50	.3140	0.3470	0.5486	.1699	0.1392E 03	0.6548	0.7248	2.39
250	46.29	114.89	.4100	0.4600	0.8236	.1478	0.4346E 02	0.5747	0.6827	1.62
251	46.29	80.20	.6600	0.5850	1.1799	.1660	0.1098E 02	0.6494	0.6402	1.14
252	46.29	64.00	.6920	-----*	1.4786	.1389	0.3043E 01	0.5448	0.6214	0.92
253	61.82	64.00	.7150	-----*	1.4786	.1436	0.1966E-01	0.4884	0.5827	0.69
254	61.82	71.00	.7060	-----*	1.3328	.1572	0.3469E-00	0.5345	0.5975	0.76
255	61.82	80.20	.6450	0.6280	1.1799	.1623	0.1381E 01	0.5510	0.6093	0.86
256	61.82	102.00	.6010	0.5360	0.9277	.1923	0.6496E 01	0.6512	0.6309	1.09
257	61.82	135.32	.5250	0.4950	0.6993	.2229	0.2122E 02	0.7517	0.6593	1.43

Notes:

Runs 213 - 236 Evaporation of ether from ethanol into CO_2.

Runs 237 - 257 Evaporation of ether from ethanol into helium.

* Computer solution not carried out to this Graetz number VEL. RATIO = U_m/U_o

Table C - 8
Countercurrent Interphase Experimental Data

RUN	Q CC/SEC LIQUID	Q CC/SEC GAS	FR. SATN.	GRAETZ NO	MASS TRANSFER COEFFICIENT EXPTL	MASS TRANSFER COEFFICIENT GRAETZ	MASS TRANSFER COEFFICIENT MODEL
258	61.82	63.75	.5710	1.4844	.1142	.1245	.1177
259	61.82	77.93	.5400	1.2143	.1320	.1391	.1316
260	61.82	80.00	.5340	1.1829	.1340	.1410	.1334
261	61.82	102.00	.4640	0.9277	.1485	.1576	.1495
262	61.82	135.22	.4050	0.6998	.1718	.1745	.1665
263	46.29	63.75	.5970	1.4844	.1194	.1175	.1124
264	46.29	80.00	.5150	1.1829	.1292	.1320	.1264
265	46.29	114.89	.3980	0.8236	.1434	.1526	.1470
266	46.29	172.00	.3780	0.5502	.2040	.1704	.1654
267	46.29	240.41	.3330	0.3936	.2511	.1811	.1769
268	30.86	240.41	.2410	0.3936	.1818	.1556	.1535
269	30.86	172.00	.2790	0.5502	.1505	.1485	.1458
270	30.86	114.89	.3980	0.8236	.1434	.1352	.1321
271	30.86	80.00	.4540	1.1829	.1139	.1191	.1158
272	30.86	63.75	.4730	1.4844	.0946	.1074	.1041
273	15.43	63.75	.5830	1.4844	.1166	.0894	.0882
274	15.43	80.00	.5380	1.1829	.1350	.0971	.0959
275	15.43	114.89	.4730	0.8236	.1705	.1066	.1056
276	15.43	172.00	.3880	0.5502	.2094	.1128	.1121
277	15.43	240.41	.3660	0.3936	.2760	.1142	.1137
279	46.29	240.41	.2820	0.3936	.2127	.1811	.1769
280	46.29	172.00	.3580	0.5502	.1932	.1704	.1654
281	46.29	114.89	.4140	0.8236	.1492	.1526	.1470
282	46.29	80.00	.5480	1.1829	.1375	.1320	.1264
283	46.29	63.75	.5900	1.4844	.1180	.1175	.1124
284	30.86	193.50	.1640	0.0981	.0996	.1011	.0957
285	30.86	102.90	.2190	0.1844	.0707	.0892	.0819
286	30.86	77.40	.3250	0.2452	.0789	.0834	.0755
287	30.86	51.60	.4050	0.3677	.0656	.0745	.0661
288	30.86	25.25	.5210	0.7515	.0413	.0548	.0479

Runs 258 -283 Data using helium
Runs 284 -288 Data using carbon dioxide

Analysis of Data in which Water was used as the Solvent

In Runs 105 to 211, which are interphase mass transfer data using ether-water solutions, it was found that there was a surfactant film on the interface. This is discussed in Chapter V. The object of "SURFER", the computer program reproduced on the next three pages, is to carry out the calculations indicated in Chapter V. The results of all the runs are included in the succeeding seven pages.

A. Description of "SURFER"

Necessary Input Data: All data are read from one card, statement 100, according to the Format given in statement 101. The necessary data are

NO - The run number

SG - The equilibration gas phase reading of the integrator on the chromatograph recorder reduced to 25°C.

SL - The liquid reading on the differential interferometer corresponding the gas reading, SG, using pure water as the reference liquid.

DIFFG - The diffusion coefficient of the gas phase. Cm^2/sec. (The liquid phase value is set at the value for infinitely dilute ether solutions in water as part of the program).

VISCL - The viscosity of the liquid phase in poises.

VISCG - The viscosity of the gas phase in poises.

QL - Flow rate of the liquid phase in cc/sec. (Dimensions of the channel are set within the program).

QG - Flow rate of the gas phase in cc/sec.

EL - Liquid phase reading of the run in question.

EXG - Gas phase reading of the run in question reduced to 25°C.

GRP - $C2G^2$ DIFFG $L/C3^3$, The Beek and Bakker distance group, (it is meaningless if C2G is negative).

AVGK - Average mass transfer coefficient assuming no surface contaminants, in cm/sec (invalid if C2G is negative).

CHB - AVGK $(L/C3\ DIFFG)^{1/2}$ Beek and Bakker mass transfer group. (Invalid if C2G is negative).

FR. SATN. - Experimental fraction saturation of the gas phase.

KAVG EXPTL - Experimental mass transfer coefficient in cm/sec.

EX. MT. GRP. - KAVG EXPTL $(L/C3\ DIFFG)^{1/2}$.

LEVEQUE MT COEFFICIENT - The mass transfer coefficient calculated for the case where there is a zero interfacial velocity. Cm/sec

INDICATED VELOCITY IS - Second to last calculated velocity in cm/sec.

J - Convergence at the Jth iteration

U(J-2) - Third to last calculated velocity cm/sec.

O and ORK - Last and second to last mass transfer coefficient. cm/sec.

VACT/C3 - Ratio of calculated velocity to velocity if there were no contaminants.

TOTAL SHEAR - Shear stress of both phases upon the interface. Dynes/cm.

GAS SHEAR - Shear stress of the gas phase alone upon the interface. Dynes/cm.

NOTE: If the Printout only includes information down to "INDIATED VELOCITY IS" the program has found a negative velocity on its first trial and has terminated.

B. Internal Calculations

From the given flow data, the program computes the interfacial velocity and the slope of the velocity in the gas phase at the interface assuming no retardation due to surfactants. It calculates the corresponding mass transfer coefficient for these flow conditions. The mass transfer coefficient for the case where there is zero interfacial velocity and the given flow conditions calculated. Finally the experimental mass transfer coefficient is computed. A first approximation to the interfacial velocity is derived by a simple interpolation. If the velocity proves to the negative, the computation is terminated, and the next run is considered. If it is positive, a slope of the velocity at the interface is calculated for each phase. From these three values a mass transfer coefficient is computed. It is checked with the experimental value, and it is either accepted or a new interpolation is made. A very small velocities, the calculation is unstable, and therefore one must resort to changing the velocity by fixed increments until there is a change of sign in the direction of change in the interfacial velocity. The calculation is terminated at that point, and the final three velocities are printed. After an interfacial velocity has been found, the shear stress on the interface is computed.

C. Output

The program prints the following information:

The run number, the two flow rates, and the diffusivity of the gas phase in cm^2/sec, all of which are self explanatory.

C2G - The slope of the gas phase velocity profile at the interface. (If Q_g if less than Q_1, this value is negative; no minus sign is printed). This assumes no interfacial contaminants. Units sec^{-1}.

C3 - Interfacial velocity assuming no contaminants in cm/sec.

```
      WRITE(3,402)
  402 FORMAT(62H  COMPUTATION OF DATA WITH A SURFACTANT ON THE WATER INT
     1ERFACE)
  100 READ(2,101) NO,SG,SL,DIFFG,VISCL,VISCG,QL,QG,EL,EXG
  101 FORMAT(I3,2F5.3,3F5.5,2F5.2,2F5.3)
      WRITE(3,400) NO
  400 FORMAT (12H RUN NUMBER ,I3)
      B=1.27
      W= 7.62*.915
      C3=(1.5/(W*B))*(QG + QL*(VISCL/VISCG))/(1.0 + VISCL/VISCG)
      C2G=(1.0/B**2)*(4.0*B*C3 - 6.0*QL/W)*(VISCL/VISCG)
      C2L= C2G*(VISCG/VISCL)
      C1G=-(C2G*B + C3)/B**2
      C1L= (B*C2L - C3)/B**2
      WRITE (3,405) QG ,QL
  405 FORMAT(9H Q GAS = ,F10.4,18H CC/SEC    Q LIQ = ,F10.4,7H CC/SEC)
      XO = 2.54*12.0*1.5
      GRP = (C2G**2)*DIFFG*XO/C3**3
      GUMP = C3**3/(C2G*C2G*DIFFG)
      STAR = C2G*DIFFG/(XO*C3)
      IF (GRP - 0.1) 503,503,504
  503 AVGK = STAR*((4.0/3.1416)**.5*XO**.5*GUMP**.5 + XO/4.0)
      GO TO 515
  504 IF (GRP - 10.0)505,505,506
 5050 AVGK = (C3*DIFFG/XO)**.5*(1.2036 + .0616*GRP - .00787*GRP**2
     1 + .00037*GRP**3)
      GO TO 515
  506 AVGK=(C3*DG/XO)**.5*(1.615*GRP**.1667*(.5+.375/(GRP**.333))-.193)
  515 CONTINUE
      AR=2.0*(0.96E-5*C3/(XO*3.1416))**0.5
      AVGK=AVGK*AR/(0.03264*AVGK+AR)
      PCS=EXG*SL/(SG*EL)
      XPTK=PCS*QG/355.5
      CH=          (XO/(C3*DIFFG))**0.5
      CHB = AVGK*CH
      CHE = XPTK*CH
      WRITE(3,516) DIFFG, C2G, C3
  516 FORMAT(7H DIFFG= 1PE10.4, 6H  C2G= E10.4, 5H  C3= E10.4 )
      WRITE(3,517) GRP, CHB, AVGK
  517 FORMAT(5H GRP= 1PE10.4, 6H  CHB= E10.4, 7H  AVGK= E10.4, 1H )
      WRITE(3,401) PCS,XPTK,CHE
  401 FORMAT(10H FR. SATN=,F5.4,13H KAVG EXPTL= ,F7.5,11H EX.MT.GRP=,F8.
     16)
      UO=C3
      AG=.683*QG
      AL=.683*QL
      DG=DIFFG
      GL=(AG*DG*DG/46.8)**0.333
      RL=(AG*DG*DG/(AL*0.92E-10))**0.3333
      J=1
      RL=0.0326*RL
      AV=0.808*GL/(1.0+RL)
      WRITE (3,35)    AV
   35 FORMAT(27H LEVESQUE MT COEFFICIENT =  ,E10.4)
      U=(UO     *(XPTK-AV)/(AVGK-AV))
```

```
      IF(U) 12,12,41
   12 WRITE(3,13)  U,J
   13 FORMAT(23H INDICATED VELOCITY IS ,E10.4,4H J= ,I3)
      GO TO 10
   41 CONTINUE
      VAV=QG/(B*W*B)
      VAW=QL/(B*W*B)
    1 C2G=6.0*VAV-4.0*U
      IF(C2G)   15,15,14
   15 WRITE(3,16) C2G,J
   16 FORMAT(14H GAS SLOPE IS ,E10.4,4H J= ,I3)
      GO TO 10
   14 C2L=6.0*VAW-4.0*U
      IF(C2L)   18,18,17
   18 WRITE(3,19)  C2L,J
   19 FORMAT(17H LIQUID SLOPE IS ,E10.4,4H J= ,I3)
      GO TO 10
   17 C3=U
      GRP = (C2G**2)*DIFFG*XO/C3**3
      GUMP = C3**3/(C2G*C2G*DIFFG)
      STAR = C2G*DIFFG/(XO*C3)
      IF (GRP - 0.1) 523,523,524
  523 AVG  = STAR*((4.0/3.1416)**.5*XO**.5*GUMP**.5 + XO/4.0)
      GO TO 527
  524 IF (GRP - 10.0)525,525,526
 5250 AVG  = (C3*DIFFG/XO)**.5*(1.2036 + .0616*GRP - .00787*GRP**2
     1 + .00037*GRP**3)
      GO TO 527
  526 AVG =(C3*DG/XO)**.5*(1.615*GRP**.1667*(.5+.375/(GRP**.333))-.193)
  527 CONTINUE
      DL=0.96E-5
      GRP = (C2L**2)*DL   *XO/C3**3
      GUMP = C3**3/(C2L*C2L*DL)
      STAR = C2L*DL   /(XO*C3)
      IF (GRP - 0.1) 533,533,534
  533 AVL  = STAR*((4.0/3.1416)**.5*XO**.5*GUMP**.5 + XO/4.0)
      GO TO 537
  534 IF (GRP - 10.0)535,535,536
 5350 AVL  = (C3*DL   /XO)**.5*(1.2036 + .0616*GRP - .00787*GRP**2
     1 + .00037*GRP**3)
      GO TO 537
  536 AVL =(C3*DL/XO)**.5*(1.615*GRP**.1667*(.5+.375/(GRP**.333))-.193)
  537 CONTINUE
      OKG=AVG*AVL/(0.03264*AVG+AVL)
      CHK=ABS(OKG-XPTK)
      IF(CHK-0.0001)   7,7,3
    3 IF(J-100)  4,4,5
    4 IF(C3-.1*UO)   26,26,27
   27 IF(J-1)  8,8,9
    8 U=(C3     *(XPTK-AV)/(OKG -AV))
      IF(U)  20,20,21
   20 WRITE(3,22)  U
   22 FORMAT(23H INDICATED VELOCITY IS   ,E10.4)
      GO TO 10
   21 O=OKG
      C=C3
```

```
      J=2
      GO TO 1
    9 U=(C3      +(C     -C3     )*(XPTK-OKG)/(O-OKG))
      J=J+1
      IF(U)  24,24,23
   24 WRITE(3,25)  U,J
   25 FORMAT(23H INDICATED VELOCITY IS    ,E10.4,4H J= ,I3)
      GO TO 10
   23 O=OKG
      C=C3
      GO TO 1
   26 IF(XPTK-OKG)  28,28,29
   28 U=.9*C3
      IF(C-C3)   30,30,31
   30 WRITE(3,32)      U,J,C
   32 FORMAT(23H INDICATED VELOCITY IS    ,E10.4,4H J= ,I3 ,10H U(J-2) =
     1,E10.4)
      WRITE(3,36) O,OKG
   36 FORMAT( 6H O =  ,E10.4, 7H OKG = ,E10.4)
      GO TO 7
   29 U=1.1*C3
      IF(C-C3)   31,31,33
   33 WRITE(3,34)      U,J,C
   34 FORMAT(23H INDICATED VELOCITY IS    ,E10.4,4H J= ,I3 ,10H U(J-2) =
     1,E10.4)
      WRITE(3,37) O,OKG
   37 FORMAT( 6H O =  ,E10.4, 7H OKG = ,E10.4)
      GO TO 7
   31 C=C3
      O=OKG
      J=J+1
      GO TO 1
    5 WRITE(3,6)
    6 FORMAT(23H NO CONVERGENCE          )
      GO TO 10
    7 VR=C3/UO
      TAU=VISCL*C2L +VISCG*C2G
      TA=VISCG*C2G
      WRITE(3,11) VR,TAU,TA
   11 FORMAT( 9H VACT/C3=,          F7.5,15H TOTAL SHEAR = ,E10.4,12H GAS
     1 SHEAR =,E10.4/)
   10 GO TO 100
      STOP
      END
RUN NUMBER 105
Q GAS =     16.6700 CC/SEC    Q LIQ =     15.4300 CC/SEC
DIFFG=9.3800E-02  C2G=6.4705E-01  C3=2.6184E 00
GRP=1.0001E-01  CHB=2.7130E-01  AVGK=1.9885E-02
FR. SATN=.2365 KAVG EXPTL= 0.01109 EX.MT.GRP=0.151311
LEVESQUE MT COEFFICIENT = 0.6406E-02
VACT/C3=0.21329 TOTAL SHEAR = 0.5472E-01 GAS SHEAR =0.1332E-02
RUN NUMBER 106
Q GAS =      8.3400 CC/SEC    Q LIQ =     15.4300 CC/SEC
DIFFG=9.3800E-02  C2G=3.6997E 00  C3=2.5874E 00
GRP=3.3886E 00  CHB=2.7719E-01  AVGK=2.0196E-02
```

```
FR. SATN=.3664 KAVG EXPTL= 0.00860 EX.MT.GRP=0.117969
LEVESQUE MT COEFFICIENT = 0.6307E-02
VACT/C3=0.12345 TOTAL SHEAR = 0.6253E-01 GAS SHEAR =0.6344E-03
RUN NUMBER 107
Q GAS =    25.0000 CC/SEC    Q LIQ =    15.4300 CC/SEC
DIFFG=9.3800E-02  C2G=4.9938E 00  C3=2.6495E 00
GRP=5.7503E 00  CHB=2.7853E-01  AVGK=2.0535E-02
FR. SATN=.1600 KAVG EXPTL= 0.01125 EX.MT.GRP=0.152603
LEVESQUE MT COEFFICIENT = 0.6456E-02
VACT/C3=0.20843 TOTAL SHEAR = 0.5584E-01 GAS SHEAR =0.2226E-02
RUN NUMBER 108
Q GAS =    33.3000 CC/SEC    Q LIQ =    15.4300 CC/SEC
DIFFG=9.3800E-02  C2G=9.3248E 00  C3=2.6804E 00
GRP=1.9365E 01  CHB=2.8362E-01  AVGK=2.1032E-02
FR. SATN=.1206 KAVG EXPTL= 0.01129 EX.MT.GRP=0.152308
LEVESQUE MT COEFFICIENT = 0.6487E-02
VACT/C3=0.20186 TOTAL SHEAR = 0.5713E-01 GAS SHEAR =0.3121E-02
RUN NUMBER 109
Q GAS =    41.7000 CC/SEC    Q LIQ =    15.4300 CC/SEC
DIFFG=9.3800E-02  C2G=1.3708E 01  C3=2.7116E 00
GRP=4.0417E 01  CHB=2.8797E-01  AVGK=2.1479E-02
FR. SATN=.0941 KAVG EXPTL= 0.01103 EX.MT.GRP=0.147944
LEVESQUE MT COEFFICIENT = 0.6510E-02
VACT/C3=0.18725 TOTAL SHEAR = 0.5924E-01 GAS SHEAR =0.4044E-02
RUN NUMBER 110
Q GAS =    50.0000 CC/SEC    Q LIQ =    15.4300 CC/SEC
DIFFG=9.3800E-02  C2G=1.8039E 01  C3=2.7425E 00
GRP=6.7652E 01  CHB=2.9114E-01  AVGK=2.1839E-02
FR. SATN=.0763 KAVG EXPTL= 0.01073 EX.MT.GRP=0.143105
LEVESQUE MT COEFFICIENT = 0.6527E-02
VACT/C3=0.17111 TOTAL SHEAR = 0.6152E-01 GAS SHEAR =0.4960E-02
RUN NUMBER 111
Q GAS =    66.7000 CC/SEC    Q LIQ =    15.4300 CC/SEC
DIFFG=9.3800E-02  C2G=2.6753E 01  C3=2.8047E 00
GRP=1.3912E 02  CHB=2.9565E-01  AVGK=2.2427E-02
FR. SATN=.0569 KAVG EXPTL= 0.01067 EX.MT.GRP=0.140680
LEVESQUE MT COEFFICIENT = 0.6553E-02
VACT/C3=0.15946 TOTAL SHEAR = 0.6411E-01 GAS SHEAR =0.6760E-02
RUN NUMBER 112
Q GAS =   100.0000 CC/SEC    Q LIQ =    15.4300 CC/SEC
DIFFG=9.3800E-02  C2G=4.4130E 01  C3=2.9287E 00
GRP=3.3247E 02  CHB=3.0106E-01  AVGK=2.3337E-02
FR. SATN=.0370 KAVG EXPTL= 0.01039 EX.MT.GRP=0.134097
LEVESQUE MT COEFFICIENT = 0.6585E-02
VACT/C3=0.14549 TOTAL SHEAR = 0.6843E-01 GAS SHEAR =0.1033E-01
RUN NUMBER 113
Q GAS =   133.0000 CC/SEC    Q LIQ =    15.4300 CC/SEC
DIFFG=9.3800E-02  C2G=6.1350E 01  C3=3.0516E 00
GRP=5.6803E 02  CHB=3.0430E-01  AVGK=2.4077E-02
FR. SATN=.0280 KAVG EXPTL= 0.01048 EX.MT.GRP=0.132470
LEVESQUE MT COEFFICIENT = 0.6605E-02
VACT/C3=0.14093 TOTAL SHEAR = 0.7181E-01 GAS SHEAR =0.1385E-01
RUN NUMBER 114
Q GAS =   250.0000 CC/SEC    Q LIQ =    15.4300 CC/SEC
DIFFG=9.3800E-02  C2G=1.2240E 02  C3=3.4871E 00
GRP=1.5152E 03  CHB=3.0993E-01  AVGK=2.6215E-02
FR. SATN=.0125 KAVG EXPTL= 0.00880 EX.MT.GRP=0.104068
LEVESQUE MT COEFFICIENT = 0.6644E-02
INDICATED VELOCITY IS 0.2574E-00 J=   2 U(J-2) = 0.3846E-00
D =  0.1019E-01 DKG = 0.8458E-02
VACT/C3=0.06711 TOTAL SHEAR = 0.9143E-01 GAS SHEAR =0.2649E-01
RUN NUMBER 115
Q GAS =   417.0000 CC/SEC    Q LIQ =    15.4300 CC/SEC
DIFFG=9.3800E-02  C2G=2.0955E 02  C3=4.1089E 00
GRP=2.7145E 03  CHB=3.1307E-01  AVGK=2.8744E-02
FR. SATN=.0078 KAVG EXPTL= 0.00919 EX.MT.GRP=0.130146
LEVESQUE MT COEFFICIENT = 0.6670E-02
INDICATED VELOCITY IS 0.2875E-00 J=   2 U(J-2) = 0.4700E-00
D =  0.1121E-01 DKG = 0.8825E-02
VACT/C3=0.06360 TOTAL SHEAR = 0.1083E-00 GAS SHEAR =0.4429E-01
RUN NUMBER 138
Q GAS =     8.3400 CC/SEC    Q LIQ =    30.8600 CC/SEC
DIFFG=9.3800E-02  C2G=1.1751E 01  C3=5.1438E 00
GRP=4.3513E 00  CHB=2.7791E-01  AVGK=2.8549E-02
FR. SATN=.4193 KAVG EXPTL= 0.00984 EX.MT.GRP=0.095766
LEVESQUE MT COEFFICIENT = 0.7792E-02
INDICATED VELOCITY IS 0.4563E-00 J=   1 U(J-2) = 0.4700E-00
D =  0.1121E-01 DKG = 0.1042E-01
VACT/C3=0.09856 TOTAL SHEAR = 0.1290E-00 GAS SHEAR =0.4944E-03
RUN NUMBER 139
Q GAS =    15.4600 CC/SEC    Q LIQ =    30.8600 CC/SEC
DIFFG=9.3800E-02  C2G=8.0360E 00  C3=5.1703E 00
GRP=2.0037E 00  CHB=2.7552E-01  AVGK=2.8377E-02
FR. SATN=.2486 KAVG EXPTL= 0.01081 EX.MT.GRP=0.104956
LEVESQUE MT COEFFICIENT = 0.7929E-02
INDICATED VELOCITY IS 0.5168E 00 J=   2 U(J-2) = 0.7283E 00
D =  0.1239E-01 DKG = 0.1057E-01
VACT/C3=0.09086 TOTAL SHEAR = 0.1311E-00 GAS SHEAR =0.1274E-02
RUN NUMBER 140
Q GAS =    25.0000 CC/SEC    Q LIQ =    30.8600 CC/SEC
DIFFG=9.3800E-02  C2G=3.0578E 00  C3=5.2058E 00
GRP=2.8423E-01  CHB=2.7184E-01  AVGK=2.8093E-02
FR. SATN=.1572 KAVG EXPTL= 0.01106 EX.MT.GRP=0.106996
LEVESQUE MT COEFFICIENT = 0.8021E-02
INDICATED VELOCITY IS 0.5129E 00 J=   2 U(J-2) = 0.7876E 00
D =  0.1315E-01 DKG = 0.1077E-01
VACT/C3=0.08956 TOTAL SHEAR = 0.1322E-00 GAS SHEAR =0.2295E-02
RUN NUMBER 141
Q GAS =    33.3000 CC/SEC    Q LIQ =    30.8600 CC/SEC
DIFFG=9.3800E-02  C2G=1.2732E 00  C3=5.2367E 00
GRP=4.8410E-02  CHB=2.6995E-01  AVGK=2.7981E-02
FR. SATN=.1187 KAVG EXPTL= 0.01112 EX.MT.GRP=0.107299
LEVESQUE MT COEFFICIENT = 0.8069E-02
INDICATED VELOCITY IS 0.5018E 00 J=   2 U(J-2) = 0.8028E 00
D =  0.1344E-01 DKG = 0.1081E-01
VACT/C3=0.08712 TOTAL SHEAR = 0.1335E-00 GAS SHEAR =0.3188E-02
RUN NUMBER 142
Q GAS =    41.7000 CC/SEC    Q LIQ =    30.8600 CC/SEC
DIFFG=9.3800E-02  C2G=5.6565E 00  C3=5.2680E 00
GRP=9.3855E-01  CHB=2.7350E-01  AVGK=2.8434E-02
FR. SATN=.0955 KAVG EXPTL= 0.01121 EX.MT.GRP=0.107787
LEVESQUE MT COEFFICIENT = 0.8105E-02
INDICATED VELOCITY IS 0.5008E 00 J=   2 U(J-2) = 0.8035E 00
D =  0.1358E-01 DKG = 0.1088E-01
VACT/C3=0.08642 TOTAL SHEAR = 0.1344E-00 GAS SHEAR =0.4086E-02
RUN NUMBER 143
Q GAS =    50.0000 CC/SEC    Q LIQ =    30.8600 CC/SEC
DIFFG=9.3800E-02  C2G=9.9875E 00  C3=5.2989E 00
GRP=2.8752E 00  CHB=2.7668E-01  AVGK=2.8848E-02
FR. SATN=.0766 KAVG EXPTL= 0.01077 EX.MT.GRP=0.103312
LEVESQUE MT COEFFICIENT = 0.8132E-02
INDICATED VELOCITY IS 0.4276E-00 J=   2 U(J-2) = 0.6753E 00
D =  0.1272E-01 DKG = 0.1038E-01
VACT/C3=0.07335 TOTAL SHEAR = 0.1377E-00 GAS SHEAR =0.5024E-02
```

```
RUN NUMBER 144
Q GAS =    100.0000 CC/SEC    Q LIQ =     30.8600 CC/SEC
DIFFG=9.3800E-02  C2G=3.6078E 01  C3=5.4851E 00
GRP=3.3826E 01  CHB=2.8689E-01  AVGK=3.0434E-02
FR. SATN=.0360 KAVG EXPTL= 0.01011 EX.MT.GRP=0.095335
LEVESQUE MT COEFFICIENT = 0.8222E-02
VACT/C3=0.06208 TOTAL SHEAR = 0.1448E-00 GAS SHEAR =0.1040F-01
RUN NUMBER 145
Q GAS =     66.7000 CC/SEC    Q LIQ =     30.8600 CC/SEC
DIFFG=9.3800E-02  C2G=1.8702E 01  C3=5.3611E 00
GRP=9.7346E 00  CHB=2.7978E-01  AVGK=2.9342E-02
FR. SATN=.0569 KAVG EXPTL= 0.01068 EX.MT.GRP=0.101797
LEVESQUE MT COEFFICIENT = 0.8171E-02
INDICATED VELOCITY IS 0.4025E-00 J=   2 U(J-2) = 0.6342E 00
D =  0.1251E-01 DKG = 0.1027E-01
VACT/C3=0.06826 TOTAL SHEAR = 0.1403E-00 GAS SHEAR =0.6825E-02
RUN NUMBER 146
Q GAS =    133.0000 CC/SEC    Q LIQ =     30.8600 CC/SEC
DIFFG=9.3800E-02  C2G=5.3298E 01  C3=5.6079E 00
GRP=6.9076E 01  CHB=2.9127E-01  AVGK=3.1242E-02
FR. SATN=.0252 KAVG EXPTL= 0.00944 EX.MT.GRP=0.088026
LEVESQUE MT COEFFICIENT = 0.8253E-02
INDICATED VELOCITY IS 0.2870E-00 J=   2 U(J-2) = 0.2899E-00
D =  0.9690E-02 DKG = 0.9332E-02
VACT/C3=0.04653 TOTAL SHEAR = 0.1512E-00 GAS SHEAR =0.1398E-01
RUN NUMBER 147
Q GAS =    250.0000 CC/SEC    Q LIQ =     30.8600 CC/SEC
DIFFG=9.3800E-02  C2G=1.1435E 02  C3=6.0435E 00
GRP=2.5405E 02  CHB=2.9941E-01  AVGK=3.3339E-02
FR. SATN=.0121 KAVG EXPTL= 0.00854 EX.MT.GRP=0.076682
LEVESQUE MT COEFFICIENT = 0.8314E-02
INDICATED VELOCITY IS 0.5957E-01 J=   1 U(J-2) = 0.2899E-00
D =  0.9690E-02 DKG = 0.7689E-02
VACT/C3=0.00896 TOTAL SHEAR = 0.1712E-00 GAS SHEAR =0.2663E-01
RUN NUMBER 163
Q GAS =    417.0000 CC/SEC    Q LIQ =     30.8600 CC/SEC
DIFFG=9.3800E-02  C2G=2.0149E 02  C3=6.6653E 00
GRP=5.8800E 02  CHB=3.0450E-01  AVGK=3.5608E-02
FR. SATN=.0075 KAVG EXPTL= 0.00881 EX.MT.GRP=0.075349
LEVESQUE MT COEFFICIENT = 0.8355E-02
INDICATED VELOCITY IS 0.1226E-00 J=   1 U(J-2) = 0.2899E-00
D =  0.9690E-02 DKG = 0.8099E-02
VACT/C3=0.01672 TOTAL SHEAR = 0.1870E-00 GAS SHEAR =0.4441E-01
RUN NUMBER 148
Q GAS =    417.0000 CC/SEC    Q LIQ =     37.1500 CC/SEC
DIFFG=9.3800E-02  C2G=1.9821E 02  C3=7.7074E 00
GRP=3.6800E 02  CHB=3.0168E-01  AVGK=3.7936E-02
FR. SATN=.0092 KAVG EXPTL= 0.01084 EX.MT.GRP=0.086215
LEVESQUE MT COEFFICIENT = 0.8873E-02
INDICATED VELOCITY IS 0.4698E-00 J=   1 U(J-2) = 0.2899E-00
D =  0.9690E-02 DKG = 0.1218E-01
VACT/C3=0.06773 TOTAL SHEAR = 0.2019E-00 GAS SHEAR =0.4408E-01
RUN NUMBER 176
Q GAS =      8.3400 CC/SEC    Q LIQ =     49.7000 CC/SEC
DIFFG=9.3800E-02  C2G=2.1582E 01  C3=8.2652E 00
GRP=3.5379E 00  CHB=2.7732E-01  AVGK=3.6113E-02
FR. SATN=.3912 KAVG EXPTL= 0.00918 EX.MT.GRP=0.070484
LEVESQUE MT COEFFICIENT = 0.8988E-02
INDICATED VELOCITY IS 0.6382E-01 J=   1 U(J-2) = 0.2899E-00
D =  0.9690E-02 DKG = 0.8219E-02
VACT/C3=0.00702 TOTAL SHEAR = 0.2348E-00 GAS SHEAR =0.8435E-03
RUN NUMBER 177
Q GAS =     16.6700 CC/SEC    Q LIQ =     49.7000 CC/SEC
DIFFG=9.3800E-02  C2G=1.7236E 01  C3=8.2962E 00
GRP=2.2311E 00  CHB=2.7586E-01  AVGK=3.5990E-02
FR. SATN=.2414 KAVG EXPTL= 0.01132 EX.MT.GRP=0.086766
LEVESQUE MT COEFFICIENT = 0.9192E-02
INDICATED VELOCITY IS 0.5929E 00 J=   1 U(J-2) = 0.2899E-00
D =  0.9690E-02 DKG = 0.1225E-01
VACT/C3=0.07941 TOTAL SHEAR = 0.2138E-00 GAS SHEAR =0.1252E-02
RUN NUMBER 288
Q GAS =      8.9200 CC/SEC    Q LIQ =     51.6400 CC/SEC
DIFFG=9.3800E-02  C2G=2.2292E 01  C3=8.5887E 00
GRP=3.3637E 00  CHB=2.7717E-01  AVGK=3.6792E-02
FR. SATN=.3873 KAVG EXPTL= 0.00972 EX.MT.GRP=0.073209
LEVESQUE MT COEFFICIENT = 0.9113E-02
INDICATED VELOCITY IS 0.2066E-00 J=   1 U(J-2) = 0.2899E-00
D =  0.9690E-02 DKG = 0.8884E-02
VACT/C3=0.02187 TOTAL SHEAR = 0.2393E-00 GAS SHEAR =0.9016E-03
RUN NUMBER 289
Q GAS =     16.6700 CC/SEC    Q LIQ =     51.6400 CC/SEC
DIFFG=9.3800E-02  C2G=1.8248E 01  C3=8.6176E 00
GRP=2.2314E 00  CHB=2.7586E-01  AVGK=3.6680E-02
FR. SATN=.2173 KAVG EXPTL= 0.01019 EX.MT.GRP=0.076648
LEVESQUE MT COEFFICIENT = 0.9299E-02
INDICATED VELOCITY IS 0.3090E-00 J=   1 U(J-2) = 0.2899E-00
D =  0.9690E-02 DKG = 0.9640E-02
VACT/C3=0.03259 TOTAL SHEAR = 0.2368E-00 GAS SHEAR =0.1554E-02
RUN NUMBER 178
Q GAS =     25.0000 CC/SEC    Q LIQ =     51.6400 CC/SEC
DIFFG=9.3800E-02  C2G=1.3901E 01  C3=8.6486E 00
GRP=1.2811E 00  CHB=2.7424E-01  AVGK=3.6530E-02
FR. SATN=.1548 KAVG EXPTL= 0.01098 EX.MT.GRP=0.081713
LEVESQUE MT COEFFICIENT = 0.9404E-02
INDICATED VELOCITY IS 0.4249E-00 J=   1 U(J-2) = 0.2899E-00
D =  0.9690E-02 DKG = 0.1135E-01
VACT/C3=0.05458 TOTAL SHEAR = 0.2307E-00 GAS SHEAR =0.2290E-02
RUN NUMBER 179
Q GAS =     33.0000 CC/SEC    Q LIQ =     51.6400 CC/SEC
DIFFG=9.3800E-02  C2G=9.7266E 00  C3=8.6784E 00
GRP=6.2075E-01  CHB=2.7274E-01  AVGK=3.6393E-02
FR. SATN=.1177 KAVG EXPTL= 0.01093 EX.MT.GRP=0.081905
LEVESQUE MT COEFFICIENT = 0.9469E-02
INDICATED VELOCITY IS 0.4235E-00 J=   1 U(J-2) = 0.2899E-00
D =  0.9690E-02 DKG = 0.1146E-01
VACT/C3=0.05422 TOTAL SHEAR = 0.2316E-00 GAS SHEAR =0.3145E-02
RUN NUMBER 180
Q GAS =     41.7000 CC/SEC    Q LIQ =     51.6400 CC/SEC
DIFFG=9.3800E-02  C2G=5.1869E 00  C3=8.7108E 00
GRP=1.7456E-01  CHB=2.7152E-01  AVGK=3.6298E-02
FR. SATN=.0948 KAVG EXPTL= 0.01112 EX.MT.GRP=0.083180
LEVESQUE MT COEFFICIENT = 0.9520E-02
INDICATED VELOCITY IS 0.4684E-00 J=   1 U(J-2) = 0.2899E-00
D =  0.9690E-02 DKG = 0.1190E-01
VACT/C3=0.05974 TOTAL SHEAR = 0.2307E-00 GAS SHEAR =0.4033E-02
RUN NUMBER 181
Q GAS =     50.0000 CC/SEC    Q LIQ =     51.6400 CC/SEC
DIFFG=9.3800E-02  C2G=8.5577E-01  C3=8.7417E 00
GRP=4.7015E-03  CHB=5.0344E-01  AVGK=6.7420E-02
FR. SATN=.0791 KAVG EXPTL= 0.01113 EX.MT.GRP=0.083120
LEVESQUE MT COEFFICIENT = 0.9557E-02
INDICATED VELOCITY IS 0.2616E-00 J=   1 U(J-2) = 0.2899E-00
D =  0.9690E-02 DKG = 0.9716E-02
VACT/C3=0.02720 TOTAL SHEAR = 0.2419E-00 GAS SHEAR =0.5145E-02
```

```
RUN NUMBER 182
Q GAS =    66.7000 CC/SEC   Q LIQ =    51.6400 CC/SEC
DIFFG=9.3800E-02  C2G=7.8585E 00  C3=8.8038E 00
GRP=3.8813E-01  CHB=2.7213E-01  AVGK=3.6573E-02
FR. SATN=.0677 KAVG EXPTL= 0.01270 EX.MT.GRP=0.094533
LEVESQUE MT COEFFICIENT = 0.9612E-02
INDICATED VELOCITY IS 0.5972E 00 J=   2 U(J-2) = 0.1010E 01
D =  0.1536E-01 DKG = 0.1224E-01
VACT/C3=0.06167 TOTAL SHEAR = 0.2326E-00 GAS SHEAR =0.6683E-02
RUN NUMBER 183
Q GAS =   100.0000 CC/SEC   Q LIQ =    51.6400 CC/SEC
DIFFG=9.3800E-02  C2G=2.5235E 01  C3=8.9278E 00
GRP=3.8378E 00  CHB=2.7756E-01  AVGK=3.7565E-02
FR. SATN=.0342 KAVG EXPTL= 0.00961 EX.MT.GRP=0.071009
LEVESQUE MT COEFFICIENT = 0.9682E-02
INDICATED VELOCITY IS 0.2302E-01 J=   1
RUN NUMBER 184
Q GAS =   133.0000 CC/SEC   Q LIQ =    51.6400 CC/SEC
DIFFG=9.3800E-02  C2G=4.2455E 01  C3=9.0507E 00
GRP=1.0426E 01  CHB=2.8026E-01  AVGK=3.8189E-02
FR. SATN=.0256 KAVG EXPTL= 0.00957 EX.MT.GRP=0.070235
LEVESQUE MT COEFFICIENT = 0.9726E-02
INDICATED VELOCITY IS 0.4950E-01 J=   1
RUN NUMBER 185
Q GAS =   250.0000 CC/SEC   Q LIQ =    51.6400 CC/SEC
DIFFG=9.3800E-02  C2G=1.0351E 02  C3=9.4863E 00
GRP=5.3822E 01  CHB=2.8972E-01  AVGK=4.0418E-02
FR. SATN=.0127 KAVG EXPTL= 0.00896 EX.MT.GRP=0.064213
LEVESQUE MT COEFFICIENT = 0.9811E-02
INDICATED VELOCITY IS 0.2644E-00 J=   1
RUN NUMBER 186
Q GAS =   524.0000 CC/SEC   Q LIQ =    51.6400 CC/SEC
DIFFG=9.3800E-02  C2G=2.4648E 02  C3=1.0506E 01
GRP=2.2466E 02  CHB=2.9865E-01  AVGK=4.3846E-02
FR. SATN=.0074 KAVG EXPTL= 0.01092 EX.MT.GRP=0.074381
LEVESQUE MT COEFFICIENT = 0.9892E-02
INDICATED VELOCITY IS 0.3501E-00 J=   1 U(J-2) = 0.1010E 01
D =  0.1536E-01 DKG = 0.1065E-01
VACT/C3=0.03029 TOTAL SHEAR = 0.2895E-00 GAS SHEAR =0.5566E-01
RUN NUMBER 116
Q GAS =     6.4500 CC/SEC   Q LIQ =    15.4300 CC/SEC
DIFFG=7.5600E-02  C2G=4.7118E 00  C3=2.5886E 00
GRP=4.4238E 00  CHB=3.0253E-01  AVGK=1.9793E-02
FR. SATN=.3899 KAVG EXPTL= 0.00707 EX.MT.GRP=0.108113
LEVESQUE MT COEFFICIENT = 0.6187E-02
INDICATED VELOCITY IS 0.1855E-00 J=   1 U(J-2) = 0.1010E 01
D =  0.1536E-01 DKG = 0.6891E-02
VACT/C3=0.06514 TOTAL SHEAR = 0.6768E-01 GAS SHEAR =0.4150E-03
RUN NUMBER 117
Q GAS =    12.8900 CC/SEC   Q LIQ =    15.4300 CC/SEC
DIFFG=7.5600E-02  C2G=1.3327E 00  C3=2.6067E 00
GRP=3.4661E-01  CHB=2.9551E-01  AVGK=1.9401E-02
FR. SATN=.2468 KAVG EXPTL= 0.00895 EX.MT.GRP=0.136281
LEVESQUE MT COEFFICIENT = 0.6308E-02
VACT/C3=0.13543 TOTAL SHEAR = 0.6152E-01 GAS SHEAR =0.8198E-03
RUN NUMBER 118
Q GAS =    19.3500 CC/SEC   Q LIQ =    15.4300 CC/SEC
DIFFG=7.5600E-02  C2G=2.0568E 00  C3=2.6248E 00
GRP=8.0856E-01  CHB=2.9692E-01  AVGK=1.9561E-02
FR. SATN=.1753 KAVG EXPTL= 0.00954 EX.MT.GRP=0.144869
LEVESQUE MT COEFFICIENT = 0.6368E-02
VACT/C3=0.15265 TOTAL SHEAR = 0.6031E-01 GAS SHEAR =0.1308E-02
RUN NUMBER 119
Q GAS =    24.5000 CC/SEC   Q LIQ =    15.4300 CC/SEC
DIFFG=7.5600E-02  C2G=4.7590E 00  C3=2.6393E 00
GRP=4.2579E 00  CHB=3.0241E-01  AVGK=1.9978E-02
FR. SATN=.1313 KAVG EXPTL= 0.00905 EX.MT.GRP=0.136983
LEVESQUE MT COEFFICIENT = 0.6400E-02
VACT/C3=0.12809 TOTAL SHEAR = 0.6299E-01 GAS SHEAR =0.1758E-02
RUN NUMBER 120
Q GAS =    32.2800 CC/SEC   Q LIQ =    15.4300 CC/SEC
DIFFG=7.5600E-02  C2G=8.8412E 00  C3=2.6611E 00
GRP=1.4336E 01  CHB=3.0727E-01  AVGK=2.0383E-02
FR. SATN=.0954 KAVG EXPTL= 0.00866 EX.MT.GRP=0.130586
LEVESQUE MT COEFFICIENT = 0.6435E-02
INDICATED VELOCITY IS 0.2904E-00 J=   2 U(J-2) = 0.4250E-00
D =  0.1002E-01 DKG = 0.8382E-02
VACT/C3=0.09920 TOTAL SHEAR = 0.6630E-01 GAS SHEAR =0.2425E-02
RUN NUMBER 121
Q GAS =    38.7000 CC/SEC   Q LIQ =    15.4300 CC/SEC
DIFFG=7.5600E-02  C2G=1.2210E 01  C3=2.6792E 00
GRP=2.6794E 01  CHB=3.1150E-01  AVGK=2.0733E-02
FR. SATN=.0802 KAVG EXPTL= 0.00873 EX.MT.GRP=0.131149
LEVESQUE MT COEFFICIENT = 0.6456E-02
INDICATED VELOCITY IS 0.2926E-00 J=   2 U(J-2) = 0.4265E-00
D =  0.1010E-01 DKG = 0.8447E-02
VACT/C3=0.09929 TOTAL SHEAR = 0.6674E-01 GAS SHEAR =0.2938E-02
RUN NUMBER 122
Q GAS =    51.6000 CC/SEC   Q LIQ =    15.4300 CC/SEC
DIFFG=7.5600E-02  C2G=1.8978E 01  C3=2.7154E 00
GRP=6.2180E 01  CHB=3.1760E-01  AVGK=2.1281E-02
FR. SATN=.0628 KAVG EXPTL= 0.00911 EX.MT.GRP=0.135945
LEVESQUE MT COEFFICIENT = 0.6488E-02
VACT/C3=0.11894 TOTAL SHEAR = 0.6571E-01 GAS SHEAR =0.3936E-02
RUN NUMBER 123
Q GAS =    77.4000 CC/SEC   Q LIQ =    15.4300 CC/SEC
DIFFG=7.5600E-02  C2G=3.2516E 01  C3=2.7878E 00
GRP=1.6866E 02  CHB=3.2507E-01  AVGK=2.2071E-02
FR. SATN=.0388 KAVG EXPTL= 0.00845 EX.MT.GRP=0.124482
LEVESQUE MT COEFFICIENT = 0.6528E-02
INDICATED VELOCITY IS 0.2495E-00 J=   2 U(J-2) = 0.3451E-00
D =  0.9456E-02 DKG = 0.8164E-02
VACT/C3=0.08135 TOTAL SHEAR = 0.7125E-01 GAS SHEAR =0.6058E-02
RUN NUMBER 124
Q GAS =   102.9000 CC/SEC   Q LIQ =    15.4300 CC/SEC
DIFFG=7.5600E-02  C2G=4.5895E 01  C3=2.8594E 00
GRP=3.1141E 02  CHB=3.2964E-01  AVGK=2.2666E-02
FR. SATN=.0258 KAVG EXPTL= 0.00748 EX.MT.GRP=0.108719
LEVESQUE MT COEFFICIENT = 0.6553E-02
VACT/C3=0.05728 TOTAL SHEAR = 0.7558E-01 GAS SHEAR =0.8137E-02
RUN NUMBER 125
Q GAS =   193.5000 CC/SEC   Q LIQ =    15.4300 CC/SEC
DIFFG=7.5600E-02  C2G=9.3433E 01  C3=3.1138E 00
GRP=9.9944E 02  CHB=3.3799E-01  AVGK=2.4252E-02
FR. SATN=.0112 KAVG EXPTL= 0.00607 EX.MT.GRP=0.084608
LEVESQUE MT COEFFICIENT = 0.6601E-02
INDICATED VELOCITY IS 0.9349E-01 J=   1
RUN NUMBER 126
Q GAS =   322.7000 CC/SEC   Q LIQ =    15.4300 CC/SEC
DIFFG=7.5600E-02  C2G=1.6122E 02  C3=3.4766E 00
GRP=2.1381E 03  CHB=3.4308E-01  AVGK=2.6012E-02
FR. SATN=.0073 KAVG EXPTL= 0.00659 EX.MT.GRP=0.096943
LEVESQUE MT COEFFICIENT = 0.6634E-02
INDICATED VELOCITY IS 0.7463E-02 J=   1
```

```
RUN NUMBER 149
Q GAS =      6.4500 CC/SEC    Q LIQ =     37.1500 CC/SEC
DIFFG=7.5600E-02  C2G=1.6108E 01  C3=6.2070E 00
GRP=3.7504E 00  CHB=3.0199E-01  AVGK=3.0595E-02
FR. SATN=.3552 KAVG EXPTL= 0.00645 EX.MT.GRP=0.063618
LEVESQUE MT COEFFICIENT = 0.8035E-02
INDICATED VELOCITY IS 0.4375E-00 J=   1
RUN NUMBER 150
Q GAS =     12.8900 CC/SEC    Q LIQ =     37.1500 CC/SEC
DIFFG=7.5600E-02  C2G=1.2729E 01  C3=6.2251E 00
GRP=2.3216E 00  CHB=3.0021E-01  AVGK=3.0458E-02
FR. SATN=.2334 KAVG EXPTL= 0.00846 EX.MT.GRP=0.093398
LEVESQUE MT COEFFICIENT = 0.8241E-02
INDICATED VELOCITY IS 0.6797E-01 J=   1 U(J-2) = 0.3451E-00
0 =  0.9456E-02 OKG = 0.7598E-02
VACT/C3=0.00993 TOTAL SHEAR = 0.1752E-00 GAS SHEAR =0.9945E-03
RUN NUMBER 151
Q GAS =     19.3500 CC/SEC    Q LIQ =     37.1500 CC/SEC
DIFFG=7.5600E-02  C2G=9.3396E 00  C3=6.2432E 00
GRP=1.2390E 00  CHB=2.9804E-01  AVGK=3.0282E-02
FR. SATN=.1637 KAVG EXPTL= 0.00891 EX.MT.GRP=0.087710
LEVESQUE MT COEFFICIENT = 0.8345E-02
INDICATED VELOCITY IS 0.1775E-00 J=   1 U(J-2) = 0.3451E-00
0 =  0.9456E-02 OKG = 0.8247E-02
VACT/C3=0.02585 TOTAL SHEAR = 0.1721E-00 GAS SHEAR =0.1452E-02
RUN NUMBER 152
Q GAS =     24.5000 CC/SEC    Q LIQ =     30.9600 CC/SEC
DIFFG=7.5600E-02  C2G=3.3895E 00  C3=5.2265E 00
GRP=2.7815E-01  CHB=2.9529E-01  AVGK=2.7451E-02
FR. SATN=.1300 KAVG EXPTL= 0.00896 EX.MT.GRP=0.096366
LEVESQUE MT COEFFICIENT = 0.7943E-02
VACT/C3=0.05205 TOTAL SHEAR = 0.1391E-00 GAS SHEAR =0.1798E-02
RUN NUMBER 153
Q GAS =     19.3500 CC/SEC    Q LIQ =     30.9600 CC/SEC
DIFFG=7.5600E-02  C2G=6.0917E 00  C3=5.2120E 00
GRP=9.0594E-01  CHB=2.9718E-01  AVGK=2.7589E-02
FR. SATN=.1642 KAVG EXPTL= 0.00894 EX.MT.GRP=0.096252
LEVESQUE MT COEFFICIENT = 0.7894E-02
VACT/C3=0.05290 TOTAL SHEAR = 0.1386E-00 GAS SHEAR =0.1383E-02
RUN NUMBER 154
Q GAS =     12.8900 CC/SEC    Q LIQ =     30.9600 CC/SEC
DIFFG=7.5600E-02  C2G=9.4813E 00  C3=5.1939E 00
GRP=2.2176E 00  CHB=3.0004E-01  AVGK=2.7805E-02
FR. SATN=.2270 KAVG EXPTL= 0.00823 EX.MT.GRP=0.088814
LEVESQUE MT COEFFICIENT = 0.7801E-02
INDICATED VELOCITY IS 0.1228E-00 J=   1 U(J-2) = 0.3451E-00
0 =  0.9456E-02 OKG = 0.7499E-02
VACT/C3=0.02149 TOTAL SHEAR = 0.1440E-00 GAS SHEAR =0.9646E-03
RUN NUMBER 155
Q GAS =      6.4500 CC/SEC    Q LIQ =     30.9600 CC/SEC
DIFFG=7.5600E-02  C2G=1.2860E 01  C3=5.1758E 00
GRP=4.1229E 00  CHB=3.0231E-01  AVGK=2.7967E-02
FR. SATN=.3891 KAVG EXPTL= 0.00706 EX.MT.GRP=0.076306
LEVESQUE MT COEFFICIENT = 0.7616E-02
INDICATED VELOCITY IS 0.1417E-00 J=   1
RUN NUMBER 156
Q GAS =     32.2800 CC/SEC    Q LIQ =     30.8600 CC/SEC
DIFFG=7.5600E-02  C2G=7.4506E-01  C3=5.2316E 00
GRP=1.3400E-02  CHB=2.9146E-01  AVGK=2.7108E-02
FR. SATN=.0928 KAVG EXPTL= 0.00842 EX.MT.GRP=0.090550
LEVESQUE MT COEFFICIENT = 0.7989E-02
INDICATED VELOCITY IS 0.1304E-00 J=   1 U(J-2) = 0.3451E-00
0 =  0.9456E-02 OKG = 0.7754E-02
VACT/C3=0.02266 TOTAL SHEAR = 0.1448E-00 GAS SHEAR =0.2512E-02
RUN NUMBER 157
Q GAS =     38.7000 CC/SEC    Q LIQ =     30.8600 CC/SEC
DIFFG=7.5600E-02  C2G=4.1136E 00  C3=5.2497E 00
GRP=4.0428E-01  CHB=2.9570E-01  AVGK=2.7550E-02
FR. SATN=.0816 KAVG EXPTL= 0.00889 EX.MT.GRP=0.095377
LEVESQUE MT COEFFICIENT = 0.8022E-02
INDICATED VELOCITY IS 0.2557E-00 J=   1 U(J-2) = 0.3451E-00
0 =  0.9456E-02 OKG = 0.8621E-02
VACT/C3=0.04427 TOTAL SHEAR = 0.1412E-00 GAS SHEAR =0.2958E-02
RUN NUMBER 158
Q GAS =     51.6000 CC/SEC    Q LIQ =     30.8600 CC/SEC
DIFFG=7.5600E-02  C2G=1.0882E 01  C3=5.2859E 00
GRP=2.7715E 00  CHB=3.0088E-01  AVGK=2.8130E-02
FR. SATN=.0591 KAVG EXPTL= 0.00858 EX.MT.GRP=0.091758
LEVESQUE MT COEFFICIENT = 0.8070E-02
INDICATED VELOCITY IS 0.1473E-00 J=   1 U(J-2) = 0.3451E-00
0 =  0.9456E-02 OKG = 0.7948E-02
VACT/C3=0.02533 TOTAL SHEAR = 0.1458E-00 GAS SHEAR =0.4049E-02
RUN NUMBER 159
Q GAS =     77.4000 CC/SEC    Q LIQ =     30.8600 CC/SEC
DIFFG=7.5600E-02  C2G=2.4419E 01  C3=5.3583E 00
GRP=1.3397E 01  CHB=3.0684E-01  AVGK=2.8882E-02
FR. SATN=.0357 KAVG EXPTL= 0.00777 EX.MT.GRP=0.082590
LEVESQUE MT COEFFICIENT = 0.8133E-02
INDICATED VELOCITY IS 0.9255E-01 J=   1
RUN NUMBER 160
Q GAS =    102.9000 CC/SEC    Q LIQ =     30.8600 CC/SEC
DIFFG=7.5600E-02  C2G=3.7799E 01  C3=5.4299E 00
GRP=3.0847E 01  CHB=3.1250E-01  AVGK=2.9611E-02
FR. SATN=.0285 KAVG EXPTL= 0.00824 EX.MT.GRP=0.086966
LEVESQUE MT COEFFICIENT = 0.8172E-02
INDICATED VELOCITY IS 0.1915E-01 J=   1 U(J-2) = 0.3451E-00
0 =  0.9456E-02 OKG = 0.7417E-02
VACT/C3=0.00321 TOTAL SHEAR = 0.1541E-00 GAS SHEAR =0.8225E-02
RUN NUMBER 161
Q GAS =    193.5000 CC/SEC    Q LIQ =     30.8600 CC/SEC
DIFFG=7.5600E-02  C2G=8.5337E 01  C3=5.6843E 00
GRP=1.3705E 02  CHB=3.2351E-01  AVGK=3.1364E-02
FR. SATN=.0104 KAVG EXPTL= 0.00564 EX.MT.GRP=0.058211
LEVESQUE MT COEFFICIENT = 0.8247E-02
INDICATED VELOCITY IS 0.6403E 00 J=   1
RUN NUMBER 162
Q GAS =    322.7000 CC/SEC    Q LIQ =     30.8600 CC/SEC
DIFFG=7.5600E-02  C2G=1.5313E 02  C3=6.0471E 00
GRP=3.6652E 02  CHB=3.3083E-01  AVGK=3.3082E-02
FR. SATN=.0085 KAVG EXPTL= 0.00774 EX.MT.GRP=0.077388
LEVESQUE MT COEFFICIENT = 0.8299E-02
INDICATED VELOCITY IS 0.1367E-00 J=   1
RUN NUMBER 187
Q GAS =    405.0000 CC/SEC    Q LIQ =     51.6400 CC/SEC
DIFFG=7.5600E-02  C2G=1.8541E 02  C3=9.7399E 00
GRP=1.2859E 02  CHB=3.2303E-01  AVGK=4.0995E-02
FR. SATN=.0052 KAVG EXPTL= 0.00588 EX.MT.GRP=0.046308
LEVESQUE MT COEFFICIENT = 0.9818E-02
INDICATED VELOCITY IS 0.1231E 01 J=   1
RUN NUMBER 188
Q GAS =    193.5000 CC/SEC    Q LIQ =     51.6400 CC/SEC
DIFFG=7.5600E-02  C2G=7.4434E 01  C3=9.1461E 00
GRP=2.5030E 01  CHB=3.1103E-01  AVGK=3.8249E-02
FR. SATN=.0104 KAVG EXPTL= 0.00564 EX.MT.GRP=0.045891
```

```
LEVESQUE MT COEFFICIENT = 0.9718E-02
INDICATED VELOCITY IS 0.1306E 01 J=   1
RUN NUMBER 189
Q GAS =   102.9000 CC/SEC   Q LIQ =   51.6400 CC/SEC
DIFFG=7.5600E-02  C2G=2.6896E 01  C3=8.8917E 00
GRP=3.5567E 00  CHB=3.0181E-01  AVGK=3.6596E-02
FR. SATN=.0271 KAVG EXPTL= 0.00784 EX.MT.GRP=0.064626
LEVESQUE MT COEFFICIENT = 0.9613E-02
INDICATED VELOCITY IS 0.5854E 00 J=   1
RUN NUMBER  90
Q GAS =    95.2000 CC/SEC   Q LIQ =   51.6400 CC/SEC
DIFFG=7.5600E-02  C2G=2.2856E 01  C3=8.8701E 00
GRP=2.5873E 00  CHB=3.0062E-01  AVGK=3.6408E-02
FR. SATN=.0298 KAVG EXPTL= 0.00798 EX.MT.GRP=0.065876
LEVESQUE MT COEFFICIENT = 0.9598E-02
INDICATED VELOCITY IS 0.5360E 00 J=   1
RUN NUMBER 191
Q GAS =    77.4000 CC/SEC   Q LIQ =   51.6400 CC/SEC
DIFFG=7.5600E-02  C2G=1.3516E 01  C3=8.8201E 00
GRP=9.2027E-01  CHB=2.9722E-01  AVGK=3.5894E-02
FR. SATN=.0376 KAVG EXPTL= 0.00818 EX.MT.GRP=0.067730
LEVESQUE MT COEFFICIENT = 0.9558E-02
INDICATED VELOCITY IS 0.4618E-00 J=   1
RUN NUMBER 192
Q GAS =    51.6500 CC/SEC   Q LIQ =   51.6400 CC/SEC
DIFFG=7.5600E-02  C2G=5.2273E-03  C3=8.7478E 00
GRP=1.4109E-07  CHB=2.8959E-01  AVGK=3.4829E-02
FR. SATN=.0561 KAVG EXPTL= 0.00815 EX.MT.GRP=0.067727
LEVESQUE MT COEFFICIENT = 0.9473E-02
INDICATED VELOCITY IS 0.4579E-00 J=   1
RUN NUMBER 193
Q GAS =    38.7000 CC/SEC   Q LIQ =   51.6400 CC/SEC
DIFFG=7.5600E-02  C2G=6.7896E 00  C3=8.7114E 00
GRP=2.4101E-01  CHB=2.9516E-01  AVGK=3.5425E-02
FR. SATN=.0734 KAVG EXPTL= 0.00799 EX.MT.GRP=0.066597
LEVESQUE MT COEFFICIENT = 0.9405E-02
INDICATED VELOCITY IS 0.4729E-00 J=   1
RUN NUMBER 194
Q GAS =    32.2800 CC/SEC   Q LIQ =   51.6400 CC/SEC
DIFFG=7.5600E-02  C2G=1.0158E 01  C3=8.6934E 00
GRP=5.4286E-01  CHB=2.9614E-01  AVGK=3.5505E-02
FR. SATN=.1080 KAVG EXPTL= 0.00980 EX.MT.GRP=0.081759
LEVESQUE MT COEFFICIENT = 0.9360E-02
INDICATED VELOCITY IS 0.1619E-00 J=   1 U(J-2) = 0.3451E-00
O =  0.9456E-02 OKG = 0.8976E-02
VACT/C3=0.01693 TOTAL SHEAR = 0.2425E-00 GAS SHEAR =0.2495E-02
RUN NUMBER 195
Q GAS =    24.5000 CC/SEC   Q LIQ =   51.6400 CC/SEC
DIFFG=7.5600E-02  C2G=1.4240E 01  C3=8.6716E 00
GRP=1.0749E 00  CHB=2.9763E-01  AVGK=3.5640E-02
FR. SATN=.1256 KAVG EXPTL= 0.00865 EX.MT.GRP=0.072259
LEVESQUE MT COEFFICIENT = 0.9286E-02
INDICATED VELOCITY IS 0.2086E-00 J=   1
RUN NUMBER 196
Q GAS =    19.3500 CC/SEC   Q LIQ =   51.6400 CC/SEC
DIFFG=7.5600E-02  C2G=1.6943E 01  C3=8.6571E 00
GRP=1.5292E 00  CHB=2.9871E-01  AVGK=3.5739E-02
FR. SATN=.1651 KAVG EXPTL= 0.00899 EX.MT.GRP=0.075116
LEVESQUE MT COEFFICIENT = 0.9219E-02
INDICATED VELOCITY IS 0.7561E-01 J=   1
RUN NUMBER 197
Q GAS =    12.8900 CC/SEC   Q LIQ =   51.6400 CC/SEC
DIFFG=7.5600E-02  C2G=2.0332E 01  C3=8.6390E 00
GRP=2.2162E 00  CHB=3.0003E-01  AVGK=3.5860E-02
FR. SATN=.2254 KAVG EXPTL= 0.00817 EX.MT.GRP=0.068394
LEVESQUE MT COEFFICIENT = 0.9092E-02
INDICATED VELOCITY IS 0.2962E-00 J=   1
RUN NUMBER 198
Q GAS =     6.4000 CC/SEC   Q LIQ =   51.6400 CC/SEC
DIFFG=7.5600E-02  C2G=2.3737E 01  C3=8.6208E 00
GRP=3.0399E 00  CHB=3.0123E-01  AVGK=3.5965E-02
FR. SATN=.4070 KAVG EXPTL= 0.00733 EX.MT.GRP=0.061369
LEVESQUE MT COEFFICIENT = 0.8839E-02
INDICATED VELOCITY IS 0.4806E-00 J=   1
RUN NUMBER 127
Q GAS =    44.5000 CC/SEC   Q LIQ =   15.4300 CC/SEC
DIFFG=3.7700E-01  C2G=1.5338E 01  C3=2.6685E 00
GRP=2.1338E 02  CHB=1.4636E-01  AVGK=2.1710E-02
FR. SATN=.1313 KAVG EXPTL= 0.01644 EX.MT.GRP=0.110814
LEVESQUE MT COEFFICIENT = 0.6693E-02
VACT/C3=0.43263 TOTAL SHEAR = 0.3408E-01 GAS SHEAR =0.1912E-02
RUN NUMBER 128
Q GAS =    67.5000 CC/SEC   Q LIQ =   15.4300 CC/SEC
DIFFG=3.7700E-01  C2G=2.7473E 01  C3=2.7118E 00
GRP=6.5232E 02  CHB=1.6259E-01  AVGK=2.4313E-02
FR. SATN=.0840 KAVG EXPTL= 0.01595 EX.MT.GRP=0.106641
LEVESQUE MT COEFFICIENT = 0.6708E-02
VACT/C3=0.39316 TOTAL SHEAR = 0.3849E-01 GAS SHEAR =0.3175E-02
RUN NUMBER 129
Q GAS =    89.1000 CC/SEC   Q LIQ =   15.4300 CC/SEC
DIFFG=3.7700E-01  C2G=3.8869E 01  C3=2.7525E 00
GRP=1.2488E 03  CHB=1.6365E-01  AVGK=2.4654E-02
FR. SATN=.0645 KAVG EXPTL= 0.01617 EX.MT.GRP=0.107355
LEVESQUE MT COEFFICIENT = 0.6717E-02
VACT/C3=0.39622 TOTAL SHEAR = 0.3876E-01 GAS SHEAR =0.4318E-02
RUN NUMBER 130
Q GAS =   112.5000 CC/SEC   Q LIQ =   15.4300 CC/SEC
DIFFG=3.7700E-01  C2G=5.1215E 01  C3=2.7965E 00
GRP=2.0672E 03  CHB=1.6442E-01  AVGK=2.4968E-02
FR. SATN=.0565 KAVG EXPTL= 0.01789 EX.MT.GRP=0.117834
LEVESQUE MT COEFFICIENT = 0.6724E-02
VACT/C3=0.48603 TOTAL SHEAR = 0.3034E-01 GAS SHEAR =0.5459E-02
RUN NUMBER 131
Q GAS =   135.0000 CC/SEC   Q LIQ =   15.4300 CC/SEC
DIFFG=3.7700E-01  C2G=6.3087E 01  C3=2.8389E 00
GRP=2.9983E 03  CHB=1.6496E-01  AVGK=2.5240E-02
FR. SATN=.0433 KAVG EXPTL= 0.01644 EX.MT.GRP=0.107434
LEVESQUE MT COEFFICIENT = 0.6729E-02
VACT/C3=0.39348 TOTAL SHEAR = 0.4026E-01 GAS SHEAR =0.6756E-02
RUN NUMBER 132
Q GAS =   224.0000 CC/SEC   Q LIQ =   15.4300 CC/SEC
DIFFG=3.7700E-01  C2G=1.1004E 02  C3=3.0064E 00
GRP=7.6814E 03  CHB=1.6624E-01  AVGK=2.6174E-02
FR. SATN=.0278 KAVG EXPTL= 0.01749 EX.MT.GRP=0.111078
LEVESQUE MT COEFFICIENT = 0.6741E-02
VACT/C3=0.42113 TOTAL SHEAR = 0.3964E-01 GAS SHEAR =0.1144E-01
RUN NUMBER 133
Q GAS =   270.0000 CC/SEC   Q LIQ =   15.4300 CC/SEC
DIFFG=3.7700E-01  C2G=1.3431E 02  C3=3.0930E 00
GRP=1.0509E 04  CHB=1.6663E-01  AVGK=2.6611E-02
FR. SATN=.0206 KAVG EXPTL= 0.01564 EX.MT.GRP=0.097934
LEVESQUE MT COEFFICIENT = 0.6745E-02
VACT/C3=0.31698 TOTAL SHEAR = 0.5238E-01 GAS SHEAR =0.1401E-01
RUN NUMBER 134
```

```
Q GAS =    359.0000 CC/SEC    Q LIQ =     15.4300 CC/SEC
DIFFG=3.7700E-01  C2G=1.8127E 02  C3=3.2605E 00
GRP=1.6340E 04  CHB=1.6715E-01  AVGK=2.7408E-02
FR. SATN=.0148 KAVG EXPTL= 0.01496 EX.MT.GRP=0.091221
LEVESQUE MT COEFFICIENT = 0.6751E-02
VACT/C3=0.26972 TOTAL SHEAR = 0.6076E-01 GAS SHEAR =0.1880E-01
RUN NUMBER 164
Q GAS =     44.5000 CC/SEC    Q LIQ =     30.8600 CC/SEC
DIFFG=3.7700E-01  C2G=7.1966E 00  C3=5.2533E 00
GRP=6.1575E 00  CHB=1.5476E-01  AVGK=3.2209E-02
FR. SATN=.1440 KAVG EXPTL= 0.01803 EX.MT.GRP=0.086612
LEVESQUE MT COEFFICIENT = 0.8392E-02
VACT/C3=0.26141 TOTAL SHEAR = 0.9948E-01 GAS SHEAR =0.1825E-02
RUN NUMBER 165
Q GAS =     67.5000 CC/SEC    Q LIQ =     30.8600 CC/SEC
DIFFG=3.7700E-01  C2G=1.9332E 01  C3=5.2966E 00
GRP=4.3350E 01  CHB=1.5772E-01  AVGK=3.2960E-02
FR. SATN=.0826 KAVG EXPTL= 0.01569 EX.MT.GRP=0.075061
LEVESQUE MT COEFFICIENT = 0.8416E-02
VACT/C3=0.17645 TOTAL SHEAR = 0.1165E-00 GAS SHEAR =0.3228E-02
RUN NUMBER 166
Q GAS =     90.0000 CC/SEC    Q LIQ =     30.8600 CC/SEC
DIFFG=3.7700E-01  C2G=3.1203E 01  C3=5.3390E 00
GRP=1.1027E 02  CHB=1.5944E-01  AVGK=3.3453E-02
FR. SATN=.0597 KAVG EXPTL= 0.01513 EX.MT.GRP=0.072088
LEVESQUE MT COEFFICIENT = 0.8431E-02
VACT/C3=0.16030 TOTAL SHEAR = 0.1205E-00 GAS SHEAR =0.4460E-02
RUN NUMBER 167
Q GAS =    112.5000 CC/SEC    Q LIQ =     30.8600 CC/SEC
DIFFG=3.7700E-01  C2G=4.3074E 01  C3=5.3813E 00
GRP=2.0522E 02  CHB=1.6057E-01  AVGK=3.3824E-02
FR. SATN=.0524 KAVG EXPTL= 0.01658 EX.MT.GRP=0.078731
LEVESQUE MT COEFFICIENT = 0.8441E-02
VACT/C3=0.19694 TOTAL SHEAR = 0.1144E-00 GAS SHEAR =0.5578E-02
RUN NUMBER 168
Q GAS =    135.0000 CC/SEC    Q LIQ =     30.8600 CC/SEC
DIFFG=3.7700E-01  C2G=5.4946E 01  C3=5.4237E 00
GRP=3.2616E 02  CHB=1.6140E-01  AVGK=3.4132E-02
FR. SATN=.0428 KAVG EXPTL= 0.01627 EX.MT.GRP=0.076918
LEVESQUE MT COEFFICIENT = 0.8449E-02
VACT/C3=0.18493 TOTAL SHEAR = 0.1176E-00 GAS SHEAR =0.6802E-02
RUN NUMBER 169
Q GAS =    177.0000 CC/SEC    Q LIQ =     30.8600 CC/SEC
DIFFG=3.7700E-01  C2G=7.7105E 01  C3=5.5027E 00
GRP=6.1501E 02  CHB=1.6249E-01  AVGK=3.4613E-02
FR. SATN=.0263 KAVG EXPTL= 0.01312 EX.MT.GRP=0.061573
LEVESQUE MT COEFFICIENT = 0.8460E-02
VACT/C3=0.11143 TOTAL SHEAR = 0.1339E-00 GAS SHEAR =0.9198E-02
RUN NUMBER 170
Q GAS =    224.0000 CC/SEC    Q LIQ =     30.8600 CC/SEC
DIFFG=3.7700E-01  C2G=1.0190E 02  C3=5.5912E 00
GRP=1.0240E 03  CHB=1.6333E-01  AVGK=3.5070E-02
FR. SATN=.0244 KAVG EXPTL= 0.01539 EX.MT.GRP=0.071688
LEVESQUE MT COEFFICIENT = 0.8469E-02
VACT/C3=0.15297 TOTAL SHEAR = 0.1277E-00 GAS SHEAR =0.1161E-01
RUN NUMBER 171
Q GAS =    270.0000 CC/SEC    Q LIQ =     30.8600 CC/SEC
DIFFG=3.7700E-01  C2G=1.2617E 02  C3=5.6778E 00
GRP=1.4992E 03  CHB=1.6393E-01  AVGK=3.5471E-02
FR. SATN=.0176 KAVG EXPTL= 0.01337 EX.MT.GRP=0.061770
LEVESQUE MT COEFFICIENT = 0.8476E-02
VACT/C3=0.11061 TOTAL SHEAR = 0.1383E-00 GAS SHEAR =0.1415E-01
RUN NUMBER 172
Q GAS =    359.0000 CC/SEC    Q LIQ =     30.8600 CC/SEC
DIFFG=3.7700E-01  C2G=1.7313E 02  C3=5.8453E 00
GRP=2.5869E 03  CHB=1.6475E-01  AVGK=3.6170E-02
FR. SATN=.0143 KAVG EXPTL= 0.01445 EX.MT.GRP=0.065807
LEVESQUE MT COEFFICIENT = 0.8485E-02
VACT/C3=0.12827 TOTAL SHEAR = 0.1387E-00 GAS SHEAR =0.1885E-01
RUN NUMBER 199
Q GAS =     67.5000 CC/SEC    Q LIQ =     51.6400 CC/SEC
DIFFG=3.7700E-01  C2G=8.3679E 00  C3=8.7776E 00
GRP=1.7846E 00  CHB=1.5368E-01  AVGK=4.1344E-02
FR. SATN=.0956 KAVG EXPTL= 0.01816 EX.MT.GRP=0.067490
LEVESQUE MT COEFFICIENT = 0.9954E-02
VACT/C3=0.14472 TOTAL SHEAR = 0.2031E-00 GAS SHEAR =0.3093E-02
RUN NUMBER 200
Q GAS =     44.5000 CC/SEC    Q LIQ =     51.6400 CC/SEC
DIFFG=3.7700E-01  C2G=3.7672E 00  C3=8.7343E 00
GRP=3.6710E-01  CHB=1.5271E-01  AVGK=4.0982E-02
FR. SATN=.1443 KAVG EXPTL= 0.01806 EX.MT.GRP=0.067307
LEVESQUE MT COEFFICIENT = 0.9921E-02
VACT/C3=0.14663 TOTAL SHEAR = 0.2015E-00 GAS SHEAR =0.1862E-02
RUN NUMBER 201
Q GAS =     89.1000 CC/SEC    Q LIQ =     51.6400 CC/SEC
DIFFG=3.7700E-01  C2G=1.9764E 01  C3=8.8183E 00
GRP=9.8188E 00  CHB=1.5512E-01  AVGK=4.1829E-02
FR. SATN=.0645 KAVG EXPTL= 0.01617 EX.MT.GRP=0.059982
LEVESQUE MT COEFFICIENT = 0.9975E-02
VACT/C3=0.10846 TOTAL SHEAR = 0.2155E-00 GAS SHEAR =0.4371E-02
RUN NUMBER 202
Q GAS =    112.5000 CC/SEC    Q LIQ =     51.6400 CC/SEC
DIFFG=3.7700E-01  C2G=3.2110E 01  C3=8.8623E 00
GRP=2.5533E 01  CHB=1.5676E-01  AVGK=4.2377E-02
FR. SATN=.0554 KAVG EXPTL= 0.01754 EX.MT.GRP=0.064895
LEVESQUE MT COEFFICIENT = 0.9990E-02
VACT/C3=0.13004 TOTAL SHEAR = 0.2097E-00 GAS SHEAR =0.5541E-02
RUN NUMBER 203
Q GAS =    135.0000 CC/SEC    Q LIQ =     51.6400 CC/SEC
DIFFG=3.7700E-01  C2G=4.3982E 01  C3=8.9047E 00
GRP=4.7221E 01  CHB=1.5787E-01  AVGK=4.2779E-02
FR. SATN=.0435 KAVG EXPTL= 0.01653 EX.MT.GRP=0.061008
LEVESQUE MT COEFFICIENT = 0.1000E-01
VACT/C3=0.11275 TOTAL SHEAR = 0.2163E-00 GAS SHEAR =0.6801E-02
RUN NUMBER 204
Q GAS =    177.0000 CC/SEC    Q LIQ =     51.6400 CC/SEC
DIFFG=3.7700E-01  C2G=6.6141E 01  C3=8.9837E 00
GRP=1.0400E 02  CHB=1.5933E-01  AVGK=4.3365E-02
FR. SATN=.0331 KAVG EXPTL= 0.01649 EX.MT.GRP=0.060603
LEVESQUE MT COEFFICIENT = 0.1002E-01
VACT/C3=0.10896 TOTAL SHEAR = 0.2194E-00 GAS SHEAR =0.9052E-02
RUN NUMBER 205
Q GAS =    224.0000 CC/SEC    Q LIQ =     51.6400 CC/SEC
DIFFG=3.7700E-01  C2G=9.0939E 01  C3=9.0722E 00
GRP=1.9090E 02  CHB=1.6044E-01  AVGK=4.3882E-02
FR. SATN=.0248 KAVG EXPTL= 0.01560 EX.MT.GRP=0.057053
LEVESQUE MT COEFFICIENT = 0.1003E-01
VACT/C3=0.09488 TOTAL SHEAR = 0.2262E-00 GAS SHEAR =0.1161E-01
RUN NUMBER 206
Q GAS =    270.0000 CC/SEC    Q LIQ =     51.6400 CC/SEC
DIFFG=3.7700E-01  C2G=1.1521E 02  C3=9.1588E 00
GRP=2.9779E 02  CHB=1.6124E-01  AVGK=4.4310E-02
FR. SATN=.0182 KAVG EXPTL= 0.01379 EX.MT.GRP=0.050168
LEVESQUE MT COEFFICIENT = 0.1004E-01
```

```
INDICATED VELOCITY IS 0.6255E 00 J=   2 U(J-2) = 0.1002E 01
O =  0.1664E-01 OKG = 0.1326E-01
VACT/C3=0.06209 TOTAL SHEAR = 0.2391E-00 GAS SHEAR =0.1418E-01
RUN NUMBER 207
Q GAS =   332.0000 CC/SEC   Q LIQ =    51.6400 CC/SEC
DIFFG=3.7700E-01  C2G=1.4792E 02  C3=9.2755E 00
GRP=4.7261E 02  CHB=1.6204E-01  AVGK=4.4814E-02
FR. SATN=.0155 KAVG EXPTL= 0.01447 EX.MT.GRP=0.052330
LEVESQUE MT COEFFICIENT = 0.1005E-01
INDICATED VELOCITY IS 0.7251E 00 J=   2 U(J-2) = 0.1180E 01
O =  0.1797E-01 OKG = 0.1400E-01
VACT/C3=0.07107 TOTAL SHEAR = 0.2392E-00 GAS SHEAR =0.1745E-01
RUN NUMBER 208
Q GAS =   359.0000 CC/SEC   Q LIQ =    51.6400 CC/SEC
DIFFG=3.7700E-01  C2G=1.6217E 02  C3=9.3263E 00
GRP=5.5879E 02  CHB=1.6233E-01  AVGK=4.5016E-02
FR. SATN=.0142 KAVG EXPTL= 0.01429 EX.MT.GRP=0.051546
LEVESQUE MT COEFFICIENT = 0.1005E-01
INDICATED VELOCITY IS 0.6963E 00 J=   2 U(J-2) = 0.1132E 01
O =  0.1764E-01 OKG = 0.1380E-01
VACT/C3=0.06787 TOTAL SHEAR = 0.2416E-00 GAS SHEAR =0.1890E-01
```

APPENDIX D

COLLECTION OF PROGRAMS SOLVING THE CONVECTIVE TRANSPORT EQUATION

This section includes all the computer programs which were written for the solutions of the problems which were suggested in the course of this work. These include:

(a) "GRINT" - A program which solves the convective mass transfer equation for a single phase with a parabolic profile and one moving wall.

(b) "BAKKER" - A program which solves the convective mass transfer equation for an infinite medium with a moving interface and a linear slope in velocity.

(c) "GRAGRA" - A program which solves the interphase mass transfer problem where is flow between two flat plates and hence there are parabolic profiles in both phases.

(d) "GRAPEN" - A program which solves the interphase mass transfer problem where the upper phase has a parabolic velocity profile and the lower phase has a constant velocity and is infinite in extent.

(e) "CJKING" - A program which solves the interphase mass transfer problem where the upper phase is infinite in extent and has a linear gradient in velocity and the lower phase has a constant velocity and is also infinite in extent.

All of these programs are written in Fortran IV and were compiled and executed on the UCLRL IBM 7094 and CDC 6600 computers. The fact that they all contain instructions for the operation of the "Calcomp" plotter will probably cause them to be inoperative on any other computer in their present form. The letters "CC" at the beginning of any term indicates that it is involved in plotting instructions.

Included with each source program are a set of instructions on how to operate the program. The print out will be explained where that is necessary.

"GRINT"

Necessary Input

Card 1 NODATA is the number of separate cases which are to be run. There must be at least two, but not more than ten

Card 2 M is the number of divisions in the y direction (from interface to wall)

N is the number of divisions taken along the wall

IND tells the computer to print and plot only every INDth profile in concentration which it generates

JELL is the allowable number of inerations in correction of the direct solution. (Set it at 10)

JS tells the computer which piece of data it is dealing with, will be 1 for the first piece of data and NODATA for the last.

IRD, if this is 0 the concentration profile is not plotted, if it is 1 the profile is plotted.

Card 3 R is set at 0.001 times VAV. Experience has shown that this gives stable results. It is the dimensionless group, DL/U_0b^2

VAV is the ratio of the average velocity to the interfacial velocity.

Card 4 This is really a series of cards which appear in each of the five programs and serve the function of extending the length of the exposure. If R is set at the value given above, the first exposure will be to a Graetz number of 0.001. To extend this, add the following card, LR, if set equal to 1 extends calculation, if set at zero it terminates.

MD tells the computer by how much to extend the range; eg. MD = 2 doubles the range. Note MD must be such that N is divisible by it without remainder eg. if N = 50 then MD = 2 is admissable while MD = 3 is not admissable

IND gives you the opportunity to change the number of profiles which you print

NOTE: A card with 00 in the first two columns must appear as the last card in a sequence.

This card has brought the calculation to a second Graetz number, say 0.002. The next #4 card will bring us to MD times 0.002 so that if the new MD is 5 then the new card will bring the calculation to Gz = 0.010. Repeat the procedure until the desired Gz is obtained.

```
$IBFTC GRINT
C     GRAETZ MODEL WITH INTERFACIAL VELOCITY
      DIMENSION Q(200),GL(90),GG(90),XNU(90),W(200)
          DIMENSION  YD(200),RU(10,500),RUT(10,500)     ,S(200)
      DIMENSION X(200),A(200),B(200),C(200),VAR(200),G(200),O(200)
      DIMENSION         T(0500),XR(0500),XTS(0500)     ,XD(200)
      COMMON/CCPOOL/XMIN,XMAX,YMIN,YMAX,CCXMIN,CCXMAX,CCYMIN,CCYMAX
      CALL CCBGN
      READ(2,57)  NODATA
   57 FORMAT  (I2)
   50 READ(2,1)   M,N,IND,JELL,JS,IRD
    1 FORMAT (4I5,I2,I1   )
      READ(2,107) R,VAV
  107 FORMAT(2F12.6)
      WRITE(3,67)
   67 FORMAT(53H1RESULTS OF GRAETZ SOLUTION WITH INTERFACIAL VELOCITY//)
      WRITE(3,104) R
  104 FORMAT (              3H R=,F10.7)
      P=1./FLOAT(N)
      H2=1./FLOAT(M)
      WRITE(3, 4 ) H2
    4 FORMAT(                                F6.4,17H GAS Y INCREMENT ///)
      WRITE(3, 5 ) P
    5 FORMAT(F6.4,22H X DIRECTION INCREMENT///)
      WRITE(3,110)   VAV
  110 FORMAT( 7H VAV = ,F10.5)
      M=M-1
      L=M+1
      LO=L+1
      II=0.0
      XMIN=0.0
      YMIN=0.0
      XMAX=1.0
      YMAX=1.0
      CCYMIN=100./1024.
      CCYMAX=1000./1024.
      CCXMIN= 80./1024.
      CCXMAX=1080./1024.
      IF(IRD)   44,44,46
   44 CALL CCGRID (1,10,5,6HLABELS,1,10,5)
       CALL CCLTR (400./1024.,10./1024.,0.2,5H Y/B )
      CALL CCLTR (10./1024.,350./1024.,1,2,14H CONCENTRATION)
   46 MR=1
      DO  15  J=1,L
   15 X(J)=0.0
      XNUI= 1./H2
      AY=6.*VAV-4.
      AYS=3.-6.*VAV
   18 ALP=(H2*H2)/(R*P)
      CARG=ALP*0.25*H2*(3.*VAV-1.+H2/2.-VAV*H2)
      WRITE(3,60)  ALP,CARG
   60 FORMAT(6H ALP=  ,F10.5,6H CARG= ,E10.4)
      YD(L+1)=H2*FLOAT(L)
      YD(1)=0.0
      DO 9 J= 1 ,M
      Z=H2*FLOAT(J )
      YD(J+1)=Z
      VAR(J)=(1.+AY*Z+AYS*Z*Z)*ALP
      A(J)=-(1.+VAR(J))*2.0
```

```
      C(J)=1.
    9 B(J)=1.
      C(L)=1.-2.*CARG/3.
      A(L)=-(1.+4.*CARG/3.)
      O(1)=A(1)
      DO 19 I=MR,N
      II=II+1
      IF(I-1)  68,69,68
   69 O(1)=-(2.+VAR(1))
      DO 70 J=2  ,L
      Q(J-1)=B(J-1)/O(J-1)
   70 O(J)=A(J)-C(J)*Q(J-1)
      G(1)=-1.0/O(1)
      MR1=MR+1
      GO TO 71
   68 IF (I-MR1) 45,72,45
   72 DO 54 J=2  ,L
      Q(J-1)=B(J-1)/O(J-1)
   54 O(J)=A(J)-C(J)*Q(J-1)
   45 G(1)=-(2.-2.*(1.-VAR(1))*X(1)+X(2))/A(1)
   71 DO 12 J= 2 ,M
      W(J)=X(J)
   12 G(J)=(2.*(1.-VAR(J))*X(J)-X(J-1)-X(J+1)-C(J)*G(J-1))/O(J)
      G(L)=((1.-4.*CARG/3.)*X(L)-(1.+2.*CARG/3.)*X(M)-C(L)*G(M))/O(L)
      W(1)=X(1)
      W(L)=X(L)
      X(L)=G(L)
      DO 13 J=1,M
      J1=L-J
      J2=J1+1
   13 X(J1)=G(J1)-Q(J1)*X(J2)
      DO 75 JO=1,JELL
      IF(I-1)   76,77,76
   77 SET=X(1)
      X(1)=-(X(2)+1.)/O(1)
      S(1)=ABS(X(1)-SET)
      GO TO 78
   76 SET=X(1)
      X(1)=-(X(2)-2.*(1.-VAR(1))*W(1)+2.+W(2))/A(1)
      S(1)=ABS(X(1)-SET)
   78 DO 79 J=2,M
      SET=X(J)
      X(J)=-(X(J+1)+X(J-1)-2.*(1.-VAR(J))*W(J)+W(J+1)+W(J-1))/A(J)
   79 S(J)=ABS(X(J)-SET)
      SET=X(L)
      X(L)=-(X(M)*C(L)-(1.-4.*CARG/3.)*W(L)+(1.+2.*CARG/3.)*W(M))/A(L)
      S(L)=ABS(X(L)-SET)
      DO 80 J=1,L
      IF(S(J)-0.00001)  80,80,75
   80 CONTINUE
      GO TO 81
   75 CONTINUE
   81 CONTINUE
      Y=P*FLOAT (I)*R/VAV
      WRITE(3, 14)  Y
   14 FORMAT(16H GRAETZ NUMBER= ,F9.5    )
      T(II)=Y
      XN   =(19.-30.*X(1)+18.*X(2)-10.*X(3)+3.*X(4))/(12.*H2)
```

```
      XD(1)=1.0
      DO 91  J=1,L
   91 XD(J+1)=X(J)
      IF( MOD (I,IND))20,16,20
   16 WRITE(3,22 )
   22 FORMAT(//30X,3H P ,28H GAS PROFILE FROM INTERFACE //)
      DO 31 J=1,L
      IF(X(J)  -0.00001)       32,32,31
   32 LOW=J
      GO TO 33
   31 CONTINUE
      LOW=L
   33 WRITE(3,23 )( X(J),J= 1 ,LOW)
   23 FORMAT(25X,E10.4)
      IF(IRD)   43,43,20
   43 CALL  CCPLOT(YD,XD,LO,4HJOIN,0,0)
   20 XNU(I)=XN
      RU(JS,II)=XNU(I)
      WRITE(3,30)  XN
   30 FORMAT(23H LOCAL NUSSELT NUMBER =,E10.4)
      SUM1=0.
      SUM2=0.
      DO 28 J= 1 ,M,2
      SUM1=(VAR(J)/ALP)*X(J)+SUM1
   28 SUM2=(VAR(J+1)/ALP)*X(J+1)+SUM2
      CUP =H2*      (4.*SUM1+2.*SUM2+1.00)/(VAV*3.00)
      XNS=CUP/Y
      RUT(JS,II)=CUP
      WRITE (3,17)   CUP,XNS
   17 FORMAT(25H CUP MIXING CONCENTRATION,E12.6,16H AVG NUSSELT NO=,E12.
     16//)
   19 CONTINUE
      READ (2,2)  LR,MD  ,IND
    2 FORMAT(2I2,I5)
      IF(LR)  3,6,3
    3 DIV=FLOAT(MD)
      R=R*DIV
      DO 8  I=1,N
      MO=I/MD
      IF(MOD(I,MD))   8,11,8
   11 XNU(MO)=XNU(I)
    8 CONTINUE
      MR=N/MD +1
      MR1=MR
      GO TO 18
    6 SUM1=0.
      SUM2=0.
      NO=N-2
      DO 24 J=1,NO,2
      SUM1=XNU(J)+SUM1
   24 SUM2=XNU(J+1)+SUM2
      XNUSLT=P*(4.*SUM1+2.*SUM2+4.*XNU(N-1)+XNU(N)+XNUI) /3.
      WRITE (3,25) XNUSLT
   25 FORMAT(27H THE AVE NUSSELT NUMBER IS ,E10.4)
      SUM1=0.
      SUM2=0.
      DO 26 J= 1 ,M,2
      SUM1=(VAR(J)/ALP)*X(J)+SUM1
```

```
26 SUM2=(VAR(J+1)/ALP)*X(J+1)+SUM2
   CUP1=H2*      (4.*SUM1+2.*SUM2+1.00)/(VAV*3.00)
   WRITE(3,27 )  CUP1
27 FORMAT(//37H CUP MIXING CONC FROM EXIT PROFILE = ,E10.4///)
    VEL=XNUSLT*R/VAV
   WRITE(3,29 )  VEL
29 FORMAT(43H CUP MIXING CONC FROM INTERFACIAL FLUXES = ,E10.4 )
   CALL CCNEXT
   IF(NODATA-JS)  83,83,82
82 GO TO 50
83 CONTINUE
   XMIN=0.0
   YMIN=0.0
   XMAX=Y
   YMAX=1.0
   CCXMAX=1280./1024.
   CALL CCGRID (1,10,5,6HLABELS,1,10,5)
    CALL CCLTR (400./1024.,10./1024.,0,2,11H GRAETZ NO. )
   CALL CCLTR (10./1024.,350./1024.,1,2,21H FRACTION SATURATION  )
   DO 89 J=1,JS
   DO 85 I=1,II
85 XR(I)=RUT(J,I)
   CALL CCPLOT (T,XR ,II,4HJOIN,0,0)
89 CONTINUE
   CALL CCNEXT
   UP=0.0
   DN=100.
   DO 7 J=1,JS
   IF(RU(J,II)-DN)   87,87,84
87 DN=RU(J,II)
84 DO 21 I=1,10
   IF(RU (J,I)-UP) 21,21,88
88 UP=RU (J,I)
21 CONTINUE
 7 CONTINUE
   XMIN=-5.
   XMAX=1.0
   YMIN=FLOAT(IFIX(ALOG10(DN)-1.))
   YMAX=FLOAT(IFIX(ALOG10(UP)+1.))
   KI=IFIX(YMAX-YMIN)
   CALL CCGRID (6,6HLABELS,KI )
   DO 42  I=1,II
42 T(I)=ALOG10(T(I))
    CALL CCLTR (400./1024.,10./1024.,0,2,16H LOG(GRAETZ NO.)  )
   CALL CCLTR (10./1024.,350./1024.,1,2,24H LOG(NUSSELT NUMBER)      )
   DO 86 J=1,JS
   DO 90 I=1,II
90 XTS(I)=ALOG10(RU(J,I))
   CALL CCPLOT (T,XTS,II,4HJOIN,0,0)
86 CONTINUE
   CALL CCEND
   STOP
   END
```

Output

The output is self explanatory . All results are in nondimensional form . Profiles proceed from the interface to the wall. Only concentrations greater than a certain value (10^{-5}) are printed to conserve paper. A sample of the output is given below.

```
GRAETZ NUMBER=    0.00050

                                P  GAS PROFILE FROM INTERFACE

                              0.8404E 00
                              0.6848E 00
                              0.5383E 00
                              0.4060E-00
                              0.2922E-00
                              0.1996E-00
                              0.1288E-00
                              0.7811E-01
                              0.4436E-01
                              0.2352E-01

LOCAL NUSSELT NUMBER =0.1625E 02
CUP MIXING CONCENTRATION0.143944E-01 AVG NUSSELT NO=0.143944E 02

GRAETZ NUMBER=    0.00052
LOCAL NUSSELT NUMBER =0.1597E 02
CUP MIXING CONCENTRATION0.147116E-01 AVG NUSSELT NO=0.147116E 02

GRAETZ NUMBER=    0.00054
LOCAL NUSSELT NUMBER =0.1571E 02
CUP MIXING CONCENTRATION0.150236E-01 AVG NUSSELT NO=0.150236E 02

GRAETZ NUMBER=    0.00056
LOCAL NUSSELT NUMBER =0.1546E 02
CUP MIXING CONCENTRATION0.153307E-01 AVG NUSSELT NO=0.153307E 02

GRAETZ NUMBER=    0.00058
LOCAL NUSSELT NUMBER =0.1522E 02
CUP MIXING CONCENTRATION0.156331E-01 AVG NUSSELT NO=0.156331E 02
```

Figures 59 to 65 are plotted concentration profiles associated with the "GRINT" program. The table given below is a listing of the values of the modified Graetz numbers ($DL/U_m b^2$) for which concentration profiles are drawn in each graph in the order of increasing fraction saturation. The value of the parameter U_m/U_0 is also given.

Table D-1

Graetz Numbers for which Profiles are Plotted in Figures 59 to 65

Number of Curve	Graetz Number
1	0.00050
2	0.00100
3	0.00200
4	0.00400
5	0.00800
6	0.00160
7	0.03200
8	0.04800
9	0.06400
10	0.08000
11	0.09600
12	0.11200
13	0.12800
14	0.14400
15	0.16000
16	0.24000
17	0.32000
18	0.40000
19	0.48000
20	0.56000
21	0.64000
22	0.72000
23	0.80000
24	1.60000

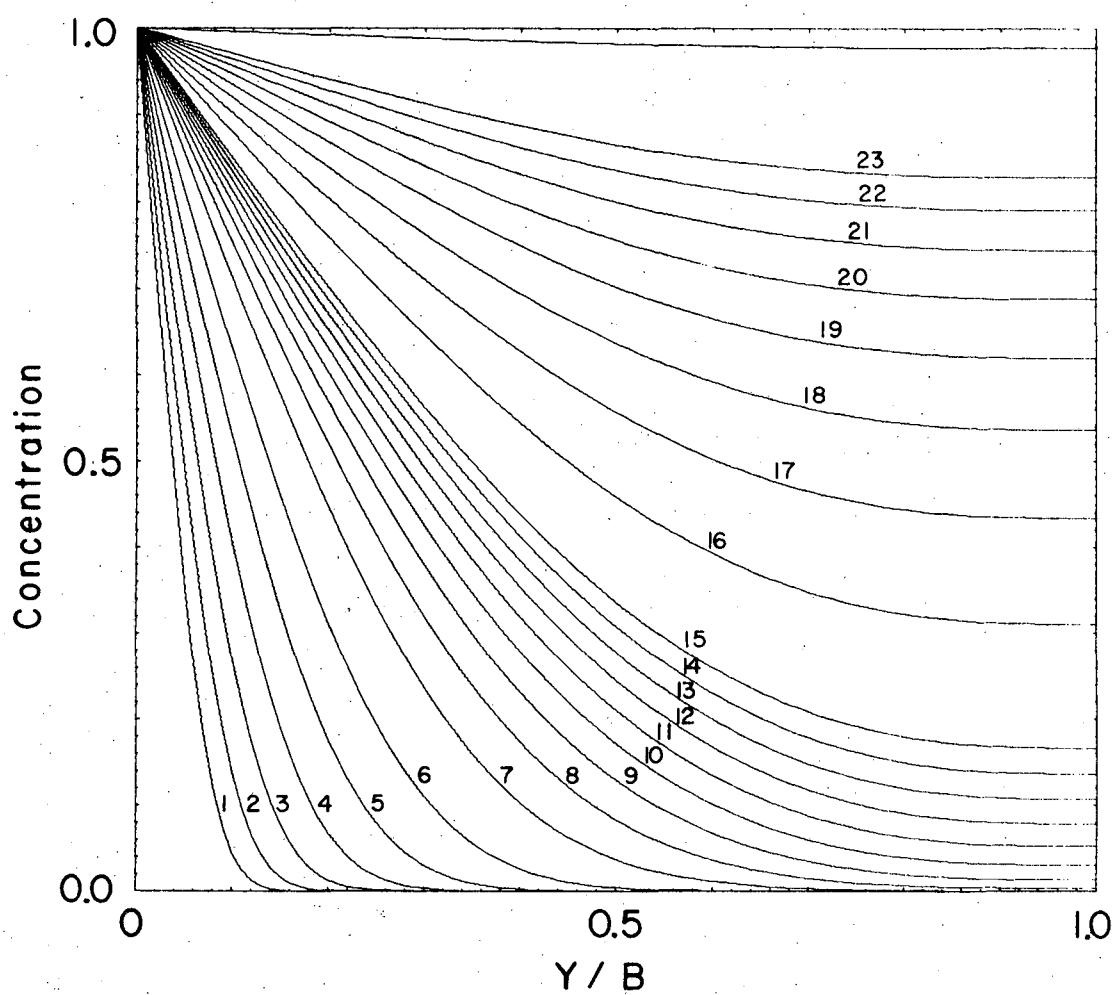

MUB 11324

Fig. 59. Concentration profiles for single phase controlled mass transfer showing profiles for various values of the Graetz number. The velocity ratio, $U_m/U_o = 10.0$.

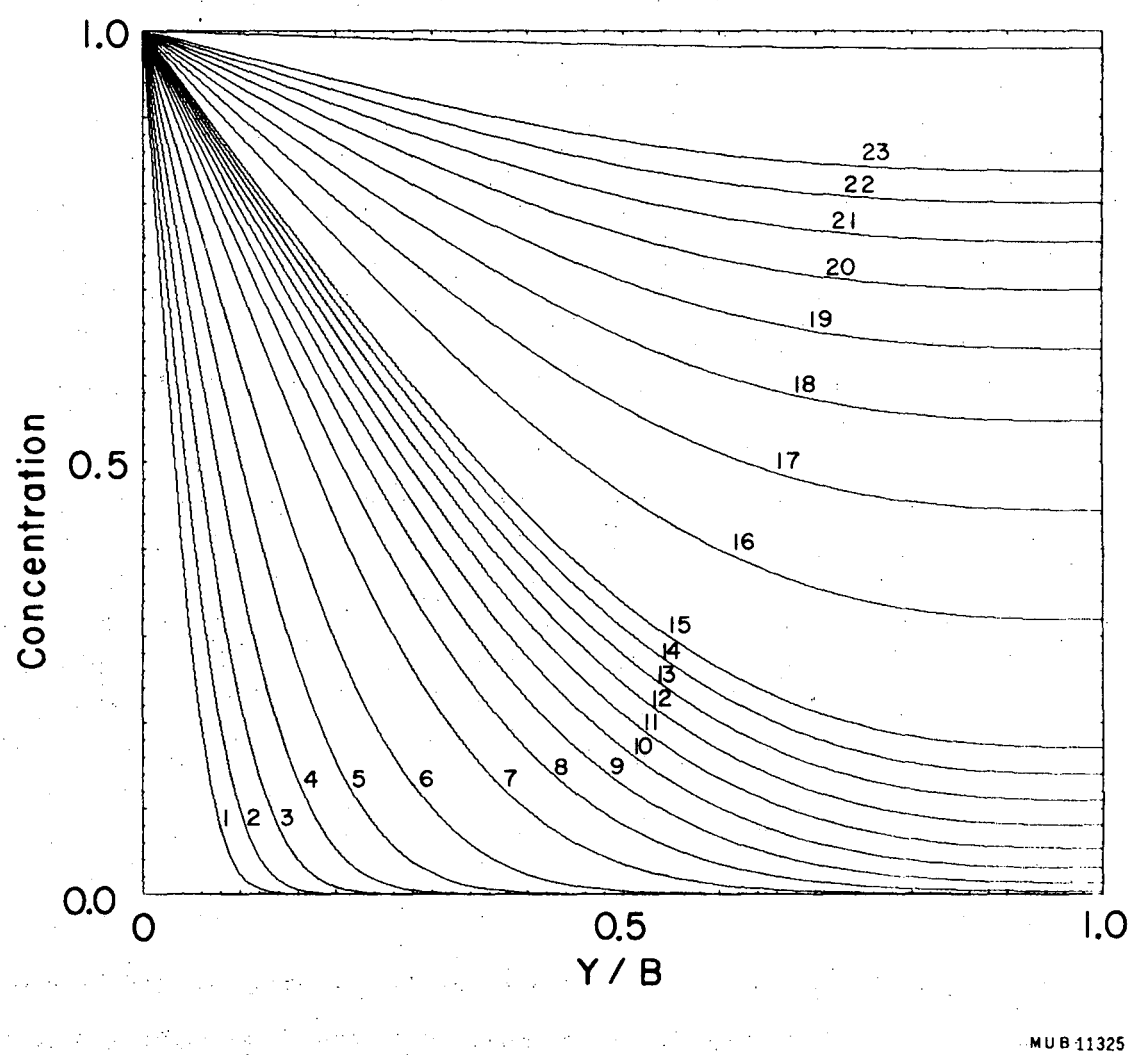

Fig. 60

Concentration profiles for single phase controlled mass transfer showing profiles for various values of the Graetz number. The velocity ratio, $U_m/U_o = 4.0$.

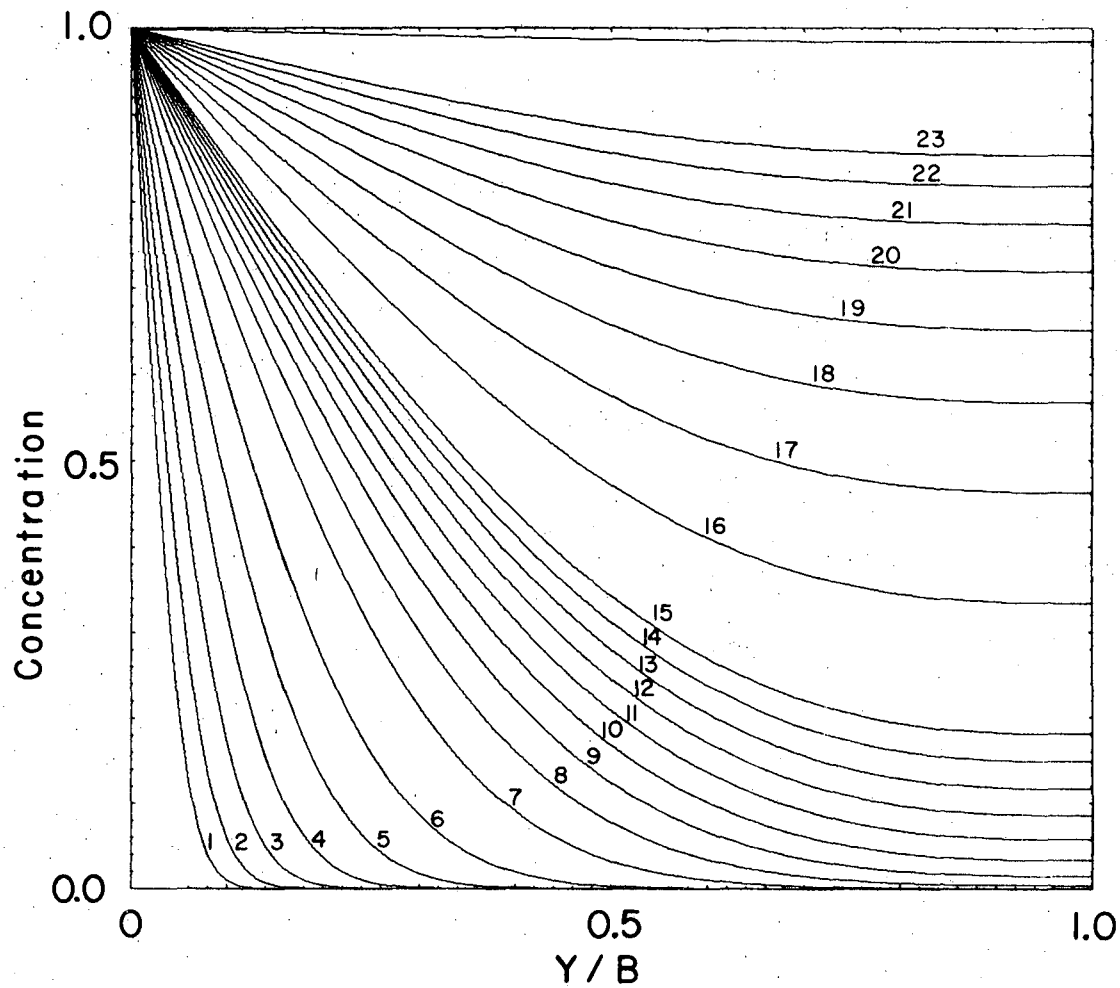

MUB11326

Fig. 61. Concentration profiles for single phase controlled mass transfer showing profiles for various values of the Graetz number. The velocity ratio, $U_m/U_o = 2.0$.

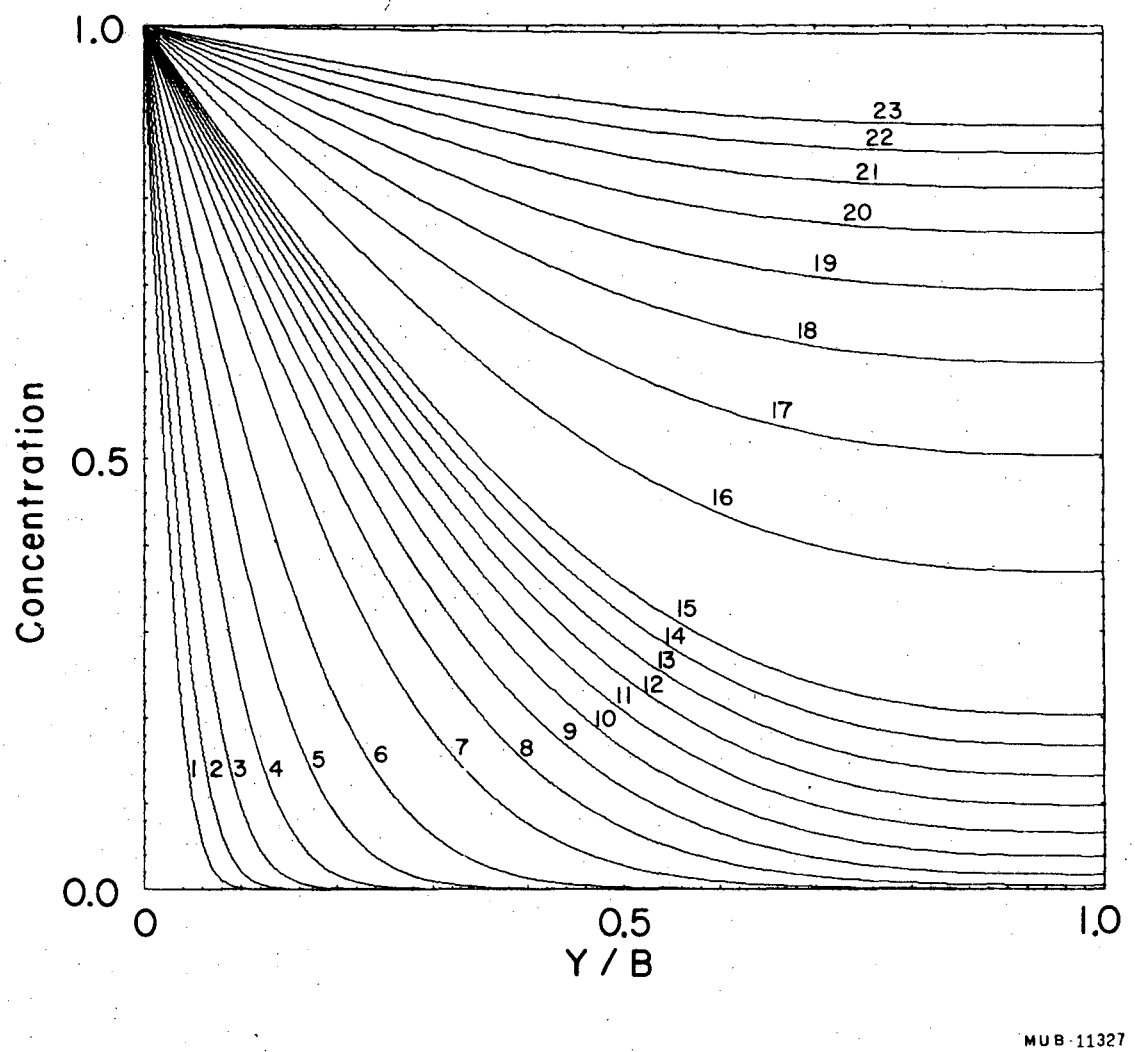

Fig. 62. Concentration profiles for single phase controlled mass transfer showing profiles for various values of the Graetz number. The velocity ratio, $U_m/U_o = 1.0$.

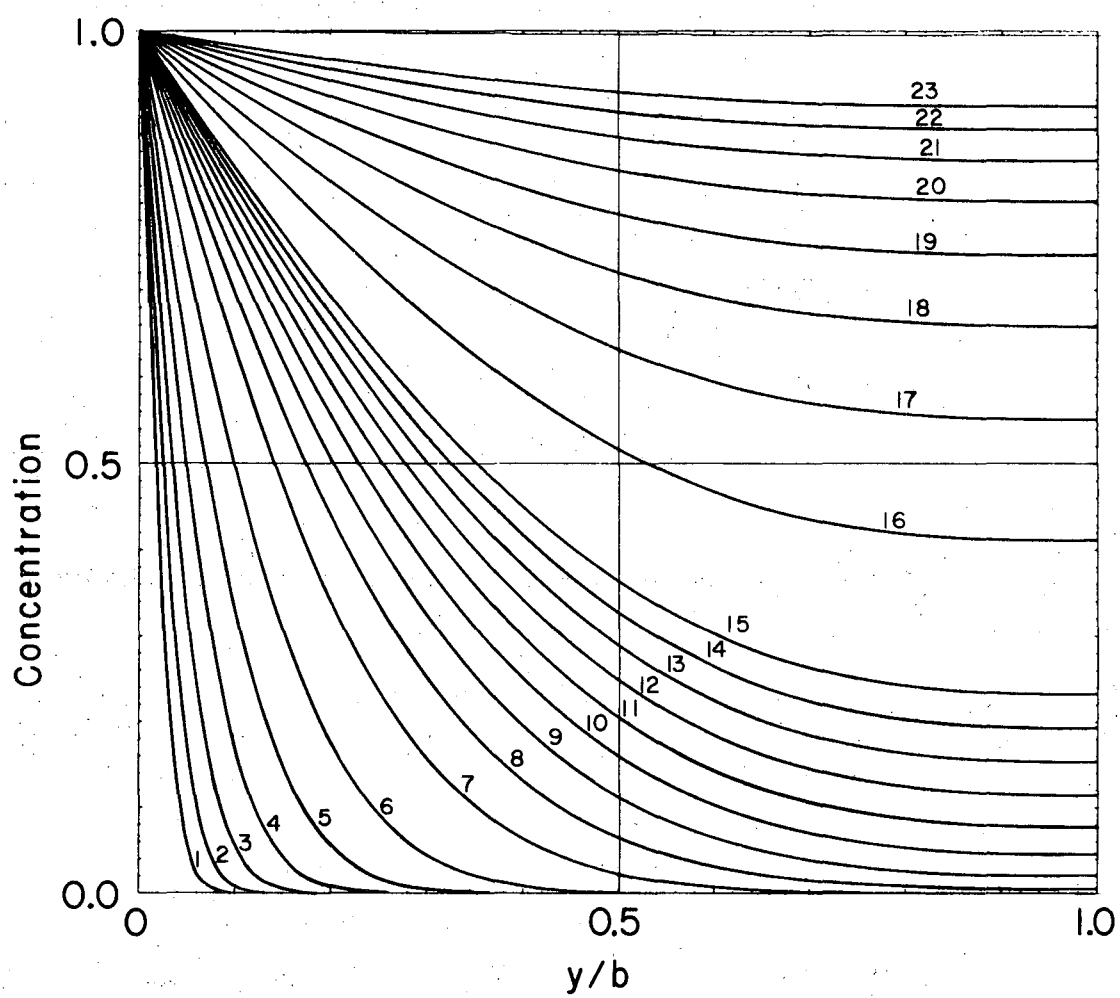

Fig. 63. Concentration profiles for single phase controlled mass transfer showing profiles for various values of the Graetz number. The velocity ratio, $U_m/U_o = 0.667$.

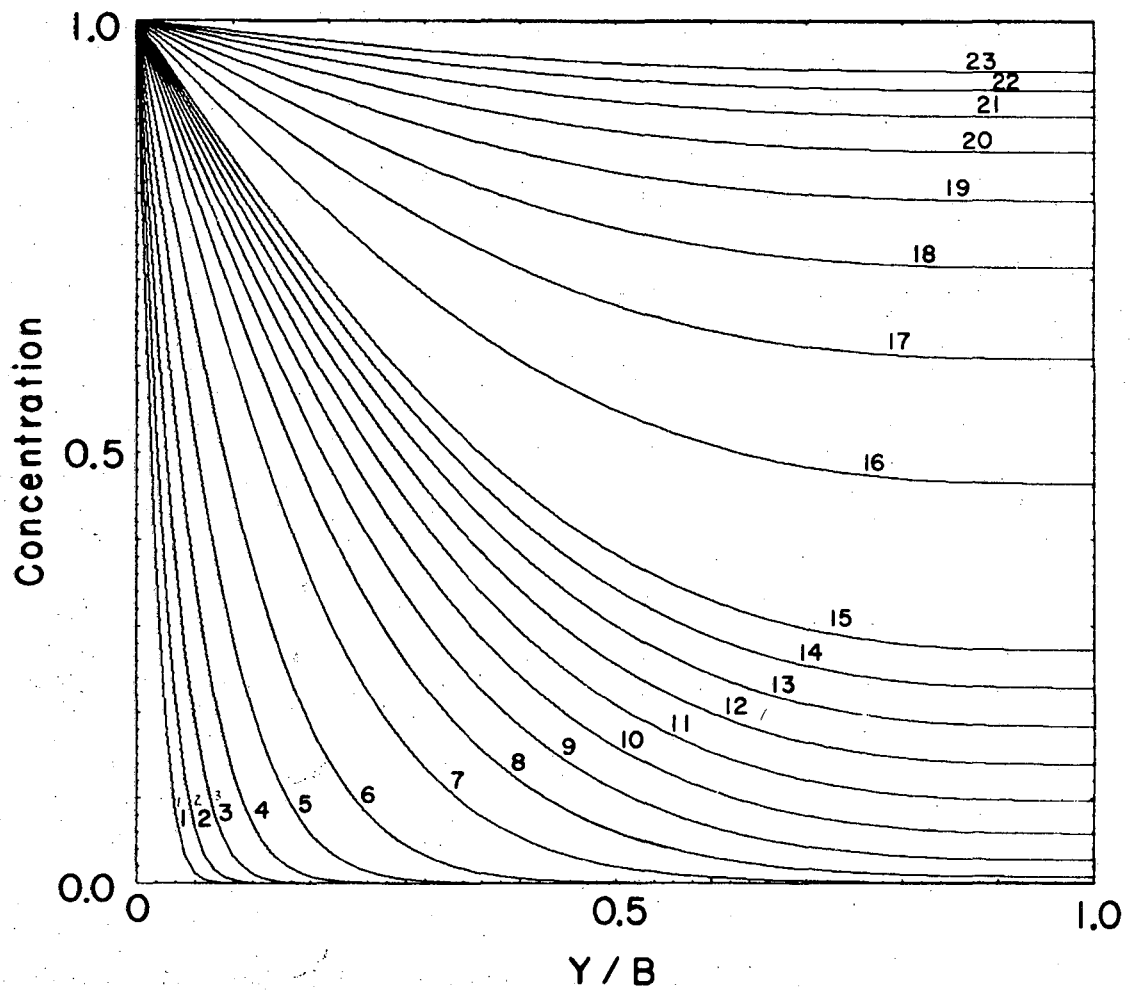

MUB-11322

Fig. 64. Concentration profiles for single phase controlled mass transfer showing profiles for various values of the Graetz number. The velocity ratio, $U_m/U_o = 0.5$.

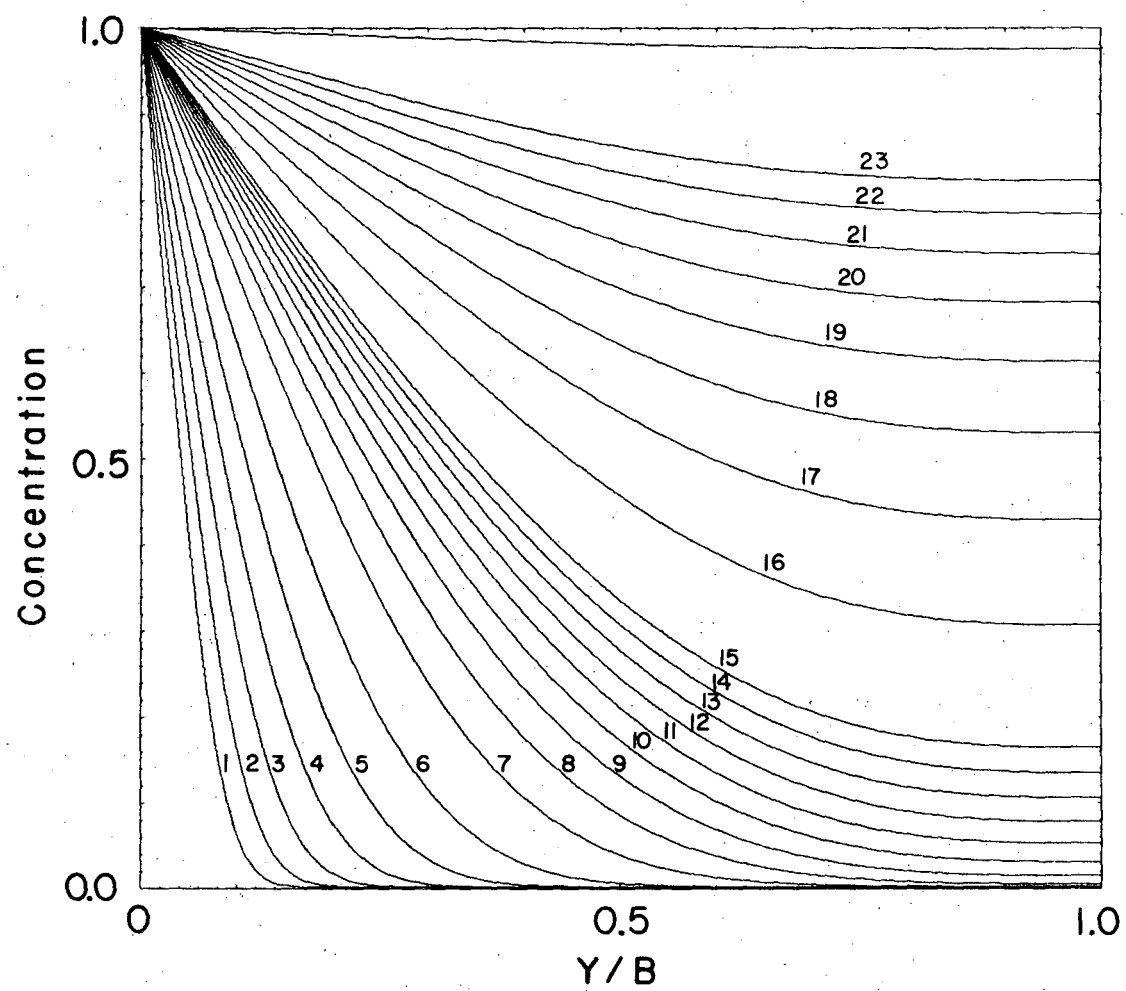

MUB 11323

Fig. 65. Concentration profiles for single phase controlled mass transfer showing profiles for various values of the Graetz number. The velocity ratio, U_m/U_o = 100.0 (may be assumed to be the Graetz solution).

"BAKKER"

Necessary Input Data: The following changes are necessary in the input data of the GRINT program.

Card 1 is omitted.

Card 2 JS and IRD are not used.

LARK - The number of divisions, which are added to the y-direction, in order to keep the mass transfer from penetrating to the wall. Care must be exercised in not over-running the field of the dimension statemant.

Card 3 VAV now takes on the value of the interfacial slope in the velocity profile.

Card 4 IND is not included.

Output

Some typical output from the program is shown below. BB GROUP is $a^2 D x/ U_o^3$. The Cup Mixing concentration and KAVG-- are meaningless. K(LOC)*(X/UO*D)**0.5 is the Beek and Bakker Mass Transfer Group.

```
PROFILE AT BB GROUP =    0.00960

GAS GRADIENT 0.1211E 02

 K(LOC)*(X/UO*D)**0.5 = 0.5933E 00
CUP MIXING CONCENTRATION0.282342E-01 KAVG*(A**2*D*L/UO**3)**0.5 = 0.112937E 02

NO. OF ROW  IS  25 CONVERGENCE AT J =    1
PROFILE AT BB GROUP =    0.01000
```

P GAS PROFILE FROM INTERFACE

```
0.8828E 00
0.7678E 00
0.6574E 00
0.5535E 00
0.4579E-00
0.3719E-00
0.2963E-00
0.2314E-00
```

Note: Profile Continues but was not all included

```
C     BEEK  AND BAKKER SOLUTION
      DIMENSION Q(200),GL(200),GG(200),XNU(200),W(200),VAR(200)
      DIMENSION X(200),A(200),B(200),C(200),S(200) ,G(200) ,O(200)
   50 READ(2,1)   M,N,IND,JELL  ,LARK
    1 FORMAT (5I5)
      READ(2,107) R,VAV
  107 FORMAT(2F12.6)
      WRITE(3,67)
   67 FORMAT(53H1RESULTS OF LEVESQ SOLUTION WITH INTERFACIAL VELOCITY//)
      WRITE(3,104) R
  104 FORMAT(10H D/UO*X = ,F10.3)
      P=1./FLOAT(N)
      H2=1./FLOAT(M)
      WRITE(3, 4 ) H2
    4 FORMAT(                                F6.4,17H GAS Y INCREMENT ///)
      WRITE(3, 5 ) P
    5 FORMAT(F6.4,22H X DIRECTION INCREMENT///)
      WRITE(3,110)   VAV
  110 FORMAT(9H A*X/UO= ,F10.5)
      M=M+LARK
      L=M+1
      MR=1
      DO  15  J=1,L
   15 X(J)=0.0
      XNUI= 1./H2
   18 ALP=(H2*H2)/(R*P)
      FA=H2/FLOAT(L)
      FAR=FA/(H2*100.)
      CARG=ALP*0.5*(1.+VAV-0.5*VAV*H2*FAR)*FAR
      WRITE(3,60)  ALP,CARG
   60 FORMAT(6H ALP=  ,F10.5,6H CARG= ,E10.4)
      DO 9 J= 1 ,M
      Z=H2*FLOAT(J )
      VAR(J)=(1.+VAV*Z)*ALP
      A(J)=-(1.+VAR(J))*2.0
      C(J)=1.
    9 B(J)=1.
      C(L)=1.-2.*CARG/3.
      A(L)=-(1.+4.*CARG/3.)
      O(1)=A(1)
      DO 19 I=MR,N
      IF(I-1)  68,69,68
   69 O(1)=-(2.+VAR(1))
      DO 70 J=2  ,L
      Q(J-1)=B(J-1)/O(J-1)
   70 O(J)=A(J)-C(J)*Q(J-1)
      G(1)=-1.0/O(1)
      MR1=MR+1
      GO TO 71
   68 IF (I-MR1) 45,72,45
   72 DO 54 J=2  ,L
      Q(J-1)=B(J-1)/O(J-1)
   54 O(J)=A(J)-C(J)*Q(J-1)
   45 G(1)=-(2.-2.*(1.-VAR(1))*X(1)+X(2))/A(1)
   71 DO 12 J= 2 ,M
      W(J)=X(J)
   12 G(J)=(2.*(1.-VAR(J))*X(J)-X(J-1)-X(J+1)-C(J)*G(J-1))/O(J)
      G(L)=((1.-4.*CARG/3.)*X(L)-(1.+2.*CARG/3.)*X(M)-C(L)*G(M))/O(L)
      W(1)=X(1)
```

```
      W(L)=X(L)
      X(L)=G(L)
      DO 13 J=1,M
      J1=L-J
      J2=J1+1
   13 X(J1)=G(J1)-Q(J1)*X(J2)
      DO 75 JO=1,JELL
      IF(I-1)   76,77,76
   77 SET=X(1)
      X(1)=-(X(2)+1.)/O(1)
      S(1)=ABS(X(1)-SET)
      GO TO 78
   76 SET=X(1)
      X(1)=-(X(2)-2.*(1.-VAR(1))*W(1)+2.+W(2))/A(1)
      S(1)=ABS(X(1)-SET)
   78 DO 79 J=2,M
      SET=X(J)
      X(J)=-(X(J+1)+X(J-1)-2.*(1.-VAR(J))*W(J)+W(J+1)+W(J-1))/A(J)
   79 S(J)=ABS(X(J)-SET)
      SET=X(L)
      X(L)=-(X(M)*C(L)-(1.-4.*CARG/3.)*W(L)+(1.+2.*CARG/3.)*W(M))/A(L)
      S(L)=ABS(X(L)-SET)
      DO 80 J=1,L
      IF(S(J)-0.00001)  80,80,75
   80 CONTINUE
      GO TO 81
   75 CONTINUE
   81 WRITE(3,82)  I,JO
   82 FORMAT(16H NO. OF ROW  IS ,I3, 20H CONVERGENCE AT J = ,I3)
      Y=P*FLOAT (I)
      XY=VAV*VAV*R*Y
      WRITE(3, 14) XY
   14 FORMAT(22H PROFILE AT BB GROUP = ,F10.5///)
      GG(I)=(19.-30.*X(1)+18.*X(2)-10.*X(3)+3.*X(4))/(12.*H2)
      IF( MOD (I,IND))20,16,20
   16 WRITE(3,22 )
   22 FORMAT(//30X,3H P ,28H GAS PROFILE FROM INTERFACE //)
      WRITE(3,23 )( X(J),J= 1 ,L)
   23 FORMAT(25X,E10.4)
   20 SGG=GG(I)
      WRITE(3, 21)   SGG
   21 FORMAT(                              14H GAS GRADIENT E10.4///)
   57 XNU(I)=GG(I)
    7 XN=XNU(I) *(R*Y)**0.5
      WRITE(3,30)  XN
   30 FORMAT (25H  K(LOC)*(X/UO*D)**0.5 = ,E10.4)
      SUM1=0.
      SUM2=0.
      DO 28 J= 1 ,M,2
      SUM1=(VAR(J)/ALP)*X(J)+SUM1
   28 SUM2=(VAR(J+1)/ALP)*X(J+1)+SUM2
      CUP =H2*      (4.*SUM1+2.*SUM2+1.JO)/((1.+VAV/2.)*3.)
      XNS=CUP*VAV/R
      WRITE (3,17)   CUP,XNS
   17 FORMAT(25H CUP MIXING CONCENTRATION,E12.6,30H KAVG*(A**2*D*L/UO**3
     1)**0.5 = , E12.6//)
   19 CONTINUE
      READ (2,2)  LR,MD
```

```
 2 FORMAT(2I2)
   IF(LR)  3,6,3
 3 DIV=FLOAT(MD)
   R=R*DIV
   DO 8  I=1,N
   MO=I/MD
   IF(MOD(I,MD))   8,11,8
11 XNU(MO)=XNU(I)
 8 CONTINUE
   MR=N/MD +1
   MR1=MR
   GO TO 18
 6 SUM1=0.
   SUM2=0.
   NO=N-2
   DO 24 J=1,NO,2
   SUM1=XNU(J)+SUM1
24 SUM2=XNU(J+1)+SUM2
   XNUSLT=P*(4.*SUM1+2.*SUM2+4.*XNU(N-1)+XNU(N)+XNUI) /3.
   WRITE (3,25) XNUSLT
25 FORMAT(27H THE AVE NUSSELT NUMBER IS ,E10.4)
   SUM1=0.
   SUM2=0.
   DO 26 J= 1 ,M,2
   SUM1=(VAR(J)/ALP)*X(J)+SUM1
26 SUM2=(VAR(J+1)/ALP)*X(J+1)+SUM2
   CUP1=H2*     (4.*SUM1+2.*SUM2+1.00)/((1.+VAV/2.)*3.)
   WRITE(3,27 )  CUP1
27 FORMAT(//37H CUP MIXING CONC FROM EXIT PROFILE = ,E10.4///)
    VEL=XNUSLT*R/VAV
   WRITE(3,29 )  VEL
29 FORMAT(43H CUP MIXING CONC FROM INTERFACIAL FLUXES = ,E10.4 )
   GO TO 50
   END
```

Concentration profiles have been plotted for various values of the distance group, a^2Dx/U_0^3, in Fig. 15. Each curve has been assigned a number. The following is a listing of the values of the distance grouping corresponding to each number on the curves.

Curve Number	a^2Dx/U_0^3	Curve Number	a^2Dx/U_0^3
1	0.01	20	3.60
2	0.02	21	4.00
3	0.04	22	6.00
4	0.08	23	8.00
5	0.16	24	10.00
6	0.24	25	12.00
7	0.32	26	14.00
8	0.40	27	16.00
9	0.48	28	18.00
10	0.56	29	20.00
11	0.64	30	40.00
12	0.72	31	60.00
13	0.80	32	80.00
14	1.20	33	100.00
15	1.60	34	120.00
16	2.00	35	140.00
17	2.40	36	160.00
18	2.80	37	180.00
19	3.20	38	200.00

"GRAGRA"

Necessary Input

Card 1 NODATA is the number of separate cases which are to be run. There must be at least two and not more than ten.

Card 2 This card is the same as the corresponding card in the "GRINT" program with two changes.

- K is the number of subdivisions in the liquid phase.
- M is the number of subdivisions in the entire channel width. Therefore there are K-M divisions in the gas phase.
- TOL provides for the fact that the liquid is not normally penetrated by the exposure. If TOL is set at 2, for example, only the half of the liquid phase nearest the interface is calculated. As a result the mesh in the liquid is twice as fine as the original mesh which is based upon the entire width.

Card 3
- GP is the liquid phase parameter. It is set equal to D_1L/U_0b^2 where L is the length of the first exposure in the series.
- R is the gas phase parameter. It is set equal to D_gL/U_0a^2 with L being the same as in the liquid phase.
- F is the interfacial parameter. It is equal to $D_gb\mathcal{H}/D_1a$, where $\mathcal{H}$ is the dimensionless Henry's law constant, H/RT
- VAV is the ratio of the average velocity in the gas phase to the interfacial velocity.
- AA is the width of the gas phase.
- BB is the width of the liquid phase.

Card 4 This card is identical to the corresponding card in the "GRINT" program.

Any set of units may be used in this program since all parameters are dimensionless.

Output

The output from this program is similar to that of the "GRINT" program, except of course the output now includes both phases. The concentration profiles start at a finite depth in the liquid phase and proceed up through the

liquid to the interface. The interfacial concentration is printed, and then the gas phase concentrations are printed. In order to conserve paper, all liquid concentrations greater than 0.999 and all gas concentrations less than 10^{-5} are not printed. Thus, at least initially, only concentrations near the interface are printed.

It is found that the program consumes about 0.5 minutes to run each case. This assumes that eight lengths are used to cover the interface. The printout from such a run is approximately 3000 to 10,000 lines depending upon the number or concentration profiles which one chooses to print.

Care must be taken in selecting a grid. No more than 199 points may be used in M. N must be less than 500. No extension can be made of the grid since the core of the computer is close to saturation with this grid.

```
GRAGRA,4,300,120000, 468001 , BYERS
MODE 7.
RUNJ(S,,,,,,120000)
REQUEST TAPE99.  CAL-COMP PLOT TAPE
DENSITY TAPE99,5.   SET DENSITY TO 556.
GRAGRA.
EXIT.
DMP.
DMP(36003,36020)
-
      PROGRAM GRAGRA (INPUT,OUTPUT,TAPE98,TAPE99,TAPE2=INPUT,TAPE3=OUTPU
     1T)
      DIMENSION S(202),T(0500),XR(0500),XTS(0500)
      DIMENSION UL(202)         ,X(202),A(202),B(202),C(202),VAR(202)
      DIMENSION G(202),O(202),Q(202),                  XNU(202),W(202)
      DIMENSION  YD(202),RU(10,500),RUT(10,500)
C     GAS LIQUID MASS TRANSFER IN CONFINED COCURRENT FLOW
      COMMON/CCPOOL/XMIN,XMAX,YMIN,YMAX,CCXMIN,CCXMAX,CCYMIN,CCYMAX
      FACTOR =1024.
      COMMON/CCFACT/FACTOR
      READ(2,57)  NODATA
   57 FORMAT  (I2)
   50 READ(2,1) K,M,N ,IND,JELL,TOL,JS
    1 FORMAT(5I5,F6.3,I2)
   71 READ(2,107) GP,R,F ,VAV,AA,BB
  107 FORMAT(6F12.6)
      CON=(GP/R)**0.5/F
      WRITE(3,67)
   67 FORMAT(53H1RESULTS OF GRAETZ SOLUTION WITH INTERFACIAL VELOCITY)
      WRITE (3,80)
   80 FORMAT (28H AND LIQUID PHASE RESISTANCE //)
      WRITE(3,104) F,R,GP
  104 FORMAT (3H F=,F10.3,3H R=,F10.6,4H GP=,F10.6)
      H1=1./(FLOAT(K)*TOL)
      KRUMB=M-K
      H2=1./FLOAT(KRUMB)
      P=1./FLOAT(N)
      WRITE(3, 4 ) H1,H2
    4 FORMAT(F6.4,19H LIQUID Y INCREMENT,F6.4,17H GAS Y INCREMENT     )
      WRITE(3, 5 ) P
    5 FORMAT(F6.4,22H X DIRECTION INCREMENT    )
      WRITE(3,110)    VAV,AA,BB
  110 FORMAT( 7H VAV = ,F10.5,4H AA=,F10.5,5H BB= ,F10.5)
      RAG=R/VAV
      WRITE (3,91)  CON
   91 FORMAT(10H SIGMA*H= ,E10.4)
      CON=F  *H2/H1
      DIV=1.0
      MD=1
      TR=1./TOL
      II=0
      KO=K+1
      KO1=KO+1
      L=M+1
      MR=1
      DO  15  J=1,K
   15 X(J)=1.0
      DO 81 J=KO,L
   81 X(J)=0.0
```

```
      ALP=(H2*H2)/(R*P)
      BET=(H1*H1)/(GP*P)
      X(K+1)=(BET*CON)/(BET*CON+ALP)
      VEX=X(K+1)
      XNUI=(1.0-VEX)/H1
      AY=6.*VAV-4.
      AYS=3.-6.*VAV
      XMIN=-1.0/TOL
      YMIN=0.0
      XMAX=1.0
      YMAX=1.0
      CCYMIN=100./1024.
      CCYMAX=1000./1024.
      CCXMIN= 80./1024.
      CCXMAX=1080./1024.
      KJ=10+IFIX(10.*TR)
      CALL CCGRID (1,10,5,6HLABELS,1,KJ,5)
       CALL CCLTR (400./1024.,10./1024.,0,2,5H Y/L )
      CALL CCLTR (10./1024.,350./1024.,1,2,14H CONCENTRATION)
   18 ALP=(H2*H2)/(R*P)
      BET=(H1*H1)/(GP*P)
      CARL=0.5*BET*((1.-TR*TR)-TR*H1/2.0-H1*H1/12.)
      CARG=ALP*0.25*H2*(3.*VAV-1.+H2/2.-VAV*H2)
      WRITE(3,60)  ALP,CARG,CARL  ,BET
   60 FORMAT(6H ALP=  ,F10.5,6H CARG= ,E10.4,6H CARL= ,E10.4,6H BET= ,E1
     10.4//)
      A(1)=-(1.+4.*CARL/3.)
      YD(L)=1.0
      YD(1)=-  TR
      YD(KO)=0.0
      B(1) =1.-2.*CARL/3.
      DO 8 J=2,K
      YL   =H1*(FLOAT(J)-FLOAT(KO))
      YD(J)=TR* YL
      UL(J)=1.-YL   *YL
      A(J) =-(1.+ BET*UL(J))*2.0
      C(J  ) = 1.
    8 B(J) = 1.
      A(K+1)=-(CON*(1.+BET)+     (1.+ALP))
      B(K+1)=1.
      C(K+1)=CON
      DO 9 J=KO1,M
      J1=J-KO
      Z=H2*FLOAT(J1)
      YD(J)=Z
      VAR(J)=(1.+AY*Z+AYS*Z*Z)*ALP
      A(J)=-(1.+VAR(J))*2.0
      C(J)=1.
    9 B(J)=1.
      C(L)=1.-2.*CARG/3.
      A(L)=-(1.+4.*CARG/3.)
      O(1)=A(1)
      DO 10 J=2,L
      Q(J-1)=B(J-1)/O(J-1)
   10 O(J)=A(J)-C(J)*Q(J-1)
      DO 19 I=MR,N
      II=II+1
      G(1)=((1.-4.*CARL/3.)*X(1)-(1.+2.*CARL/3.)*X(2))/O(1)
```

/

```
      DO 31 J=2,K
      W(J)=X(J)
   31 G(J)=(-X(J-1)-X(J+1)+2.*(1.-BET*UL(J))*X(J)-C(J)*G(J-1))/O(J)
      G(K+1)=(-CON*X(K)-X(KO1)+(CON*(1.-BET)+(1.-ALP    )        )*X(K+1)-
     1C(KO)*G(K))/O(KO)
      DO 12 J=KO1,M
      W(J)=X(J)
   12 G(J)=(2.*(1.-VAR(J))*X(J)-X(J-1)-X(J+1)-C(J)*G(J-1))/O(J)
      G(L)=((1.-4.*CARG/3.)*X(L)-(1.+2.*CARG/3.)*X(M)-C(L)*G(M))/O(L)
      W(K+1)=X(K+1)
      W(1)=X(1)
      W(L)=X(L)
      X(L)=G(L)
      DO 13 J=1,M
      J1=L-J
      J2=J1+1
   13 X(J1)=G(J1)-Q(J1)*X(J2)
      DO 75 JO=1,JELL
      SET=X(1)
      X(1)=1.25*((1.-2.*CARL/3.)*X(2)-(1.-4.*CARL/3.)*W(1)+(1.+.667*CARL
     1)*W(2))/(1.+4.*CARL/3.)-0.25*SET
      S(1)=ABS(X(1)-SET)
      DO  32 J=2,K
      SET=X(J)
      X(J)=-1.25*(X(J+1)+X(J-1)-2.*(1.-BET*UL(J))*W(J)+W(J+1)+W(J-1))/A(
     1J)-0.25*SET
   32 S(J)=ABS(X(J)-SET)
      SET=X(K+1)
      X(KO)= -1.25*(X(K)*CON+X(KO1)+W(K)*CON-(CON*(1.-BET)+    (1.-ALP))
     1*W(KO)+W(KO1))/A(KO )-0.25*SET
      S(KO )=ABS(X(K+1)-SET)
      DO 79 J=KO1,M
      SET=X(J)
      X(J)=-(X(J+1)+X(J-1)-2.*(1.-VAR(J))*W(J)+W(J+1)+W(J-1))/A(J)*1.25-
     10.25*SET
   79 S(J)=ABS(X(J)-SET)
      SET=X(L)
      X(L)=-(X(M)*C(L)-(1.-4.*CARG/3.)*W(L)+(1.+2.*CARG/3.)*W(M))/A(L)
     1*1.25-0.25*SET
      S(L)=ABS(X(L)-SET)
      DO 33 JOKE= 1,L
      IF(S(JOKE)-0.0001)  33,33,75
   33 CONTINUE
      GO TO 34
   75 CONTINUE
   34 CONTINUE
      DO 11 J=1,L
      IF(X(J)-1.0)   11,11,40
   40 X(J)=1.00
   11 CONTINUE
      Y=P*FLOAT (I)   *DIV*RAG
      WRITE(3, 14)  Y
   14 FORMAT(16H GRAETZ NUMBER= ,F9.5    )
      T(II)=Y
      XN   =(19.*X(KO)-30.*X(KO1)+18.*X(K+2)-10.*  X(K+3) +3.*X(K+4))/
     1(12.*H2)
      XS2=X(K+1)
      IF( MOD (I,IND))20,42,20
```

```
 42 DO 131 J=1,KO
    IF (X(J)-0.999)     132,132,131
132 LOL=J
    GO TO 133
131 CONTINUE
    LOL=K   -1
133 DO  134   J=KO,L
    IF (X(J) -0.001)    135,135,134
135 LOW =J
    GO TO 136
134 CONTINUE
    LOW=L
136 WRITE(3,38 )( X(J),J=LOL,K)
 38 FORMAT(25X,F10.6)
    WRITE(3, 35)  XS2
 35 FORMAT(30H INTERFACIAL CONCENTRATION IS F7.5///)
    WRITE(3,22 )
 22 FORMAT(//30X,3H P ,28H GAS PROFILE FROM INTERFACE //)
    WRITE(3,23 )( X(J),J=KO1,LOW)
 23 FORMAT(25X,F10.6)
    CALL CCPLOT (YD,X,L,  4HJOIN,0,0)
    WRITE(3,137) LOL,KO,LOW,KRUMB
137 FORMAT(I4,29H DIVISIONS PRINTED IN LIQ OF ,I3,5X,I3,29H DIVISIONS
   1PRINTED IN GAS OF ,I3)
 20 VEX=X(K+1)
    XNU(I)=XN
    RU(JS,II)=XNU(I)
    WRITE(3,30)  XN ,JO
 30 FORMAT(5X,25H LOCAL NUSSELT NUMBER = ,E10.4,20H CONVERGENCE AT J =
   1 ,I3)
    SUM1=0.
    SUM2=0.
    DO 28 J=KO1,M,2
    SUM1=(VAR(J)/ALP)*X(J)+SUM1
 28 SUM2=(VAR(J+1)/ALP)*X(J+1)+SUM2
    CUP     =H2 * (4.*SUM1+2.*SUM2+1.00)/(VAV*3.00)
    XNS=CUP*VAV*DIV/R
    RUT(JS,II)=CUP
    WRITE (3,17)    CUP,XNS
 17 FORMAT(5X,25H CUP MIXING CONCENTRATION ,E12.6,16H AVG NUSSELT NO=,
   1E12.6//)
 19 CONTINUE
    READ (2,2)  LR,MD  ,IND
  2 FORMAT(2I2,I5)
    IF(LR)  3,6,3
  3 DI =FLOAT(MD)
    R=R*DI
    GP =GP*DI
    DIV=DIV*DI
    DO 41  I=1,N
    MO=I/MD
    IF(MOD(I,MD))   41,16,41
 16 XNU(MO)=XNU(I)
 41 CONTINUE
    MR=N/MD +1
    MR1=MR
    GO TO 18
  6 SUM1=0.
```

```
      SUM1=0.
      SUM2=0.
      NO=N-2
      DO 24 J=1,NO,2
      SUM1=XNU(J)+SUM1
   24 SUM2=XNU(J+1)+SUM2
      XNUSLT=P*(4.*SUM1+2.*SUM2+4.*XNU(N-1)+XNU(N)+XNUI) /3.
      WRITE (3,25) XNUSLT
   25 FORMAT(27H THE AVE NUSSELT NUMBER IS ,E10.4)
      SUM1=0.
      SUM2=0.
      SUM3=0.0
      SUM4=0.0
      DO 26 J=KO1,M,2
      SUM1=(VAR(J)/ALP)*X(J)+SUM1
      SUM3=VAR(J)/ALP +SUM3
      SUM4=VAR(J+1)/ALP+SUM4
   26 SUM2=(VAR(J+1)/ALP)*X(J+1)+SUM2
      CUP1=H2*      (4.*SUM1+2.*SUM2+1.00)/(VAV*3.00)
      WRITE(3,27 )  CUP1
   27 FORMAT(//37H CUP MIXING CONC FROM EXIT PROFILE = ,E10.4    )
       VEL=XNUSLT*R/VAV
      WRITE(3,29 )  VEL
   29 FORMAT(43H CUP MIXING CONC FROM INTERFACIAL FLUXES = ,E10.4 )
      CALL CCNEXT
      IF(NODATA-JS)  83,83,82
   82 GO TO 50
   83 CONTINUE
      XMIN=0.0
      YMIN=0.0
      XMAX=Y
      YMAX=1.0
      CCXMAX=1280./1024.
      CALL CCGRID (1,10,5,6HLABELS,1,10,5)
       CALL CCLTR (400./1024.,10./1024.,0,2,11H GRAETZ NO. )
      CALL CCLTR (10./1024.,350./1024.,1,2,21H FRACTION SATURATION  )
      DO 89 J=1,JS
      DO 85 I=1,II
   85 XR(I)=RUT(J,I)
      CALL CCPLOT (T,XR ,II,4HJOIN,0,0)
   89 CONTINUE
      CALL CCNEXT
      UP=0.0
      DN=100.
      DO 7 J=1,JS
      IF(RU(J,II)-DN)   87,87,84
   87 DN=RU(J,II)
   84 DO 21 I=1,10
      IF(RU (J,I)-UP) 21,21,88
   88 UP=RU (J,I)
   21 CONTINUE
    7 CONTINUE
      XMIN=-5.
      XMAX=1.0
      YMIN=FLOAT(IFIX(ALOG10(DN)-1.))
      YMAX=FLOAT(IFIX(ALOG10(UP)+1.))
      KI=IFIX(YMAX-YMIN)
      CALL CCGRID (6,6HLABELS,KI )
```

```
      DO 52  I=1,II
   52 T(I)=ALOG10(T(I))
       CALL CCLTR (400./1024.,10./1024.,0,2,16H LOG(GRAETZ NO.)  )
      CALL CCLTR (10./1024.,350./1024.,1,2,24H LOG(NUSSELT NUMBER)      )
      DO 86 J=1,JS
      DO 90 I=1,II
   90 XTS(I)=ALOG10(RU(J,I))
      CALL CCPLOT (T,XTS,II,4HJOIN,0,0)
   86 CONTINUE
      CALL CCEND
      STOP
      END
```

Results of the GRAGRA Program for the Experimental Systems

Two gases, helium and carbon dioxide, were used as the gas phase in the interphase experiments in which ether was evaporated from 0.5 mole% alcohol solutions into a gas phase. GRAGRA was used to compute the theoretical curves for these two situations. Since in both cases a wide range of velocities were used, six series of solutions were made with the velocity ratios, U_m/U_0, ranging from 0.5 to 10.0 for both systems. Figures 66 and 67 are the overall Nusselt numbers for different values of the parameter U_m/U_0 plotted as a function of the Graetz number. The former gives the results for carbon dioxide while the latter gives the values for helium. The value of the velocity ratio is given on each curve. The Nusselt number is based upon on initial driving force.

The remainder of the curves (Figs. 68 to 79) are concentration profiles for the two systems. Negative values of the ordinate are an indication of a concentration in the liquid phase; positive ones are in the gas phase. The pertinent information on each curve is given in Table D-2.

Table D-2
Concentration Profile Plots

U_m/U_0	Figure Number	
	Helium	Carbon dioxide
10.0	68	74
4.0	69	75
2.0	70	76
1.0	71	77
0.667	72	78
0.5	73	79

In each case profiles are plotted for the values of Graetz number given in Table D-3.

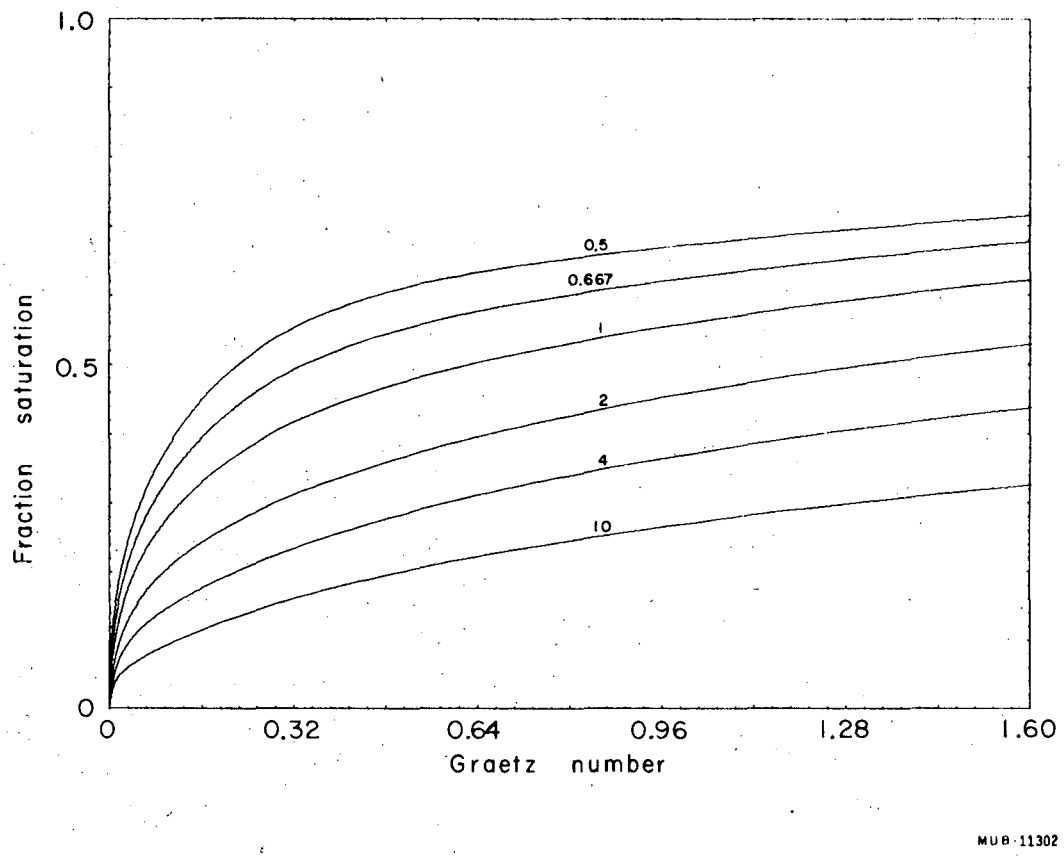

Fig. 66. Cup mixing concentration as a function of Graetz number (theoretical) for evaporation of ether from ethanol into helium flowing at different values of the parameter U_m/U_o.

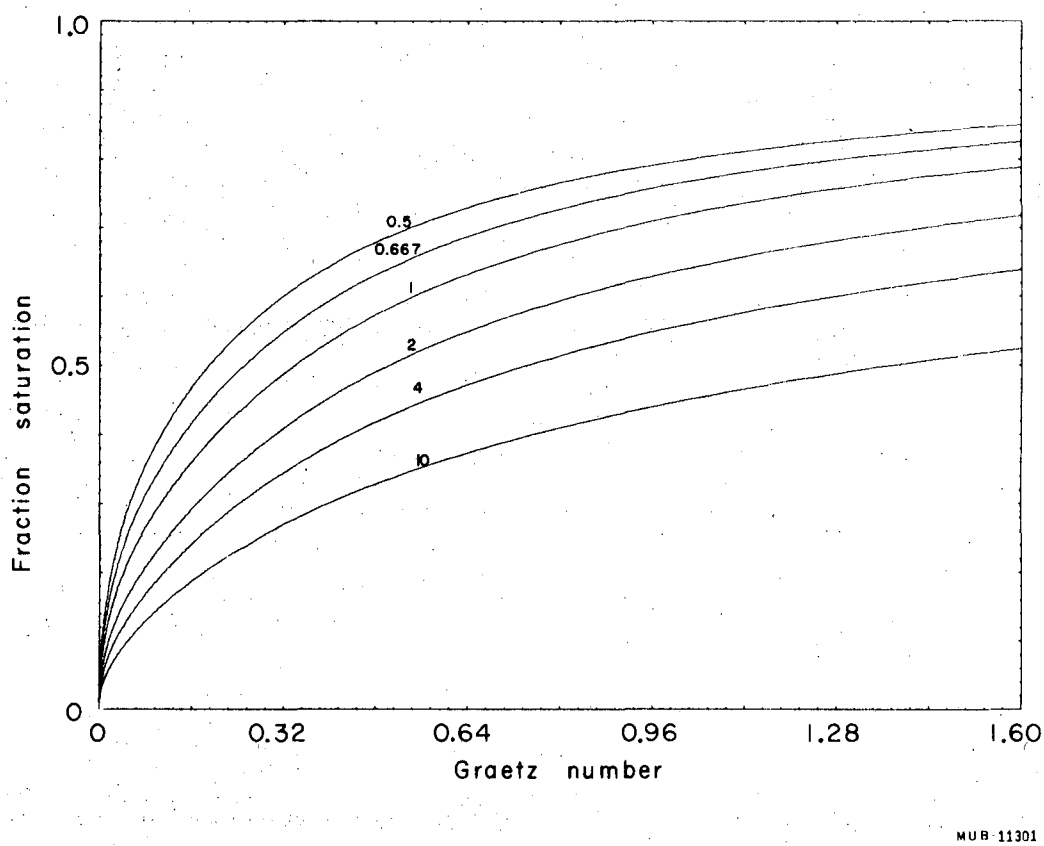

Fig. 67. Cup mixing concentration as a function of Graetz number (theoretical) for evaporation of ether from ethanol into CO_2 flowing at different values of the parameter U_m/U_o.

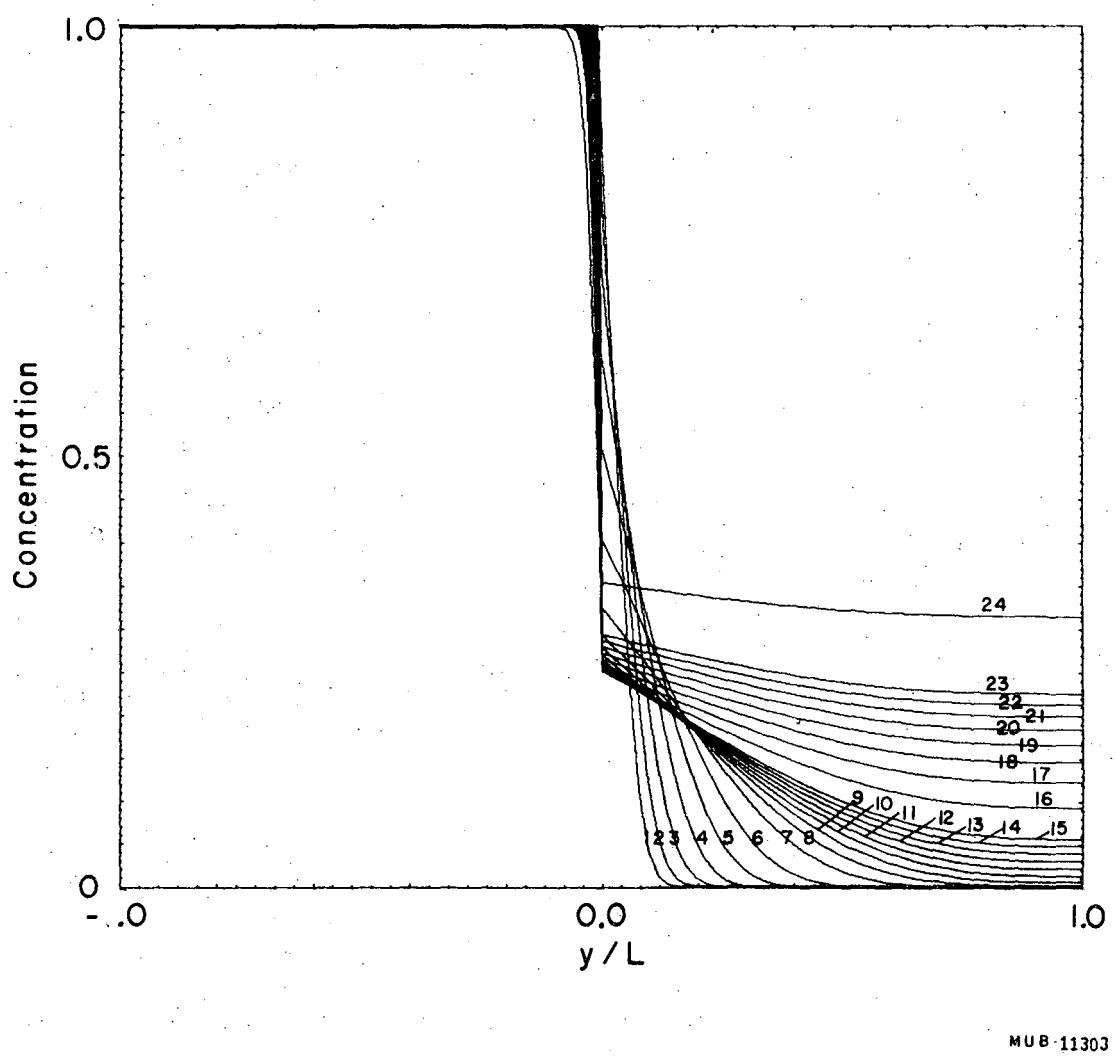

Fig. 68. Interphase concentration profiles for the evaporation of ether from ethanol solution into helium for different values of the Graetz number. $U_m/U_o = 10$.

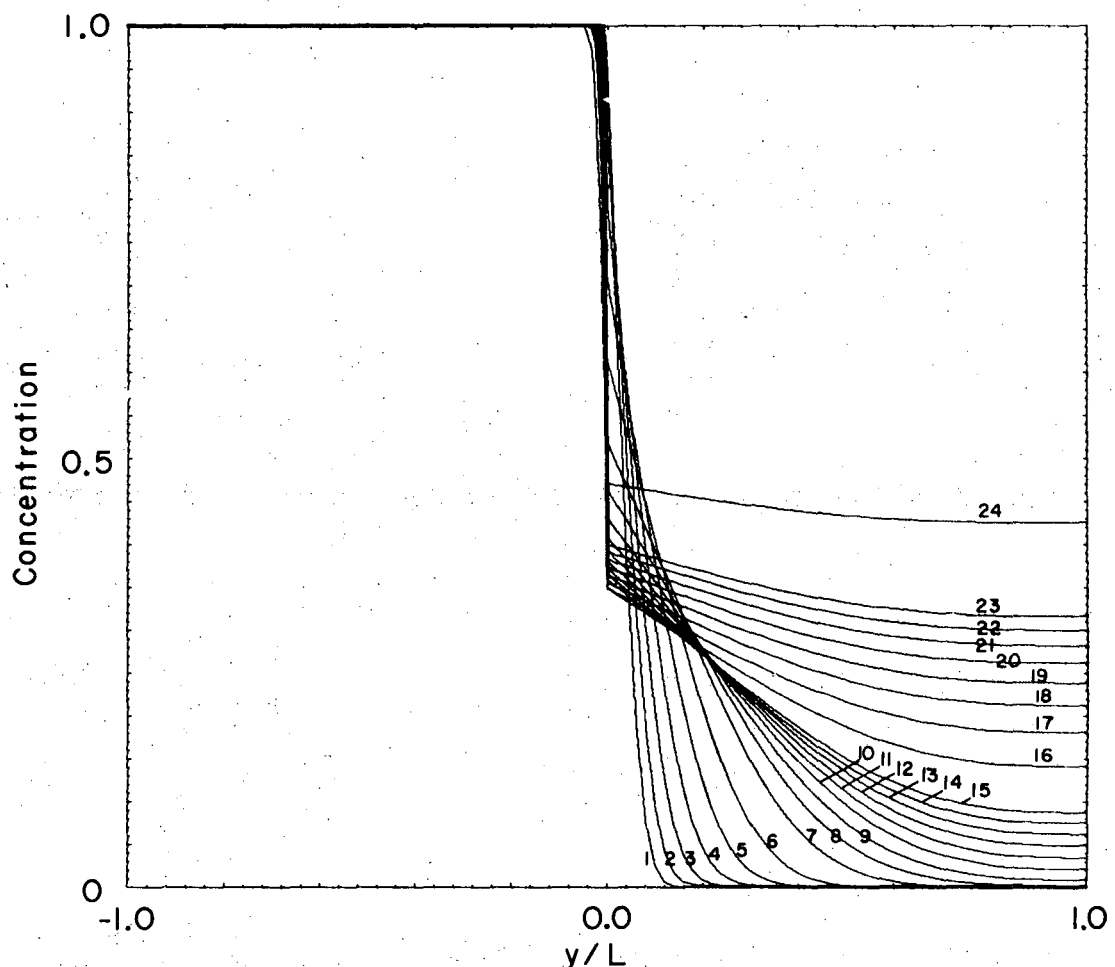

MUB 11314

Fig. 69. Interphase concentration profiles for the evaporation of ether from ethanol solution into helium for different values of the Graetz number. $U_m/U_o = 4.0$.

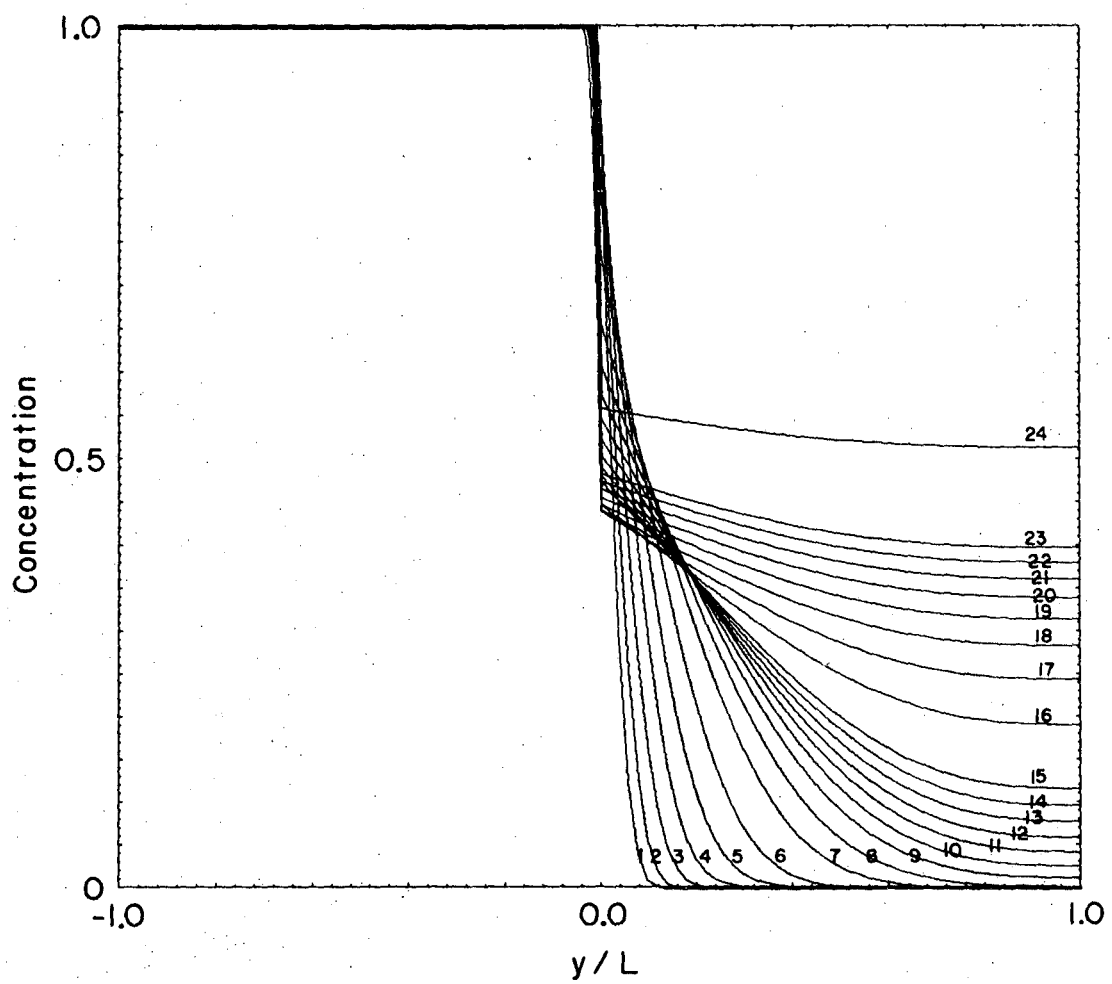

MUB-11313

Fig. 70. Interphase concentration profiles for the evaporation of ether from ethanol solution into helium for different values of the Graetz number. $U_m/U_o = 2.0$.

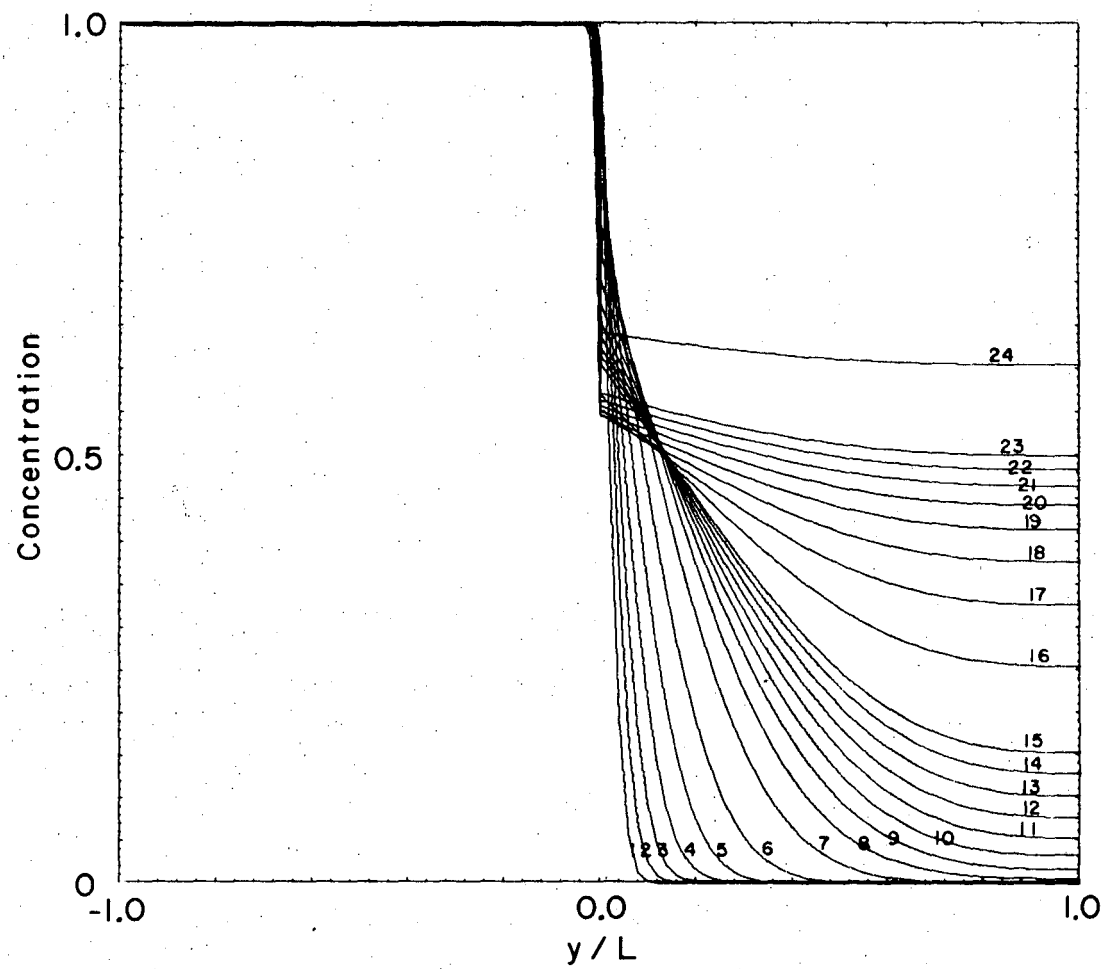

Fig. 71. Interphase concentration profiles for the evaporation of ether from ethanol solution into helium for different values of the Graetz number. $U_m/U_o = 1.0$.

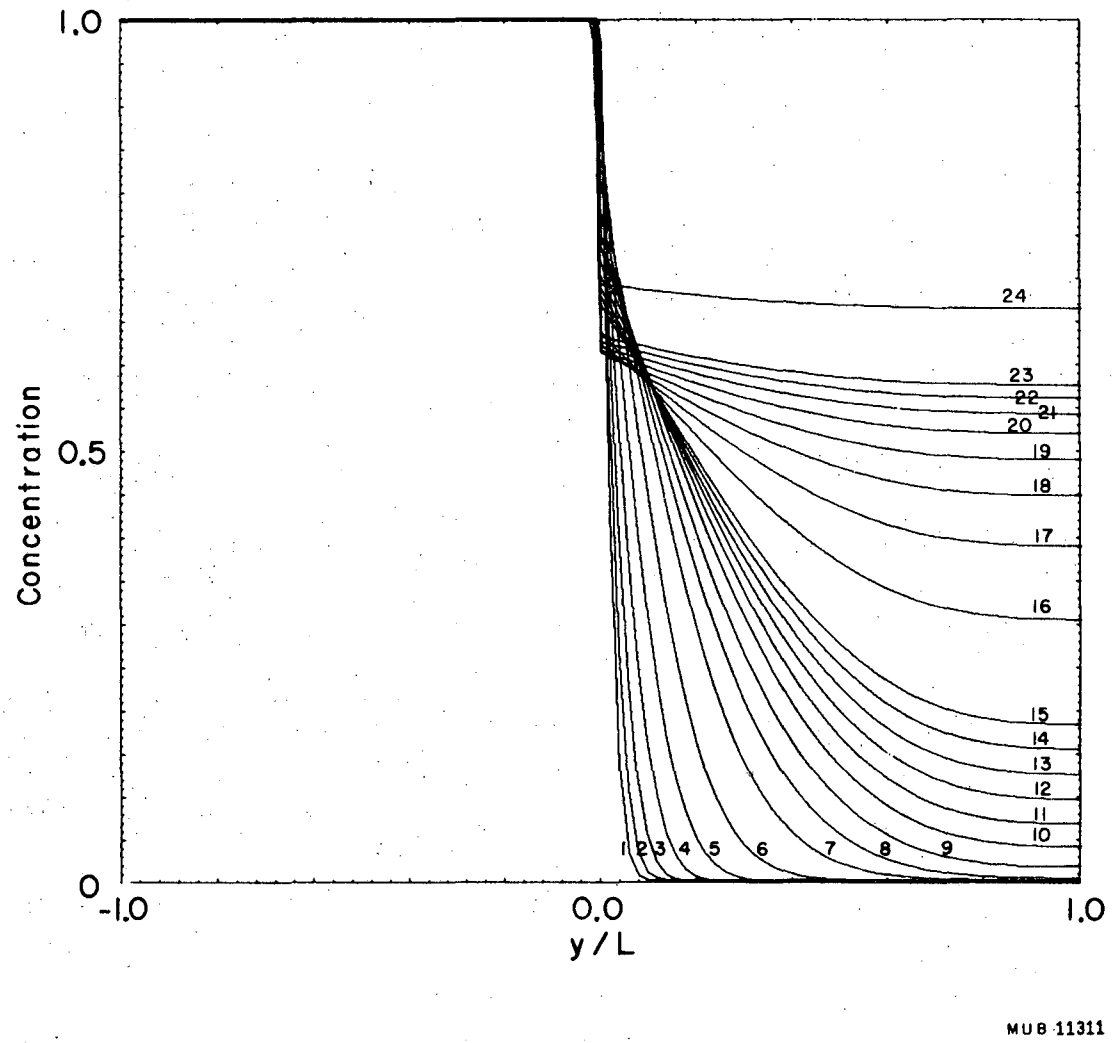

Fig. 72. Interphase concentration profiles for the evaporation of ether from ethanol solution into helium for different values of the Graetz number. $U_m/U_o = 0.667$.

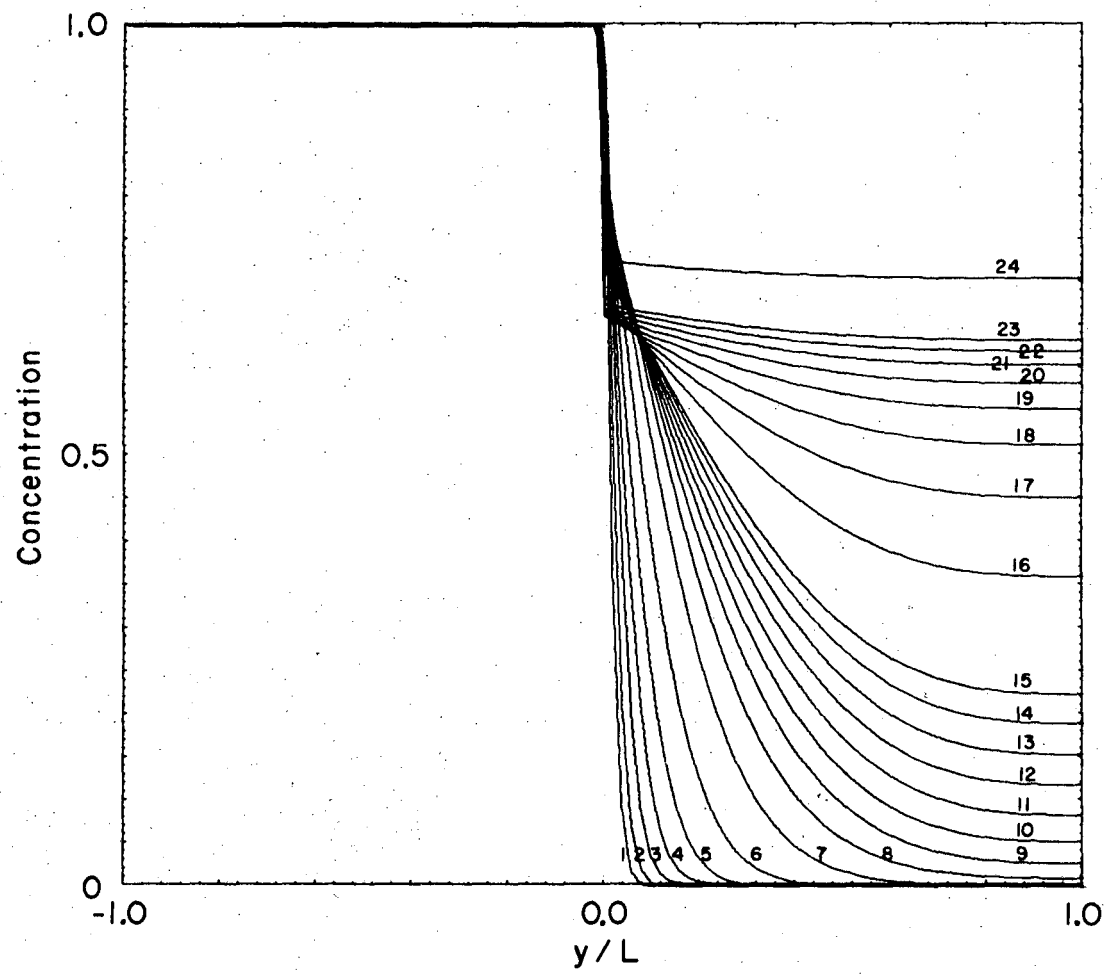

Fig. 73. Interphase concentration profiles for the evaporation of ether from ethanol solution into helium for different values of the Graetz number. $U_m/U_o = 0.5$.

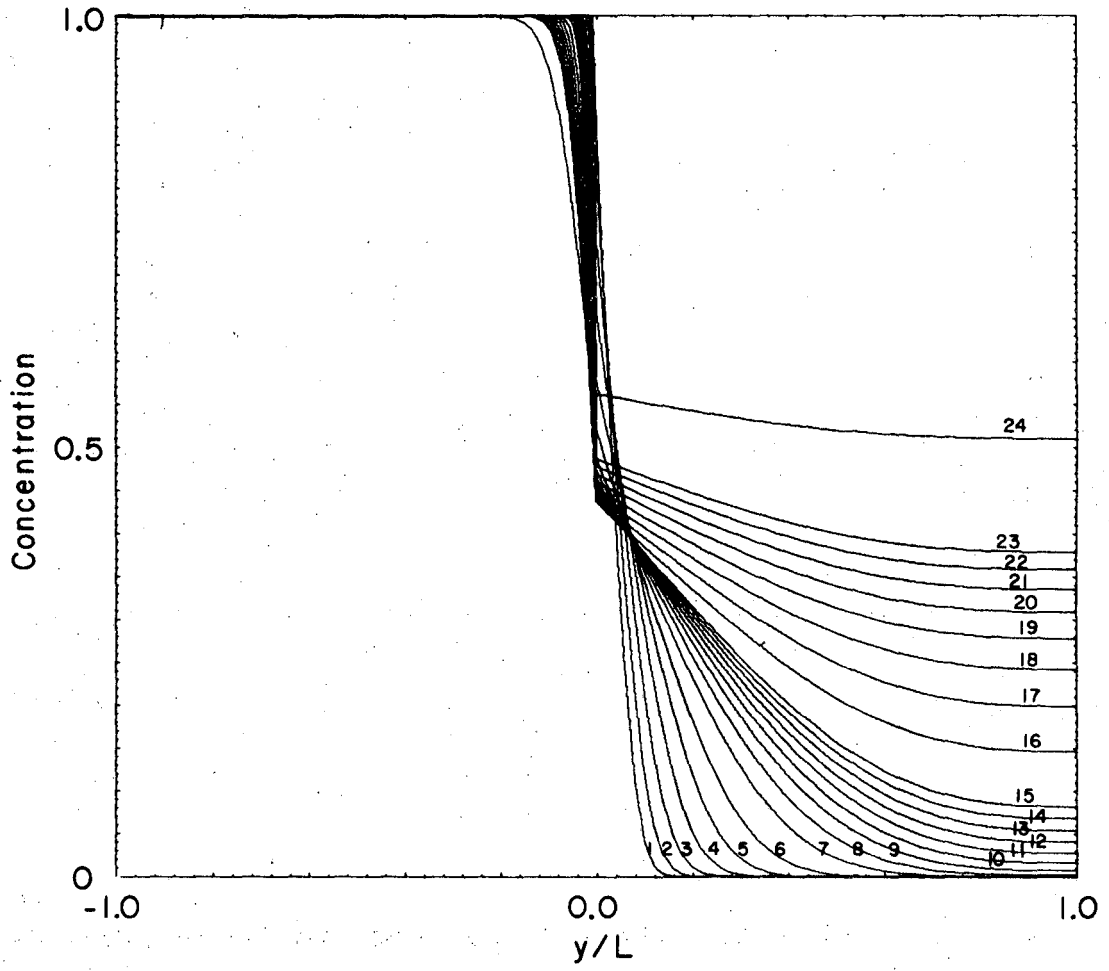

MUB-11309

Fig. 74. Interphase concentration profiles for the evaporation of ether from ethanol solution into CO_2 for different values of the Graetz number. $U_m/U_o = 10$.

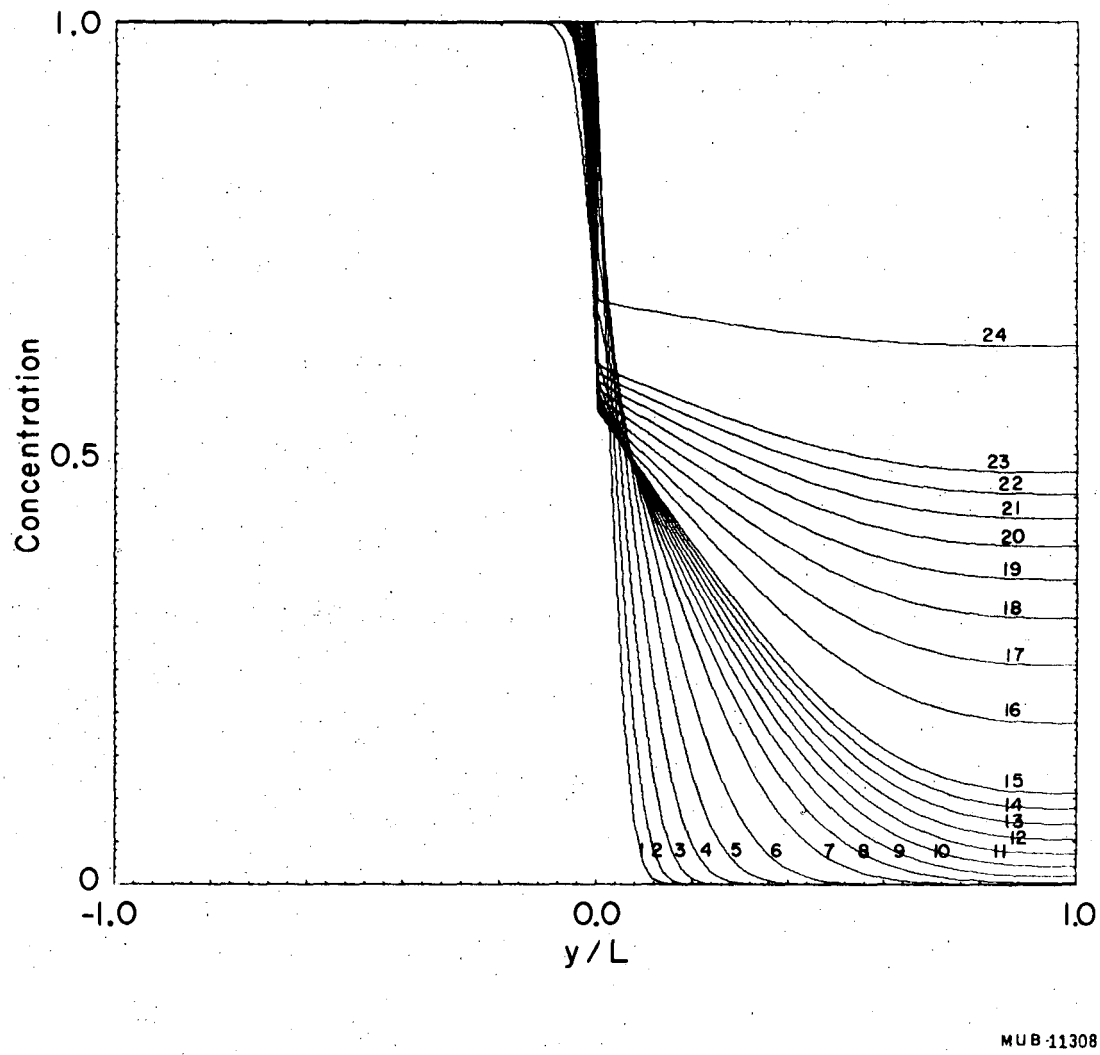

Fig. 75. Interphase concentration profiles for the evaporation of ether from ethanol solution into CO_2 for different values of the Graetz number. $U_m/U_o = 4.0$.

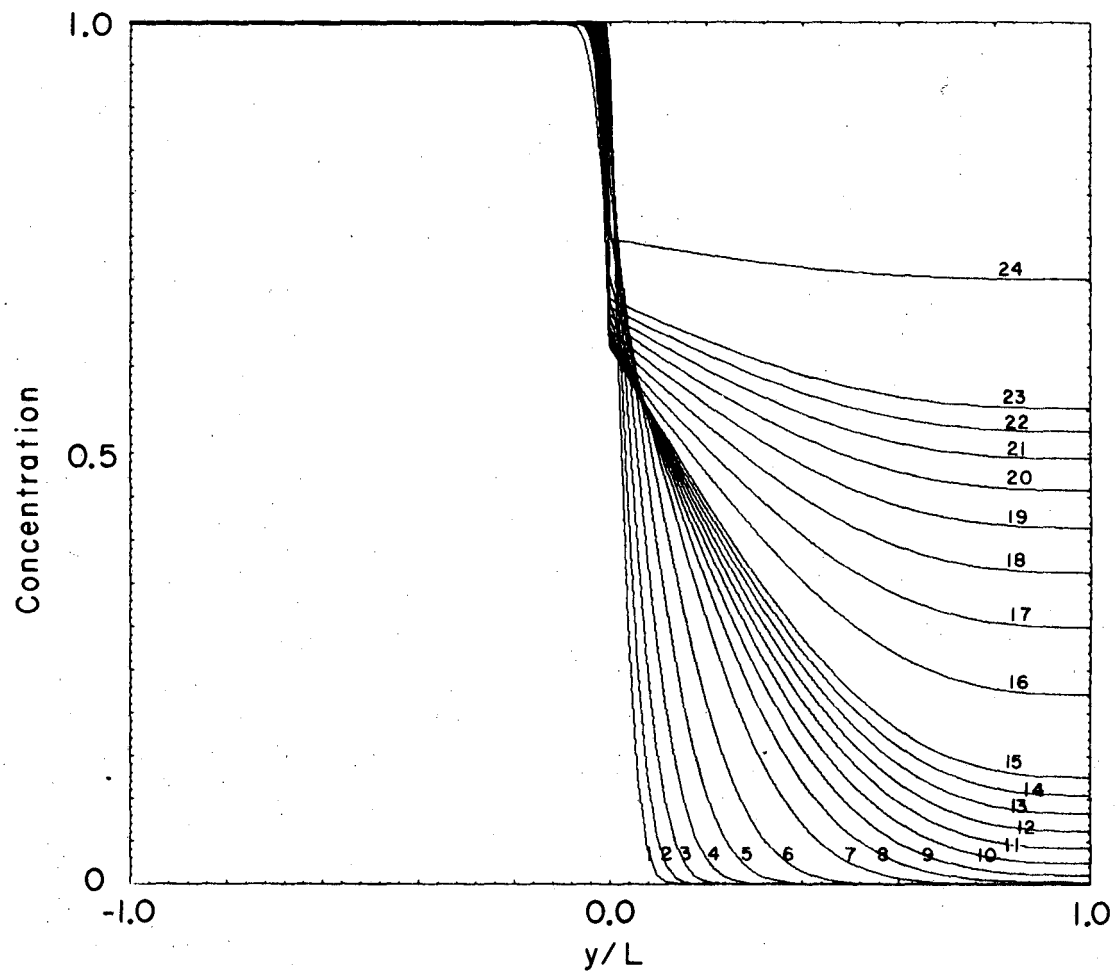

MUB 11307

Fig. 76. Interphase concentration profiles for the evaporation of ether from ethanol solution into CO_2 for different values of the Graetz number. $U_m/U_o = 2.0$.

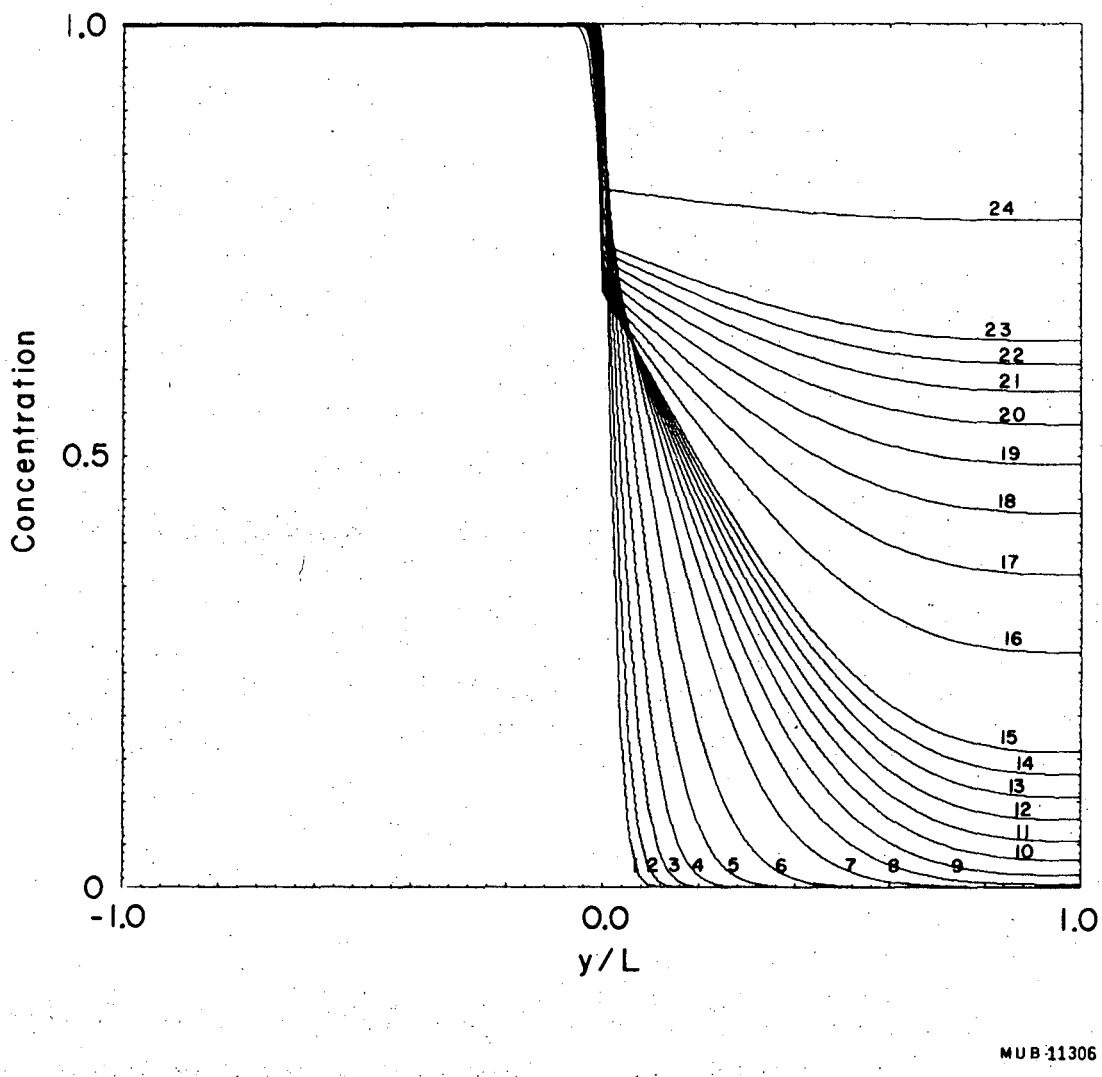

Fig. 77. Interphase concentration profiles for the evaporation of ether from ethanol solution into CO_2 for different values of the Graetz number. $U_m/U_o = 1.0$.

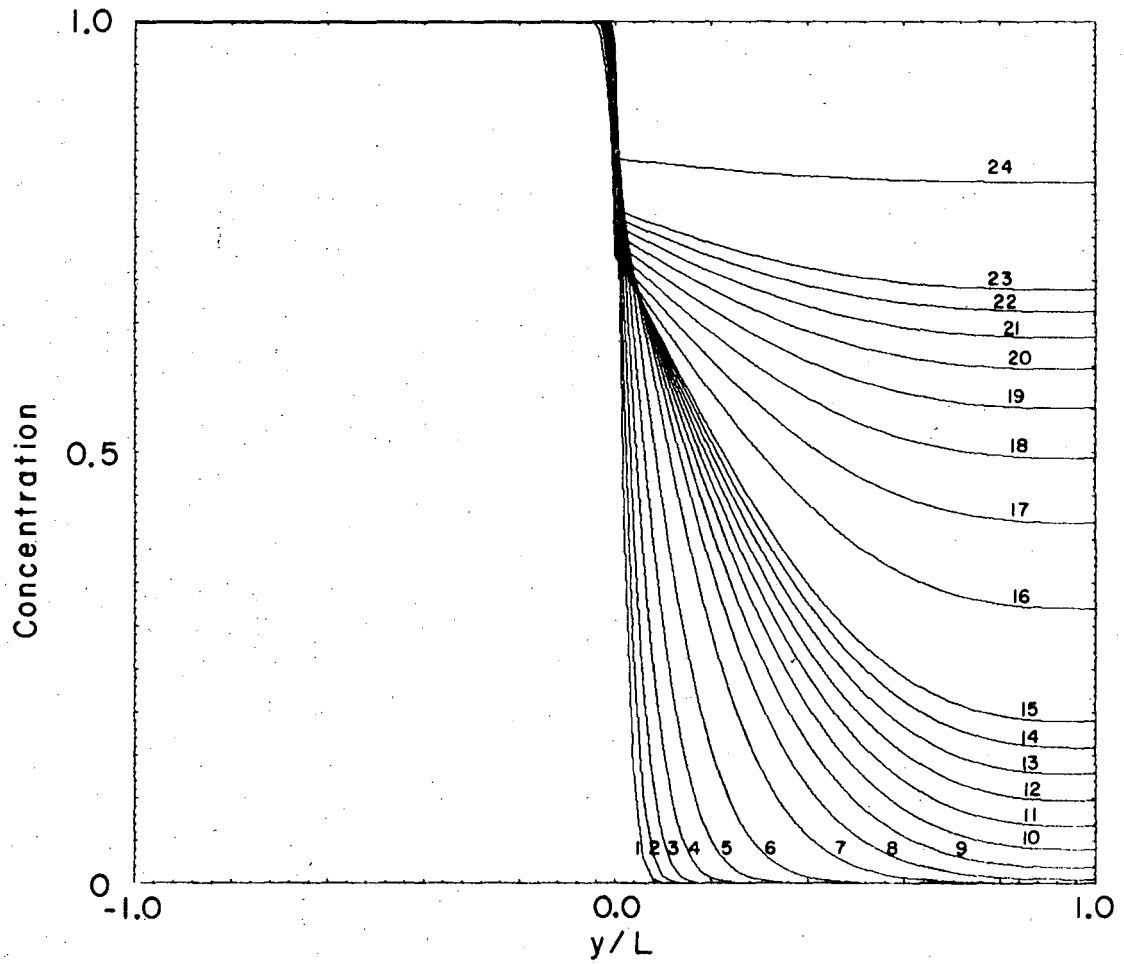

MUB-11305

Fig. 78. Interphase concentration profiles for the evaporation of ether from ethanol solution into CO_2 for different values of the Graetz number. $U_m/U_o = 0.667$.

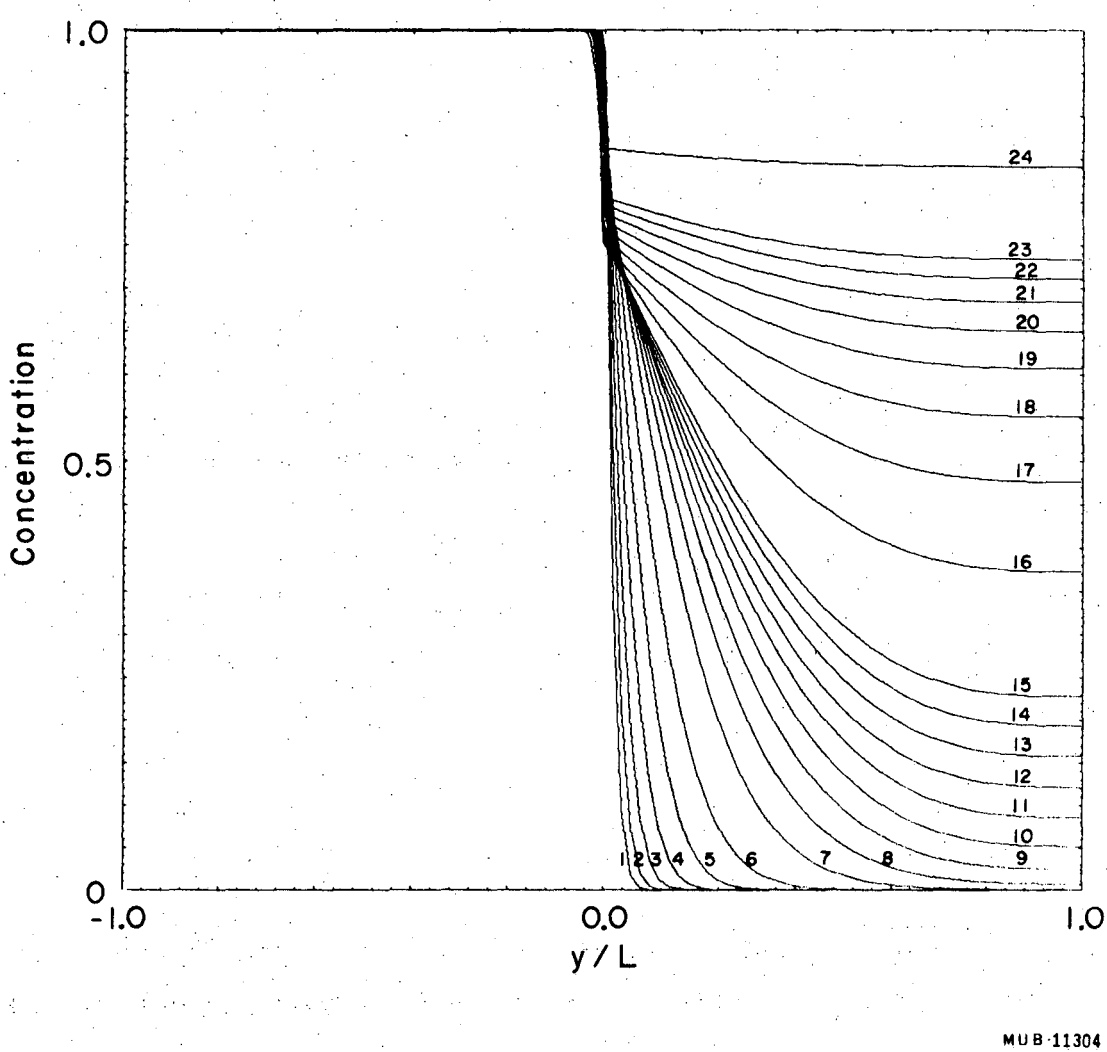

Fig. 79. Interphase concentration profiles for the evaporation of ether from ethanol solution into CO_2 for different values of the Graetz number. $U_m/U_o = 0.50$.

Table D-3

Graetz Numbers of Profiles in Figures 68 to 79

Profile Number	Graetz Number
1	0.00050
2	0.00100
3	0.00200
4	0.00400
5	0.00800
6	0.01600
7	0.03200
8	0.04800
9	0.06400
10	0.08000
11	0.09600
12	0.11200
13	0.12800
14	0.14400
15	0.16000
16	0.24000
17	0.32000
18	0.40000
19	0.48000
20	0.56000
21	0.64000
22	0.72000
23	0.80000
24	1.60000

"GRAPEN"

Necessary Input

The necessary data are basically the same as in GRAGRA except for the changes noted below.

Card 2 TOL is removed, and in its place KOL is needed. This is the number of divisions which are added to the liquid in order to make the solution infinite in extent. This value must be found by trial and error.

Card 3 Only two parameters are necessary in this case, F and VAV. They both have the same definition as in the previous case.

Output

The output is self-explanatory for the most part. It is basically the same as in GRAGRA.

```
GRAPEN, 4, 300,120000.  468001, BYERS
MODE 7.
RUNJ(S,,,,,,120000)
REQUEST TAPE99. CAL-COMP PLOT TAPE
DENSITY TAPE99,5. SET DENSITY TO 556.
GRAPEN.
EXIT.
DMP.
-
      PROGRAM GRAPEN (INPUT,OUTPUT,TAPE99,TAPE98,TAPE2=INPUT,TAPE3=OUTPU
     1T)
      DIMENSION    XR(500),      X(500),A(500),B(500),C(500),VAR(200)
      DIMENSION G(500),O(500),Q(500),                  XNU(200),W(500)
      DIMENSION  RU(6,500),          RUT(06,500)
C     GAS LIQUID MASS TRANSFER IN CONFINED COCURRENT FLOW
      COMMON/CCPOOL/XMIN,XMAX,YMIN,YMAX,CCXMIN,CCXMAX,CCYMIN,CCYMAX
      COMMON/CCFACT/FACTOR
      FACTOR=1024.
      READ(2,57)  NODATA
   57 FORMAT  (I2)
   50 READ(2,1) K,M,N ,IND,JELL,KOL,JS
    1 FORMAT(6I5      ,I2)
   71 READ(2,107)  F,VAV
  107 FORMAT(2F12.6)
      R=0.001*VAV
      GP=R/2.
      WRITE(3,67)
   67 FORMAT(53H1RESULTS OF GRAETZ SOLUTION WITH INTERFACIAL VELOCITY)
      WRITE (3,80)
   80 FORMAT (28H AND LIQUID PHASE RESISTANCE //)
      WRITE(3,104) F
  104 FORMAT (3H F=,F10.3)
      H1=1./(FLOAT(K))
      KRUMB=M-K
      H2=1./FLOAT(KRUMB)
      P=1./FLOAT(N)
      WRITE(3, 4 ) H1,H2
    4 FORMAT(F6.4,19H LIQUID Y INCREMENT,F6.4,17H GAS Y INCREMENT     )
      WRITE(3, 5 ) P
    5 FORMAT(F6.4,22H X DIRECTION INCREMENT    )
      WRITE(3,110)    VAV
  110 FORMAT( 7H VAV = ,F10.5)
      RAG=R/VAV
      CON=F  *H2/H1
      DIV=1.0
      MD=1
      M=M+KOL
      K=K+KOL
      II=0
      KO=K+1
      KO1=KO+1
      L=M+1
      MR=1
      DO  15  J=1,K
   15 X(J)=1.0
      DO 81 J=KO,L
   81 X(J)=0.0
      ALP=(H2*H2)/(R*P)
      BET=(H1*H1)/(GP*P)
```

```
      X(K+1)=(BET*CON)/(BET*CON+ALP)
      VEX=X(K+1)
      XNUI=(1.0-VEX)/H1
      AY=6.*VAV-4.
      AYS=3.-6.*VAV
   18 ALP=(H2*H2)/(R*P)
      BET=(H1*H1)/(GP*P)
      CARL=0.5*BET
      CARG=ALP*0.25*H2*(3.*VAV-1.+H2/2.-VAV*H2)
      WRITE(3,60)  ALP,CARG,CARL  ,BET
   60 FORMAT(6H ALP=  ,F10.5,6H CARG= ,E10.4,6H CARL= ,E10.4,6H BET= ,E1
     10.4//)
      A(1)=-(1.+4.*CARL/3.)
      B(1) =1.-2.*CARL/3.
      DO 8 J=2,K
      A(J) =-(1.+ BET       )*2.0
      C(J  ) = 1.
    8 B(J) = 1.
      A(K+1)=-(CON*(1.+BET)+     (1.+ALP))
      B(K+1)=1.
      C(K+1)=CON
      DO 9 J=KO1,M
      J1=J-KO
      Z=H2*FLOAT(J1)
      VAR(J)=(1.+AY*Z+AYS*Z*Z)*ALP
      A(J)=-(1.+VAR(J))*2.0
      C(J)=1.
    9 B(J)=1.
      C(L)=1.-2.*CARG/3.
      A(L)=-(1.+4.*CARG/3.)
      O(1)=A(1)
      DO 10 J=2,L
      Q(J-1)=B(J-1)/O(J-1)
   10 O(J)=A(J)-C(J)*Q(J-1)
      DO 19 I=MR,N
      II=II+1
      G(1)=((1.-4.*CARL/3.)*X(1)-(1.+2.*CARL/3.)*X(2))/O(1)
      DO 31 J=2,K
      W(J)=X(J)
   31 G(J)=(-X(J-1)-X(J+1)+2.*(1.-BET       )*X(J)-C(J)*G(J-1))/O(J)
      G(K+1)=(-CON*X(K)-X(KO1)+(CON*(1.-BET)+(1.-ALP    )       )*X(K+1)-
     1C(KO)*G(K))/O(KO)
      DO 12 J=KO1,M
      W(J)=X(J)
   12 G(J)=(2.*(1.-VAR(J))*X(J)-X(J-1)-X(J+1)-C(J)*G(J-1))/O(J)
      G(L)=((1.-4.*CARG/3.)*X(L)-(1.+2.*CARG/3.)*X(M)-C(L)*G(M))/O(L)
      W(K+1)=X(K+1)
      W(1)=X(1)
      W(L)=X(L)
      X(L)=G(L)
      DO 13 J=1,M
      J1=L-J
      J2=J1+1
   13 X(J1)=G(J1)-Q(J1)*X(J2)
      DO 75 JO=1,JELL
      SET=X(1)
      X(1)=1.25*((1.-2.*CARL/3.)*X(2)-(1.-4.*CARL/3.)*W(1)+(1.+.667*CARL
     1)*W(2))/(1.+4.*CARL/3.)-0.25*SET
```

```
      S(1)=ABS(X(1)-SET)
      DO  32 J=2,K
      SET=X(J)
      X(J)=-1.25*(X(J+1)+X(J-1)-2.*(1.-BET       )*W(J)+W(J+1)+W(J-1))/A(
     1J)-0.25*SET
   32 S(J)=ABS(X(J)-SET)
      SET=X(K+1)
      X(KO)= -1.25*(X(K)*CON+X(KO1)+W(K)*CON-(CON*(1.-BET)+     (1.-ALP))
     1*W(KO)+W(KO1))/A(KO )-0.25*SET
      S(KO )=ABS(X(K+1)-SET)
      DO 79 J=KO1,M
      SET=X(J)
      X(J)=-(X(J+1)+X(J-1)-2.*(1.-VAR(J))*W(J)+W(J+1)+W(J-1))/A(J)*1.25-
     10.25*SET
   79 S(J)=ABS(X(J)-SET)
      SET=X(L)
      X(L)=-(X(M)*C(L)-(1.-4.*CARG/3.)*W(L)+(1.+2.*CARG/3.)*W(M))/A(L)
     1*1.25-0.25*SET
      S(L)=ABS(X(L)-SET)
      DO 33 JOKE= 1,L
      IF(S(JOKE)-0.0001)  33,33,75
   33 CONTINUE
      GO TO 34
   75 CONTINUE
   34 CONTINUE
      DO 11 J=1,L
      IF(X(J)-1.0)   11,11,40
   40 X(J)=1.00
   11 CONTINUE
      Y=P*FLOAT (I)   *DIV*RAG
      WRITE(3, 14)  Y
   14 FORMAT(16H GRAETZ NUMBER= ,F9.5   )
      T(II)=Y
      XN   =(19.*X(KO)-30.*X(KO1)+18.*X(K+2)-10.*  X(K+3) +3.*X(K+4))/
     1(12.*H2)
      XS2=X(K+1)
      IF( MOD (I,IND))20,42,20
   42 DO 131 J=1,KO
      IF (X(J)-0.999)    132,132,131
  132 LOL=J
      GO TO 133
  131 CONTINUE
      LOL=K   -1
  133 DO  134   J=KO,L
      IF (X(J) -0.001)   135,135,134
  135 LOW =J
      GO TO 136
  134 CONTINUE
      LOW=L
  136 WRITE(3,38 )( X(J),J=LOL,K)
   38 FORMAT(25X,F10.6)
      WRITE(3, 35)  XS2
   35 FORMAT(30H INTERFACIAL CONCENTRATION IS F7.5///)
      WRITE(3,22 )
   22 FORMAT(//30X,3H P ,28H GAS PROFILE FROM INTERFACE //)
      WRITE(3,23 )( X(J),J=KO1,LOW)
   23 FORMAT(25X,F10.6)
   20 VEX=X(K+1)
```

```
      XNU(I)=XN
      RUT(JS,II)=XNU(I)
      WRITE(3,30)  XN ,JO
   30 FORMAT(5X,24H LOCAL NUSSELT NUMBER = ,E10.4,20H CONVERGENCE AT J =
     1 ,I3)
      SUM1=0.
      SUM2=0.
      DO 28 J=KO1,M,2
      SUM1=(VAR(J)/ALP)*X(J)+SUM1
   28 SUM2=(VAR(J+1)/ALP)*X(J+1)+SUM2
      CUP     =P*    (4.*SUM1+2.*SUM2+1.00)/(VAV*3.00)
      XNS=CUP*VAV*DIV/R
      RUT(JS,II)=CUP
      WRITE (3,17)    CUP,XNS
   17 FORMAT(5X,25H CUP MIXING CONCENTRATION ,E12.6,16H AVG NUSSELT NO=,
     1E12.6//)
   19 CONTINUE
      READ(2,2)  LR,MD,IND
    2 FORMAT(2I2,I5)
      IF(LR)  3,6,3
    3 DI =FLOAT(MD)
      R=R*DI
      GP =GP*DI
      DIV=DIV*DI
      DO 41  I=1,N
      MO=I/MD
      IF(MOD(I,MD))    41,16,41
   16 XNU(MO)=XNU(I)
   41 CONTINUE
      MR=N/MD +1
      MR1=MR
      GO TO 18
    6 SUM1=0.
      SUM1=0.
      SUM2=0.
      NO=N-2
      DO 24 J=1,NO,2
      SUM1=XNU(J)+SUM1
   24 SUM2=XNU(J+1)+SUM2
      XNUSLT=P*(4.*SUM1+2.*SUM2+4.*XNU(N-1)+XNU(N)+XNUI) /3.
      WRITE (3,25) XNUSLT
   25 FORMAT(27H THE AVE NUSSELT NUMBER IS ,E10.4)
      SUM1=0.
      SUM2=0.
      SUM3=0.0
      SUM4=0.0
      DO 26 J=KO1,M,2
      SUM1=(VAR(J)/ALP)*X(J)+SUM1
      SUM3=VAR(J)/ALP +SUM3
      SUM4=VAR(J+1)/ALP+SUM4
   26 SUM2=(VAR(J+1)/ALP)*X(J+1)+SUM2
      CUP1=P*       (4.*SUM1+2.*SUM2+1.00)/(VAV*3.00)
      WRITE(3,27 )  CUP1
   27 FORMAT(//37H CUP MIXING CONC FROM EXIT PROFILE = ,E10.4    )
       VEL=XNUSLT*R/VAV
      WRITE(3,29 )  VEL
   29 FORMAT(43H CUP MIXING CONC FROM INTERFACIAL FLUXES = ,E10.4 )
      CALL CCNEXT
```

```
      IF(NODATA-JS)  83,83,82
   82 GO TO 50
   83 CONTINUE
      XMIN=0.0
      YMIN=0.0
      XMAX=Y
      YMAX=1.0
      CCXMIN= 80./1024.
      CCYMIN=100./1024.
      CCYMAX=1000./1024.
      CCXMAX=1280./1024.
      CALL CCGRID (1,10,5,6HLABELS,1,10,5)
       CALL CCLTR (400./1024.,10./1024.,0,2,11H GRAETZ NO. )
      CALL CCLTR (10./1024.,350./1024.,1,2,21H FRACTION SATURATION  )
      DO 89 J=1,JS
      DO 85 I=1,II
   85 XR(I)=RUT(J,I)
      CALL CCPLOT (T,XR ,II,4HJOIN,0,0)
   89 CONTINUE
      CALL CCNEXT
      UP=0.0
      DN=100.
      DO 7 J=1,JS
      IF(RU(J,II)-DN)   87,87,84
   87 DN=RU(J,II)
   84 DO 21 I=1,10
      IF(RU (J,I)-UP) 21,21,88
   88 UP=RU (J,I)
   21 CONTINUE
    7 CONTINUE
      XMIN=-5.
      XMAX=1.0
      YMIN=FLOAT(IFIX(ALOG10(DN)-1.))
      YMAX=FLOAT(IFIX(ALOG10(UP)+1.))
      KI=IFIX(YMAX-YMIN)
      CALL CCGRID (6,6HLABELS,KI )
      DO 52  I=1,II
   52 T(I)=ALOG10(T(I))
       CALL CCLTR (400./1024.,10./1024.,0,2,16H LOG(GRAETZ NO.)  )
      CALL CCLTR (10./1024.,350./1024.,1,2,24H LOG(NUSSELT NUMBER)      )
      DO 86 J=1,JS
      DO 90 I=1,II
   90 XTS(I)=ALOG10(RU(J,I))
      CALL CCPLOT (T,XTS,II,4HJOIN,0,0)
   86 CONTINUE
      CALL CCEND
      STOP
      END
```

Results of the General Solution using the GRAPEN Program

The velocity profiles which are assumed are a constant velocity in the liquid phase and a parabolic profile in the gas. This requires the setting of two independent parameters, in this case these were chosen to be $\alpha\mathcal{H}$, the mass transfer control parameter, and U_m/U_0, the velocity ratio. Solutions were computed for five values of the control parameter, 5, 2, 1, 0.5 and 0.25. At each of these values a series of six values of the velocity parameter were set. These were 10, 4, 2, 1, 0.667, and 0.5. They are represented by a series of six curves on each graph (Figs. 80 to 88). For each value of the control parameter two graphs are given; the first is a logarithmic plotting of local Nusselt number as a function of the Graetz number of the gas phase, and the second is a plotting of the cup-mixing concentration as a function of the Graetz number. A directory of these graphs is given as Table D-4.

Table D-4
A Listing of the Plots for Different Values of $\alpha\mathcal{H}$

$\alpha\mathcal{H}$	Figure Number of Graph	
	Local Nusselt Number Plot	Cup-Mixing Concentration Plot
1.00	36	84
2.00	80	85
5.00	81	86
0.50	82	87
0.25	83	88

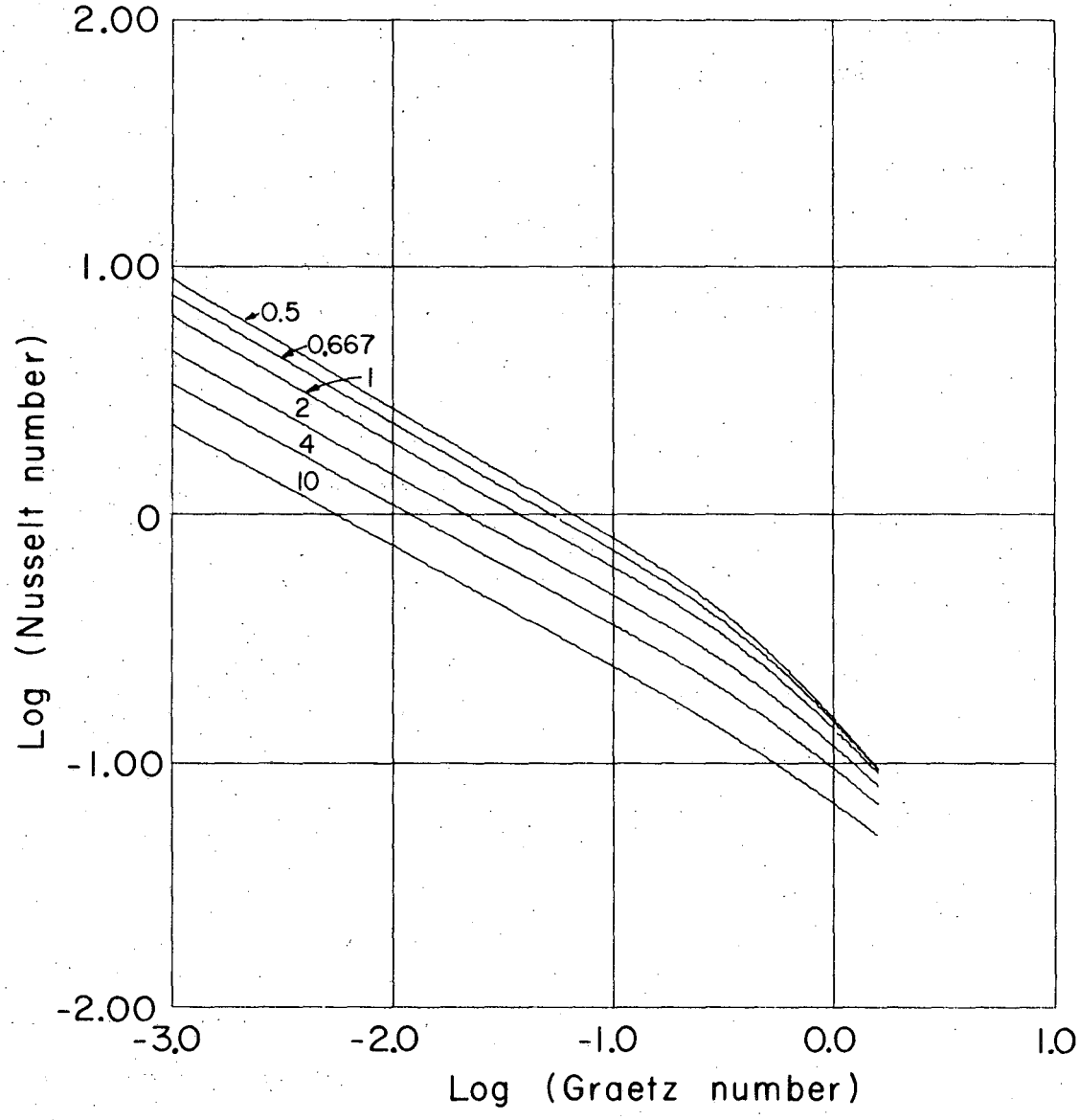

MUB 11319

Fig. 80. Local Nusselt number as a function of the Graetz number for interphase mass transfer with the liquid phase velocity constant. The parameter is U_m/U_o and $\alpha N = 2.00$.

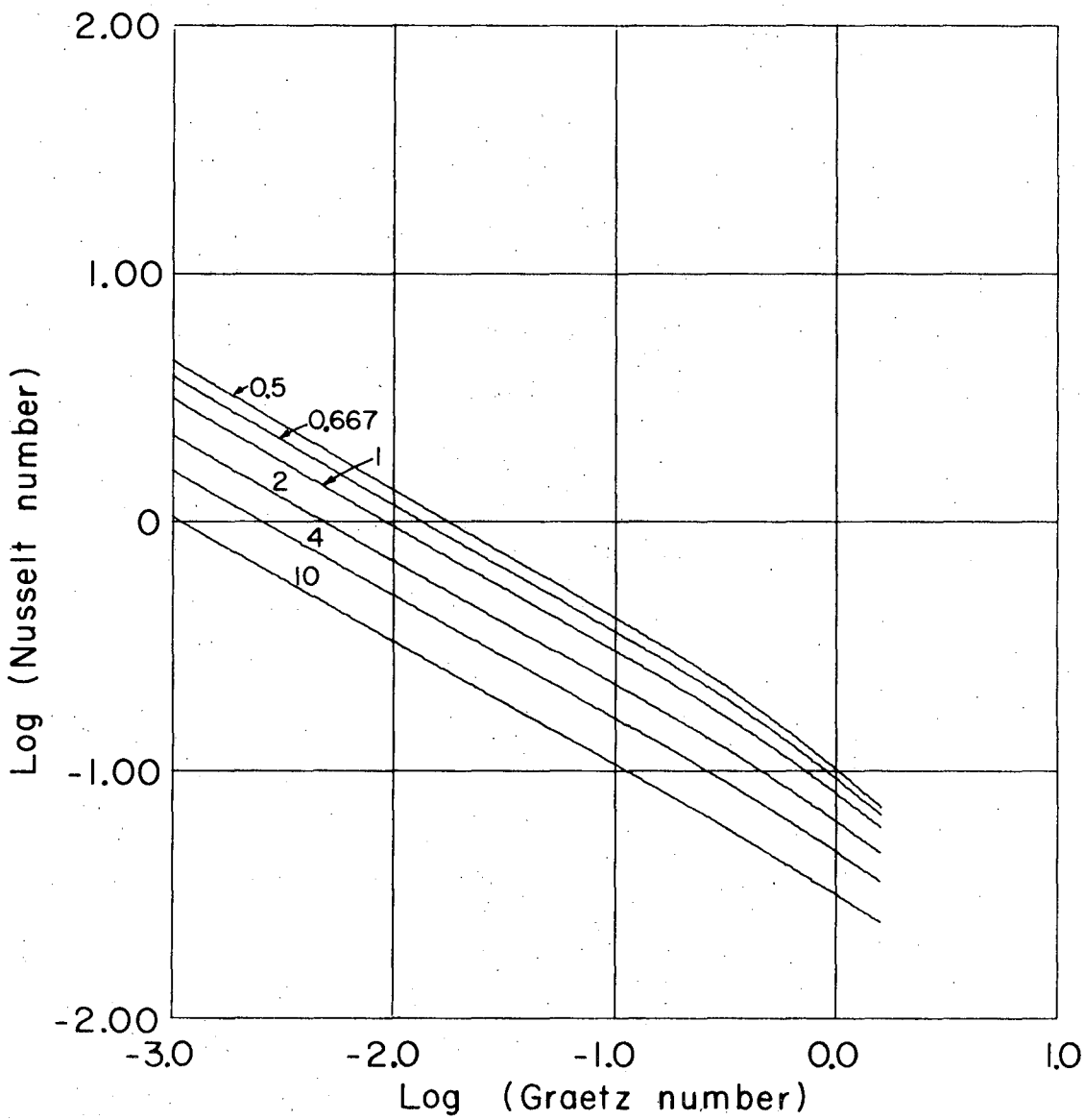

MUB 11320

Fig. 81. Local Nusselt number as a function of the Graetz number for interphase mass transfer with the liquid phase velocity constant. The parameter is U_m/U_o and $\alpha H = 5.00$.

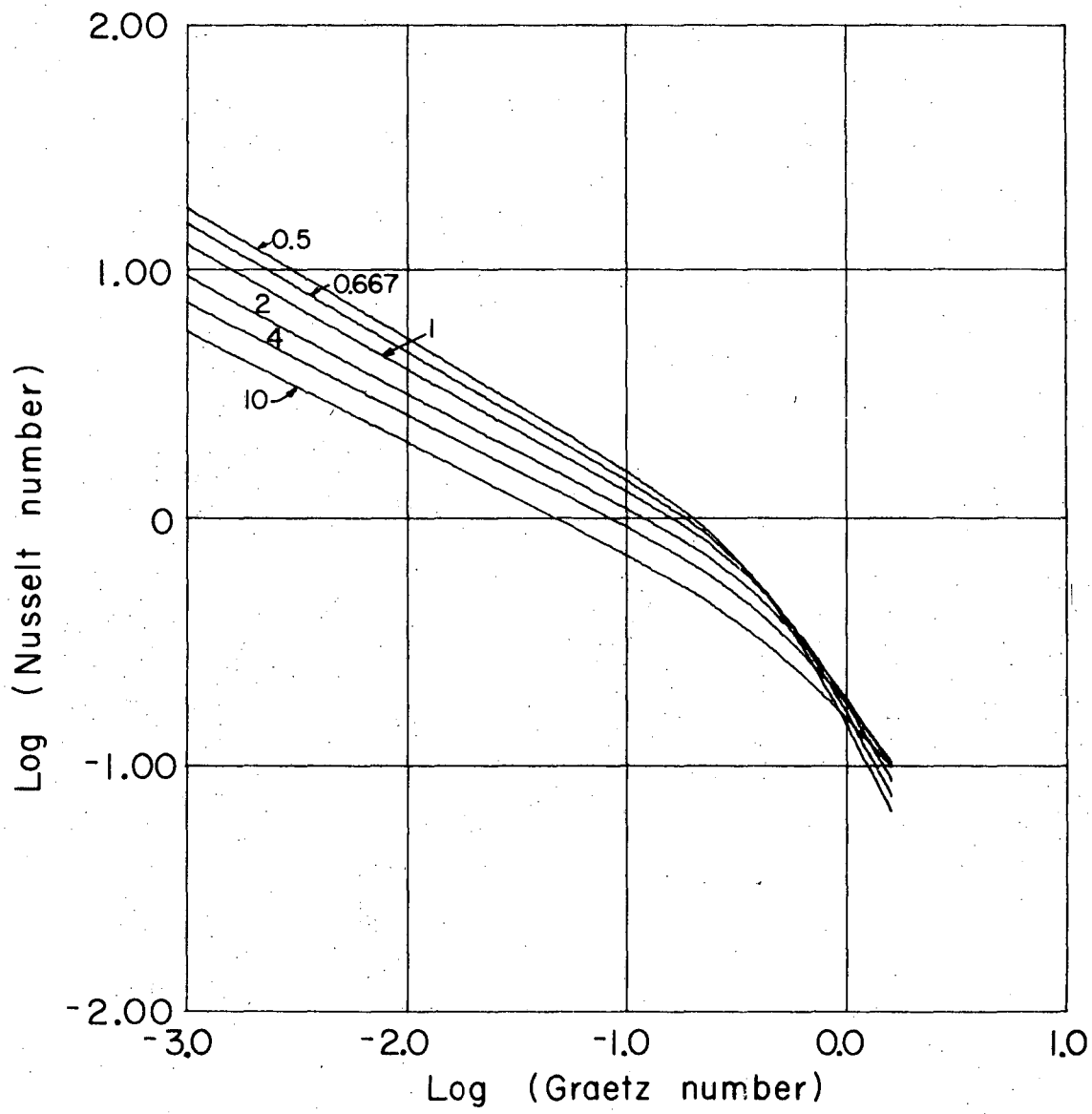

Fig. 82. Local Nusselt number as a function of the Graetz number for interphase mass transfer with the liquid phase velocity constant. The parameter is U_m/U_o and $\alpha H = 0.50$.

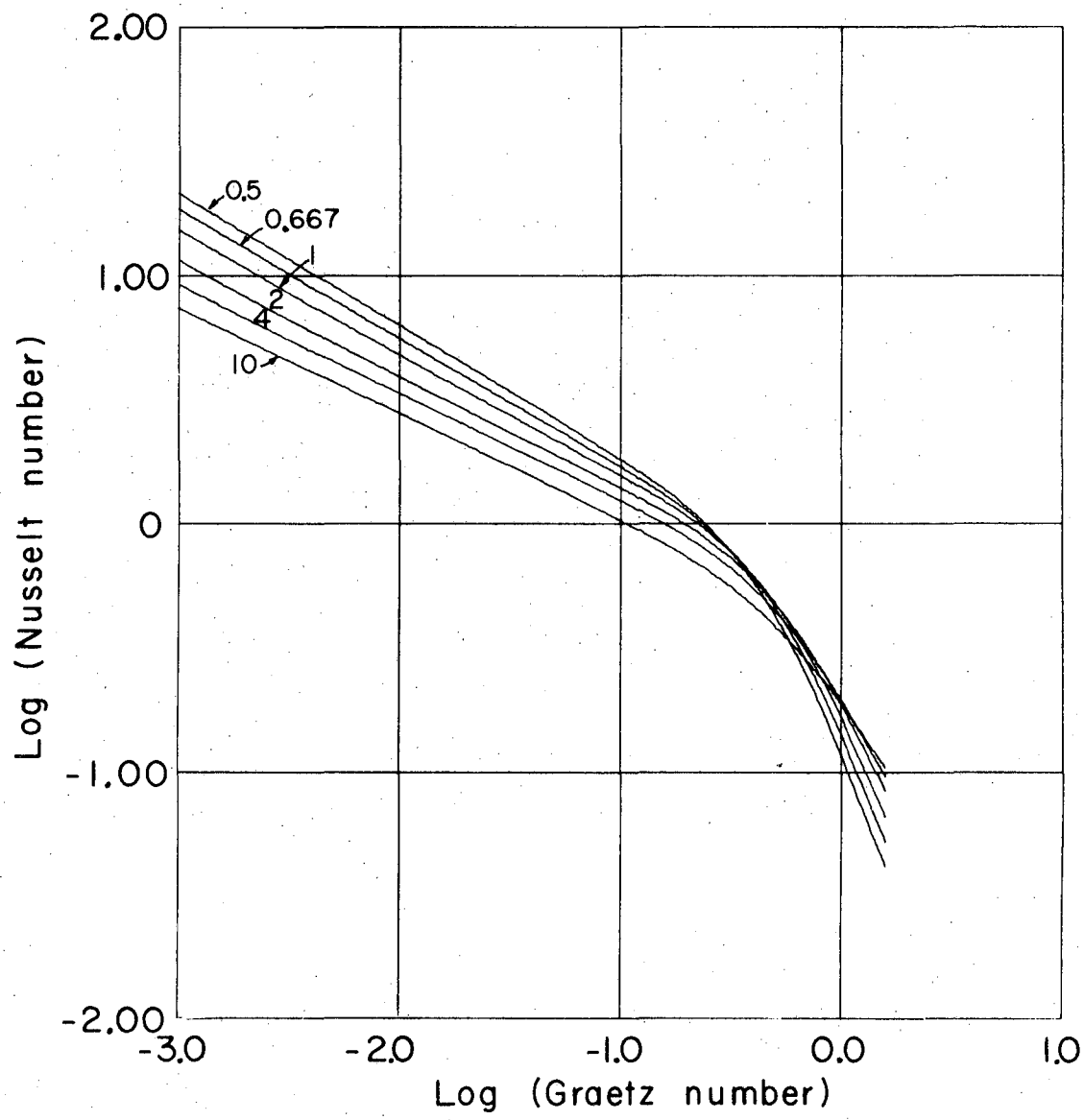

MUB 11318

Fig. 83. Local Nusselt number as a function of the Graetz number for interphase mass transfer with the liquid phase velocity constant. The parameter is U_m/U_o and $\alpha H = 0.25$.

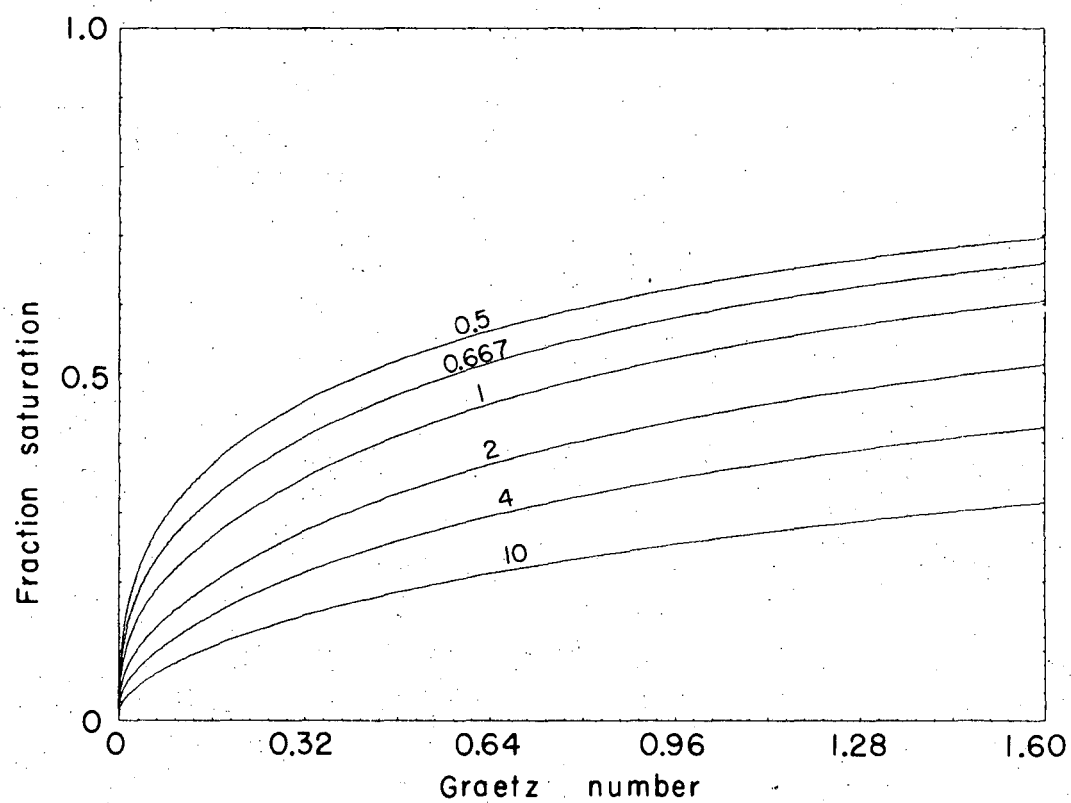

MUB-11251

Fig. 84. Cup mixing concentration as a function of Graetz number for interphase mass transfer with the liquid phase velocity constant. The parameter is U_m/U_o and $\alpha H = 1.00$.

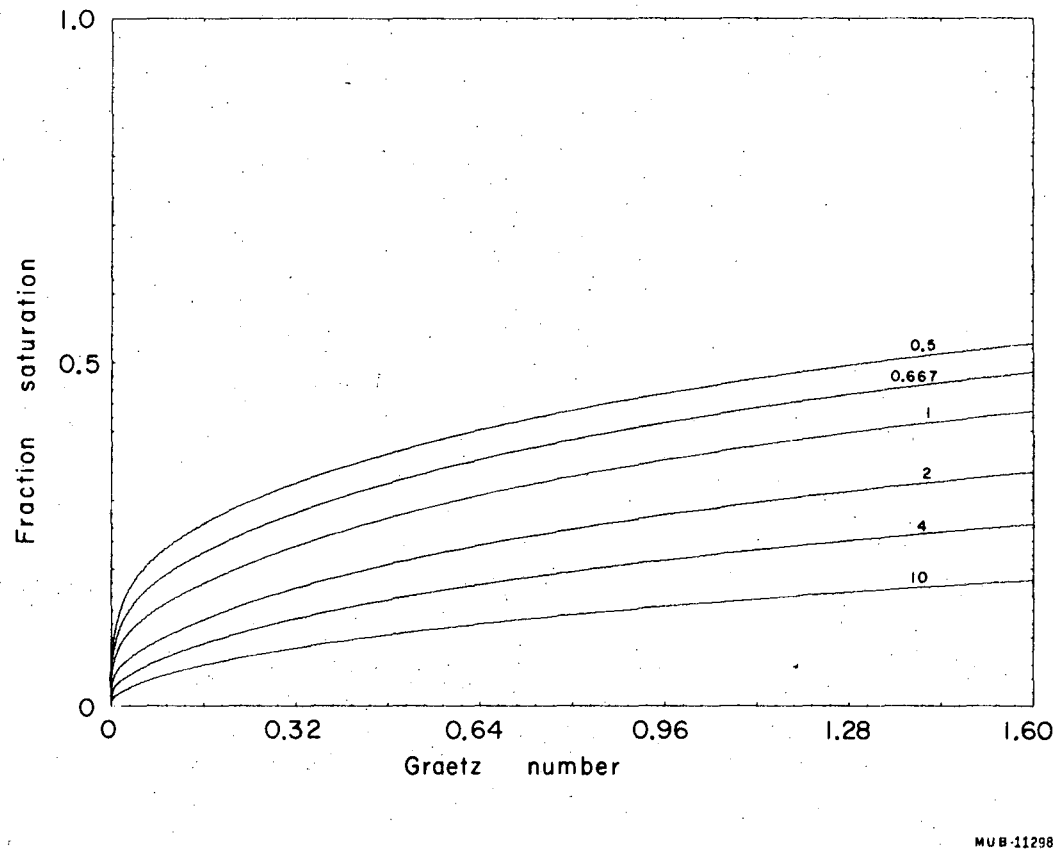

Fig. 85. Cup mixing concentration as a function of Graetz number for interphase mass transfer with the liquid phase velocity constant. The parameter is U_m/U_o and $\alpha H = 2.00$.

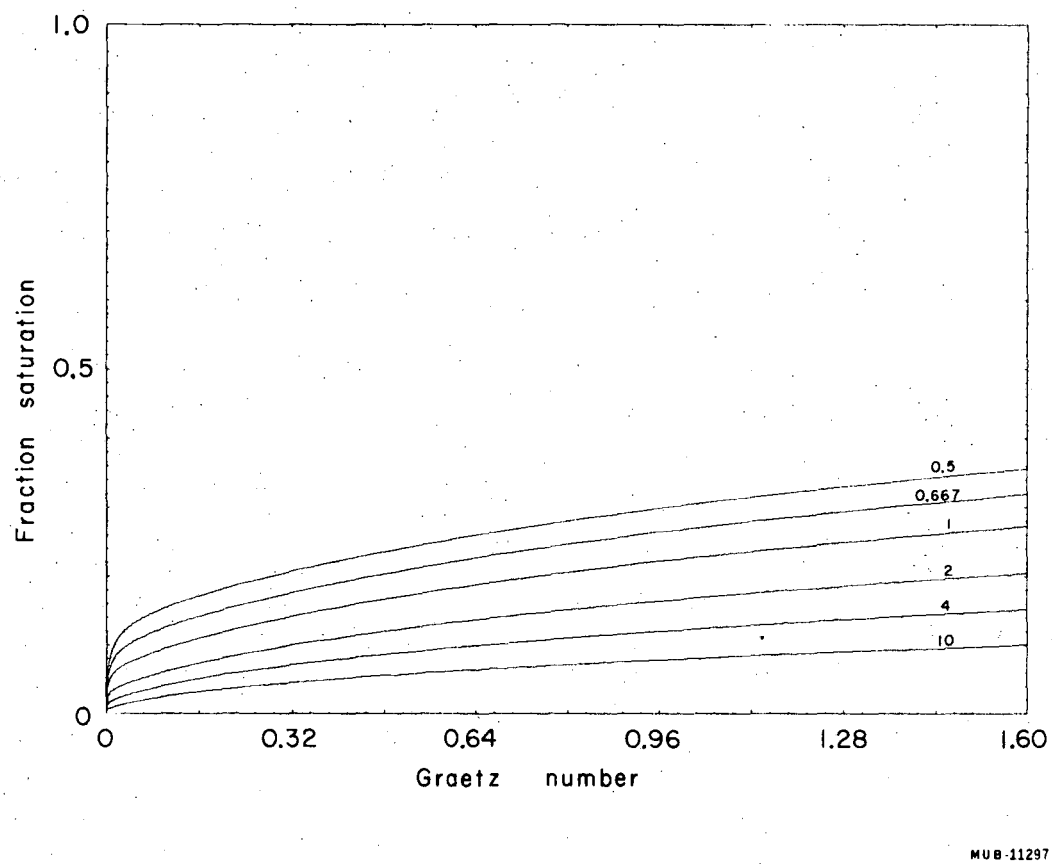

Fig. 86. Cup mixing concentration as a function of Graetz number for interphase mass transfer with the liquid phase velocity constant. The parameter is U_m/U_o and $\alpha\tilde{H} = 5.00$.

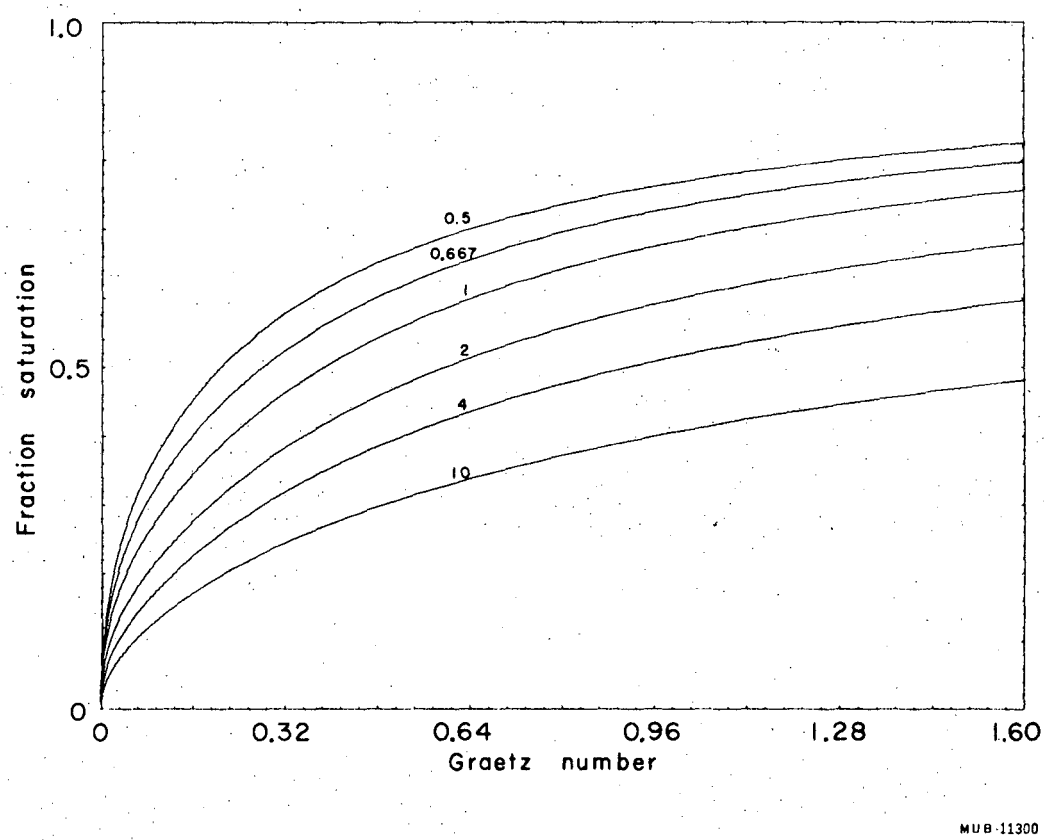

Fig. 87. Cup mixing concentration as a function of Graetz number for interphase mass transfer with the liquid phase velocity constant. The parameter is U_m/U_o and $\alpha H = 0.50$.

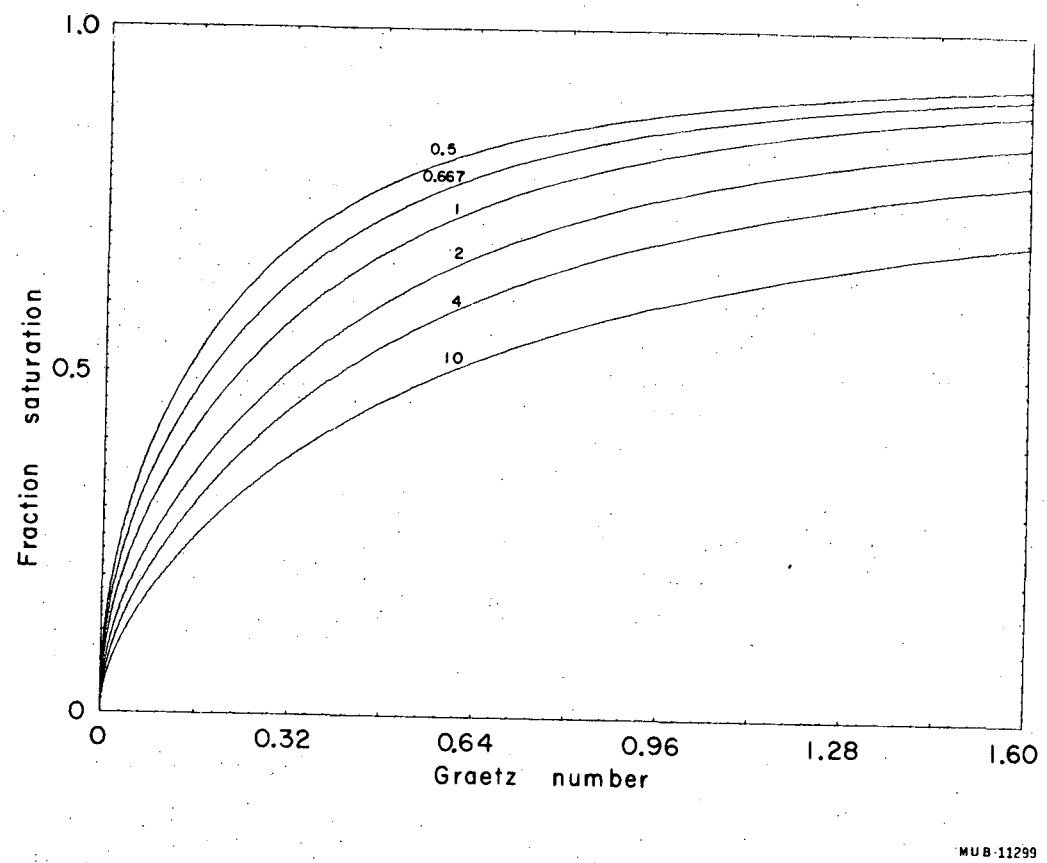

Fig. 88. Cup mixing concentration as a function of Graetz number for interphase mass transfer with the liquid phase velocity constant. The parameter is U_m/U_o and $\alpha H = 0.25$.

"CJKING"

Input Data

Again the input is basically the same as in the previous programs with the following changes from GRAPEN.

Card 2 Add the variable LARK which is the number of divisions to be added to the gas phase to prevent penetration from occuring. It must be established by trial for any particular case.

Card 3 VAV now is the slope of the velocity profile in the gas phase.

Output

This is given in terms of the variables in the Beek and Bakker solution. These are written with the appropriate symbols in the output.

```
$ID   468001,CJKING, 8,C.H.BYERS
$IBJOB
$IBFTC CJKING
      DIMENSION S(500),T(0500),XR(0500)
      DIMENSION                X(500),A(500),B(500),C(500),VAR(500)
      DIMENSION G(500),O(500),Q(500),                XNU(500),W(500)
      DIMENSION  YD(500),RU(10,500)
C     GAS LIQUID MASS TRANSFER IN CONFINED COCURRENT FLOW
      COMMON/CCPOOL/XMIN,XMAX,YMIN,YMAX,CCXMIN,CCXMAX,CCYMIN,CCYMAX
      CALL CCBGN
      READ(2,57)  NODATA
   57 FORMAT  (I2)
   50 READ(2,1) K,M,N ,IND,JELL,KOL,LARK,JS
    1 FORMAT(7I5     ,I2)
   71 READ(2,107)  F,VAV
  107 FORMAT(2F12.6)
      R=0.001*VAV/10.
      GP=R
      CON=1./F
      WRITE(3,67)
   67 FORMAT(53H1RESULTS OF LEVEQU SOLUTION WITH INTERFACIAL VELOCITY)
      WRITE (3,80)
   80 FORMAT (28H AND LIQUID PHASE RESISTANCE //)
      WRITE(3,104) F,CON
  104 FORMAT (3H F=,F10.3,11H SIGMA*H = ,F10.5)
      H1=1./(FLOAT(K))
      KRUMB=M-K
      KA=LARK/KRUMB
      H2=1./FLOAT(KRUMB)
      P=1./FLOAT(N)
      WRITE(3, 4 ) H1,H2
    4 FORMAT(F6.4,19H LIQUID Y INCREMENT,F6.4,17H GAS Y INCREMENT    )
      WRITE(3, 5 ) P
    5 FORMAT(F6.4,22H X DIRECTION INCREMENT    )
      WRITE(3,110)   VAV
  110 FORMAT( 7H VAV = ,F10.5)
      RAG=R/VAV
      CON=F  *H2/H1
      DIV=1.0
      MD=1
      TR=1.+FLOAT(KOL)/FLOAT(K)
      M=M+KOL
      K=K+KOL
      II=0
      KO=K+1
      KO1=KO+1
      M=M+LARK
      L=M+1
      MR=1
      DO  15  J=1,K
   15 X(J)=1.0
      DO 81 J=KO,L
   81 X(J)=0.0
      ALP=(H2*H2)/(R*P)
      BET=(H1*H1)/(GP*P)
      X(K+1)=(BET*CON)/(BET*CON+ALP)
      VEX=X(K+1)
      XNUI=(1.0-VEX)/H1
      XMIN=-TR
```

```
      XMAX=FLOAT(KA+1  )
      YMIN=0.0
      YMAX=1.0
      CCYMIN=100./1024.
      CCYMAX=1000./1024.
      CCXMIN= 80./1024.
      CCXMAX=1280./1024.0
      KJ=IFIX(TR) +KA          +1
      CALL CCGRID (KJ,5,6HLABELS,1,10 )
       CALL CCLTR (400./1024.,10./1024.,0,2,5H Y/L )
      CALL CCLTR (10./1024.,350./1024.,1,2,14H CONCENTRATION)
   18 ALP=(H2*H2)/(R*P)
      BET=(H1*H1)/(GP*P)
      CARL=0.5*BET
      FA=H2/FLOAT(L)
      FAR=FA/(H2*100.)
      CARG=ALP*0.5*(1.+VAV-0.5*VAV*H2*FAR)*FAR
      WRITE(3,60)  ALP,CARG,CARL  ,BET
   60 FORMAT(6H ALP=  ,F10.5,6H CARG= ,E10.4,6H CARL= ,E10.4,6H BET= ,E1
     10.4//)
      A(1)=-(1.+4.*CARL/3.)
      YD(L)=1.0
      YD(1)=-  TR
      YD(KO)=0.0
      B(1) =1.-2.*CARL/3.
      DO 8 J=2,K
      YL    =H1*(FLOAT(J)-FLOAT(KO))
      YD(J)=     YL
      A(J) =-(1.+ BET       )*2.0
      C(J  ) = 1.
    8 B(J) = 1.
      A(K+1)=-(CON*(1.+BET)+     (1.+ALP))
      B(K+1)=1.
      C(K+1)=CON
      DO 9 J=KO1,M
      J1=J-KO
      Z=H2*FLOAT(J1)
      YD(J)=Z
      VAR(J)=(1.+VAV*Z)*ALP
      A(J)=-(1.+VAR(J))*2.0
      C(J)=1.
    9 B(J)=1.
      C(L)=1.-2.*CARG/3.
      A(L)=-(1.+4.*CARG/3.)
      O(1)=A(1)
      DO 10 J=2,L
      Q(J-1)=B(J-1)/O(J-1)
   10 O(J)=A(J)-C(J)*Q(J-1)
      DO 19 I=MR,N
      II=II+1
      G(1)=((1.-4.*CARL/3.)*X(1)-(1.+2.*CARL/3.)*X(2))/O(1)
      DO 31 J=2,K
      W(J)=X(J)
   31 G(J)=(-X(J-1)-X(J+1)+2.*(1.-BET       )*X(J)-C(J)*G(J-1))/O(J)
      G(K+1)=(-CON*X(K)-X(KO1)+(CON*(1.-BET)+(1.-ALP    )       )*X(K+1)-
     1C(KO)*G(K))/O(KO)
      DO 12 J=KO1,M
      W(J)=X(J)
```

```
133 DO  134   J=KO,L
    IF (X(J) -0.001)   135,135,134
135 LOW =J
    GO TO 136
134 CONTINUE
    LOW=L
136 WRITE(3,38 )( X(J),J=LOL,K)
 38 FORMAT(25X,F10.6)
    WRITE(3, 35)  XS2
 35 FORMAT(30H INTERFACIAL CONCENTRATION IS F7.5///)
    WRITE(3,22 )
 22 FORMAT(//30X,3H P ,28H GAS PROFILE FROM INTERFACE //)
    WRITE(3,23 )( X(J),J=KO1,LOW)
 23 FORMAT(25X,F10.6)
    CALL CCPLOT (YD,X,L,  4HJOIN,0,0)
 20 VEX=X(K+1)
    XN=XN*Y**0.5/VAV
    XNU(I)=XN
    RU(JS,II)=XNU(I)
    WRITE(3,30)  XN ,JO
 30 FORMAT(5X,24H KAV*(X/DUO)**0.5      = ,E10.4,20H CONVERGENCE AT J =
   1 ,I3)
 19 CONTINUE
    READ(2,2)  LR,MD,IND
  2 FORMAT(2I2,I5)
    IF(LR)  3,6,3
  3 DI =FLOAT(MD)
    R=R*DI
    GP =GP*DI
    DIV=DIV*DI
    DO 41  I=1,N
    MO=I/MD
    IF(MOD(I,MD))   41,16,41
 16 XNU(MO)=XNU(I)
 41 CONTINUE
    MR=N/MD +1
    MR1=MR
    GO TO 18
  6 CONTINUE
    CALL CCNEXT
    IF(NODATA-JS)  83,83,82
 82 GO TO 50
 83 CONTINUE
    UP=0.0
    DO 7 J=1,JS
    IF(RU (J ,II)-UP)   7, 7,87
 87 UP=RU (J ,II)
  7 CONTINUE
    MUP=IFIX(ALOG10(UP))
     LUP=IFIX    (1.+UP/(10.**(MUP)))
    UP=FLOAT(LUP) *10.**(MUP  )
 88 PUI=ALOG10(T(1))
 25 PUII= ALOG10(T(II))
    PUII=FLOAT(IFIX(PUII)+1)
    PUI= FLOAT(IFIX(PUI)-1)
    XMIN=PUI
    XMAX=PUII
    YMIN=0.0
```

```
 12 G(J)=(2.*(1.-VAR(J))*X(J)-X(J-1)-X(J+1)-C(J)*G(J-1))/O(J)
    G(L)=((1.-4.*CARG/3.)*X(L)-(1.+2.*CARG/3.)*X(M)-C(L)*G(M))/O(L)
    W(K+1)=X(K+1)
    W(1)=X(1)
    W(L)=X(L)
    X(L)=G(L)
    DO 13 J=1,M
    J1=L-J
    J2=J1+1
 13 X(J1)=G(J1)-Q(J1)*X(J2)
    DO 75 JO=1,JELL
    SET=X(1)
    X(1)=1.25*((1.-2.*CARL/3.)*X(2)-(1.-4.*CARL/3.)*W(1)+(1.+.667*CARL
   1)*W(2))/(1.+4.*CARL/3.)-0.25*SET
    S(1)=ABS(X(1)-SET)
    DO  32 J=2,K
    SET=X(J)
    X(J)=-1.25*(X(J+1)+X(J-1)-2.*(1.-BET       )*W(J)+W(J+1)+W(J-1))/A(
   1J)-0.25*SET
 32 S(J)=ABS(X(J)-SET)
    SET=X(K+1)
    X(KO)= -1.25*(X(K)*CON+X(KO1)+W(K)*CON-(CON*(1.-BET)+     (1.-ALP))
   1*W(KO)+W(KO1))/A(KO )-0.25*SET
    S(KO )=ABS(X(K+1)-SET)
    DO 79 J=KO1,M
    SET=X(J)
    X(J)=-(X(J+1)+X(J-1)-2.*(1.-VAR(J))*W(J)+W(J+1)+W(J-1))/A(J)*1.25-
   10.25*SET
 79 S(J)=ABS(X(J)-SET)
    SET=X(L)
    X(L)=-(X(M)*C(L)-(1.-4.*CARG/3.)*W(L)+(1.+2.*CARG/3.)*W(M))/A(L)
   1*1.25-0.25*SET
    S(L)=ABS(X(L)-SET)
    DO 33 JOKE= 1,L
    IF(S(JOKE)-0.0001)  33,33,75
 33 CONTINUE
    GO TO 34
 75 CONTINUE
 34 CONTINUE
    DO 11 J=1,L
    IF(X(J)-1.0)   11,11,40
 40 X(J)=1.00
 11 CONTINUE
    Y=P*FLOAT (I)*R*VAV*VAV
    WRITE(3, 14)  Y
 14 FORMAT(22H PROFILE AT BB GROUP = ,F10.5   )
    T(II)=Y
    XN   =(19.*X(KO)-30.*X(KO1)+18.*X(K+2)-10.*  X(K+3) +3.*X(K+4))/
   1(12.*H2)
    XS2=X(K+1)
    LOL=1
    IF( MOD (I,IND))20,42,20
 42 DO 131 J=1,KO
    IF (X(J)-0.999)    132,132,131
132 LOL=J
    GO TO 133
131 CONTINUE
    LOL=K   -1
```

```
      YMAX=UP
      CCXMAX=1280./1024.
      KR=IFIX (PUII-PUI    )
      CALL CCGRID (KR,6HLABELS,5,5)
       CALL CCLTR (400./1024.,10./1024.,0,2,11H AADX/UO**3 )
      CALL CCLTR (10./1024.,350./1024.,1,2,17H KAVG(X/UOD)**0.5 )
      DO 89 J=1,JS
      DO 85 I=1,II
      T(I)=ALOG10(T(I))
   85 XR(I)=RU(J,I)
      CALL CCPLOT (T,XR ,II,4HJOIN,0,0)
   89 CONTINUE
      CALL CCEND
      STOP
      END
```

APPENDIX E

PHYSICAL PROPERTIES

The physical properties used throughout the entire study are collected in this chapter. The units of all variables are in the cgs system of units except for pressure and where a note to the contrary is made. All the experiments in the study were made at or near 25°C, and hence all properties are reported at this temperature. The one exception is the vapor pressure, which is tabulated over a temperature range. In the cgs system the universal gas constant is

$$R = 82.06 \text{ cm}^3 \text{ atm g-mole}^{-1} \text{ °K}^{-1}$$

A. Diffusion Coefficients

1. Gas Diffusivities

The Wilke-Lee[78] modification of the Hirschfelder, Bird and Spotz[32] equation is used to calculate all the binary gas diffusivities used in this series of experiments. Table E-1 is a compilation of the results of these calculations. Where experimental values are available in the report by Wilke and Lee,[78] these are also added. The calculated values were used in the experiments.

Table E-1

Gas Diffusivities at 25°C

Diffusing Component	Solvent Gas	Calculated $D\text{-cm}^2/\text{sec}$	Experimental $D\text{-cm}^2/\text{sec}$
Ethanol	Nitrogen	0.123	0.135*
Ethanol	Oxygen	0.123	0.135*
Ethanol	Carbon dioxide	0.0789	0.0793
Ether	Oxygen	0.0938	0.0924*
Ether	Carbon dioxide	0.0670	0.0620
Ether	Helium	0.377	--

*Data for air

An example of the type of calculation which was necessary to arrive at a value of the diffusion coefficient is now discussed. The diffusivity of ether in oxygen is calculated. The constants which are necessary are quoted by Wilke and Lee[78] as:

Oxygen	$M_2 = 32$	$e/k = 113.2$	$r_0 = 3.433$
Ether	$M_1 = 74$	$e/k = 350.$	$r_0 = 5.424$

$$e_{12}/k = \sqrt{e_1 e_2}\ /k = \sqrt{350. \times 113.2} = 198.9$$

$$kT/e_{12} = 298.0/198.9 = 1.50$$

From this information the following constants can be estimated by using tables and graphs given in Ref. 81. For this case $W_1^1 = 0.5991$ and $\Delta = 0.0$

$$r_{12} = (r_1 + r_2)/2 = 4.428$$

The predictive equation is

$$D_{12} = (10.7 - 2.46\ (\frac{M_1+M_2}{M_1M_2})^{1/2})\ \frac{T^{3/2}((M_1+M_2)/M_1M_2)^{1/2} \times 10^{4}}{P\ r_{12}^{2} W_1^1 (1 - \Delta)}$$

$$= \frac{10.179 \times 5144 \times 0.2118 \times 10^{-4}}{1 \times 4.428^2 \times 0.5991}$$

$$= 0.0938\ cm^2/sec$$

1. <u>Liquid Diffusivities</u>

Two liquid diffusivities were required for the present study, the diffusion coefficient of ether at high dilution in water and a similar value for ether in ethanol. Since these values had not been reported previously both were measured using a diaphram cell technique which is discussed else where.[7] In the case of the diffusion in water, an approximately 1.5 weight per cent ether solution diffused into pure water at 25.0°C. Analysis was

performed with a differential interferometer. Four values were found acceptable; these are shown in Table E 2. The average value is

$$D_{ether-H_2O} = 0.962 \times 10^{5} \pm 3.5\% \ cm^2/sec.$$

Rossi et al.[58] have found a value of 0.878×10^{5} cm^2/sec for the same system at 20°C. The value measured in the present study compares favorable with the value of 1.015×10^{-5} cm^2/sec calculated by the Wilke Chang equation.[77]

In the case of the diffusion of ether in alcohol, 2 mole % ether solutions diffused into ethanol. The gas liquid chromatograph was used to analyse samples. The diffusion coefficient averaged over five measurements is

$$D_{ether\ EtOH} = 0.871 \times 10^{5} \pm 5.0\% \ cm^2/sec$$

This value is consistant with experimental data systems. It is also in good agreement with the Wilke-Chang equation, which predicts a value of 0.855 cm^2/sec. No previous measurement of this system was found.

Table E-2

Experimental Diffusion Coefficients (25°C.) in $cm^2/sec \times 10^5$

	Ether-Water	Ether-Ethanol
	0.932	0.924
	0.997	0.847
	0.940	0.908
	0.980	0.795
		0.886
Average	0.962±3.5%	0.871±5.0%

B. Viscosities

The viscosities of the four gases used in this study were found in the Chemical Engineers' Handbook.[53a] The viscosities of the two liquids, ethanol and water, were also taken from this source.[53b] Table E-3 is a collection of these values.

Table E-3

Viscosities

Substance	State	Viscosity cp.
Oxygen	Gas	0.0203
Nitrogen	Gas	0.0177
Carbon dioxide	Gas	0.0146
Helium	Gas	0.0190
Water	Liquid	0.8937
Ethanol	Liquid	1.15

C. Densities

All gas densities were obtained by the use of the ideal gas law. At 25°C they are

$$\rho_{N^2} = 1.369 \text{ gm/l}$$

$$\rho O_2 = 1.561 \text{ gm/l}$$

$$\rho He = 0.1932 \text{ gm/l}$$

$$\rho CO_2 = 2.155 \text{ gm/l}$$

The density of water at 25°C was found to be 0.997 gm/ml[84c] and that of ethanol is 0.789 gm/ml[84d].

D. Vapor Pressure

In order to calculate the Henry's law constant and to correct for minor deviations in temperature from 25°C, it was necessary to know the vapor pressure of both ethanol and ether. These were found in the Chemical Engineers' Handbook[53e,f] over a large range of temperatures. Using a semilog graph of vapor pressure as a function of the reciprocal of absolute temperature, the vapor pressures over the desired range were found. These are listed in Table E-4.

Table E-4

Important Vapor Pressures

Temperature °C	V.P. of EtOH mm Hg.	V.P. of Ether mm Hg.
21	45.0	427
22	48.0	450
23	50.5	471
24	53.8	500
25	57.0	525
26	60.5	550
27	64.5	575
28	68.5	600

E. Henry's Law Constant

The dimensionless Henry's law constant (H/RT) is necessary when one is considering interphase mass transfer. The value of this constant for solutions of the partially miscible ether-water system is calculated from solubility data. Seidell[64] reports that this figure is 6.04 grams of ether per hundred grams of solution. The density of this solution of 0.98508 gm/cc. The Henry's law constant is then the ratio of the mole fraction at saturation (0.01537) to the vapor pressure of ether at 25°C(525 mm Hg). This procedure follows from the very low solubility of water in ether.

Therefore

$$H = 3.448 \quad 10^4 \text{ mm Hg/mole fraction.}$$

In nondimensional form

$$\mathcal{H} = H/RT = 3.264 \times 10^{-2}$$

In the ether-ethanol system Gordon and Hornibrook[25] have measured the vapor pressure as a function of mole fraction. At a mole fraction of ether of 0.005, its partial pressure is 7.40 mmHg. Therefore

$$H = 1.48 \times 10^3 \text{ mm Hg/mole fraction}$$

and

$$\mathcal{H} = 4.54 \times 10^{-3}$$

APPENDIX F

Nomenclature

a	Channel width, used in derivation of hydrodynamics only - cm.
a	Slope of the velocity of the gas phase at the interface - sec^{-1}.
b	Thickness of the gas phase in two phase studies - cm.
b'	Constant
c	Liquid thickness in rectangular channel hydrodynamics - cm.
C,Ca	Concentration, when unsubscripted it is a dimensionless group, when subscripted with an a, for example, it is the concentration of component a in the solution in gm moles/cc. ΔC is defined as $C_{go}/\mathcal{H}-C_{10}$. $\bar{C}$ is the concentration transformed into the Laplace domain. C_1, C_2 are dimensionless concentrations on grid points in computer solution.
Cg	In two-phase flow notation only, this is the % of total flow which is gas.
D	Diffusion coefficient (also script D) - cm^2/sec.
e	maximum energy of attraction in ergs/molecule
f	Function defined as 1/z
g	Acceleration due to gravity - cm/sec^2
G	$2\mathcal{H}U_0^2/3a$
Gz	Modified Graetz Number $DL/U_m b^2$
H	Henry's law constant - mm Hg/mole fraction.
H	Increment in y direction in computer studies.
$\mathcal{H}$	Dimensionless Henry's law constant = H/RT
i	$\sqrt{-1}$
Io	Imaginary Bessel function of the second kind to order "o"
k	Boltzmann's constant in ergs/molecule °K.
k	A general constant which is later evaluated.
k_c	Local mass transfer coefficient of the gas phase - cm/sec. $\bar{k}$ same in Laplace domain.
k_c	Overall mass transfer coefficient based upon the gas phase - cm/sec.
ko	Real Bessel function of the second kind of order "o".
l	Distance from the leading edge of a stagnant film to exit - cm.
L	Length of channel - cm.

Lc	Length of channel - cm.
m	Index defined in Eq. (A-25).
m	Equilibrium constant between gas and liquid defined by Eq. (4-2).
M	Molecular weight - grams/gram mole.
n	Index on constants in Graetz solution.
N	Mass flux in gm moles/cm^2sec.
N	Avogadro's Number.
Nu	Nusselt number.
P	Partial pressure of the transferrring component of the gas phase in mm Hg (always subscripted).
P	Total pressure in atmospheres.
P	Laplace transform variable.
Q	Volumetric flow rate in cm^3/sec.
r	Collision radius-A°.
R	Universal gas constant - cm^3 Atm $(gm\ mole)^{-1}$ $°K^{-1}$.
R	Separation solution in Eq. (3-6).
R	$(U_0^3/a^2D_g)^{1/2}$.
Re	Reynolds Number.
Rh	Hydraulic radius - cm.
R_n	Series with running variable, n, defined in Eq. (4-26).
s	Laplace transform variable. cm^{-1}
S_n	Series with running variable, n, defined in Eq. (4-26).
St	Stanton Number.
t	Time in sec.
T	Absolute temperature - °K.
u	Velocity in general or specifically the velocity in the x direction - cm/sec.
U_0	Interfacial velocity - cm/sec.
U_m	Average velocity in the gas phase _ cm/sec.
U	U_m/U_0
v	Velocity vector - cm/sec.
W	Width of channel - cm.
x	Mole fraction of a component in the liquid phase.
x	Coordinate direction or distance parallel to flow - cm.

x^+	Dimensionless distance parameter.
X	X/L
X	1/Lc
y	Coordinate direction or distance perpendicular to flow - cm.
Y	y/b
z	$2Rs^{1/2}/3$
Zo	General Bessel function of order "o".

Greek Letters

α	$(\sigma\mathcal{H}+1)$
	Equilibrium constant between vapor and interfacial surfactant film.
β	$(5-7\sigma\mathcal{H})/72$
	Angle which the channel is inclined to the vertical, in radians
β_n	Series of constants in the Graetz solution
Γ	Surface concentration - molecules/cm^2.
$\Gamma(a)$	The gamma function (always of some argument a).
δ	Thickness of a film on an inclined plane - cm.
	The thickness of a surfactant film - cm.
Δ	The distance between the interface and the flow reversal in counter-current flow - cm.
ζ_n	Variable defined as (2n + 1)b/W.
η	Variable defined in Eq. (A-25).
	y/L
	ay/U_0
θ	Constant in Eq. (4-21).
λ	xD/aL^3
Λ	Constant in Eq. (4-20).
μ	Viscosity in cp.
ν	Kinematic viscosity - cm^2/sec.
ξ	The Beek and Bakker distance group, a^2Dx/U_0^3.
π	Surface pressure-dynes/cm^2.
ρ	Density - gm/cc.
τ	Shear stress - Dynes/cm.
τ	$\sigma\mathcal{H}(-1/3)!/2^{-1/3}(-2/3)!$

σ	$(D_g/D_l)^{1/2}$
ϕ	Rate of adsorption at the interface molecules/sec.
ϕ	Fraction saturation.
χ	X direction solution in the Graetz problem.
χ	Transform variable defined in Eq. (3-17).
ψ	The Modified Graetz number - $DL/U_m b^2$.
Ω	Y direction solution in Graetz problem.

Subscripts

1,2--	Referring to the first, second, etc. quantity.
a,b	Referring to component a,b,---
av	Average of quantity.
act	Actual
cwt	With constant wall temperature.
f	Referring to the film.
fp	Referring to behavior between two flat plates.
g	Of the gas phase or based upon the gas phase.
i,int	At the interface.
l	Of the liquid or based upon the liquid.
lwt	Linear wall temperature.
m	In the moving part of the surfactant film.
o	At entry.
s	At the surface. In Chapter V refers to the stagnant region.

49. R. L. Merson and J. A. Quinn, A. I. Ch. E. J. 11, 391 (1965).
50. W. Nernst, Z. Phys. Chem. 47, 52 (1904).
51. W. Nusselt, Z. Agew. Math. Mech. 10, 105 (1930).
52. R. H. Perry, "Chemical Engineers' Handbook," Fourth Edition, (McGraw-Hill Book Co., Inc., New York, 1963).
53. R. H. Perry, "Chemical Engineers' Handbook," Fourth Edition, (McGraw-Hill Book Co., Inc., New York, 1963), a) pp. 3-196—197; b) pp. 3-199—201; c) p. 3-70; d) p. 3-22; e) p. 3-51; f) 3-52.
54. R. L. Pigford, (Ph.D. Thesis), University of Illinois, Urbana, (1941).
55. O. E. Potter, Chem. Eng. Sci. 6, 170 (1957).
56. G. A. Ratcliffe and K. J. Reid, Trans. Inst. Chem. Eng. 39, (1960).
57. G. A. Ratcliffe and K. J. Reid, Trans. Inst. Chem. Eng. 40, (1961).
58. C. Rossi, E. Bianci, and A. Rossi, J. Chim. Phys. 55, 99 (1958).
59. H. Schlichting, "Boundary Layer Theory," (McGraw-Hill Book Co., Inc., New York, 1960).
60. E. Schmidt, Z. Gesundl.-Ing. 63, 525 (1929).
61. L. E. Scriven and R. L. Pigford, A. I. Ch. E. J. 5, 397 (1959).
62. L. E. Scriven and R. L. Pigford, A. E. Ch. E. J. 4, 439 (1958).
63. J. R. Sellars, Myron Tribus, and J. S. Klein, Trans. A. S. M. E. 78, 441 (1956).
64. A. Seidell, "Solubilities of Organic Compounds," 3rd Edition, (Van Nostrand, New York, 1940).
65. T. K. Sherwood and R. L. Pigford, "Absorption and Extraction," 2nd Edition, (McGraw-Hill Book Co., Inc., New York, 1952).
66. A. E. Shulman, C. G. Savini, and R. V. Edwin, A. I. Ch. E. J. 9, 479 (1963).
67. Y. P. Tang and D. M. Himmelblau, A. I. Ch. E. J. 9, 630 (1963).
68. Y. P. Tang and D. M. Himmelblau, Chem. Eng. Sci. 18, 143 (1963).
69. H. Thoma, "Hocheislungskessel," (Springer, Berlin, 1921).
70. D. W. van Krevelan and P. J. Hoftijzer, Rec. Trans. Chim. 68, 221 (1949).
71. J. E. Vivian and C. J. King, A. I. Ch. E. J. 10, 221 (1964).
72. J. E. Vivian and D. W. Peaceman, A. I. Ch. E. J. 2, 437 (1956).

73. A. F. H. Ward and L. Tordai, J. Chem. Phys. 14, 453 (1946).
74. M. M. Wendel, (Ph.D. Thesis), University of Delaware, Newark, (1956).
75. L. E. Westkeamper and R. R. White, A. I. Ch. E. J. 3, 69 (1957).
76. W. Whitman, Chem. Met. Eng. 29, 146 (1923).
77. C. R. Wilke and Pin Chang, A. I. Ch. E. J. 1, 264 (1955).
78. C. R. Wilke and C. Y. Lee, Ind. Eng. Chem. 47, 1253 (1955).
79. C.-S. Yih, Phys. Fluids 6, 321 (1963).
80. F. Yoshida and T. Koyanagi, A. I. Ch. E. J. 8, 309 (1962).

This report was prepared as an account of Government sponsored work. Neither the United States, nor the Commission, nor any person acting on behalf of the Commission:

A. Makes any warranty or representation, expressed or implied, with respect to the accuracy, completeness, or usefulness of the information contained in this report, or that the use of any information, apparatus, method, or process disclosed in this report may not infringe privately owned rights; or

B. Assumes any liabilities with respect to the use of, or for damages resulting from the use of any information, apparatus, method, or process disclosed in this report.

As used in the above, "person acting on behalf of the Commission" includes any employee or contractor of the Commission, or employee of such contractor, to the extent that such employee or contractor of the Commission, or employee of such contractor prepares, disseminates, or provides access to, any information pursuant to his employment or contract with the Commission, or his employment with such contractor.